CHEMICALLY MODIFIED FORMS OF MAGNETIC CHITOSAN AS POTENTIAL ENZYME CARRIERS: A GATEWAY TO UPLIFT INDUSTRIAL APPLICATIONS

Thesis submitted to
Cochin University of Science and Technology
in partial fulfillment of the requirements for the degree of

Doctor of Philosophy

in

Chemistry

under the Faculty of Science

By

Bindu V.U

Under the Supervision of

Dr. P.V. Mohanan

DEPARTMENT OF APPLIED CHEMISTRY
COCHIN UNIVERSITY OF SCIENCE AND TECHNOLOGY
KOCHI – 682 022

January 2019

Chemically Modified Forms of Magnetic Chitosan as Potential Enzyme Carriers: A Gateway to Uplift Industrial Applications

Ph.D. Thesis under the Faculty of Science

Author

Bindu V.U.
Research Scholar
Department of Applied Chemistry
Cochin University of Science and Technology
Kochi 682022
Kerala, India
Email id: bindukish@gmail.com

Supervising Guide

Dr. P.V. Mohanan
Associate Professor
Department of Applied Chemistry
Cochin University of Science and Technology
Kochi 682022
Kerala, India
Email id: pvmohanan@gmail.com

Department of Applied Chemistry
Cochin University of Science and Technology
Kochi 682022
Kerala, India

January 2019

Department of Applied Chemistry
Cochin University of Science and Technology
Kochi – 682 022

Dr. P.V. Mohanan
Associate Professor

Certificate

This is to certify that the thesis entitled ***"Chemically modified forms of magnetic chitosan as potential enzyme carriers: A gateway to uplift industrial applications"*** *submitted by* ***Mrs. Bindu V.V.*** *is an authentic record of research work carried out by her under my supervision and guidance at the Department of Applied Chemistry in partial fulfillment of the requirements for the degree of Doctor of Philosophy in Chemistry of Cochin University of Science and Technology and has not been included in any other thesis previously for the award of any other degree. All the relevant corrections and modifications suggested by the audience during the pre-synopsis seminar and recommended by the Doctoral Committee have been incorporated in the thesis.*

.

Kochi
Date:

Dr. P.V. Mohanan
Associate Professor
Department of Applied Chemistry
Cochin University of Science and Technology
Kochi-682 022

Declaration

I hereby declare that the thesis entitled ***"Chemically modified forms of magnetic chitosan as potential enzyme carriers: A gateway to uplift industrial applications"*** *submitted for the award of Ph.D. Degree, is based on original research work done by me under the guidance of* ***Dr. P.V. Mohanan,*** *Associate Professor, Department of Applied Chemistry, Cochin University of Science and Technology and further that it has not previously formed the basis for the award of any other degree.*

Kochi-22 ***Bindu V.V.***
Date:

Acknowledgement

"Think of what you have rather than of what you lack. Of the things you have, select the best and then reflect how eagerly you would have sought them if you did not have them."

Marcus Aurelius

"GOD Thank you for bestowing me the opportunity to step in the excellent world of research and pouring me the strength and capability throughout my research work, especially during the challenging moments in completing this thesis. I am candidly grateful for your grace and blessings during this entire journey.

Fulfillment of this doctoral dissertation was associated with the contribution of several people. I would like to take this opportunity to express my sincere gratitude and admiration to all those have contributed to the research in many ways and I need to give them special thanks at this most cherished moment.

At the outset, I would like to convey my sincere gratitude to my research supervisor, Dr. P. V. Mohanan for his valuable guidance, constant support, patience, scholarly inputs and consistent encouragement. I owe him lots of indebtedness for providing amiable research atmosphere, freedom of thought, motivation which imparted in me a confidence in solving my research problems. As my supervisor, he has eternally encouraged me to remain alert on achieving my goal. His surveillance and comments boosted me to accomplish the overall growth of research and to bring the investigation in depth. I perceive fortunate to be associated with his research team and there are no other words to express my extensive regard towards him.

Besides my advisor, I extend my heartfelt gratitude to my doctoral committee member, Dr. P. A. Unnikrishnan for his insightful comments and encouragement.

I express profound gratitude to Dr. K. Girish Kumar, Head, Department of Applied Chemistry for providing all necessary facilities and making it possible to carry out this work in this department. I am very grateful to Dr. K. Sreekumar, former Head, Department of Applied Chemistry for his advices and valuable suggestions related to my research work. I am sincerely indebted to the former heads, Prof. M. R. Prathapachandra Kurup, Dr. N. Manoj and other faculty members Prof. S. Sugunan, Prof. K. K. Muhammed Yusuff, Dr. S. Prathapan and Dr. P.M. Sabura Begum for their enormous support and encouragement during my research period.

I am truly thankful to all non-teaching staff, librarians and administrative staff for their timely help and supports.

I am immensely indebted to Prof. Nirmala Rachel James, Department of Chemistry, Trivandrum for providing permission to carry out surface area analysis at their institution. I express my gratitude to Abdul Basith, Kerala University for carrying out EDS analysis and I extend my special thanks to Christeena John for spending her precious time for helping me to this analysis.

I am also grateful to SAIF, IIT Madras for VSM analysis and SAIF at STIC, CUSAT for carrying out several analyses.

I take the opportunity to acknowledge the funding agency, the University Grant Commission (UGC), Government of India, for providing financial support as UGC-JRF/SRF to complete my research work.

I wish to extend my warmest thanks to all my lab mates for their constant support and co-operation during the course of research work. I am lucky to have made such great friends and their friendship provided me a marvelous work place which enabled to complete the research work without any burden. I remember the wonderful moments with them; during tea times and treats for each and every small happiness. My acknowledgement will never be perfect without giving special mention of my lab seniors. I would like to acknowledge Dr. Priya Rajan and Dr. Navya Antony for their support and motivation during the initial days of my stay in the lab.

I express my sincere affection to Maria chechi, who led me to the field of enzyme immobilization. She was always available to me for the discussions in research area when I was in any trouble. Without her support and motivation I could not complete my thesis work. Shanty chechi, you are the person who gave me the relief at the first sight, when I came to the lab for asking any research scholar vacancy to our sir. After that, you have influenced me a lot by your good advices and motivational talks. I remember with grateful, the occasions with you in several national and international seminars and conferences. Divya, the familiar face when I joined the lab and I missed you a lot as a good friend during my research period. I am grateful to Jessica and Sneha, as my young sisters for their love and affection and also their support and corporation during my research period. Geetha, Savitha and Anjali, my sweet 'enzyme' mates, I am very thankful to you for your great support especially during my pre-synopsis presentation. I felt more comfort with you all when I tell some problems related to my research work since you all understood that's own spirit. Thank you very much Dhanya for your love and liberality even though you came at the end period of my course. Best wishes to Krishnendu, the newcomer to our lab. Thank you once again to my lab mates for creating an excellent work environment where I enjoyed working every day!

I extend my sincere thanks to other lab mates, especially the polymer lab mates, who considered us as their good neighbor and their friendship has made my research life dynamic and vibrant. I thank Sherly miss, Anjali Pathmanabhan, Soumya Xavier, Anjali Jacob and Jisha for giving me the wonderful experience, attending a seminar presentation at Coimbatore. I appreciate the juniors in this lab who maintain the relation as in the same manner.

I owe a special thanks to my Amma and Achan for their love, prayers, timely encouragement and endless patience. It was their blessings that raised me up again when I got weary. They really recognized my pain and pressures during my PhD course and became part of my journey. A big thank to my Father and Mother in laws who really supported me to strive towards my goal. I am indebted to them for providing a loving environment for me. I am extremely thankful to my brother, sister, cousins, brother in laws, sister in laws and their kids for their love and moral support. All of them have given me constant inspiration and encouragement when I was being really frustrated and passed through the difficult situations. I feel extremely lucky as I am very much blessed by God to be gifted such a lovely, caring and supportive family.

There are no words and I don't know how to begin with saying thanks to my soul mate, my dearest husband, Amrith Kishor. He is my most enthusiastic cheer leader, made my ambition also of him and has given up so much to make my career a priority in our lives. His love, inspiration and forbearances have been vital to me throughout the entire period of my course. I really thank him for being so understanding and for putting up with me through the toughest moments of my life. I love you for everything and I thank God for enlightening my life with your presence.

I owe very much to my beloved kids, Aadi Narayan (Appoos) and Aadi Lakshmi (Kunjus) for their patience and support and I dedicate this PhD thesis to both of them. Words would never say how grateful I am to both of you. Appoos, you are my little hero by your cute advices and inspirations towards my thesis completion. Kunjus, your naughty and smiling face is enough for me to reduce my stresses especially during the thesis writing.

Besides this, I extend my thanks to several people who helped me in the successful completion of this thesis knowingly and unknowingly.

Bindu

Preface

Enzyme technology stands for an important keystone of industrial biotechnology since this technology facilitates commercial production of various enzymes with varied applications in food, textile, detergents, medicine and paper industry. The use of many more enzymes is restricted due to their cost and could not be economical if not reused. The immobilization techniques have been developed which leads to the physical confinement of the enzyme onto a solid material and provide retention of its catalytic activities. This makes the enzyme to use repeatedly and improve the industrial profit by creating the whole process economically feasible. Several inorganic and organic materials have been assessed as efficient carrier for enzyme immobilization. The magnetite particles have gained more attention as enzyme carrier due to the presence of hydroxyl groups on their surfaces that enable their functionalization and interaction with the enzyme. Their magnetic properties promote facile separation from the reaction system which allows the rapid termination of the enzymatic reaction and the recovery for their repeated uses. The biopolymers possess distinctive properties such as biocompatibility, non-toxicity, biodegradability and high affinity towards protein those make them suitable for enzyme immobilization. Chitosan can be regarded as the most commonly used biopolymer as carrier for enzyme immobilization. The reactive amino and hydroxyl groups on chitosan enable direct interaction with the enzyme and facilitate their surface modification. These can be applied in various forms and sizes for enzyme immobilization and also promote the adsorption and covalent methods.

In our study we have used magnetic chitosan as base carrier for α-amylase immobilization. The magnetic property of the carrier made its simple recovery and it was very easy to handle the enzymatic reaction. The surface modification of magnetic chitosan was carried out using cross-linking agents, synthetic polymers, inorganic layered solids and PAMAM dendrimers.

The thesis is divided into eight chapters,

Chapter 1 presents an introduction to industrial biocatalysis and a literature review on enzymes on industrial applications. A brief note on importance of enzyme and need for enzyme immobilization are also outlined. The significance of enzyme and carrier selected for our work are mentioned. The scope and objectives of the current study are also emphasized at the end of this chapter.

Chapter 2 selects magnetic chitosan as base enzyme carrier from chitosan-metal oxide composites such as CSM, CSZ and CST composites. Magnetic chitosan was modified with cross-linking agents such as gluteraldehyde, glyoxal and epichlorohydrin and performed as α-amylase carriers. Experimental methods for physico-chemical techniques and biochemical characterization are also depicted in this chapter.

Chapter 3 to chapter 5 describes the surface modification of magnetic chitosan with synthetic polymers, inorganic layered solids and dendritic polymers respectively. Immobilization studies of α-amylase on these modified forms have been depicted.

Chapter 6 deals with the thermal deactivation study of free and all immobilized enzymes. Kinetic and thermodynamic parameters for thermal deactivation of free and immobilized enzymes were also evaluated.

Chapter 7 illustrates the washing performance of α-amylase immobilized magnetic chitosan in laundry detergents. The performance of immobilized enzyme in enzymatic desizing was also described in this chapter.

Chapter 8 presents the summary and conclusion of the present work. This also comprised of future outlook of the work done.

Contents

Chapter 1

Industrial Biocatalysis: A tactical green technology

Contents

1.1 Industrial biocatalysis

The biocatalysis plays an essential role in industrial technologies and environmentally comfortable characteristics of biocatalysts make the chemical processes greener. Biocatalysis stands for both green and sustainable technology; since the biological catalysts are biodegradable, non-toxic, non-hazardous and they implemented under mild experimental conditions, the processes have become environmentally more attractive and cost-effective [1]. The first modern biocatalysis was developed by Louis Pasteur in 1858, presented the resolution of racemic tartaric acid by various microorganisms and thereafter Emil Fischer introduced the lock and key model to enzymatic catalysis [2]. The first enzyme for industrial purpose was developed by Christian Hansen in 1874 which has been extracted from the dried calves' stomachs using saline solution. Wilhelm Kuhne invented the term 'enzyme' in 1878 derived from Latin word, which mean 'in yeast' and in 1897 Eduard Buchner has discovered the enzyme, 'zymase' which caused the fermentation of sucrose. Trypsin, the first commercial enzyme was prepared by Rohm in 1914, which was isolated from animals and used

in the detergents for the degradation of protein. The *Bacillus* protease was first commercialized in 1959 for detergent manufacturing. The starch industry has utilized alpha amylases and glucoamylases for the starch hydrolysis since they have provided 95 % yield to glucose.

The technical enzymes have been used in other industries like detergents, paper, textile, leather, fuel and pharmaceuticals. The introduction of enzymes on various industrial applications provided financial and ecological benefits as they are cost effective and environment friendly. Since the enzymatic reactions are carried out under mild reaction conditions, the processes can be easily controlled and the negative influences on environment are minimized. Because of the high specificity of enzymes, the reaction can be taken place with decrease of by-products and thereby reduced the waste disposal problems. The enzymes have certain affinity towards the substrate like complex molecules and they exhibited catalysis reactions with unique enantio and regio selectivities. These peculiarities are essential for myriad industrial applications such as food and pharmaceuticals where high reaction selectivities were required towards the complex substrates [3]. The isomerization of D-glucose leads to the formation of D-fructose by the catalytic reaction of xylose isomerase which included the selective catalysis [4]. The chemical industry also necessitated the selective catalysis of enzyme for the synthesis of polymers and chemical materials [5]. The phenolic resins were synthesized by the catalysis of peroxidases and the hydration of acrylonitrile to acrylamide was catalyzed by nitrile hydratase [6, 7]. This high selectivity of enzyme catalysis imparted effective reactions with little by-products and thus making this type of catalysis more advantageous than standard chemical catalysis. The biocatalysts such as hydrolases, oxidases, reductases and transferases are mainly used for the synthesis of organic compounds [8, 9]. The important

enzymes applied in the textile industry are cellulases, α-amylases, lipases, pectate lyases, laccases and peroxidases [10]. The principal hydrolases like proteases, amylases, cellulases and lipases are widely employed in detergent industry from *Bacillus subtilis* species and recently *psychrophilic* enzymes are arrived in this field which can operate at low temperature and impart economic and environmental benefits by attaining energy savings [11, 12]. The role of proteases in leather industry was widely reported which involved in skin processing, protein removal from collagen and also in replacing the toxic chemicals [13]. In paper industry, the important enzymes used are lipases, laccases, cellulases and xylanases [14]. Cellulases and hemicellulases have achieved increased attention in the production of biofuels which involved in the conversion of lignocelluloses [15, 16].

Although the use of enzymes in industrial applications was getting more attention, their isolation from the solution has become very inconvenient since they are used in soluble forms. The stability of the enzymes have also been faced major challenges in their industrial usages as they could not much tolerated in the biochemical reaction conditions. These facts have caused their recovery from the reaction systems to become very difficult. The various enzyme immobilization techniques could diminish these problems as immobilization can remarkably augment the enzyme stability. The insolubility of the immobilized forms can also make their recovery easy. The immobilized enzymes on nanomaterials can impart effective industrial bioprocesses and leads to the development of selective biosensors [17-19].

1.1.1 Enzymes, The green catalysts

Enzymes are macromolecular biological catalysts that accelerate the biochemical reaction rate in living organisms and also catalyze wide variety of chemical reactions by lowering the activation energy without affecting

the reaction products [20]. The enzymes are treated as green catalysts since they are involved in organic chemical transformation and acquired reduced energy cost as well as increased safety. Commonly they are biodegradable in nature and the products formed as a result of biocatalytic reaction can be easily purified due to the decreased waste products. They exhibit enhanced catalytic efficiency and reaction specificity even at mild conditions of pH and temperature with the same reaction rates as that attained by chemical catalysts. Enzymes are proteinaceous in nature and formed by the linkage of amino acid chains through peptide bonds. Their catalytic function depends on the structure of protein and the activity relates to the structural integrity of the protein conformation. The catalytic reaction takes place only at the active site of the enzyme and makes it specific for single reaction [21, 22].

1.1.2 Chemical nature of enzyme

Enzymes are high molecular weight compounds that ranging from 10,000 to 20,00,000 and are composed by the joining of amino acid chains together via peptide bonds.

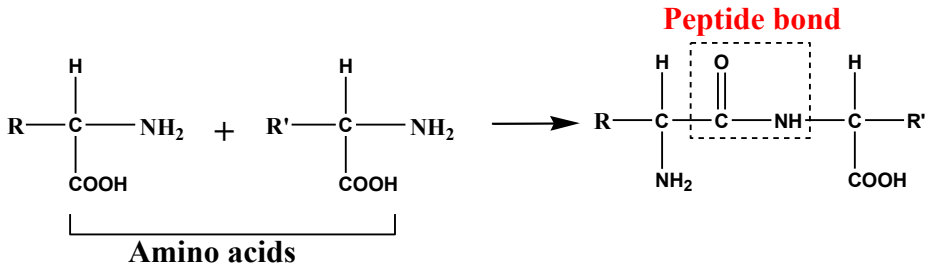

Figure 1.1 General protein structure- Joining of two amino acids through a peptide bond

The enzymes can be precipitated and denatured by solvents, salts and certain reagents. They exhibit catalytic activity in the presence of other compounds such as cofactors.

The cofactor can be comprised of,

Coenzyme - This stands for a non-protein organic substance that weakly attached to the protein part.

Prosthetic group - This can be an organic substance that strongly attached to the protein part.

Metal ion activator - This consist of Fe^{2+}, Fe^{3+}, Cu^{2+}, Zn^{2+}, Mn^{2+}, Ca^{2+}, Mg^{2+}, Mo^{3+}, Co^{2+} and K^{+}

The protein part of the enzyme is referred to as apoenzyme and the entire active complex can be represented as apoenzyme plus cofactor which is mentioned as holoenzyme.

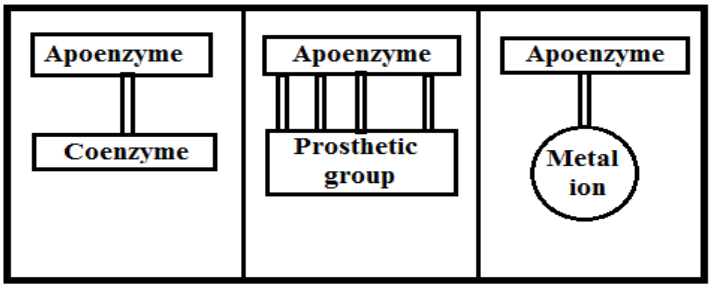

Figure 1.2 Representation of holoenzyme

1.1.3 Structure of enzyme

The enzymes that based on the linkages of amino acid chains are globular proteins in which one or more polypeptide chains are folded to obtain three dimensional structures with definite conformational characteristic to the enzyme. This structure incorporates with small area at which the substrate actually binds with it, known as active site. This active site may consist of about less than 10 of constituent units of amino acids. Enzyme structure can be classified in to four levels depending on the arrangement of amino acids.

1.1.3.1 Primary structure

The sequence of amino acids of the peptide chains is the primary structure of enzyme. In this structure the amino acid chains are linked through –CO–NH– bonds; amino group ($–NH_2$) of one amino acid linked with carboxyl group (–COOH) of another by the liberation of water molecules.

1.1.3.2 Secondary structure

The secondary structure of enzyme arises as a result of interaction of amino acids in the same chain at which they are closely situated. Secondary structures are of two types,

- **α- helix**

  It is a helical structure coiled around an axis and is right handed in nature. Here the intermolecular H-bonds held within the same strand that exist between C=O and N–H groups of each peptide bonds.

- **β-pleated sheet**

  In this structure intermolecular H-bonding exists between two or more strands. The C=O group of peptide bond in one strand may hydrogen bonds with N–H group of peptide bond in another strand.

1.1.3.3 Tertiary structure

The tertiary structure can attain by the array of amino acid chains in the three dimensional space. Here the arrangement is such that in order to achieve low energy and hence maximum stability. The various interactive forces involved in this case are H-bonds, hydrophobic interaction, ionic interaction, polar-polar interaction, van der Waals interaction and disulfide bonds. The hydrophobic interactions are commonly generated from the alkyl groups of alanine, leucine, isoleucine and valine. The protein surface exhibit hydrophilic nature due to the presence of acidic or basic amino acid

chains and the disulfide linkages provide maximum stability to the tertiary structure through covalent binding on different parts of protein chain. The positive and negative charged sites on amino acid chains allow ionic interactive forces which also stabilize the tertiary structure.

1.1.3.4 Quaternary structure

In quaternary structure, the interactive forces exist between more than one peptide chains and the various interactions that stabilizing the overall complex are H-bonding, disulfide bridges and salt bridges. This structure describes the interactions of different protein subunits and their arrangement to form larger protein aggregates.

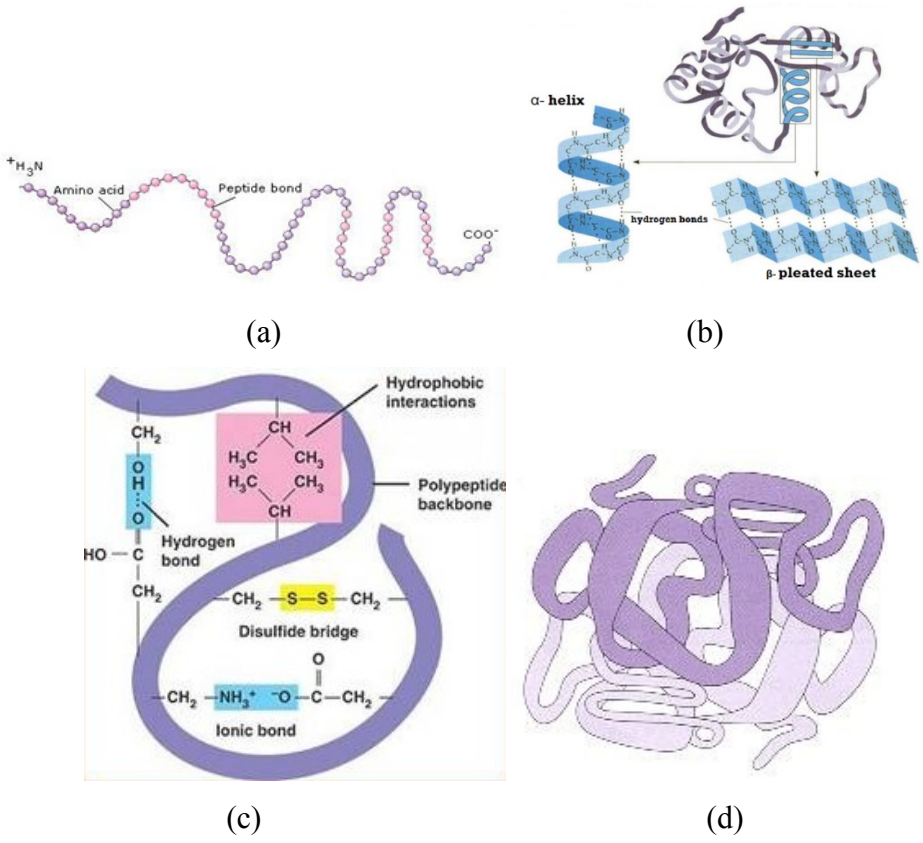

(a) (b)

(c) (d)

Figure 1.3 Structure of protein (a) primary structure (b) secondary structure (c) tertiary structure and (d) quaternary structure

1.1.4 Types of enzymes

The enzymes are classified into six major types on the basis of catalytic reaction and these were approved by the nomenclature committee of the International Union of Biochemistry and Molecular Biology (IUBMB). An important numerical classification stratagem for enzymes is the Enzyme Commission Number (EC number), which do not describe about the enzyme, but specify the enzyme catalyzed reaction. The same EC number can be attained by different enzymes for the same catalyzed reaction. This represented as code number which consist of four constituent elements prefixed by EC and are separated by points. The first element assign to enzyme class; the second and third represent the general and specific groups to which the enzyme acts respectively. The fourth element denotes the specific substrate at which the enzyme acts.

The six types of enzymes are,

Oxidoreductases : Catalyze different oxidation-reduction reactions at which the electron transfer occurs. The common names used are dehydrogenase, reductase and oxidase.

Transferases : Catalyze the transfer of groups such as acetyl, methyl and phosphate. The common names used to represent are acetyl transferase, protein kinase, methylase and polymerase.

Hydrolases : Catalyze the hydrolysis reaction which includes the transfer of functional groups to water and so can be grouped under transferases.

Lyases : Catalyze the reactions which involve the cleavage of C–C, C–O, C–N and C–S bonds. Here the addition of functional groups caused to cleave the double bonds or the elimination of functional groups leads to the formation of double bonds. This type has the common names such as aldolase and decarboxylase.

Isomerases : These catalyze the reactions in which the atomic rearrangements are taken place within a molecule. This results in the formation of isomers due to the transfer of functional groups. An intramolecular oxidoreduction may also be related with this type enzyme.

Ligases : This type of enzyme catalyzes the reaction where the two substrates taken are ligated and the reaction involves the joining of two molecules. These include DNA ligase, RNA ligase and peptide synthase.

1.1.5 Activity of enzyme

Enzyme activity is a measure of the capacity of an enzyme to catalyze a specific reaction. This catalytic effect can be expressed as units per mg of enzyme (specific activity) or in terms of substrate molecules transformed per minute per enzyme molecule (molecular activity). This can be measured either on the basis of decrease of substrate concentration during the time period or increase of product concentration after the time period. Since most of the enzymes are proteins, the factors that distort the protein structure such as temperature and pH can affect the activity of enzyme. The factors that affect the catalysts such as reactant (substrate)

concentration and catalyst (enzyme) concentration are also control the enzyme activity.

The enzymes are highly sensitive to thermal changes due to its protein nature and they show activity within a limited temperature ranges. Each enzyme has exhibited maximum activity at certain temperature, called optimum temperature and over this temperature the enzyme activity decreased to lower values due to the conformational changes in the enzyme structure. At extreme high temperatures, the enzyme lost it activity completely and become denatured. All enzymes are proteinaceous in nature and consist of acidic group such as –COOH and basic group such as $–NH_2$. These groups provide certain charges to the enzyme structure and are affected by the changes of pH value. Every enzyme shows maximum activity at a particular pH called optimum pH and at above and below this optimum value the enzyme activity decreases until it loses its complete activity. The enzymes tend to denature at the most extreme pH values due to the unfavorable charge distribution on the enzyme structure. The concentrations of enzyme and substrate that are involved in the enzymatic reaction affect the activity of enzyme. As the enzyme concentration increases, the activity of enzyme also tends to increases with respect to the availability of substrate molecules. After all the substrate molecules are bound with the enzyme active site, the further reaction rate decreases even the concentration of enzyme increases and this could be due to the lack of substrate molecules for the catalytic reaction. The substrate concentration also affects the rate reaction and the rate of the reaction increases to a particular point as the substrate concentration increases. Once all the active sites of enzymes are saturated with the substrate molecules, there is no further increase in reaction rate even the substrate concentration increased to

higher region and this could be due to the unavailability of enzyme active site in order to bind with the substrate molecules. The effect of activators takes an important role in maintaining the activity of enzyme. The cations like Zn^{2+}, Mg^{2+}, Ca^{2+}, Mn^{2+}, Cu^{2+}, Co^{2+}, Na^{+}, K^{+} etc and anions like Cl^{-} facilitate the enzyme to acquire optimum activity.

1.1.6 Specificity of enzyme

All enzymatic reactions are very specific and this specificity depends on the shape of active site of the enzyme as well as that of substrate. The arrangement of atoms in the active site of enzyme determines the specificity of enzyme binding. The active site of the enzyme consists of amino acid residues, called the catalytic groups which directly involved in the enzymatic reaction via transition state formation. The enzyme specificity towards a chemical reaction is influenced by the orientation of active site on the basis of atomic configuration. Enzymes have shown different types of specificity.

(i) Absolute specificity: Enzyme specific to one substrate and catalyze only one reaction.

eg: maltase only acts on maltose, sucrase only acts on sucrose.

(ii) Group specificity: The enzyme exhibit specificity towards structure as well as chemical groups. They catalyze same type of reaction for similar substrates and act on specific functional groups such as methyl, amino and phosphate groups.

eg: hexokinases transfer phosphates to hexoses.

(iii) Linkage specificity: The enzyme specific to substrates with similar structures and similar bonds. They catalyze on particular chemical bond and this property of enzyme is also known as bond specificity.

eg: Amylase hydrolyze α-1,4-glycosidic linkages of starch and glycogen, lipase hydrolyze ester bond between glycerol and fatty acid.

(iv) Stereochemical specificity: In this case the enzyme is specific to substrate and also to stereo or optical configuration.

eg: L-amino acid oxidase only acts on L-amino acid, starch can be digested with α-glycosidase but cellulose required β-glycosidase.

(v) Dual specificity: Here the enzyme exhibited same type of reaction for the two substrates and also acts on same substrate with two types of reactions.

eg: Xanthine oxidase acts on hypoxanthine and xanthine for the same type of reaction such as oxidation, iso-citrate dehydrogenase used for two types of reactions such as oxidation and decarboxylation.

1.1.7 Enzyme action

Like all chemical catalysts, enzymes also enhance the reaction rates without undergoing any chemical modifications. The enzymatic catalysis occurs commonly in the restricted temperature range and the enzyme exhibit appreciable activity at optimal pH range. The three dimensional structure of enzyme takes an important role in determining the effectiveness of enzyme catalysis. The changes in temperature and pH may cause the reduction in the conformational integrity of the enzyme structure which in turn leads to the loss of enzyme activity and denaturation of enzyme.

During the enzymatic catalysis, the substrate molecules are attracted towards the active site of the enzyme and their combination leads to the formation of enzyme-substrate complex. The chemical bonds are not involved in this complex formation, but associated with the electrostatic and

hydrophobic forces. After the formation of enzyme-substrate complex, the enzyme facilitates the catalytic reaction in which the products formed are liberated from the surface of enzyme.

The interactions between enzyme-substrate complexes are described by several theories. The lock and key model, proposed by Emil Fischer in 1890 explain the binding between the enzyme and substrate molecules. Here the shape of the enzyme's active site is such that which is complementary to that of shape of substrate and so the substrate can fit into the active site of enzyme just like a key into a lock. Then the enzyme catalyzes a specific chemical reaction, release the products formed and become free for further reaction [23]. Koshland put forward another theory, induced fit model in order to describe the specificity of enzyme. Based on this theory, when substrate attracted towards the enzyme, it induces certain conformational changes in the active site of the enzyme. As a result of this the amino acid residues at the active site of the enzyme acquired favorable alignment in order to promote catalytic reaction. Hence the interaction between the flexible enzyme active site and substrate leads to the formation of E-S complex. As the enzyme molecule is not stable at this active conformation, it tends to return to its original form after the formation of products. This theory explains the role of substrate in determining the occurrence of catalytic reaction. As the enzyme structure is flexible, the substrate controls its ultimate shape. If the enzyme structure is too distorted, the substrate molecules cannot bind with the active site of the enzyme and this hinders the catalytic reaction. Also the substrate molecules with very small size cannot induce suitable alignment to the enzyme active site and this also prevents the enzymatic reaction [24]. The occurrence of enzymatic reaction is also explained by the transition state theory. This theory described that in

transition state the enzyme bind more strongly with the substrate than that in the ground state. At the transition state the enzyme acquire decreased activation energy as it distort the shape of active site and hence required less energy in order to break the bond at the beginning of the reaction. The enzyme thus stabilizes the transition state by lowering its activation energy. The reaction rate is proportional to the amount of reactants presented in the transition state complex. Linus pauling explained the catalytic action of enzyme due to the tight binding in the transition state species. Wolfenden and coworkers rationalized that the rate of the enzymatic reaction is proportional to the affinity of the enzyme for the development of transition state species [25].

1.1.8 Enzyme kinetics

This reveals the rate of enzyme catalyzed reactions and correlates the effect of different experimental conditions on reaction rate. The kinetic studies provide the basic mechanism for the enzymatic reaction and the other parameters that distinguish the properties of the enzyme. Brown developed the complex formation of enzyme with its substrate and then the complex split in to the products by regenerating the enzyme. The mechanism of enzyme-substrate reaction can be demonstrated as

$$E + S \underset{K_{-1}}{\overset{K_1}{\rightleftharpoons}} ES \qquad (1.1)$$

$$ES \xrightarrow{K_2} P + E \qquad (1.2)$$

The kinetics of single substrate-enzyme catalyzed reaction commonly referred to as Michaelis-Menten model of enzyme kinetics or saturation kinetics. This model describe the rate of enzymatic reaction

which relate the reaction rate or rate of product formation to the substrate concentration and the formula is represented as,

$$v = \frac{d[P]}{dt} = \frac{V_{\max}[S]}{K_m + [S]} \qquad (1.3)$$

This is the Michaelis-Menten equation, where V_{max} is the maximum rate attained by the enzyme system at saturate substrate concentration and K_m represents the substrate concentration at which the rate of reaction reach half of V_{max}. The K_m measures the affinity of enzyme towards the substrate molecules and higher the K_m value gives the lower affinity of enzyme for substrate and vice versa. This value gives the binding capacity of substrate molecules in to the enzyme active site. The catalytic reaction with lower K_m value reveals tight binding of substrate to the enzyme active site and the higher value corresponds to its loose binding. K_m value also determines the substrate concentration when the rate of the reaction is half of V_{max}.

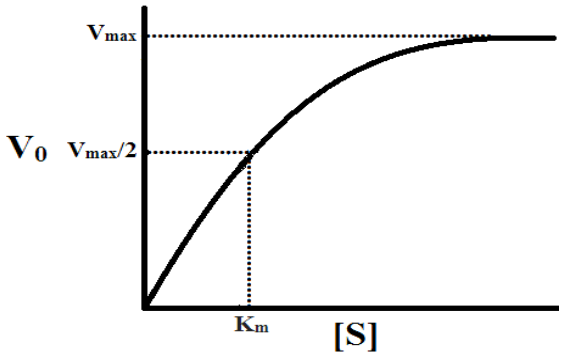

Figure 1.4 Graphical representation of determination of kinetic parameters

At low substrate concentration the reaction rate changes linearly and follows the first order kinetics. Hence,

$$V = K_{cat}[E]_0 \frac{[S]}{K_m} \qquad (1.4)$$

At higher substrate concentration the reaction rate follows zero order and reaches the maximum rate,

$$V_{\max} = K_{cat}[E]_0 \qquad (1.5)$$

Where $[E]_0$ represents the initial concentration of enzyme and K_{cat} is the turn over number.

The increase of substrate concentration provides the increase of reaction rate at which the enzyme and substrate molecules encounter to each other. At high substrate concentrations, the enzyme active sites are almost fully occupied by the substrate molecules, leads to the saturation state and the reaction rate tends to increase to maximum range. As the K_m reveals the information on enzyme affinity, the V_{max} value provides the measurement of catalytic efficiency of enzyme towards the substrate. The K_{cat} value of an enzymatic reaction represents the maximum number of substrate molecules that converted into product at the active site of a single enzyme molecule per unit time. The enzyme with higher K_{cat} value indicates that it involved in the rapid catalytic reaction. The term K_{cat}/K_m gives the catalytic efficiency which measures the effectiveness of enzyme. This is frequently referred to as specificity constant, which compare the rates of enzyme action on competing and alternating substrates. The K_{cat}/K_m values for the two enzymes or for the same enzyme towards different substrates can be compared in order to measure the enzyme effectiveness. The higher ranges for catalytic efficiency lies between 10^8 and 10^9 $S^{-1}M^{-1}$ and the enzymes having these ranges considered to be gained kinetic perfection and dependent only on the concentration of substrate.

By using Michaelis Menten Kinetic equation, the kinetic parameters K_m and V_{max} can be determined from different plots such as Lineweaver-Burk plot, Hanes-Woolf plot and Eadie-Hofstee plot.

The reciprocal of Michaelis Menten equation gives the straight line equation relating $1/V_0$ and 1/[S], which is Lineweaver-Burk plot. This plot used to determine the kinetic parameters precisely and also help for the analysis of inhibited and multi substrate enzymatic reactions.

$$\frac{1}{V_0} = \frac{K_m}{V_{\max}} \frac{1}{[S]} + \frac{1}{V_{\max}} \qquad (1.6)$$

Here K_m/V_{max} and $1/V_{max}$ stand for slope and intercept of the straight line respectively.

Another graphical representation of enzyme kinetics is the Hanes-Woolf plot which is the straight line rearrangement of Michaelis Menten equation. Here the proportion of initial concentration of substrate to reaction velocity, [S]/V was plotted against [S]. This plot used for the determination of kinetic parameters, but it is replaced by non-linear regression methods. At higher range substrate concentrations, the errors in [S]/V impart which is close agreement with that of errors in V and this make it remains very useful. One of the drawbacks of this approach is that in which both ordinate and abscissa do not represent the independent variables, but they are dependent on the concentration of substrate.

$$\frac{[S]}{V} = \frac{[S]}{V_{\max}} + \frac{K_m}{V_{\max}} \qquad (1.7)$$

The plot of [S]/V against [S] yield a straight line with slope of $1/V_{max}$ and intercept of K_m/V_{max}.

Eadie-Hofstee plot is the representation for enzyme kinetics which is obtained from another linearized Michaelis Menten equation. Here the rate of reaction is plotted against the ratio between rate and concentration of

substrate. This approach is superseded by non-linear regression method and is stronger against error susceptible data than Lineweaver-Burk plot. Like Hanes-Woolf plot, this approach also does not constitute with the independent ordinate and abscissa and both are rate dependent.

$$V_0 = V_{\max} - \frac{V_0 K_m}{[S]} \qquad (1.8)$$

The plot of V_0 against $V_0/[S]$ give a straight line with negative slope of $-K_m$ and positive intercept of V_{max}.

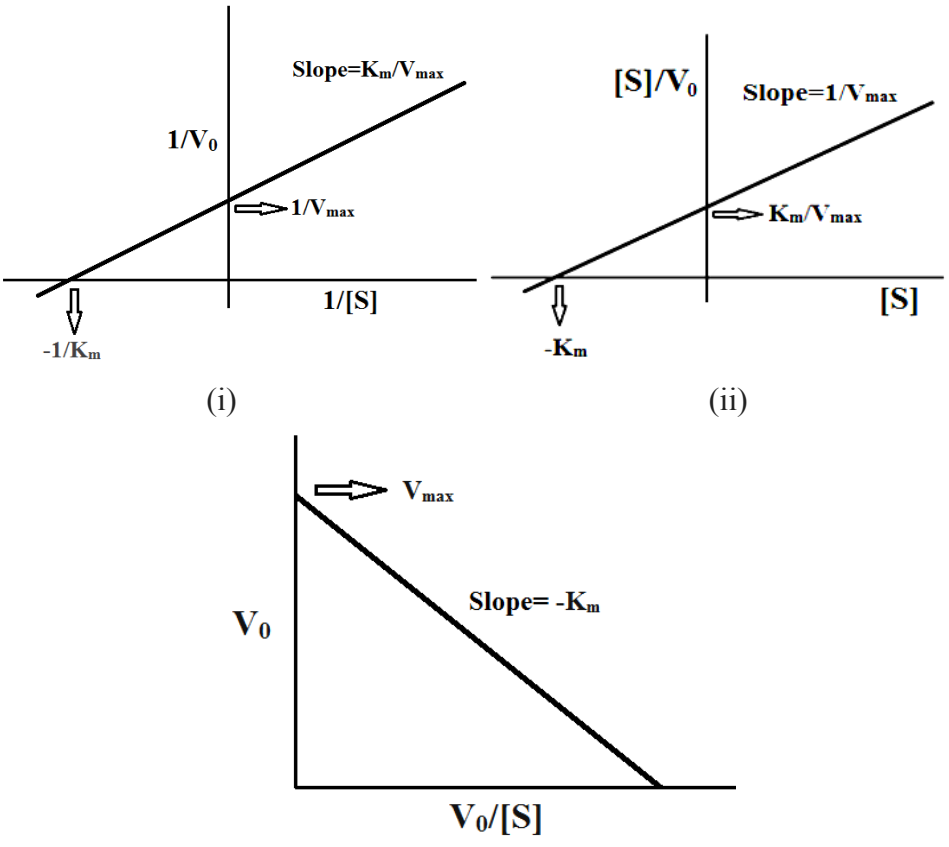

Figure 1.5 Linear representations of Michaelis Menten equation (i) Lineweaver-Burk plot (ii) Hanes-Woolf plot and (iii) Eadie-Hofstee plot.

1.2 Immobilization of enzyme

The concept of immobilization of enzyme has been established about for over hundred years. Immobilized enzyme is an enzyme system which can be used continuously and repeatedly by maintaining its catalytic activity since the enzyme is physically attached to inert and insoluble solid material. The use of immobilized enzymes has gained much attention in the field of medical and industrial sectors. The enzymes in its immobilized state provide easy separation of products, reusability, appropriate handling and higher physical and chemical stability. The immobilized enzymes with these properties make their application more economically viable, supply effort less process control, suitable for different types of reactors and also for industrial processes [26, 27]. They have also greatly influenced in the technical performances of industrial processes and thus improved the productivity and economic efficiency. Chibata and coworkers reported the first industrial use of immobilized enzyme in 1966 by the development of immobilized Aspergillus oryzae aminoacylase for the resolution of synthetic D-L amino acids [28]. The immobilized enzymes have been utilized for industrial applications such as production of amino acids, pharmaceuticals and sugars [29]. They require enhanced selectivity and specificity towards the catalytic reaction for the long term reuse in industrial processes.

All immobilized enzymes consist of two important functions; non-catalytic functions and catalytic functions. The former assist the enzyme separation from the reaction mixture and promote the reuse capability of immobilized enzyme. The later provide the chances to convert substrate molecules into products during the time period. The non-catalytic function correlate with the physical properties of immobilized enzymes, while the catalytic function associated with the biological activities of enzymes like

activity, substrate specificity etc. Hence the immobilized enzyme system should be developed with optimum non catalytic function and high catalytic function in order to confirm reuse and purification of enzyme. The catalytic function depends on the catalytic reaction and the substrate involved in it, which leads to the product formation with reduced side reactions. While the non-catalytic functions depends on the reaction medium and also on the method of product purification. Hence the carrier and immobilization method are well chosen based on the industrial requirements.

However, the immobilization may cause the loss of enzyme activity due to the denaturation of its three dimensional structure. The multiple interactions of the enzyme with carrier can cause some distortions in its structure that leads to the secondary structural changes in enzyme. Thus the protein lost its α-helical structure, but gained β-sheet structure and so it showed some alterations in its catalytic properties [30-33].

1.2.1 Properties of immobilized enzyme

The properties of immobilized enzymes depend on the nature of carrier to which the enzyme attached and also on the binding forces between them. The interactions of enzyme on carrier make certain changes in the three dimensional conformation of the protein structure and cause some alterations in the properties of immobilized enzyme with respect to its catalytic activity. The immobilization can increase the operational stability of the enzyme since it causes the controlled diffusional limitations. The stability also increased as a result of multiple interactions between the enzyme and carrier since this provides more rigidity to the enzyme structure.

The stability of the immobilized enzyme depends on the pH and temperature of the reaction medium. For immobilized enzyme, the enzyme-

substrate reaction at the microenvironment is different from that taken place in the bulk solution environment due to the unfavorable charge distributions and this leads to the conformational changes in the three dimensional structure of enzyme and thus causes changes in immobilized enzyme properties. The immobilization provides more rigidity to the enzyme structure and protects it from temperature effects and thus attains enhanced heat resistance towards the thermal denaturation of enzyme structure.

The immobilized enzyme exhibit reduced enzyme activity when compared to free enzyme as the system cannot access the substrate molecules during the catalytic reaction since the distortions in the active site of the enzyme arise due to the enzyme immobilization [34, 35]. The stability and kinetic properties of the enzyme may vary due to the modifications in the microenvironment of the enzyme as a result of immobilization. This may be due to the changes in the intrinsic activity of the immobilized enzyme. During the enzymatic reaction, the immobilized enzyme interacts with the substrate in a different manner at its microenvironment compared to that at bulk solution. When the immobilized enzyme acts on macromolecular substrate, there exists a limited accessibility of substrate to the active site of the enzyme. Only the surface groups on substrate are accessible for the catalytic action and this impart reduced immobilized enzyme activity. The steric hindrance of large substrate molecules with the active site of the enzyme can also obstruct the enzymatic reaction. Thus the stability of immobilized enzyme plays an important role for maintaining its catalytic activity. There are several studies are reported in which the immobilized enzyme attained more stability due to the multipoint covalent attachment between the enzyme and the carrier [36]. Different methods are developed that correlate the number of covalent bonds between enzyme and carrier with the stabilization of immobilized enzyme system [37, 38].

1.2.2 Immobilization methods

The functional groups present on the enzyme and carrier and the bonds involved between them decide the type of immobilization methods. The methods used for the industrial applications should be simple, easy handling and cost effective. The nature of enzyme-carrier binding determines the stability of the immobilized enzyme and the conformational integrity of the active site of the immobilized enzyme and hence influences its catalytic activity.

1.2.2.1 Adsorption

This is the simple immobilization method in which the enzyme bound with the carrier through the weak interactive forces such as van der Waals forces, hydrophobic interactions and hydrogen bonding etc. Here the immobilization is taken place directly with the carrier and does not require any pre-activation. The high enzyme adsorption is possible with the carrier having high surface area. The carriers with porous structure exhibit high surface area due to the availability of inner core of the material and can be showed enhanced enzyme loading. Since the enzyme interactions with the carrier are very weak, it does not alter the native conformation of the enzyme active site and so the enzyme maintains its activity. However, even the small changes in pH and temperature of reaction medium can simply detach the adsorbed enzymes [39]. This makes reduction in their catalytic activities and diminishes their usage in industrial sectors.

This type of immobilization technique is widely used in chemical and pharmaceutical industries and has been extensively employed for the production of enzymatic biosensors [40-42]. Even though this method provides simplicity and cost effectiveness, it results in materials and time

consuming for their practical applications. The further non-specific adsorption of enzyme may affect the properties of immobilized enzyme since the reaction rate depends on the mobility of enzyme and substrate molecules. The multilayer adsorption does not impart any homogeneity to the bound enzyme onto the carrier surface which prevents the substrate affinity towards the active site of the enzyme and reduces the catalytic activity. The adsorption via electrostatic binding of enzyme with the support depends on pH of reaction medium and isoelectric point of enzyme and carrier. The enzyme surfaces bear positively or negatively charged species depending on the pH of the medium and can interact with the oppositely charged carrier surface though ionic and polar interactions [43].

1.2.2.2 Entrapment

Here the enzyme entrapped within a polymer or gel matrix which is a permeable membrane that allow the passage of substrate and product molecules but not that of enzyme molecules. There is no chemical interaction between the enzyme and entrapping polymer, but this type of immobilization method restricts the enzyme diffusion and thus furnishes enhanced enzyme stability due to the reduction in enzyme leaching and denaturation. The main drawback of this method is the limitations in mass transfer. When the thickness of the polymer matrix is increased as a result of extensive polymerization, the substrate molecules cannot pass into the permeable matrix in order to react with the active site of the enzyme and this decreases the catalytic activity. The low enzyme loading by this method may be due to the leaching of entrapped enzymes through the large pore sized polymer matrix. The conformational distortions of enzyme structure cannot be taken place since there are no strong binding forces between the

enzyme and carrier. However the changes in pH and temperature may leads to certain enzyme deactivation.

1.2.2.3 Covalent attachment

The enzyme directly attached to the reactive functional groups of carrier such as hydroxyl, carboxyl, amino and amido groups through covalent bonds or by a spacer arm through the reactions like diazotization, Schiff base and imine bond formation [44]. The covalent immobilization leads to the formation of stable immobilized enzyme system that prevents the enzyme leaching and also provides high rigidity to the enzyme structure. The changes in structural conformation as a result of this immobilization results in the deformation of active site of the enzyme which tend to hinder the catalytic reaction and hence cause the loss of enzyme activity. The important amino acid residues of enzyme structure that involved in the covalent immobilization are cysteine, serine and threonine [45, 46]. The non-essential amino acids involved in this method causes lesser conformational changes and provides higher resistance towards heat and denaturants.

In case of inert carriers, they require pre-activation before involved in the covalent binding of enzyme. The covalent attachment through spacer arm provides increased mobility to the enzyme and so the enzyme retains its flexible conformation in order to retain the high catalytic activity. Carbodiimide performs as activating agent for carboxyl functional groups of carrier in order to bind with amino groups of enzyme. The N-hydroxy succinamide incorporated with carbodiimide also used for covalent immobilization to get improved immobilization efficiency. The amino groups of carrier can also be activated with carbodiimide for the covalent binding of enzyme through carboxyl functional groups. Another activating agent,

gluteraldehyde undergo Schiff base reaction in which each aldehyde group react with amino groups of carrier and enzyme through covalent binding.

1.2.2.4 Cross-linking

This is the irreversible method in which enzyme molecules are cross-linked with each other through bi- or multi functional reagents via covalent binding. The commonly used cross-linking agents are gluteraldehyde, glyoxal, hexamethylene diisocyanate, diazobenzidine etc. The amino acid residues such as lysine, cysteine, tyrosine, histidine are used for enzyme cross-linking under mild reaction conditions. Here the cross-linking agents generate bridges between the enzyme molecules just like back bone to carry the enzyme molecules. The enzyme leaching can be reduced much by this method due to the strong chemical bonds between the enzyme molecules. The main disadvantage of this method is the enzyme denaturation by poly functional cross-linking agents.

1.2.3 Selection of enzyme carrier

Selecting a carrier material is one of the crucial steps in enzyme immobilization process since it is not easy to predict which will be the suitable carrier for a specific enzyme. The essential conditions needed for the material in order to meet the characteristic properties of an enzyme carrier are their insolubility in water, chemical and mechanical stability, high binding capacity towards the enzyme, easy availability and low cost. The physical properties of the materials like mechanical strength, particle size and swelling and compression behavior determine the efficiency of immobilized enzyme and the kind of reactor required to use.

The surface area of the materials and the functional groups presented on them play an important role in determining their enzyme binding capacity

and hydrophilic property decide the activity of immobilized enzyme. The activity also controlled by the mass transfer and diffusional properties of the system. The porous materials offer high enzyme loading due to their high surface area and create more protected environment for the immobilized enzyme. For these types of materials the adsorption capacity can be optimized since they have exhibited controlled pore distribution. The nanomaterials due to their high surface area exhibit mass transfer resistance and improved enzyme loading and thus act as an effective enzyme carrier [47, 48].

The carriers can be conveniently classified as inorganic materials, hydrophilic biopolymers and lipophilic synthetic organic polymers. The inorganic materials are suitable because of their favorable adsorption capacity, high chemical and mechanical stability. Also their hydrophilic nature due to the presence of surface hydroxyl groups provide enhanced immobilization capacity due to the stable enzyme-carrier interactions.

The biocompatibility, biodegradability, non-toxicity and enzyme affinity make the biopolymers as ideal enzyme carriers. The immobilized enzymes on biopolymers retain enhanced catalytic activity since their biocompatible nature reduces the negative effects of structure and properties of enzyme. The plenty of functional groups present on them facilitate direct interaction with enzyme and also promote their surface modification. This makes their excessive use in adsorption and covalent enzyme immobilization. But their gel formation ability and the susceptibility to generate different geometrical configuration also lead them towards the enzyme immobilizations by entrapment and encapsulation.

The synthetic polymers serve as the effective enzyme carriers since the polymer layer protects the active site of the enzyme from the negative

effects of experimental conditions and the reagents used. Here the monomers can be selected based on the demand of enzyme since the properties and chemical structure of the polymer depend on the nature and amount of monomers used [49]. The stability, porous behavior and mechanical strength of the polymer depend on the selected monomers. The functional groups present on the polymers control its effectiveness for enzyme binding as well as its surface modification and thus determine the method of immobilization [50]. The different polymer materials used as the enzyme carrier can improve the thermal stability, storage stability and reusability of the immobilized enzyme. The length of the spacer arms used in case of polymeric carrier for enzyme immobilization should be controlled as the shorter ones decrease the enzyme leaching and enhance the thermal stability and the longer ones provide conformational flexibility to the immobilized enzyme [51].

1.3 Chitosan as carrier for enzyme immobilization

Chitosan is a biodegradable and biocompatible poly saccharide, poly [β-(1-4)-linked-2-amino-2-deoxy-D-glucose, the deacetylated form of chitin which exists in exoskeletons of insects and crustaceans. The various forms of chitosan like films, gels, powders, sponges and micro, macro and nano particles can be produced by controlling the molecular weight and deacetylation degree of chitosan [52, 53]. Chitosan has gained more attention in various applications due to its distinctive physico-chemical and biological properties [54]. It has become an ideal enzyme carrier due to its properties such as biodegradability, biocompatibility, hydrophilicity and high protein affinity. It is widely used for enzyme immobilization since they are non-toxic, inert, and inexpensive and has high mechanical strength [55, 56]. The natural origin and biocompatibility reduces its negative impact on

the structure and properties of enzyme and promote the immobilized enzyme to retain high catalytic activities. The presence of reactive functional groups such as hydroxyl and amino groups allow direct interaction with the enzyme and enable its surface modification under mild experimental conditions by hindering the hydrolysis of glycosidic linkages. The presence of amino and hydroxyl groups and the polycationic nature of chitosan make it suitable for effective enzyme immobilization. Since the pKa of chitosan is about 6.5, at lower pH (<pKa) most of the amino groups are protonated and at higher pH (>pKa) the amino groups are deprotonated. The immobilization of enzyme on chitosan depends on the isoelectric point of enzyme and the pKa of chitosan which determines the strength of electrostatic interaction between them.

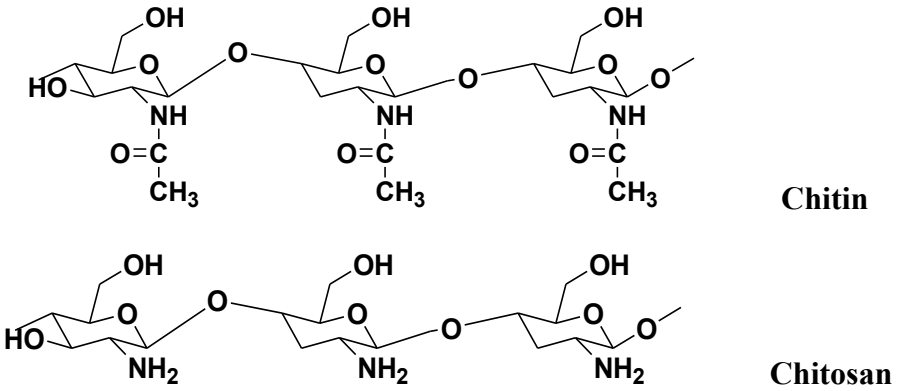

Figure 1.6 Structure of chitin and chitosan

The chitosan with different particle sizes were used as enzyme carriers and the chitosan nanoparticles attain higher enzyme binding due to its increased surface area. The enzyme immobilized on chitosan nanoparticles exhibited higher efficiency than that on chitosan microparticles [57, 58]. The particle size determines the enzyme binding sites and the reaction sites for substrate molecules. Also the chitosan

nanoparticles with increased diffusion and mobility can influence the catalytic activity of immobilized enzyme.

The porous nature of chitosan has great influence on immobilization of enzyme and if the chitosan material is highly porous, the pore size and pore size distribution determine the immobilized enzyme properties. The structure with small pore size leads to the diffusion limitation which can cause the rearrangement of enzyme structure and this conformational change of enzyme structure results in loss of its activity. Chitosan with very large pore sizes can cause the enzyme aggregation which also leads to the loss of immobilized enzyme activity. Hence for porous chitosan, the pores should be optimized in order to achieve maximum immobilized enzyme activity.

The chitosan with free amino and hydroxyl groups has great tendency for cross-linking and its cationic nature promote the ionic cross-linking with multivalent anions. The enzyme can be covalently immobilized onto chitosan via cross-linking agents such as gluteraldehyde. One aldehyde group of gluteraldehyde form Schiff base with amino group of chitosan and the other end aldehyde group covalently bound with the amino group of enzyme. The chitosan with reactive amino and hydroxyl groups make them good enzyme carrier and can offer better immobilization efficiency. As chitosan is mucoadhesive in nature, the residual time at the adsorption site can be increased which leads to the enhancement in enzyme immobilization [53].

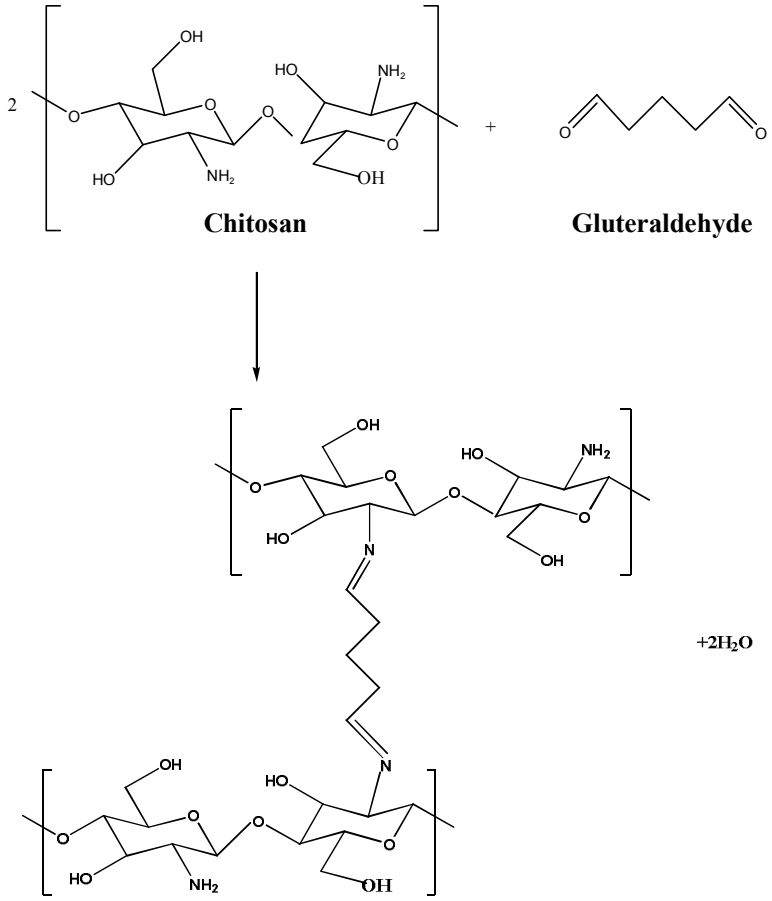

Figure 1.7 Cross-linking of chitosan with gluteraldehyde

The reactive functional groups of chitosan is used to stabilize the metal oxide particles since they aggregate in solution by dipole-dipole interaction and the chitosan-metal oxide composite can be used as efficient carrier due to its biocompatible and hydrophilic properties. The introduction of metal oxide provides enough rigidity to the chitosan matrix and the enzyme immobilized on this carrier can achieve enhanced thermal stability and reusability [59, 60]. The composites of chitosan with conducting polymers like polyaniline and polypyrrole can perform as good enzyme carrier due to the combined properties of better processability of chitosan

matrix and electrical conductivity of the polymer. The mechanical and thermal stability of synthetic polymers can be enhanced by incorporating with the chitosan biopolymer which can give improved stability to the enzyme upon immobilization. The combination of chitosan with other polymers makes it biocompatible and this provides more activity to the immobilized enzyme system by attaining specific microenvironment. The clay materials can offer enhanced thermal stability to the chitosan matrix due to its high insulation property by providing mass transfer barrier against the thermal decomposition of chitosan. The mechanical properties can be improved by the electrostatic interaction between amino and hydroxyl groups of chitosan and clay surface.

1.4 α-amylase for enzyme immobilization

α-amylase (1,4-α-D-glucan glucanohydrolase), an endo type enzyme that catalyze the hydrolysis of internal α-1,4-glycosidic linkages in carbohydrates yielding low molecular weight products such as glucose, maltose and maltotriose units with retention of α-anomeric configuration. They can be obtained from plants, microorganisms and animals. These are calcium metallo enzymes and require Ca^{2+} ions in order to acquire activity, stability and structural integrity. α-amylase is one of the most important industrial enzyme since its hydrolyzed products are widely implemented in food, pharmaceutical, textile, detergent and paper industries. In starch liquefaction process, the use of α-amylase promotes the starch hydrolysis which convert starch into glucose and fructose syrups. They are used for the production of modified starches in the paper industry, replacement of malt in the brewing industry, improvement in dough quality in baking industry, desizing in textile industry and also used as additives in detergents [61].

1.5 Scope and objectives of the current study

Immobilization of enzymes refers to the technique of anchoring the enzymes in or on an inert support for their stability and functional reuse. By employing this technique, the enzymes are made more efficient and cost-effective for their industrial purposes. The study is in accordance to maximize the advantages of α-amylase catalysis by using a carrier with low synthesis cost and high binding capacity.

The main objectives of the study are,

- ✓ To synthesize chitosan-metal oxide composites such as chitosan-Fe_3O_4, chitosan-TiO_2 and chitosan- ZnO.
- ✓ To modify the selected magnetic chitosan carrier by the cross-linking agents, gluteraldehyde, glyoxal and epichlorohydrin in order to compare efficiency and feasibility of enzyme immobilization methods.
- ✓ To synthesize the modified magnetic chitosan with synthetic polymers, inorganic layered solids and PAMAM dendrimers.
- ✓ To immobilize α-amylase on all modified forms of magnetic chitosan.
- ✓ To optimize the immobilization parameters and to estimate the immobilization efficiency in terms of immobilization yield and activity yield.
- ✓ To study the effect of reaction pH and temperature on immobilized α-amylase activity.
- ✓ To evaluate the activation energies for immobilized enzymes and to study their thermal stability.

- ✓ To study the storage stability and reusability of immobilized enzymes.
- ✓ To determine the kinetic parameters, turn over number and catalytic efficiency of immobilized enzyme systems.
- ✓ To estimate the kinetic and thermodynamic parameters for thermal deactivation of immobilized enzymes.
- ✓ To analyze the performance of α-amylase immobilized magnetic chitosan in laundry detergents and in desizing of cotton cloth.

References

[1] R.A. Sheldon, J.M. Woodley, Role of biocatalysis in sustainable chemistry, Chemical Reviews 118(2) (2018) 801-838.

[2] E. Fischer, Influence of the configuration on the effect of the enzymes, Europian Journal of Inorganic Chemistry 27(3) (1894) 2985-2993.

[3] A. Schmid, J. Dordick, B. Hauer, A. Kiener, M. Wubbolts, B. Witholt, Industrial biocatalysis today and tomorrow, Nature 409(6817) (2001) 258.

[4] V. Jensen, Industrial scale application of immobilized glucose isomerase, Methods Enzymology 136 (1989) 356-370.

[5] A. Schmid, F. Hollmann, J.B. Park, B. Buhler, The use of enzymes in the chemical industry in Europe, Current Opinion in Biotechnology 13(4) (2002) 359-366.

[6] T. Nagasawa, H. Yamada, Application of nitrite converting enzymes for the production of useful compounds, Pure and Applied Chemistry 62(7) (1990) 1441-1444.

[7] U. Hiroshi, K. Hideharu, K. Isao, K. Shiro, Synthesis of a new family of phenol resin by enzymatic oxidative polymerization, Chemistry Letters 23(3) (1994) 423-426.

[8] G.W. Huisman, S.J. Collier, On the development of new biocatalytic processes for practical pharmaceutical synthesis, Current Opinion in Chemical Biology 17(2) (2013) 284-292.

[9] B.M. Nestl, S.C. Hammer, B.A. Nebel, B. Hauer, New generation of biocatalysts for organic synthesis, Angewandte Chemie International Edition 53(12) (2014) 3070-3095.

[10] R. Araujo, M. Casal, A. Cavaco-Paulo, Application of enzymes for textile fibres processing, Biocatalysis and Biotransformation 26(5) (2008) 332-349.

[11] A.G. Mikhailova, R.F. Khairullin, I.V. Demidyuk, S.V. Kostrov, N.V. Grinberg, T.V. Burova, V.Y. Grinberg, L.D. Rumsh, Cloning, sequencing, expression, and characterization of thermostability of oligopeptidase B from Serratia proteamaculans, a novel psychrophilic protease, Protein Expression and Purification 93 (2014) 63-76.

[12] R. Cavicchioli, K.S. Siddiqui, D. Andrews, K.R. Sowers, Low-temperature extremophiles and their applications, Current Opinion in Biotechnology 13(3) (2002) 253-261.

[13] C. Arunachalam, K. Saritha, Protease enzyme: an eco-friendly alternative for leather industry, Indian Journal of Science and Technology 2(12) (2009) 29-32.

[14] B.J. Demuner, N. Pereira Junior, A. Antunes, Technology prospecting on enzymes for the pulp and paper industry, Journal of Technology Management & Innovation 6(3) (2011) 148-158.

[15] M.E. Himmel, S.Y. Ding, D.K. Johnson, W.S. Adney, M.R. Nimlos, J.W. Brady, T.D. Foust, Biomass recalcitrance: engineering plants and enzymes for biofuels production, Science 315(5813) (2007) 804-807.

[16] F. Wen, N.U. Nair, H. Zhao, Protein engineering in designing tailored enzymes and microorganisms for biofuels production, Current Opinion in Biotechnology 20(4) (2009) 412-419.

[17] L. Xu, Y. Zhu, Y. Li, X. Yang, C. Li, Bienzymatic glucose biosensor based on co-immobilization of glucose oxidase and horseradish peroxidase on gold nanoparticles-mesoporous silica matrix, 2nd IEEE International Nanoelectronics Conference, 2008, pp. 390-393.

[18] F.N. Comba, M.D. Rubianes, P. Herrasti, G.A. Rivas, Glucose biosensing at carbon paste electrodes containing iron nanoparticles, Sensors and Actuators B: Chemical 149(1) (2010) 306-309.

[19] Z.G. Xiong, L. Jian-Ping, T. Li, C. Zhi-Qiang, A novel electrochemiluminescence biosensor based on glucose oxidase immobilized on magnetic nanoparticles, Chinese Journal of Analytical Chemistry 38(6) (2010) 800-804.

[20] E. Emregul, S. Sungur, U. Akbulut, Polyacrylamide–gelatine carrier system used for invertase immobilization, Food Chemistry 97(4) (2006) 591-597.

[21] B. Krajewska, Application of chitin and chitosan-based materials for enzyme immobilizations: a review, Enzyme and Microbial Technology 35(2) (2004) 126-139.

[22] J.M. Palomo, R.L. Segura, C. Mateo, R. Fernandez-Lafuente, J.M. Guisan, Improving the activity of lipases from thermophilic organisms at mesophilic temperatures for biotechnology applications, Biomacromolecules 5(1) (2004) 249-254.

[23] R.M. Daniel, R.V. Dunn, J.L. Finney, J.C. Smith, The role of dynamics in enzyme activity, Annual Review of Biophysics and Biomolecular Structure 32(1) (2003) 69-92.

[24] W. Saenger, M. Noltemeyer, P. Manor, B. Hingerty, B. Klar, "Induced-fit"-type complex formation of the model enzyme α-cyclodextrin, Bioorganic Chemistry 5(2) (1976) 187-195.

[25] D.G. Truhlar, Transition state theory for enzyme kinetics, Archives of Biochemistry and Biophysics 582 (2015) 10-17.

[26] A.A. Homaei, R. Sariri, F. Vianello, R. Stevanato, Enzyme immobilization: an update, Journal of Chemical Biology 6(4) (2013) 185-205.

[27] V. Sirisha, A. Jain, A. Jain, Enzyme immobilization: an overview on methods, support material, and applications of immobilized enzymes, Advances in Food and Nutrition Research 79 (2016) 179-211.

[28] T. Tosa, T. Mori, I. Chibata, Studies on continuous enzyme reactions, Agricultural and Biological Chemistry 33(7) (1969) 1053-1059.

[29] B. Brena, P. Gonzalez-Pombo, F. Batista-Viera, Immobilization of enzymes: a literature survey, Methods in Molecular Biology 1051 (2013) 15-31.

[30] W. Norde, J.P. Favier, Structure of adsorbed and desorbed proteins, Colloids and Surfaces 64(1) (1992) 87-93.

[31] G. Anand, S. Sharma, A.K. Dutta, S.K. Kumar, G. Belfort, Conformational transitions of adsorbed proteins on surfaces of varying polarity, Langmuir 26(13) (2010) 10803-10811.

[32] A. Sethuraman, G. Vedantham, T. Imoto, T. Przybycien, G. Belfort, Protein unfolding at interfaces: Slow dynamics of α-helix to β-sheet transition, Proteins: Structure, Function, and Bioinformatics 56(4) (2004) 669-678.

[33] R.C. Rodrigues, C. Ortiz, A. Berenguer-Murcia, R. Torres, R. Fernandez-Lafuente, Modifying enzyme activity and selectivity by immobilization, Chemical Society Reviews 42(15) (2013) 6290-6307.

[34] Jose M.G, Immobilization of enzymes and cells, Methods in Biotechnology Second Edition (2006) 15-30.

[35] [35] S. Nisha, N. Gobi, A review on methods, application and properties of immobilized enzyme. Chemical Science Review and Letters 1(3) (2012) 148-155.

[36] R.M. Blanco, J.J. Calvete, J. Guisan, Immobilization-stabilization of enzymes; variables that control the intensity of the trypsin (amine)-agarose (aldehyde) multipoint attachment, Enzyme and Microbial Technology 11(6) (1989) 353-359.

[37] A.C. Koch-Schmidt, K. Mosbach, Studies on conformation of soluble and immobilized enzymes using differential scanning calorimetry. 2. Specific activity and thermal stability of enzymes bound weakly and strongly to Sepharose CL 4B, Biochemistry 16(10) (1977) 2105-2109.

[38] D. Gabel, E. Katchalski, I.Z. Steinberg, Changes in conformation of insolubilized trypsin and chymotrypsin, followed by fluorescence, Biochemistry 10(25) (1971) 4661-4669.

[39] D. Norouzian, Enzyme immobilization: the state of art in biotechnology, Iranian Journal of Biotechnology 1(4) (2003) 197-206.

[40] M. Mura Galelli, J. Voegel, S. Behr, E. Bres, P. Schaaf, Adsorption/desorption of human serum albumin on hydroxyapatite: a critical analysis of the Langmuir model, Proceedings of the National Academy of Sciences 88(13) (1991) 5557-5561.

[41] V. Gavalas, N. Chaniotakis, T. Gibson, Improved operational stability of biosensors based on enzyme-polyelectrolyte complex adsorbed into a porous carbon electrode1, Biosensors and Bioelectronics 13(11) (1998) 1205-1211.

[42] S. Datta, L.R. Christena, Y.R.S. Rajaram, Enzyme immobilization: an overview on techniques and support materials, 3 Biotech 3(1) (2013) 1-9.

[43] A.C. McUmber, T.W. Randolph, D.K. Schwartz, Electrostatic interactions influence protein adsorption (but not desorption) at the silica–aqueous interface, The Journal of Physical Chemistry Letters 6(13) (2015) 2583-2587.

[44] L.S. Wong, J. Thirlway, J. Micklefield, Direct site-selective covalent protein immobilization catalyzed by a phosphopantetheinyl transferase, Journal of the American Chemical Society 130(37) (2008) 12456-12464.

[45] H.J. Chae, M.J. In, E.Y. Kim, Optimization of protease immobilization by covalent binding using glutaraldehyde, Applied Biochemistry and Biotechnology 73(2-3) (1998) 195-204.

[46] R.A. Quirk, W.C. Chan, M.C. Davies, S.J. Tendler, K.M. Shakesheff, Poly (l-lysine)–GRGDS as a biomimetic surface modifier for poly (lactic acid), Biomaterials 22(8) (2001) 865-872.

[47] J. Kim, J.W. Grate, P. Wang, Nanobiocatalysis and its potential applications, Trends in Biotechnology 26(11) (2008) 639-646.

[48] W. Feng, P. Ji, Enzymes immobilized on carbon nanotubes, Biotechnology Advances 29(6) (2011) 889-895.

[49] U. Hanefeld, L. Gardossi, E. Magner, Understanding enzyme immobilization, Chemical Society Reviews 38(2) (2009) 453-468.

[50] V. Ferrario, C. Ebert, L. Knapic, D. Fattor, A. Basso, P. Spizzo, L. Gardossi, Conformational changes of lipases in aqueous media: A comparative computational study and experimental implications, Advanced Synthesis & Catalysis 353(13) (2011) 2466-2480.

[51] S. Cantone, V. Ferrario, L. Corici, C. Ebert, D. Fattor, P. Spizzo, L. Gardossi, Efficient immobilisation of industrial biocatalysts: criteria and constraints for the selection of organic polymeric carriers and immobilisation methods, Chemical Society Reviews 42(15) (2013) 6262-6276.

[52] S. Racovita, S. Vasiliu, M. Popa, C. Luca, Polysaccharides based on micro-and nanoparticles obtained by ionic gelation and their applications as drug delivery systems, Romanian Chemistry Review 54(9) (2009) 709-718.

[53] S.A. Agnihotri, N.N. Mallikarjuna, T.M. Aminabhavi, Recent advances on chitosan-based micro-and nanoparticles in drug delivery, Journal of Controlled Release 100(1) (2004) 5-28.

[54] P. Sorlier, A. Denuziere, C. Viton, A. Domard, Relation between the degree of acetylation and the electrostatic properties of chitin and chitosan, Biomacromolecules 2(3) (2001) 765-772.

[55] I.A. Alsarra, S.S. Betigeri, H. Zhang, B.A. Evans, S.H. Neau, Molecular weight and degree of deacetylation effects on lipase-loaded chitosan bead characteristics, Biomaterials 23(17) (2002) 3637-3644.

[56] A. Martino, M. Durante, P. Pifferi, G. Spagna, G. Bianchi, Immobilization of β-glucosidase from a commercial preparation. Part 1. A comparative study of natural supports, Process Biochemistry 31(3) (1996) 281-285.

[57] E. Biro, A.S. Nemeth, C. Sisak, T. Feczko, J. Gyenis, Preparation of chitosan particles suitable for enzyme immobilization, Journal of Biochemical and Biophysical Methods 70(6) (2008) 1240-1246.

[58] P.N. Nakorn, Chitin nanowhisker and chitosan nanoparticles in protein immobilization for biosensor applications, Journal of Metals, Materials and Minerals 18(2) (2017).

[59] A.U. Metin, E. Alver, Fibrous polymer-grafted chitosan/clay composite beads as a carrier for immobilization of papain and its usability for mercury elimination, Bioprocess and Biosystems Engineering 39(7) (2016) 1137-1149.

[60] A. Celik, A. Dincer, T. Aydemir, Characterization of β-glucosidase immobilized on chitosan-multiwalled carbon nanotubes (MWCNTS) and their application on tea extracts for aroma enhancement, International Journal of Biological Macromolecules 89 (2016) 406-414.

[61] R. Saini, H.S. Saini, A. Dahiya, Amylases: Characteristics and industrial applications, Journal of Pharmacognosy and Phytochemistry 6(4) (2017) 1865-1871.

Chapter 2

Experimental techniques, selection of magnetic chitosan as enzyme carrier and effect of cross-linking agents on magnetic chitosan in enzyme immobilization

Contents

2.1 Introduction

An important biopolymer, chitosan derived from chitin under strong alkaline medium and at elevated temperature was observed as an adequate immobilization carrier due to certain properties such as biocompatibility, biodegradability, non-toxicity and hydrophilicity [1, 2]. Due to its affordability, it is possible for the large scale production of cheap carriers in the field of enzyme immobilization. The reactive functional groups presented on chitosan such as amino and hydroxyl groups can be chemically modified with some cross-linking agents and enable the coupling of enzyme [3]. This cross-linking of chitosan molecules prevent the direct contact with the enzyme molecules and allow the substrate molecules to reach easily at the catalytic site. Thus chitosan is commonly used as efficient carrier for enzyme immobilization [4-6].

The amino group in chitosan has pKa of ~ 6.5 which leads to its dissolution in acidic solution, but promote the immobilization of enzyme

having isoelectric point less than 6.5. Immobilizations of amylase and cellulase have successfully reported on chitosan due to the fact that optimum pH of the corresponding enzymes were found to be at 5.5 and 5 [7, 8]. The chitosan can be used as enzyme carrier in its variety forms. Dong et al. observed that immobilized glucose oxidases on chitosan membrane exhibited excellent stability and reusability [9]. Chitosan-gel matrix was found to be an effective carrier for entrapment of biomolecules and resulted in good entrapment efficiencies. Ghanem et al. compared the entrapment of lysine, bovine serum albumin and β-galactosidase in gel beads of chitosan prepared by complexation with tripolyphosphate [10]. They observed the controlled release of bioactive compounds and found that gel chitosan beads as potential matrix for immobilization. The chitosan beads have been used as an efficient carrier in many immobilization studies [11-14]. The immobilization of catalase on gluteraldehyde activated chitosan films was shown by Cetinus et al. and also they have mentioned that the immobilized enzyme can be utilized for practical applications.

Several methods such as precipitation, ionotropic gelation, spray drying, emulsion droplet coalescence and reverse micellar method were adopted for the production of different sized chitosan particles [15-17]. Enzyme immobilization onto microparticles attained high immobilization efficiency due to their high surface area and accessibility of various fixed active sites for enzyme molecules [18, 19]. The reports showed that the obstructions in the internal diffusions get diminished by the small sized carrier particles. Shentu et al. reported the adsorption of catalase on cibacron blue F3GA-chitosan microspheres. This study revealed the high adsorption capacity of catalase and this could be possible by the carrier without generating any denaturation [20]. Recently many studies are there for the

development of macroporous chitosan membranes with high mechanical strength, increased chemical stability and controlled pore size [21-23]. Wen-Yi Yang et al. developed a new carrier such as silica gel supported macroporous chitosan membrane for enzyme immobilization [24]. The high stability and activity of immobilized β-galactosidase on chitosan nanoparticles were distinguished by Brio et al. and they argued that the highest surface area of the chitosan nanoparticles provided possibilities for better distribution of enzyme onto it when compared to that of chitosan micro and macro particles.

The introduction of inorganic nano materials to chitosan offers good mechanical and surface chemical properties and the chitosan-metal oxide composites stand for potent carrier for enzyme immobilization because of their biocompatibility, non toxicity and hydrophilic properties [25, 26] and these have applications in efficacious biosensor fabrication [27]. A novel amperometric triglyceride biosensor was constructed by Jagriti Narang and coworkers by the covalent co-immobilization of glycerol kinase, lipase and glycerol-3-phosphate oxidase onto the chitosan-ZnO composite film deposited on Pt electrode surface. Raju Khan et al. developed a novel chitosan-TiO_2 bioactive electrode and detected that the immobilization of horseradish peroxidase on chitosan-TiO_2 has shown improved charge transfer resistance [28]. Min-Yun Chang et al. investigated the stability and activity of immobilized acid phosphatase onto chitosan-ZrO_2 composite beads [29]. Deveci et al. compared the performance of immobilized lipase on chitosan-TiO_2 composite beads by adsorption and covalent binding methods [30]. Immobilization of pullulanase on chitosan-Fe_3O_4 has been reported and considered the magnetic chitosan as an effective carrier for enzyme immobilization due to its magnetic property which leads to easy

separation of immobilized enzyme from the reaction system by applying an external magnetic field [31]. Several studies have been reported on which the enzyme immobilization onto magnetic chitosan [32-36].

The chitosan coated magnetite particles attained structural stabilization via cross-linking and the most common cross-linkers for chitosan are gluteraldehyde and epichlorohydrin [37]. In case of the cross-linkers that end with dialdehyde functional groups, that promote the formation of Schiff base with amino functional groups of chitosan and caused the cross-linking of chitosan chains. The free aldehyde groups on cross-linked form also prompted the formation of Schiff base with $–NH_2$ groups of enzyme molecules and leads to the covalent enzyme immobilization [38]. Although for epichlorohydrin, the chitosan chains are linked through its –OH functional groups [39] and so the $–NH_2$ groups are available for enzyme adsorption. The covalent immobilization of β-D-galactosidase onto magnetic chitosan nanoparticles by gluteraldehyde linkage was studied by Chenliang Pan et al. and they observed the high immobilization yield, activity and stability of immobilized enzyme [40]. Gambetta et al. evaluated the effect of cross-linking agents such asglutaraldehyde, epichlorohydrin and glycidol on lipase immobilization onto chitosan and agarose [41].

The current chapter explains the details of various physico-chemical techniques used in the characterization of composites and the experimental methods adopted in the enzyme immobilization study. It discusses the α-amylase immobilization on chitosan-metal oxide composites such as chitosan-Fe_3O_4, chitosan-ZnO and chitosan-TiO_2. This chapter selects magnetic chitosan as base support for the study due to its magnetic property and easy recovery of immobilized enzyme from reaction systems. The effect

of cross-linking agents on magnetic chitosan in α-amylase immobilization is also incorporated with this chapter.

2.2 Materials and Methods

2.2.1 Materials

Diastase α-amylase (1, 4 α-D-glucanglucanohydrolase, EC 3.2.1.1) was obtained from Himedia Laboratories Pvt. Ltd, Mumbai. Bovine serum albumin and Folin & Ciocalteu's Phenol reagent were got from Sisco Research Laboratories Pvt. Ltd. Mumbai. Maltose, sodium potassium tartrate and copper sulphate were bought from Sigma Aldrich. Ferric chloride, sodium sulphite, zinc nitrate, sodium hydroxide, titanium tetraisopropoxide, soluble starch (potato) and dinitrosalicylic acid were procured from S.d. Fine Chemicals Ltd, Mumbai. Chitosan was purchased from Meron marine chemicals, Cochin. Gluteraldehyde, glyoxal and epichlorihydrin were acquired from LOBA CHEMIE Pvt. Ltd. Mumbai.

2.2.2 Physico-chemical characterization

2.2.2.1 FT-IR spectroscopy

The infrared spectra of synthesized composites were recorded on JASCO FT/IR-4100 in the frequency region 4000-400 cm^{-1} by KBr pellet method. This technique is based on the fact that the molecular absorptions which occurred at resonance frequencies characteristics to their structure. IR spectra give important data for the composite formation and also provide the information that confirms the composite modification. The shift in the characteristic peaks of chitosan and the arrival of new vibrational bands are responsible for the modification of magnetic chitosan.

2.2.2.2 X-ray powder diffraction spectra

XRD analysis was performed with Bruker AXS D8 Advance X-ray Powder Diffractometer. The powder XRD gives the diffraction pattern which is derived from powder of the material in preference to individual crystal. It also reveals the diffraction pattern of crystalline solid which need not to be representing the whole material. Here the intensity of the diffraction pattern plotted against the angle of the detector, 2θ. The diffraction pattern of the sample discloses its purity and also determines the lattice parameters of the crystal structure. For modified CSM composites, the diffraction pattern determines their crystalline nature and confirms that whether the crystallinity of chitosan and magnetite changed or not after the modification.

The average size of particles can be determined by Debye–Scherrer formula (equation 2.1) which relates the particle size to peak broadening.

$$d = k\lambda / \beta \cos\theta \qquad (2.1)$$

Where,

d is the particle size,

k is the Debye–Scherrer constant (0.89),

λ is the X-ray wavelength (0.15406nm),

θ is the Bragg angle and

β is the full width at half maximum.

2.2.2.3 Thermo-gravimetric analysis

TG-DTG analysis of composites was performed on Perkin Elmer Pyris Diamond TG analyzer under nitrogen atmosphere in the temperature

range of 40-730 °C and at a heating rate of 20 °C min^{-1}. Here the mass of the sample is determined continuously with respect to the change of temperature at constant rate. The TGA curve gives the information about the weight loss % for the corresponding thermal decomposition reaction, while the DTG curve determines the inflection points at which the thermal degradation has taken place. This technique measures the stability of the sample. The material that thermally stable shows little mass loss and the TGA curve appears with no slope at that temperature region. The thermal stability of polymers can be clearly evaluated from the TGA analysis and the stable polymers can withstand at the temperature of 300 °C in air and 500 °C in nitrogen atmosphere without causing any structural changes. In case of magnetic chitosan the weight loss % corresponding to chitosan decomposition can be reduced by the composite modification.

2.2.2.4 Surface area analysis

Surface areas of composites were determined by using surface area analyzer (TriStar II 3020 V1.04) and plotted the nitrogen adsorption isotherms at liquid nitrogen temperature. Brunauer–Emmett–Teller (BET) theory explains the measurement of specific surface area of the materials and is based on the physical adsorption of gas molecules on the surfaces of the solid material. This theory applies to describe the multilayer adsorption and the most frequently used probing gas is the nitrogen that does not undergo any chemical reaction with the material surfaces. The specific surface area of the sample was analyzed by this method at 77 K of N_2 gas including the pore distribution and this gives the dissolution rate which is proportional to the specific surface area. This study stands for an essential characterization for enzyme carrier as its specific surface area determines the binding capacity of enzyme and also decides its catalytic activity.

2.2.2.5 Scanning electron microscopy

Surface morphologies of the composites are obtained by using the JEOL Model JSM–6390LV scanning electron microscope. This is the principal magnification tool in which the images of the sample are produced by utilizing the focused beam of electrons. Here the high energy electrons interact with the atoms of the solid sample in order to generate various signals which provide the information about surface morphology, crystalline structure and chemical composition of the sample. The electron beam scanned the sample surface in a raster pattern and as a result of this interaction the energetic electrons are liberated from the surfaces of sample. These scattered electrons such as secondary, backscattered electrons and X-rays are attracted by various detectors. The backscatter electrons impart compositional data of element or compound and also provide morphological information. The diffracted backscatter electrons reveal crystalline structure and orientation of minerals. The X-rays from the surface of sample give valuable information about elements and minerals.

2.2.2.6 Vibrating sample magnetometry

VSM analysis for composites was performed on Lake Shore 7410 vibrating sample magnetometer. It measures the magnetic properties of sample material which is placed in an external magnetic field by transforming the dipole moment of the sample into AC electrical signal and the theory is based on Faraday's Law of Induction. The hysteresis loop exhibits the magnetization of a ferromagnetic material. Here the material after attaining the saturation magnetization dropped to zero and then retain its initial magnetization. The obtained saturation magnetization (Ms) values explain the magnetic characteristics of the composites. In case of modified

magnetic chitosan, the presence of non-magnetic material will reduce its magnetic property to a little.

2.2.2.7 CHN analysis

The elemental analysis on C, H and N was conducted by using the elemental analyzer, Elementar Vario EL III. It measures the elemental content in the sample with accuracy and precision. This characterization is essential for the determination of elemental composition in the composites in order to prove its modification.

2.2.3 Experimental methods in α-amylase immobilization

2.2.3.1 Synthesis of immobilized α-amylase

Two different types of methods were adopted for the synthesis of immobilized enzymes such as adsorption method and covalent method.

In adsorption method, about 0.05 g composite was mixed with definite volume of enzyme in desired buffer and then the reaction system was incubated in a shaking water bath at room temperature for 2 h. After the time period, the immobilized enzyme formed was filtered and washed many times with the same buffer for the removal of unbound enzyme. It was then dried in air and stored at 4 °C for further studies. The collected supernatant and washings were used to estimate the unbound enzyme by Lowry's method.

For covalent immobilization of enzyme, the support was initially activated with the cross-linking agents such as gluteraldehyde and glyoxal. About 1 mL of cross-linking agent was added into 1 g support in basic medium and the mixture was incubated for 3 h at room temperature under continuous stirring. After that the cross-linked support was filtered, the excess of cross-linking agent was washed out by several washings and dried

in air. This activated support, about 0.05 g was then shaken with the enzyme solution in buffer for 2 h at room temperature. Then the same procedure was followed as in the case of above method.

2.2.3.2 Total protein assay

The amount of enzyme immobilized on the support was analyzed by measuring the protein content in the solution before and after the immobilization. This was carried out by applying the Lowry's method [42] using Folin & Ciocaltaue's reagent and measuring the absorption at 660 nm in a Thermo Scientific Evolution 201 UV-Visible spectrophotometer. The amount of immobilized enzyme was determined by calculating the difference between the initial amount of protein taken for the immobilization process and the amount of protein presented in the filtrate after the immobilization process.

The immobilization yield was calculated by equation 2.2

$$IY\ \% = \frac{C1 - C2}{C1} X100 \qquad (2.2)$$

Where C1 represents the concentration of initial amount of protein taken for immobilization and C2 represents the amount of protein presented in the filtrate after immobilization.

The activity yield (AY %) was determined by measuring the activity of initial amount of enzyme and the activity of enzyme after immobilization.

$$Activity\ Yield\ (AY\ \%) = \frac{Activity\ of\ immobilized\ enzyme}{Activity\ of\ free\ enzyme} \qquad (2.3)$$

Then immobilization efficiency (IE %) can be evaluated by the equation 2.4

$$IE\,\% = \frac{AY}{IY} X100 \qquad (2.4)$$

2.2.3.3 Optimization of immobilization conditions

The immobilization conditions such as pH of the immobilization medium, incubation time and the amount of enzyme were optimized in order to get maximum immobilization for enzyme. The pH of the immobilization medium was optimized by varying from 4 to 9 using different buffers, such as acetate buffer (4-5.5), phosphate buffer (6-8) and glycine buffer (8.5-9). The incubation time was varied in the period of 30-300 min. and the enzyme concentration for immobilization was studied by its variation from 2 to 20 mg enzyme g^{-1} support.

2.2.3.4 α-amylase activity assay

The activities of free and immobilized enzymes were studied by DNS method in which 1 % of starch solution was selected as substrate for the enzymatic reaction [43]. A known amount of free and immobilized enzymes in desired buffer was mixed with 1mL starch solution in separate test tubes. Then the reaction tubes were incubated in a water bath shaker at 30 °C for 15 min. under constant stirring. The reaction was stopped by adding 1 mL DNS reagent and the tubes were placed in the boiling water bath for 5 min. The reaction tubes were allowed to cool to room temperature, diluted with 10 mL distilled water and then the absorbance was measured spectrophotometrically at 540 nm. The amount of reducing sugar formed was determined by using standard maltose curve. One unit of α-amylase activity (EU) constitute the amount of enzyme needed to liberate 1 μmol maltose per minute under the assay conditions.

2.2.4 Biochemical characterization of free and immobilized enzyme

2.2.4.1 Effect of pH on enzyme activity

The influence of reaction pH on activities of free and immobilized enzymes was investigated in the range of pH 4-9. For this study a known amount of free and immobilized enzymes in desired buffer was separately mixed with 1 mL starch substrate solution (1 %) and the reaction systems were incubated for 15 min. of continuous stirring at 30 ºC. The enzymatic reaction was repeated for varying pH and the different buffers used are acetate buffer (pH 4-5.5), phosphate buffer (pH 6-8) and glycine buffer (pH 8.5-9).

2.2.4.2 Effect of temperature on enzyme activity

The effect of temperature on activities of free and immobilized enzymes was investigated between 30 ºC and 70 ºC. The study was conducted by incubating the reaction systems in which the individual solutions of free and immobilized enzymes in buffer with optimum pH were mixed with 1 % of starch substrate solution for 15 min. at varying temperatures.

2.2.4.3 Thermal stability study

Thermal stability study was conducted in which the free and immobilized enzymes were pre-incubated at the temperatures range 30-70 ºC for 1 h in the absence of starch substrate. After that the enzymatic reaction was carried out with the addition of 1 % starch solution at optimum temperature. Thermal inactivation studies were carried out by pre-incubating the free and immobilized enzymes up to 120 min. at their optimum pH and temperatures in the absence of substrate. After each time period, the catalytic reaction was performed and their corresponding activities were measured.

2.2.4.4 Measurement of kinetic parameters

The kinetic parameters, K_m and V_{max} were determined by evaluating the rates of enzymatic reactions at varied concentrations of substrate in the range of 0.2 to 1.0 mg mL^{-1}. These parameters were calculated from the Lineweaver - Burk plot of $1/V_0$ versus $1/[S_0]$, where the y-intercept gives the values for inverse of V_{max} and the x-intercept of the plot gives $-1/k_m$. These values were also obtained from Hanes-Woolf plot of $[S_0]$ versus $[S_0]/ V_0$.

2.2.4.5 Storage stability study

The storage stability of free and immobilized enzymes was investigated by measuring their activities at regular intervals of time. In this study the enzymes have been stored at 4 °C in buffer at optimum pH for six months of period. After each definite periods of their storage, enzymatic reaction was carried out with starch substrate solution at optimum temperature and their respective activities were measured in terms of relative activity.

2.2.4.6 Reusability study

The reusability of immobilized enzymes was studied by conducting 10 cycles of repeated batch experiments. Here at the end of each enzymatic reaction, the immobilized enzyme was separated, washed with the same buffer and then new catalytic reaction was carried out with fresh substrate solution. The reaction was repeated up to 10 cycles of experiments in the same manner and the residual activities of immobilized enzymes were determined.

2.3 Chitosan-metal oxide composites as α-amylase carriers

2.3.1 Synthesis of chitosan-Fe_3O_4 (CSM) composite

The reduction precipitation process was adopted for the synthesis of chitosan-Fe_3O_4 (CSM) composite, in which the magnetite particles were precipitated by the partial reduction of Fe^{3+} ions [44]. Here $FeCl_3$ solution (70 mL, 0.13 mol L^{-1} in HCl) was added in to chitosan solution (50 mL, 2 % in HCl) under constant stirring for 1 h. The yellow colored colloidal solution obtained was mixed with Na_2SO_3 solution (30 mL, 0.1 mol L^{-1}) and stirring was continued until the yellow color again reached to the resultant solution. After that the solution rapidly poured in to ammonia solution (40 mL, 12 % (v/v)) and the solution again stirred vigorously. Then a black precipitated suspension was obtained instantly and the precipitate formed was separated by applying an external magnetic field. The collected precipitate was washed with distilled water for several times and dried at 60 °C in a vacuum oven.

The formation of chitosan-Fe_3O_4 composite is depicted in the scheme 2.1.

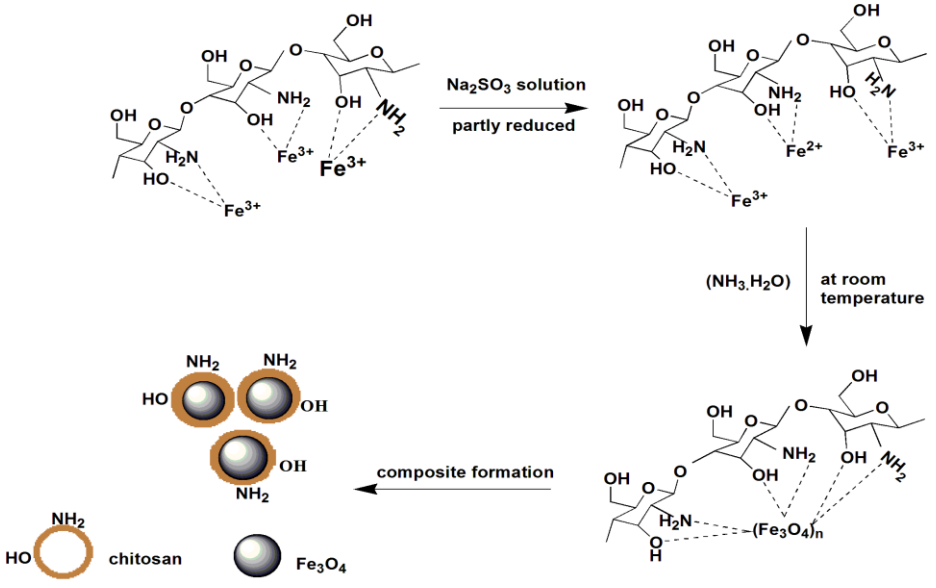

Scheme 2.1 Synthesis of chitosan-Fe_3O_4 composite

2.3.2 Synthesis of chitosan-ZnO (CSZ) composite

At first ZnO particles were synthesized by wet chemical method and for this ethanolic solution of NaOH (100 mL, 0.9 M) was put drop by drop in to ethanolic solution of $Zn(NO_3)_2$ (100 mL, 0.5 M) under continuous stirring. The resultant solution was kept overnight and there after the precipitate formed were washed with distilled water and ethanol in order to eliminate the by-products, then dried in air oven at 60 °C [45].

The chitosan-ZnO (CSZ) composite was synthesized by dissolving 1g ZnO powder in acetic acid (100 mL, 1 %) to form Zn^{2+} ions. Then about 1g chitosan powder was mixed in to it under magnetic stirring. The solution was kept at pH 10 by the addition of 1M NaOH and then it was incubated in a water bath at 80 °C for 3 h. The precipitate formed was filtered by washing several times with distilled water and after that it was dried in a vacuum oven at 50 °C for 1 h [46].

The reaction can be illustrated as shown in the scheme 2.2

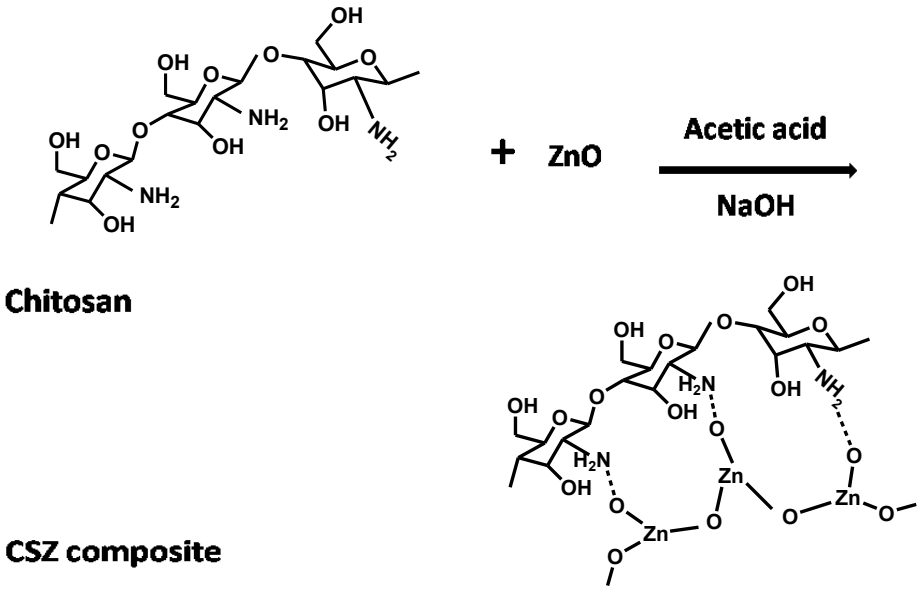

Scheme 2.2 Synthesis of chitosan-ZnO composite

2.3.3 Synthesis of chitosan-TiO_2 (CST) composite

The synthesis of TiO_2 was carried out through sol-gel method, with slight modification in the already reported work [47]. Here the precursor was used as titanium tetraisopropoxide, which was dissolved in methanol maintaining the molar ratio of titanium tetraisopropoxide to methanolis 1:3. The solution was diluted with distilled water by keeping the molar ratio of titanium tetraisopropoxide to distilled water is 1:4 and the hydrolysis during the reaction can be prevented by the addition of H_2SO_4. The resultant solution was kept under magnetic stirring for 40 min. at room temperature. After the time period the gel formed was dried at 50 °C for 1.5 h in order to remove water and organic residues presented. Then calcination was performed at 400 °C for 2 h for the formation of TiO_2 particles.

For the synthesis of chitosan-TiO_2 composite, about 1 g of TiO_2 powder was mixed with chitosan solution (1 % in 1 % (v/v) acetic acid) under sonication. After obtaining a clear sol, NaOH solution (1 M) was added drop by drop in to it until pH of the solution reached 10. The precipitated solution was then undergone 80 °C of heating for 5 h and then the precipitate was collected by washing several times with distilled water. The obtained composite was dried at 60 °C in a vacuum oven.

The composite formation can be depicted as shown in the scheme 2.3

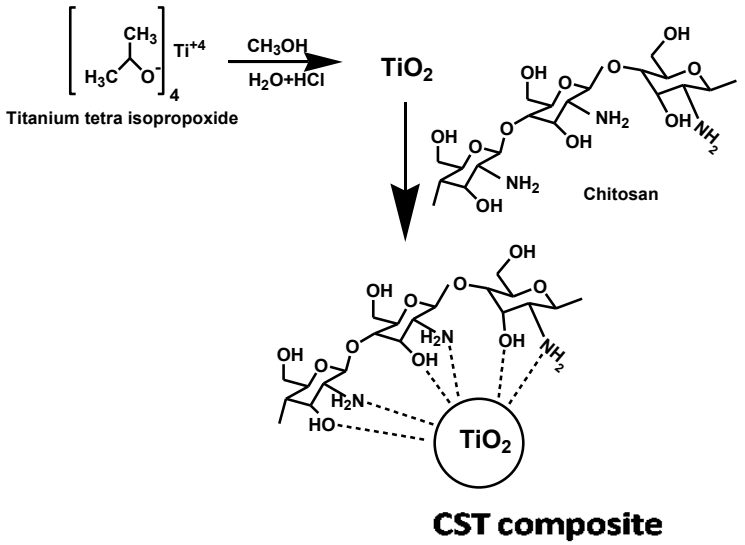

Scheme 2.3 Synthesis of chitosan-TiO_2 composite

2.3.4 Physico-chemical characterization

2.3.4.1FT-IR spectroscopy

The IR spectra of chitosan-metal oxide composites are depicted in the figure 2.1 in which the vibrational frequencies were compared with that of chitosan (CS). The peak assignments for the respective characterization are presented in the table 2.1.

The IR spectrum of chitosan showed that the absorption band at 3429 cm^{-1} corresponded to combined vibrational frequencies of hydroxyl and amino functional groups. The peak at 1644 cm^{-1} was related to C=O stretching vibrations of amide and 1540 cm^{-1} to $–NH_2$ bending vibrations. The peak at 1074 cm^{-1} represented the C–O stretching vibrations of primary alcoholic groups in chitosan and the vibrations at 2951 cm^{-1} and 2865 cm^{-1} assigned to asymmetric stretching vibrations of $–CH_3$ and $–CH_2$ groups respectively [48].

For all chitosan-metal oxide composites, the vibrations mentioned above are slightly shifted to lower frequencies, indicated that the

complexation of chitosan with metal oxide has taken place through the amino and hydroxyl functional groups presented in it. In case of CSM composite, an additional peak at 577 cm^{-1} was ascribed to Fe–O bond vibrations in magnetite and this peak appeared as a result of electrostatic interaction between positively charged chitosan and surface negatively charged magnetite. This revealed that there was no chemical bonding between chitosan and metal oxide, only the metal oxide was coated by chitosan. This composite has shown other vibrations corresponding to chitosan, but are decreased to lower frequencies and this vibrational change assigned that amino and hydroxyl groups on chitosan incorporated in the complexation with magnetite [49-51]. The infra red spectrum of CSZ exhibited a new peak at the range of 570 cm^{-1} indicated the stretching vibrations of O–Zn groups. The other peaks showed by this composite that characteristics to chitosan were located in lower frequencies [52]. In case of CST composite, the absorption band at 520 cm^{-1} ascribed to Ti–O bond vibrations in TiO_2 [30]. The high intensity of vibration at 1585 cm^{-1} attributed to the interaction of Ti^{4+} in the metal oxide with amino groups of chitosan [53].

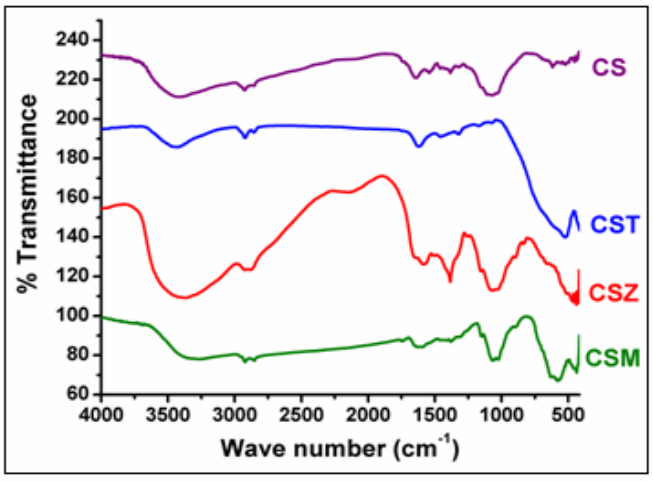

Figure: 2.1 IR Spectra of CS, CSM, CSZ and CST composites

Table 2.1 Peak assignments for chitosan and chitosan-metal oxide composites

Peak assignment (cm^{-1})	CS	CSM	CSZ	CST
Combined $–NH_2$, –OH stretching	3429	3310	3419	3400
C=O stretching of amide	1644	1614	1610	1620
NH_2 bending	1540	1514	1515	1585
C–O stretching	1074	1056	1050	1060
CH_3 asymmetric stretching	2931	2930	2925	2917
CH_2 asymmetric stretching	2863	2865	2860	2870
Fe–O /Zn–O/Ti–O bond vibration	-	577	570	520

2.3.4.2 X-ray powder diffraction spectra

The XRD spectra of chitosan-metal oxide composites are depicted in the figure 2.2 and all the spectra have shown the distinctive peaks of chitosan at about 5.5º and 20º, but these peaks were found to be less intense. The strong inter and intra molecular hydrogen bonding existed in the chitosan molecule due to the presence of amino and hydroxyl groups provided crystalline structure to it. The diminished intensity of the characteristic peaks of chitosan in the composites indicated that chitosan was successfully modified by the metal oxides. CSM has shown other sharp peaks at 2θ = 29.9°, 35.6°, 43.1°, 53.5°, 57.2°, and 62.7° which were assigned to (220), (311), (400), (422), (511) and (440) planes of face centered cubic Fe_3O_4 respectively (JCPDS File No: 75-0033) and revealed its cubic spinel structure [54]. In case of CSZ composite, the peaks at 31.7°, 34.36°, 36.2°, 56.59°, 62.7° and 67.90° were represented the (1 0 0), (0 0 2), (1 0 1), (1 1 0), (1 03), and (1 1 2) hexagonal planes of ZnO indicated the wurtzite structure of ZnO (JCPDS card 36-1451). The diffraction peaks of CST at 26.9°, 36.5°, 39°, 44°, 54° and 55.5° were good agreement with anatase structure of titanium (JCPDS 21-1272) [55].

The average crystalline sizes were evaluated by using Debye–Scherrer equation which was 30 nm for CSM, 25.8 nm for CSZ and 28 nm for CST composites.

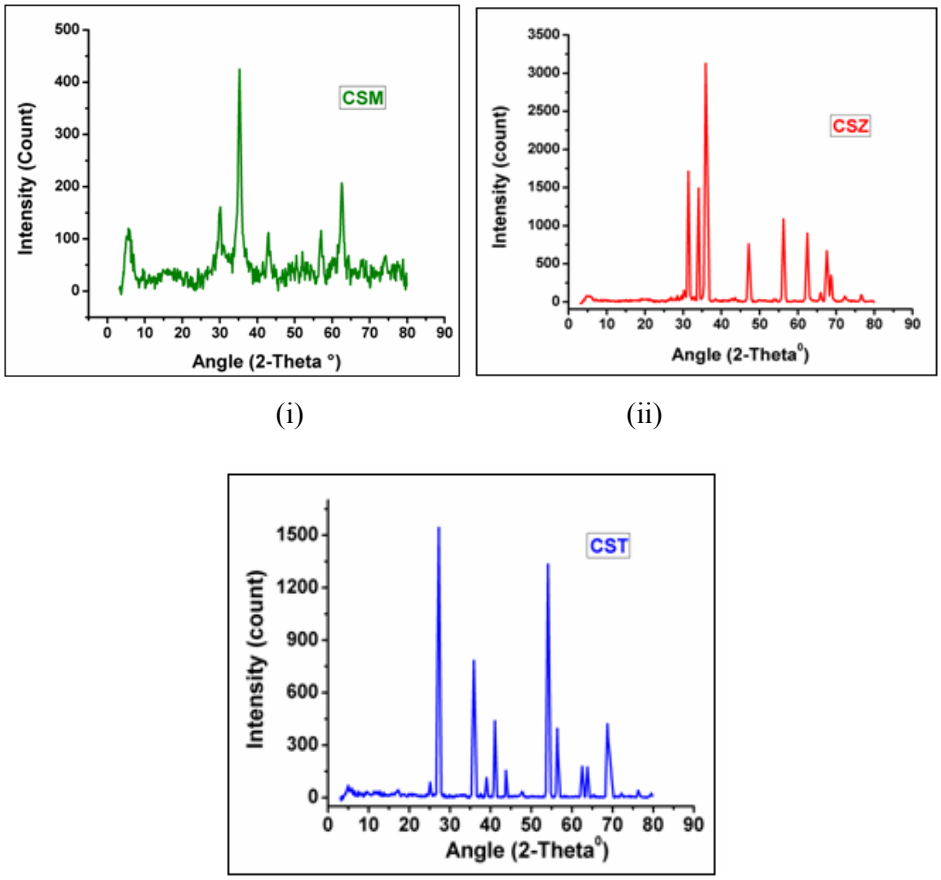

Figure: 2.2 XRD spectra of (i) CSM (ii) CSZ and (iii) CST composites

2.3.4.3 Thermo-gravimetric analysis

The TGA curve of CSM composite was constituted by three major weight losses in which first stage of weight loss about 8 % was attributed to the evaporation of physically adsorbed water. The second and third stages of main weight losses which were taken place at 200 °C – 400 °C and 600 °C – 730 °C can be due to the degradation of primary chains of chitosan and breakdown of cross-linking of chitosan with magnetite. Here we observed that the decomposition of CSM composite was occurred at higher temperatures revealed its higher thermal stability. The cross-linking of magnetite with chitosan and the conformational changes of chitosan increased its thermal stability. The similar thermogram was also reported by Wei Li et al in which magnetic chitosan nanoparticles were synthesized by a one step modified process [56]. In case of CSZ and CST composites, the first stage of weight loss below 200 °C might be due to the loss of adsorbed water and the major weight loss existed between 200 °C and 500 °C could be caused by decomposition of biopolymer and loss of hydroxyl groups presented in metal oxide. After 500 °C there was no remarkable weight losses were observed. The thermogram showed that at 700 °C, the composites exhibited 45 %, 55 % and 50 % of total weight percentage for CSM, CSZ and CST composites. The interaction between chitosan and metal oxide contributed high thermal stability to the composites.

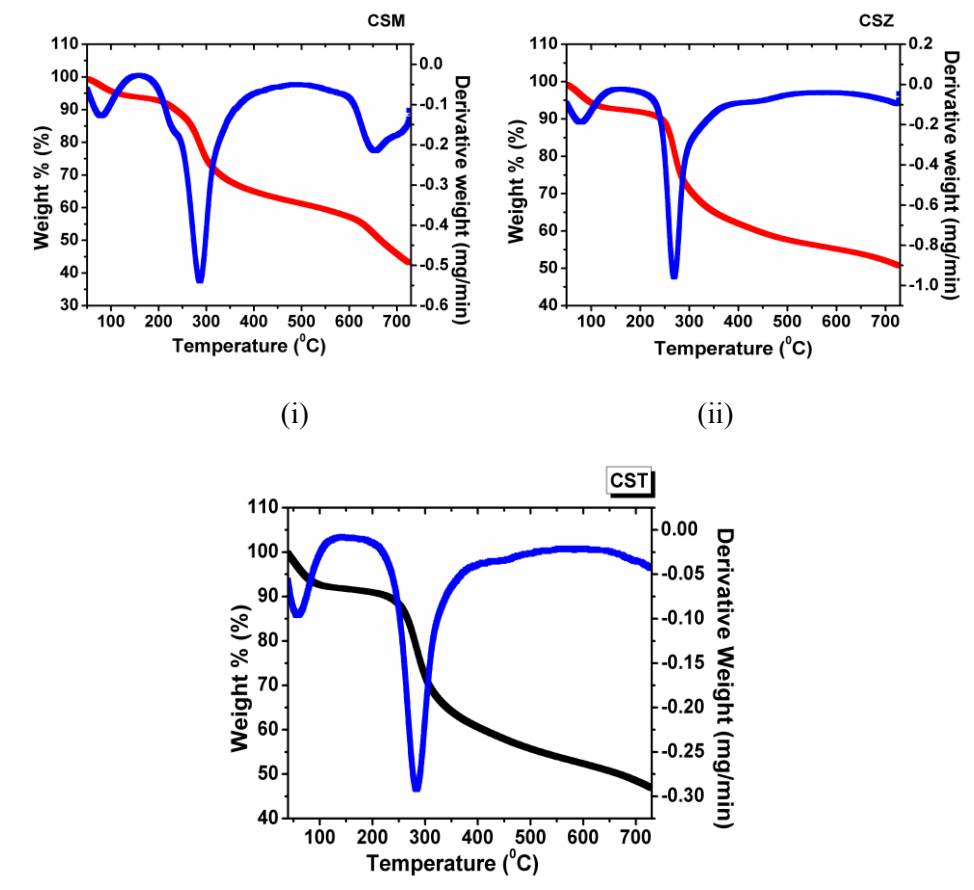

Figure: 2.3 TGA-DTG curves of (i) CSM (ii) CSZ and (iii) CST composites

2.3.4.4 Transmission electron microscopy

The transmission electron microscope images of chitosan-metal oxide composites were shown in the figure 2.4. Here we noticed that in chitosan matrix, the metal oxide particles were almost evenly embedded into it. Due to the incorporation with the polymer matrix the metal oxides in the composites were not agglomerated. The average sizes of 30 nm, 20 nm and 25 nm were obtained for CSM, CSZ and CST composites respectively and these values were in close agreement with that acquired from XRD analysis.

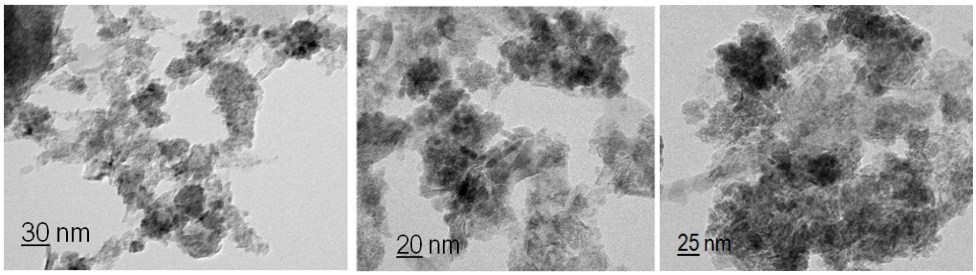

(i) (ii) (iii)

Figure: 2.4 TEM images of (i) CSM, (ii) CSZ and (iii) CST composites

2.3.4.5 Surface area analysis

The BET surface areas of chitosan-metal oxide composites were presented in the table 2.2. Among the composites it was found that CSZ composite acquired higher surface area of 2.4 $m^2 g^{-1}$ and this provide good sorption ability to it. The decrease of surface area for CSM and CST composites when compared to CSZ may arise from the agglomeration of the metal oxides in the polymer matrix.

Table 2.2 Surface areas of chitosan-metal oxide composites

Composite	Surface area ($m^2 g^{-1}$)
CSM	1.99
CSZ	2.4
CST	1.22

2.3.4.6 Vibrating sample magnetometry

The magnetic property of CSM composite was analyzed by vibrating sample magnetometer at room temperature. The magnetization curve for CSM composite was shown in the figure 2.5 and compared with that of magnetite which was given in the inset. Like magnetite the hysteresis loop obtained for CSM composite was indicated its super paramagnetic property

which confirmed the existence of single domain magnetic particles. The saturation magnetization (Ms) values were evaluated and it was 36.67 emu g^{-1} for magnetite and 11.04 emu g^{-1} for CSM composite. The occurrence of polymer layer on the surface of magnetite particles caused the decrease of uniformity as a result of quenching of surface moments and this leads to the reduction in magnetic properties. Even though, CSM composite acquired the magnetic property which was enough for its separation by external magnetic field. The decrease in Ms value of magnetic chitosan was observed in many reports [57].

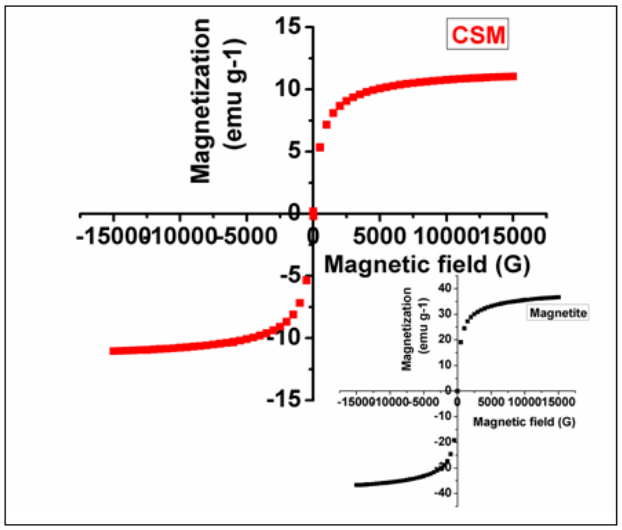

Figure: 2.5 Magnetization curve of CSM composite

2.3.5 Immobilization of α-amylase on chitosan-metal oxide composites

2.3.5.1 Optimization of α-amylase immobilization conditions

The immobilization of enzyme depends on various conditions at which the process has been taken place. During the immobilization process the microenvironment of the enzyme get altered due to the various

interactions of carrier with the enzyme. The conditions such as pH of the medium, incubation time and enzyme concentration have great influence on enzyme immobilization and so these conditions should be properly optimized in order to get maximum immobilization efficiency. The optimum immobilization pH depends on pKa of amino acid residues presented at the active site of the enzyme. The optimum pH of enzyme as a result of immobilization can be changed due to the physical and chemical properties of carrier and in addition to the immobilization methods. The incubation time also stands as an inevitable factor for determining immobilization efficiency. The high enzyme concentration leads to the obstruction of movement of substrate molecule to the active site of the immobilized enzyme and hence the enzyme concentration used in immobilization process should be controlled.

The optimization has been done by keeping the immobilization conditions constant except the variable under study. The immobilization conditions such as pH of the medium, incubation time and enzyme concentration were optimized in order to attain maximum enzyme activity and efficiency.

2.3.5.1.1 Effect of immobilization pH on α-amylase activity

The effect of immobilization pH on α-amylase activity was investigated by varying the pH ranges between 5 and 9; and the immobilization process was performed for 2 h at room temperature. The observations are illustrated in the figure 2.6 and showed that the maximum activity acquired by the enzyme was at pH 6 when immobilized on all the three composites CSM, CSZ and CST.

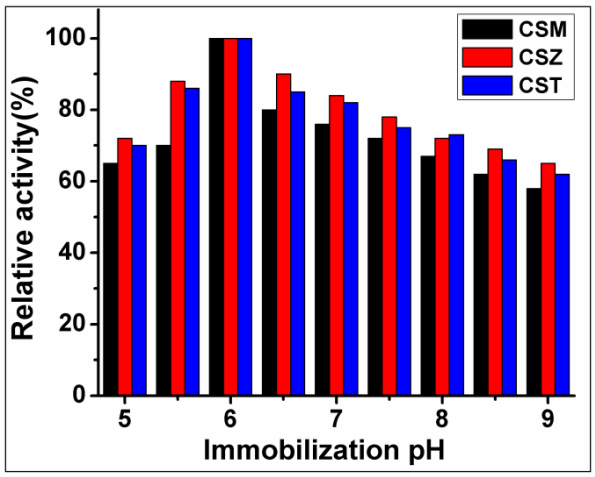

Figure: 2.6 Effect of immobilization pH on the relative activity of α-amylase

At optimum pH 6 there must be significant electrostatic interaction between the support and enzyme. The strength of interaction was determined by the isoelectric point of enzyme and carrier. The isoelectric point of metal oxides is ~ 6-7 for Fe_3O_4 and TiO_2, ~ 9 for ZnO and that of α-amylase is around 4.6. The pKa of chitosan is ~ 6.5 [58] and this value in addition with isoelectric point of metal oxides controls that of whole support. At pH 6, the α-amylase acquires net negative charge and each support may possess net positive charge. This promotes the strong electrostatic interaction between enzyme and support and leads to the high enzyme activity. The decreased enzyme activity above and below this pH indicated the poor enzyme adsorption which could be due to the unfavorable charges on the surfaces of enzyme and support. When the two surfaces maintained similar charges, the electrostatic repulsion existed between them and leads to lower enzyme activity [59].

Normally the surface of the enzyme was not evenly distributed the charges on to it. In spite of the fact that if the net charge on enzyme surface

is negative, the positively charged region on the enzyme surface may stimulate the electrostatic attraction towards the support which was negatively charged. That is why the enzyme still acquired lower activity even when the enzyme and support maintained similar charges on their surfaces and there existed electrostatic repulsive forces.

2.3.5.1.2 Effect of incubation time on α-amylase activity

The variations of enzyme activity on incubation time were studied by conducting the enzyme immobilization process on the composites for 30-150 min. of incubation at optimum pH and the results are shown in the figure 2.7. For CSM composite, the maximum enzyme activity was obtained at 120 min. of incubation and both CSZ and CST composites exhibited optimum incubation time of 90 min. The decrease of activity over this optimum incubation time could be due to the multilayer adsorption of enzyme which leads to the obstruction in the active site of the enzyme. The multilayer adsorption of enzyme also created the repulsive interaction with the already adsorbed enzyme layer which results in enzyme leakage from the support. So further adsorption was not taken place with increase of incubation time and hence no more enhancements in enzyme activity were also observed. Similar observation was reported by Zusfahair et al. when *Bacillus thuringiensis* HCB6 amylase was immobilized on chitosan beads[60]. The increased contact time of enzyme with the support changed the configuration of immobilized enzyme and hence caused the denaturation of enzyme structure.

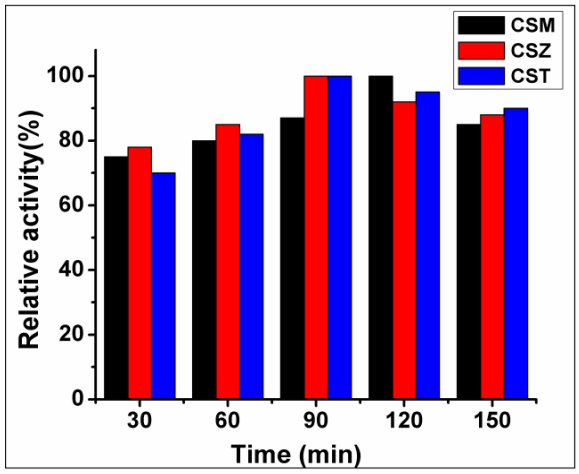

Figure: 2.7 Effect of contact time on immobilized α-amylase activity

2.3.5.1.3 Effect of initial amount of protein on protein loading on to composites

The effect of initial protein amount on protein loading on to chitosan-metal oxide composites was investigated and the results are depicted in the figure 2.8. As the initial protein used for the immobilization process was increased, the loaded protein on to the support was also found to be increased and reached the maximum intake of enzyme at particular initial enzyme concentration. Here we noticed that for all composites, after the optimum intake the enzymes desorption has taken place from the support surface which could be due to the weak interactive forces between the enzyme and carrier.

The maximum protein loading acquired by CSM composite was 7.2 mg g^{-1} support at initial amount of 12.6 mg enzyme. The CSZ and CST composites were attained the optimum protein loading of 10.8 and 8.2 mg g^{-1} support respectively at 14.2 mg and 12.6 mg of initial protein. The immobilization yield of α-amylase on composites was calculated as 57.14 %

for CSM, 76.05 % for CSZ and 65.08 % for CST composites (table 2.3). The highest IY % for CSZ composite might be due to its increased surface area compared to others which was obtained by BET surface area analysis. This was also confirmed by TEM images which provided smallest particle size to CSZ composite and hence imparted increased surface area to it.

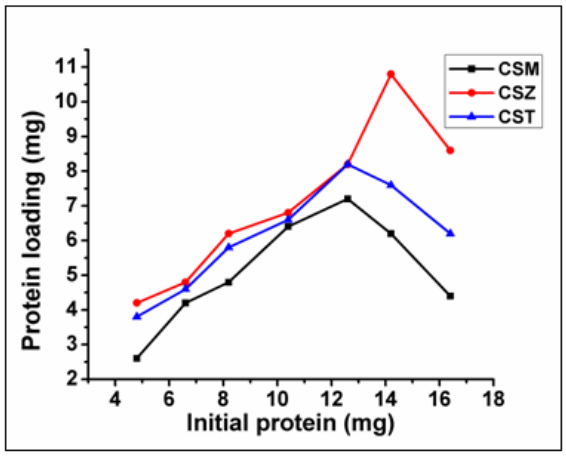

Figure: 2.8 Effect of initial protein amount on protein loading on to chitosan-metal oxide composites

2.3.5.1.4 Effect of initial protein amount on immobilized enzyme activity

The change of immobilized enzyme activity with respect to amount of initial protein was plotted in the figure 2.9. The increase of initial enzyme concentration leads to the enhancement in activity of α-amylase to some extent, but after attaining a saturation point the enzyme activity found to be decreased.

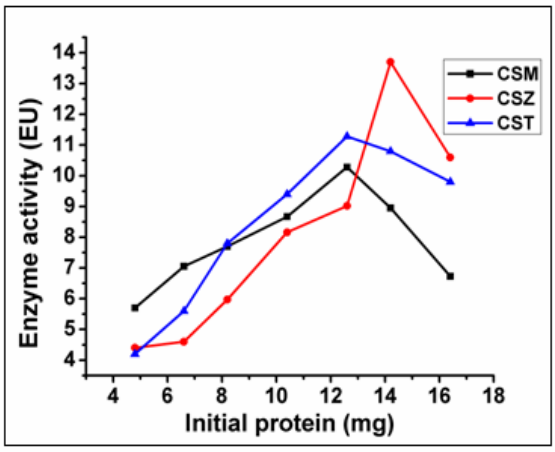

Figure: 2.9 Effect of initial protein amount on immobilized enzyme activity

The maximum activity of α-amylase on composites was 10.28 EU for CSM, 13.7 EU for CSZ and 11.28 EU for CST at initial protein of 12.6 mg, 14.2 mg and 12.6 mg respectively. As the enzyme concentration further increased after these saturation points, the accessibility of substrate molecules towards the enzyme active site may be prohibited as a result of the steric hindrance existed between the enzyme-substrate molecules. Hence the chances for enzymatic reaction were diminished which resulted in reduction of enzyme activity. The activity yield for each immobilized enzymes were calculated and presented in the table 2.3 which showed that CSM, CSZ and CST composites were attained the AY (%) of 43.76 %, 52.57 % and 54.86 % respectively.

The immobilization efficiency of α-amylase on composites were evaluated as 76.58 %, 69.12 % and 84.30 %, which showed that CST acquired highest IE % and this could be due to the high affinity of its immobilized form towards the starch substrate molecules.

Table 2.3 Immobilization efficiency of α-amylase on chitosan-metal oxide composites

Support	Initial protein (mg)	Immobilized protein mg/g support	IY (%)	Initial activity (EU)	Immobilized enzyme activity (EU)	AY (%)	IE (%)
CSM	12.6	7.2	57.14	23.49	10.28	43.76	76.58
CSZ	14.2	10.8	76.05	26.06	13.7	52.57	69.12
CST	12.6	8.2	65.08	20.56	11.28	54.86	84.30

2.3.5.2 Effect of pH on α-amylase activity

The effect of pH on α-amylase activity was studied by conducting the enzymatic reactions with free and immobilized enzymes under varied reaction pH in the range of 5-9 and then activity was measured for the respective reactions. The figure 2.10 showed the variations of relative activity of free and immobilized enzymes with respect to the reaction pH. Here the optimum activity for each enzyme was taken as 100 % and the other activities were evaluated relative to this optimum activity.

The free enzyme was exhibited maximum activity at pH 5-5.5, whereas the optimum pH for CSME was at pH 7 and for both CSZE and CSTE, it was at pH 6. Here we noticed that for all immobilized enzymes the optimum pH shifted to alkaline region and they have shown very broad pH profile compared to free enzyme. The increased positive charge on the surface of the support due to the presence of amino groups leads to the decrease of H^+ ions concentration at the microenvironment of the immobilized enzyme and this caused immobilized enzyme region more alkaline than that of external solution. The shift of optimum pH towards alkaline region was also reported by Egwim et al. in case of immobilized lipase on chitosan beads [61].

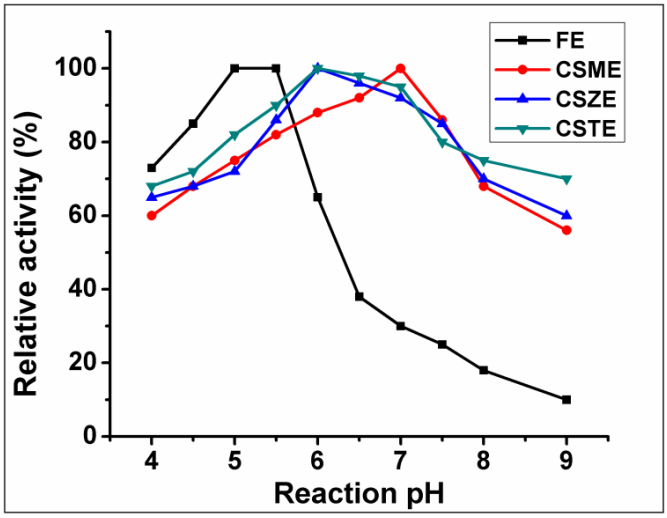

Figure: 2.10 Effect of pH on the relative activity of free and immobilized α-amylase on chitosan-metal oxide composites

2.3.5.3 Effect of temperature on α-amylase activity

The temperature variation on enzyme activity was investigated by changing the temperature of enzyme catalysis reaction at the range of 30-60 ºC. The results are depicted in the figure 2.11 and it was found that the free enzyme has shown maximum activity at 50 ºC, while for all immobilized enzymes it get shifted to 35 ºC.

The shift of optimum temperature to lower region might be due to the conformational changes of enzyme structure as a result of immobilization. This could be due to the fact that the immobilization affected the three dimensional structure of enzyme, imparted restriction in the movement of enzyme and these leads to the changes in substrate affinity towards enzyme active site. The shift of temperature optimum around 10-15 ºC to lower region was reported by Ashly et al. for the immobilization of α-amylase on polyanilines [62]. All the immobilized enzymes have exhibited

increased activity at higher temperatures. The immobilization provided increased temperature characteristics to the enzyme structure and reduced the diffusional limitations of substrate molecules at higher temperatures. This contributed improved activity to the immobilized enzymes at higher temperatures. The increased temperature stability of enzyme was also reported when β-glucosidase immobilized on chitosan beads [63]. The immobilization provided rigidity to the enzyme structure and the carrier protected this conformational integrity at higher temperatures at which the denaturation of enzyme has been taken place.

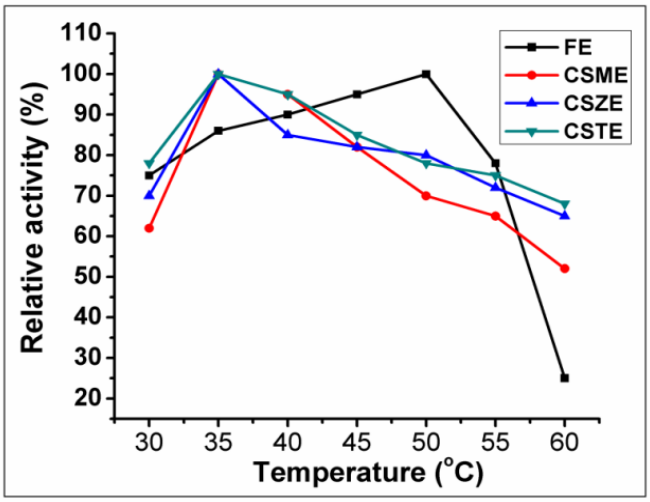

Figure: 2.11 Effect of temperature on the relative activity of free and immobilized α-amylase on chitosan-metal oxide composites

2.3.5.4 Activation energy

The activation energy (Ea) for the enzymatic reaction was evaluated from the slope of Arrhenius plot of log (relative activity %) vs 1/T. The figure 2.12 showed the Arrhenius plots of free and immobilized enzymes and the calculated activation energies are presented in the table 2.4.

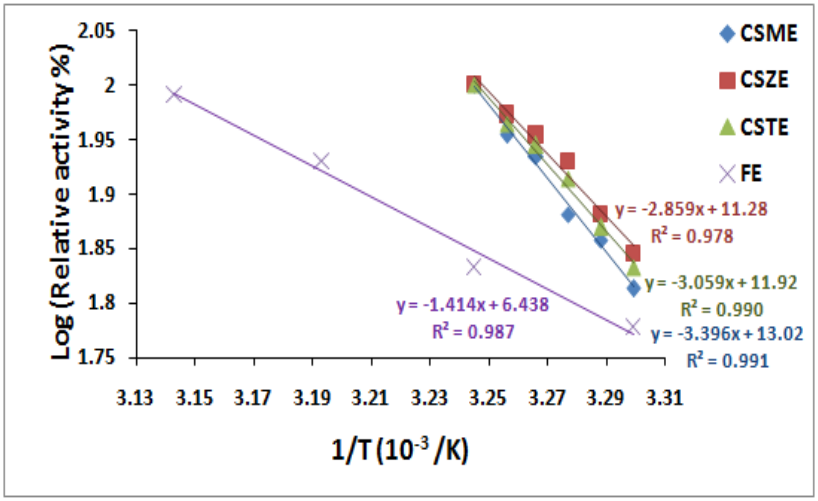

Figure: 2.12: Arrhenius plots to calculate the activation energy (Ea) of free and immobilized α-amylase on chitosan-metal oxide composites

The Ea of free enzyme was calculated as 11.75 KJ mol^{-1} and the values 28.23 KJ mol^{-1}, 23.77 KJ mol^{-1} and 25.46 KJ mol^{-1} were represented that of CSME, CSZE and CSTE respectively. Here the immobilized enzymes have attained higher Ea values than that of free enzyme. This might be due to the fact that since the immobilization affected the three dimensional structure of enzyme, the time required for the contact of enzyme with the substrate molecule has been extended which resulted in reduction in the catalytic activity. Higher Ea values for α-amylase were reported when immobilized on chitin and polyacrylamide [64].

Table 2.4 Activation energy of free and immobilized α-amylase on chitosan-metal oxide composites

Immobilized enzyme	Activation energy ($KJ\ mol^{-1}$)
FE	11.75
CSME	28.23
CSZE	23.77
CSTE	25.43

2.3.5.5 Thermal stability of the free and immobilized enzymes

Thermal stability of free and immobilized α-amylase was examined in which they have undergone 1h pre-incubation by varying the temperature from 30 ºC to 70 ºC in the absence of substrate. After that enzymatic reaction was carried out at optimum temperature and the activities were determined for the corresponding incubating temperatures. The results are illustrated in the figure 2.13 and observed that all immobilized enzymes have shown enhanced heat resistance compared to free enzyme.

After the pre-incubation at 30 ºC, the free and immobilized enzymes have shown maximum activity which was taken as 100 % and the activities at other temperatures were calculated relative to this value. After 50 ºC of pre-incubation the free enzyme was retained only 36 % of activity, whereas the immobilized enzymes retained about 80-85 % of activity. Even the temperature increased to higher ranges, the immobilized enzymes were undergone slow thermal inactivation. At 70 ºC, the activity attained by the free enzyme was only 10 %, while for immobilized enzymes the activities were kept in the range of 65-72 %. These results indicated that the thermal denaturation of enzyme can be prevented to some extend by immobilization. Since the enzyme immobilization provided rigidity to the enzyme structure and hence leads to the reduced conformational flexibility, the possibility of

protein unfolding gets restricted at higher temperatures and so the rate of thermal denaturation of enzyme tends to be decreased.

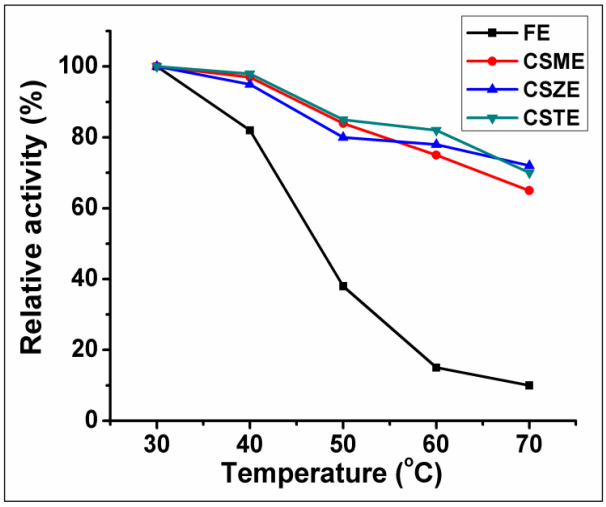

Figure: 2.13 Thermal stability of free and immobilized α-amylase on chitosan-metal oxide composites

The stability of free and immobilized enzymes was also investigated on the basis of pre-incubation time and the study as performed up to 120 min. of pre-incubation. Here at the end of the study the immobilized enzymes maintained more than 90 % of activity, indicated their slow thermal denaturation. This could be due to the immobilization of enzyme which protected the three dimensional structure of enzyme from thermal denaturation at high temperatures. The high thermal stability of α-amylase was reported by Yandri et al. when immobilized with calcium alginate [65]. The enzyme in the immobile matrix was able to prevent the protein unfolding since it has been protected itself from the temperature effect. Chang et al. observed that the thermal stability of immobilized α-amylase has improved as it protected the three dimensional structure of enzyme and decreased the conformational changes in enzyme structure [66].

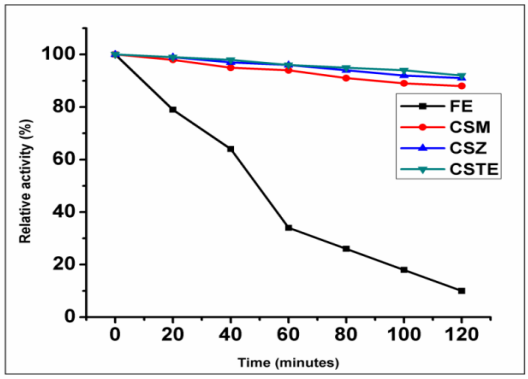

Figure: 2.14 Variation of pre-incubation time on activity of free and immobilized α-amylase on chitosan-metal oxide composites

2.3.5.6 Determination of kinetic parameters

The effect of immobilization of α-amylase on kinetic parameters was evaluated by determining the starch hydrolysis activities of free and immobilized enzymes at optimum temperature and pH for different concentrations of starch ranging between 0.2-1.0 mg mL^{-1}. The kinetic parameters K_m and V_{max} can be calculated from Lineweaver-Burk and Hanes-Woolf plots. The figure 2.15 (a) showed the Lineweaver-Burk and Hanes-Woolf plots of free enzyme and the figure 2.15 (b) is represented that of immobilized enzymes. The kinetic parameters (K_m and V_{max}), turnover number (K_{cat}) and catalytic efficiency (K_{cat}/K_m) calculated are presented in the table 2.5.

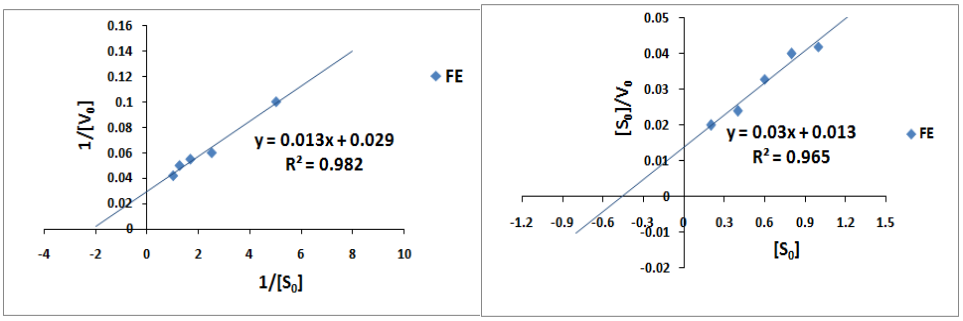

(i) (ii)

Figure: 2.15(a) (i) Lineweaver-Burk plot for free enzyme and (ii) Hanes-Woolf plot for free enzyme.

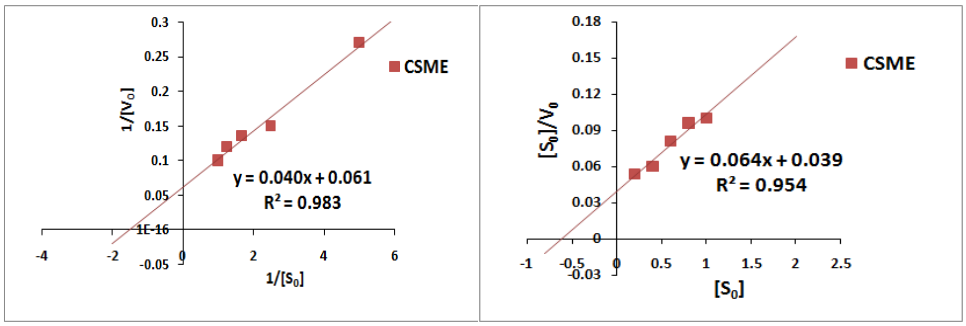

(i) (ii)

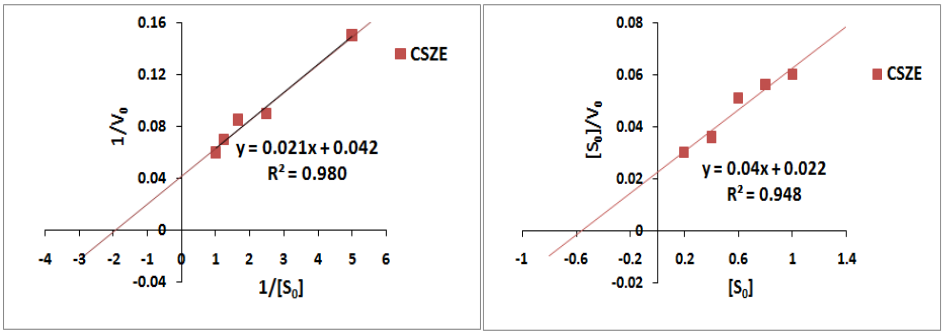

(iii) (iv)

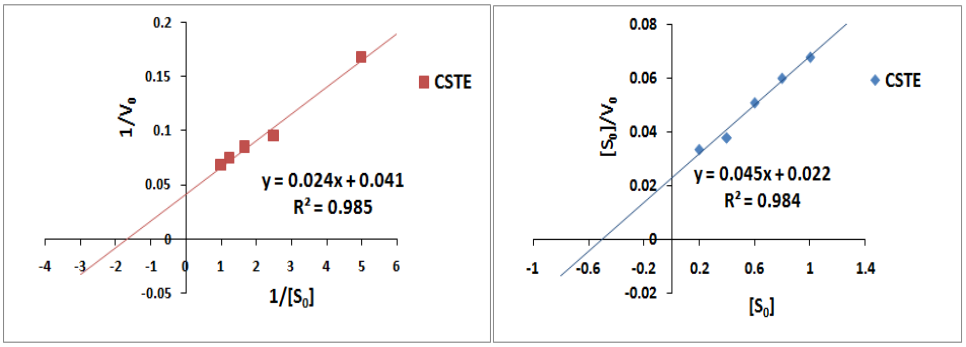

(v) (vi)

Figure: 2.15 (b) Lineweaver-Burk plots for (i) CSME (ii) CSZE (iii) CSTE and Hanes-Woolf plots for (iv) CSME (v) CSZE (vi) CSTE

Table 2.5 Kinetic parameters for free and immobilized α-amylase on chitosan-metal oxide composites

Immobilized enzyme	K_m (mg mL^{-1})	V_{max} (μmol mg^{-1} min^{-1})	K_{cat} (min^{-1})	K_{cat}/K_m ($mLmg^{-1}min^{-1}$)
Free enzyme	0.45± 0.02	34.48±0.05	1910.19	4244.87
CSME	0.65± 0.04	16.39± 0.01	908.00	1396.92
CSZE	0.5±0.04	23.81± 0.02	1319.07	2638.14
CSTE	0.58± 0.03	24.39± 0.04	1351.21	2329.67

The free enzyme exhibited K_m value of 0.45± 0.02 mg mL^{-1} and that for immobilized enzymes were 0.65± 0.04 mg mL^{-1}, 0.5±0.04 mg mL^{-1} and 0.58± 0.03 mg mL^{-1}. For all immobilized enzymes the K_m values are found to be increased when compared to free enzyme. As the K_m value denoted the affinity of enzyme towards the substrate molecule, the immobilized enzymes with higher values represented their lower affinity. This might be arising from the reduced accessibility of the substrate molecule towards the active site of the enzyme, since the immobilization has caused some conformational changes in the active site. Similar trend was obtained in many literatures [67-69]. The V_{max} explains capability of enzyme towards catalytic activity and the value for free enzyme was calculated as 34.48±0.05 μmol mg^{-1} min^{-1}. All the immobilized enzymes have attained lower V_{max} values than that of free enzyme and the values were 16.39± 0.01, 23.81± 0.02 and 24.39±0.04 μmol mg^{-1} min^{-1} for CSME, CSZE and CSTE respectively. The diffusional limitations of the substrate molecule to active site of the enzyme due to immobilization provided lower enzyme activity and hence lower V_{max} values to immobilized enzymes. The decrease of V_{max} values for α-amylase was widely reported in many literatures [70-72].

The free enzyme attained K_{cat} value of 1910.19 min^{-1} and it was found that the immobilized enzymes CSME, CSZE and CSTE were showed 52.46 %, 30.94 % and 29.26 % lower than that of free enzyme. These results

indicated that the immobilized enzymes required 66.09, 45.49 and 44.40 milliseconds in order to convert one substrate molecule into product while that for free enzyme it was only 31.41 milliseconds. The K_{cat}/K_m values were calculated as 4244.87, 1396.92, 2638.14 and 2329.67ml mg^{-1} min^{-1} for free enzyme, CSME, CSZE and CSTE respectively and this showed the lower catalytic efficiency of immobilized enzymes compared to free enzyme.

2.3.5.7 Storage stability of Immobilized α-amylase

It is very important to investigate that how long the enzyme stability existed during the storage period and this determines its applicability in industrial zones. For this study, all immobilized enzymes were kept in desired buffer at 4 ºC and their activities were analyzed at regular intervals up to six months of storage period.

After six months of storage the immobilized enzymes retained the activities of 50 % for CSME, 60 % for CSZE and 64.5 % for CSTE and this reduction in activity could be as a result of natural loss in enzyme activity during the storage. This tendency was accompanied with the changes in structural conformations of enzyme active site during the long period of storage. Here all the immobilized enzymes have attained higher stability than that of free enzyme on storage in which the free enzyme lost its entire activity within seven days (not shown in figure). Since the conformational changes of enzyme can be minimized as a result of immobilization, the loss in activity throughout the storage period can be controlled much more in case of immobilized enzyme systems. The enhanced storage stability was observed by Chia-Hung et al. for immobilized lipase on chitosan coated magnetite nanoparticles [32]. Bayramoglu et al. also reported the improved stability of immobilized α-amylase onto reactive porous membranes in

which they achieved about 71 % of initial activity during 2 months of storage [73].

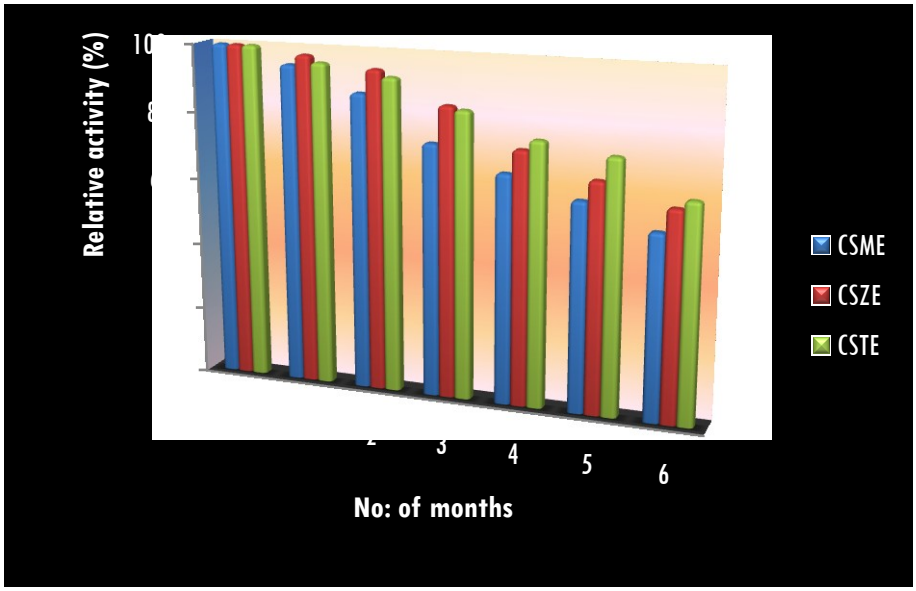

Figure:2.16 Storage stability of immobilized α-amylase on chitosan-metal oxide composites

2.3.5.8 Reusability

The repeated use of immobilized enzymes has significant role in predicting its cost effective applicability in industrial levels. We have investigated the reusability of immobilized enzymes for 10 cycles of repeated uses and the relative activities were determined at optimum conditions. The figure 2.17 showed the variation of relative activities of immobilized enzymes on reuses up to 10 cycles in which the relative activity of first cycle was assigned to 100 % and the remaining activities were expressed relative to this value.

After 10 cycles of uses the relative activities of immobilized enzymes were calculated as 50 %, 60 % and 65 % for CSME, CSZE and CSTE. The activities of immobilized enzymes were found to be decreased

on repeated uses which could be due to desorption of enzyme from the carrier surface. The reuses of immobilized enzyme caused the weakening of enzyme binding with the support and hence this leads to the loss in activity. Also the frequent encountering of substrate molecules to the active site of the immobilized enzyme distorted its conformational integrity which caused the reduction in their activities. Mahshid Defaeiet al. noticed the high preserved activity of α-amylase even after ten cycles of repeated uses when immobilized on naringin functionalized magnetic nanoparticles [74]. The similar observations were also found in many reports where α-amylase was immobilized on various supports [75, 76].

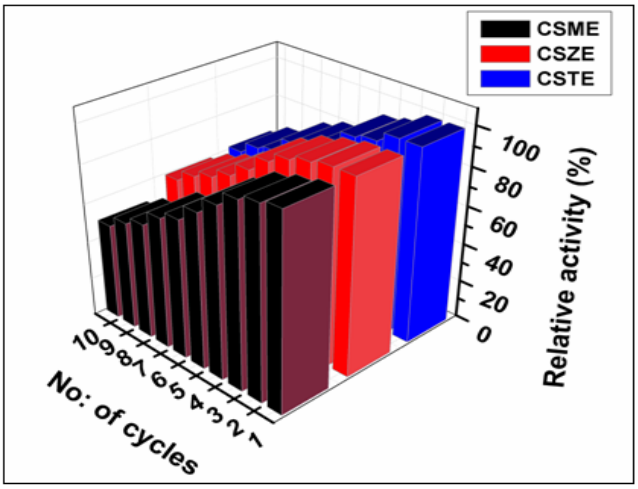

Figure: 2.17 Reusability of immobilized α-amylase on chitosan-metal oxide composites

Among the chitosan-metal oxide composites, the CSM has expected to be great significance on enzyme immobilization due to its magnetic property and it can be recovered very easily from the reaction system by applying an external magnetic field. Due to this property it is more comfortable to handle when compared with CSZ and CST composites. The immobilized α-amylase on CSM can be reused several times after the easy

recovery from the reaction mixture and this provided much benefit in industrial applications. This immobilized enzyme could be retaining more stability without causing much leaching of enzyme from the carrier. Hence we have selected CSM as the base support for the study and decided to modify this composite in order to improve its efficiency as enzyme carrier. The further studies show modifications of CSM composite and its role as enzyme carrier.

Figure: 2.18 Demonstration of magnetic separation of immobilized α-amylase on CSM composite

2.4 Effect of cross-linking agents on magnetic chitosan in enzyme immobilization

2.4.1 Cross-linking of magnetic chitosan

The magnetic chitosan was chemically modified by the cross-linking agents and the reaction was taken place in alkaline medium under continual stirring of 2 h. After the time period, the composite was magnetically separated and the excess of cross-linking agents were eliminated by washing

several times with distilled water until the neutral pH attained. The washing was subsequently performed with ethanol, acetone and then dried in air. Three types of modified forms were prepared; the cross-linking agents used were glyoxal, gluteraldehyde and epichlorohydrin and the modified composites were denoted as CSM-GLY, CSM-GLA and CSM-ECH correspondingly.

2.4.2Physico-chemical characterization

2.4.2.1 Infrared spectra of cross-linked magnetic chitosan

The IR spectra of modified forms CSM-GLY, CSM-GLA and CSM-ECH were compared with that of CSM composite. The absorption band of CSM at 3310 cm^{-1} corresponding to the combined amino, hydroxyl stretching vibrations was shifted to higher vibrational frequencies in case of modified forms and the respective vibrations were at 3492 cm^{-1}, 3495 cm^{-1} and 3500 cm^{-1}. These absorption peaks were with lower intensity than that of CSM indicated the occurrence of cross-linked reaction between CSM and the cross-linking agents. The cross-linked forms have shown distinct changes in the primary amine absorption bands. For CSM-GLY and CSM-GLA the peak corresponding to $–NH_2$ bending was disappeared due to the loss of free amino groups, while they have exhibited a new peak in the range of 1640 cm^{-1}-1660 cm^{-1} which was attributed to an imine bond (N=C) and confirmed the reaction of primary amino groups of CSM with dialdehyde cross-linking agents. These composites have not shown the absorption band corresponding to free aldehyde groups near 1720 cm^{-1} which again confirmed the cross-linking. The CSM-ECH has shown the absorption peak at 1260 cm^{-1}, which was assigned to the C–O–C stretching vibrations, indicated the cross-linking of epichlorohydrin with CSM. All the composites

have shown the absorptions in the ranges of 2920 cm^{-1}-2960 cm^{-1} attributed to the $–CH_3$ asymmetric stretching and 2850 cm^{-1}-2870 cm^{-1} to the $–CH_2$ symmetric stretching vibrations. They have shown strong absorption peak in the range of 570 cm^{-1}-577 cm^{-1} ascribed to the Fe–O bond vibration of Fe_3O_4 presented in it.

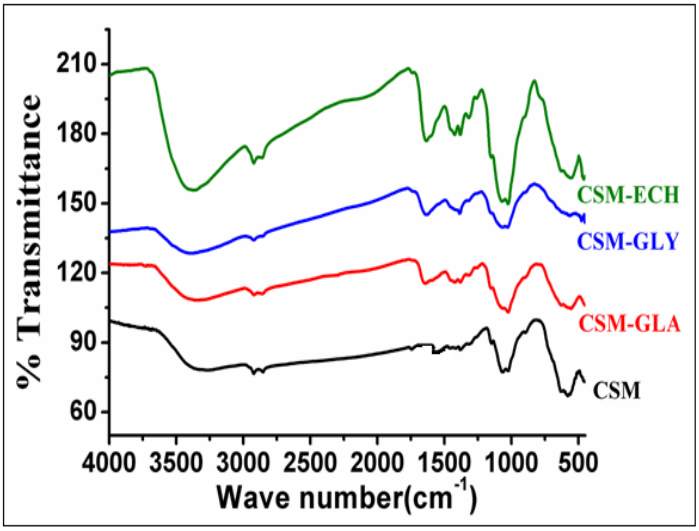

Figure: 2.19 IR Spectra of CSM, CSM-GLA, CSM-GLY and CSM-ECH

Table 2.6 Peak assignments for magnetic chitosan and its cross-linked forms

Peak assignment(cm^{-1})	CSM	CSM-GLY	CSM-GLA	CSM-ECH
Combined $–NH_2$ –OH stretching	3310	3492	3495	3500
NH_2 bending	1514	-	-	1520
N=C stretching	-	1644	1658	-
C–O–C stretching	-	-	-	1260
CH_3 asymmetric stretching	2930	2920	2936	2955
CH_2 asymmetric stretching	2865	2859	2852	2862
Fe–O bond vibration	577	570	572	575

2.4.2.2 Scanning electron microscopy

The surface morphologies of the cross-linked composites were explained on the basis of the SEM image of magnetic chitosan and are presented in the figure 2.20. All the modified forms have shown rough and aggregated surfaces compared to CSM and this could be due to the insufficient cross-linking or the imperfect grafting of cross-linking groups on magnetic chitosan. These observations have denoted that the cross-linking was performed on the surfaces of magnetic chitosan. The cross-linked forms have revealed that all the particles were looser and caused to the increase of size.

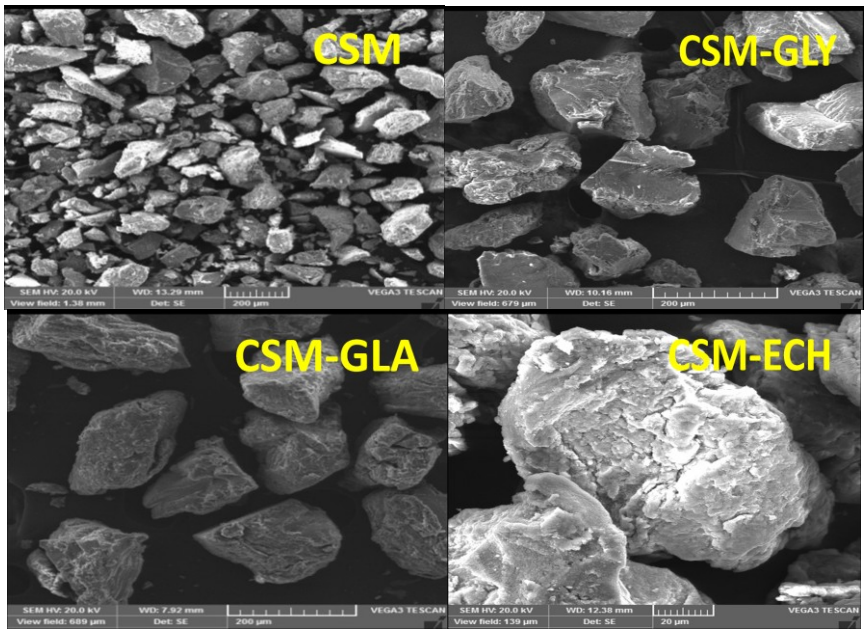

Figure: 2.20 SEM images of CSM, CSM-GLY, CSM-GLA and CSM-ECH

2.4.2.3 Surface area analysis

The BET surface areas of magnetic chitosan and its modified forms by cross-linking agents are shown in the table 2.7. They have exhibited the surface areas of 1.99 $m^2 g^{-1}$, 1.6 $m^2 g^{-1}$, 1.54 $m^2 g^{-1}$ and 1.45 $m^2 g^{-1}$ for CSM, CSM-GLY, CSM-GLA and CSM-ECH respectively. The SEM images of

modified forms confirmed that the cross-linking of magnetic chitosan resulted in the formation of aggregated surfaces and the particles became looser than that of CSM composite. This leads to the decrease in the surface areas of modified forms of magnetic chitosan.

Table 2.7 Surface areas of CSM, CSM-GLY, CSM-GLA and CSM-ECH

Composite	Surface area (m^2 g^{-1})
CSM	1.99
CSM-GLY	1.6
CSM-GLA	1.54
CSM-ECH	1.72

2.4.2.4 Vibrating sample magnetometry

The magnetic properties of the modified forms of magnetic chitosan were investigated by VSM analysis and their hysteresis loops were compared with that of magnetic chitosan. Figure 2.21 showed the hysteresis loops of composites and table 2.8 presented their magnetization saturation values.

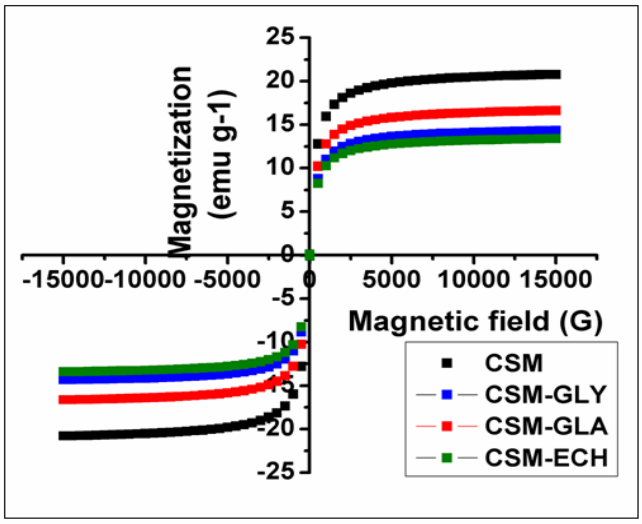

Figure: 2.21 Magnetization curves of CSM, CSM-GLY, CSM-GLA and CSM-ECH

All the composites have exhibited the S-like curves that cross the zero point indicated their super paramagnetic behavior. The calculated Ms values were 20.78 emu g^{-1}, 14.33 emu g^{-1}, 16.63 emu g^{-1} and 13.41 emu g^{-1} for CSM, CSM-GLY, CSM-GLA and CSM-ECH respectively. This indicated that the cross-linking was successfully taken place onto the surface of magnetic chitosan since the Ms values of modified forms were lower than that of magnetic chtiosan. However, these composites could response to a magnetic field and can be easily separated from the reaction system by applying an external magnetic field.

Table 2.8 Ms values of magnetic chitosan and its cross-linked forms

Composite	Magnetization (emu g^{-1}))
CSM	20.78
CSM-GLY	14.33
CSM-GLA	16.63
CSM-ECH	13.41

2.4.3 Immobilization of α-amylase on cross-linked magnetic chitosan

2.4.3.1 Optimization of α-amylase immobilization conditions

Immobilization of α-amylase on cross-linked magnetic chitosan was performed with good yield by optimizing the immobilization conditions. The immobilization pH, incubation time and enzyme concentration were optimized.

2.4.3.1.1 Effect of immobilization pH on α-amylase activity

The effect of pH on immobilization of α-amylase on cross-linked magnetic chitosan was investigated and the enzyme activities corresponding to different pH values were measured. Figure 2.22 showed that CSM exhibited maximum activity at pH 6, CSM-GLA attained the optimum pH of 5 and for CSM-GLY and CSM-ECH the maximum relative activity was obtained at pH 5.5.

For CSM-GLY and CSM-GLA, the bifunctional agents cross-linked with the support promote covalent binding with the amino groups of enzyme. This strong covalent interaction between enzyme and support provide conformational changes in enzyme structure by affecting the intra molecular forces existed in it. The covalently immobilized enzymes have shown optimum activity at which the enzyme structure attained more active conformation. But for CSM and CSM-ECH the surface amino groups electrostatically interact with the enzyme based on the isoelectric point of support and enzyme. Since the isoelectric point of α-amylase was 4.6, it attained a net positive charge and a net negative charge below and above this value respectively. The support gets charged in buffer which depends on the isoelectric point of Fe_3O_4 (6-7) and pKa of chitosan (~ 6.5). Based on these facts at optimum pH of adsorbed enzymes there existed a strong electrostatic interaction between the enzyme and support. The reduction in the enzyme activity over the optimum value might be due to the unfavorable charge distribution at which the similar charges acquired by support and enzyme.

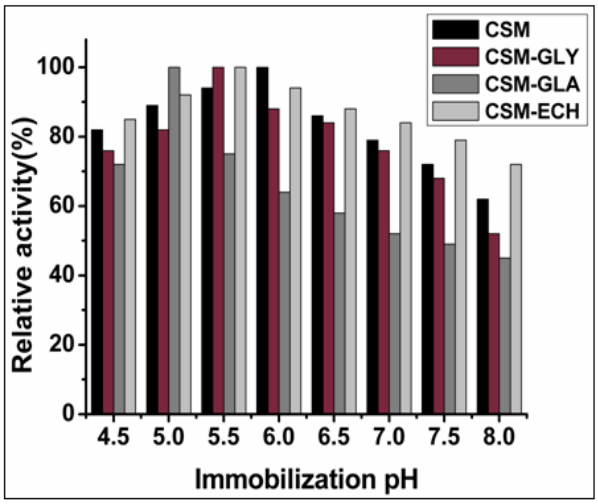

Figure: 2.22 Effect of immobilization pH on the relative activity of immobilized α-amylase on magnetic chitosan and its cross-linked forms

2.4.3.1.2 Effect of incubation time on activity of α-amylase

The incubation time needed to get maximum α-amylase activity was estimated by conducting the immobilization process on cross-linked magnetic chitosan for 30-180 min. of incubation and the results are depicted in the figure 2.23.

For CSM, CSM-GLY and CSM-GLA the maximum enzyme activity was obtained at 120 min. of incubation, but for CSM-ECH the optimum incubation time was at 90 min. Beyond these optimum values the activity of the enzyme was found to be decreased for all the composites and this could be due to the lower accessibility of the active site of the enzyme towards the substrate molecules. The excess addition of enzyme onto the carrier surface leads to the changes in the configuration of the immobilized enzyme, leads to the deformation of the enzyme active site and hence resulted into the loss of its activity. Zusfahair et al. observed the same trend in the variation of incubation time in case of immobilization of *Bacillus thuringiensis* HCB6 amylase onto chitosan beads [77].

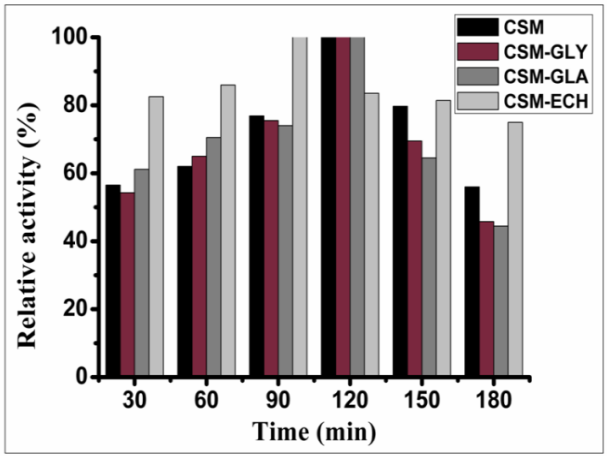

Figure: 2.23 Effect of incubation time on immobilized α-amylase activity

2.4.3.1.3 Effect of initial amount of protein on protein loading on to composites

The amount of initial protein used in the immobilization process was varied in order to get the maximum protein loading onto the carrier surfaces. The optimum protein loading acquired by the composites were 7.2, 5.8, 4.8 and 6.48 mg g^{-1} support for CSM, CSM-GLY, CSM-GLA and CSM-ECH respectively at corresponding initial protein amount of 12.6 mg, 11.2 mg, 10.4 mg and 10.8 mg. The immobilization yield was calculated and here we observed that the high values were obtained with CSM and CSM-ECH. Since gluteraldehyde and glyoxal cross-linking agents covalently bounded with the support surface, these dialdehyde ends provided binding sites for enzyme. CSM-GLY and CSM-GLA have exhibited lower immobilization yield compared to others which could be due to the lesser number of activated dialdehyde groups on the carrier surface. The adsorption method provided better protein loading even at the increased initial enzyme concentration compared to the covalently immobilized enzyme.

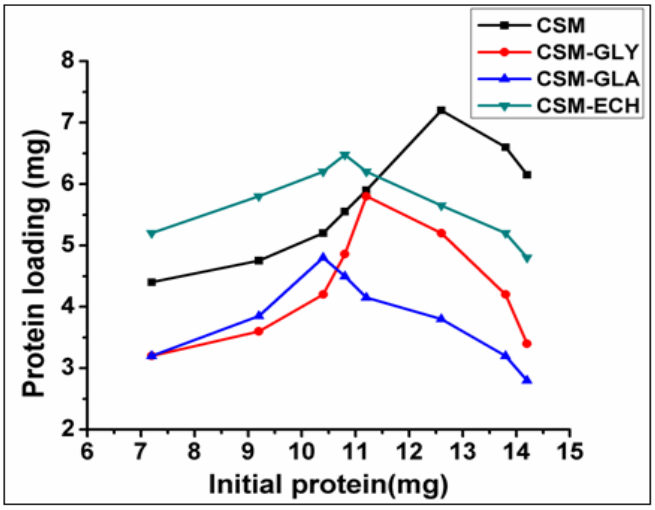

Figure: 2.24 Effect of initial protein amount on protein loading onto composites

2.4.3.1.4 Effect of initial protein amount on immobilized enzyme activity

The figure 2.25 plotted the variation of immobilized enzyme activity on magnetic chitosan composites with respect to initial amount of enzyme. The α-amylase activity for CSM, CSM-GLY, CSM-GLA and CSM-ECH were found to be as 10.28 EU, 10.15 EU, 7.8 EU and 9.14 EU respectively at initial protein of 12.6 mg, 11.2 mg, 10.4 mg and 10.8 mg. The activity for initial protein was determined and then calculated the activity yield (%).

The covalently immobilized enzymes have shown lower enzyme activity of 42.33 % for CSM-GLY and 36.53 % for CSM-GLA and the loss of activity might be as a result of the conformational changes in the active site of enzyme. The covalent immobilization of enzyme with the carrier leads to the enhanced structural deformation of enzyme due to its strong binding. The enzyme on CSM and CSM-ECH have exhibited high activity yield of 43.76 % and 46.16 %, since the interactive forces between the enzyme and carriers were only the weak electrostatic interactions which imparted only slight conformational changes in the enzyme structure.

The immobilization efficiency (%) of α-amylase on CSM and cross-linked CSM composites was evaluated from immobilization yield and activity yield and are presented in the table 2.9. The calculated immobilization efficiencies were 76.58 %, 81.75 %, 79.15 % and 76.93 % for CSM, CSM-GLY, CSM-GLA and CSM-ECH respectively. The lower values attained by the adsorbed enzymes might be due to the enzyme leaching from the carrier surfaces due to the weak interactive forces between them.

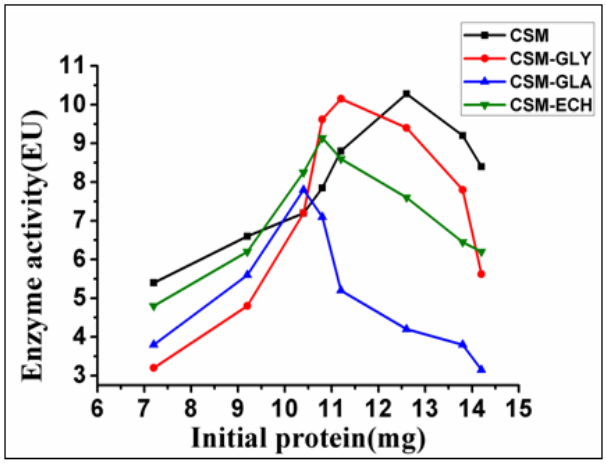

Figure: 2.25 Effect of initial protein concentration on immobilized enzyme activity

Table 2.9 Immobilization efficiency of α-amylase on CSM and cross-linked CSM composites

Support	Initial protein (mg)	Immobilized protein mg/g support	IY (%)	Initial activity (EU)	Immobilized enzyme activity (EU)	AY (%)	IE (%)
CSM	12.6	7.2	57.14	23.49	10.28	43.76	76.58
CSM-GLY	11.2	5.8	51.78	23.98	10.15	42.33	81.75
CSM-GLA	10.4	4.8	46.15	21.35	7.8	36.53	79.15
CSM-ECH	10.8	6.48	60.00	19.8	9.14	46.16	76.93

2.4.3.2 Effect of pH on α-amylase activity

The change of reaction pH in the enzymatic catalysis leads to the conformational changes in enzyme structure and so this hinders the attack of substrate molecules towards the active site of enzyme [78]. The figure 2.26 showed the variation of relative activities with respect to pH of reaction medium in the range of 4-9 and it was observed that all immobilized enzymes have shown wide pH profile compared to free enzyme. The optimum pH of adsorbed enzymes and covalently immobilized enzymes has shifted to higher

pH; CSME and CSM-ECHE have exhibited their maximum activity at pH 7, while for CSM-GLYE and CSM-GLAE the optimum pH was at 6.

For adsorbed enzymes the shift of optimum pH was determined by the H^+ ion concentration in the bulk and microenvironment of the immobilized enzyme system. The positively charged amino groups in the support caused the decrease of concentration of hydronium ions in the microenvironment of the immobilized enzyme and hence the pH shifted to alkaline region. The covalently immobilized enzymes were maintained their activity in a wider pH ranges than adsorbed and free enzymes due to the strong interaction between the enzyme and the cross-linked support. The bifunctional agents on the support formed strong covalent bond with amino lysine groups of enzyme and provided intense rigidity to the enzyme structure. The shift of optimum pH towards alkaline region was reported by Om Prakash et al. when α-amylase was immobilized on agarose and agar matrices [79]. Similar trend was observed in case of immobilized α-amylase on amberlite MB 150 and chitosan beads [80].

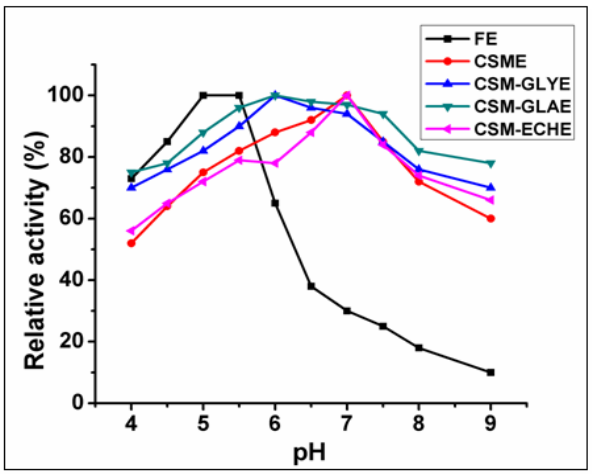

Figure: 2.26 Effect of pH on the relative activity of free and immobilized α-amylase on magnetic chitosan and its cross-linked forms

2.4.3.3 Effect of temperature on α-amylase activity

The temperature influence on enzyme activity was studied and the figure 2.27 showed that all immobilized enzymes have shown maximum activity at lower temperature ranges when compared with free enzyme. As the free enzyme has shown optimum temperature at 50 ºC, for CSME and CSM-ECHE it get shifted to 35 ºC and for CSM-GLYE and CSM-GLAE the shift was about 10 ºC and 5 ºC decrease in optimum temperature. The reduction in optimum temperature of immobilized enzymes might be due to their conformational changes of enzyme structure which resulted in less amount of activation energy for the enzyme catalytic reaction. The covalently immobilized enzymes have shown better activity in the wide temperature ranges than adsorbed ones since the immobilized enzyme have attained more rigidity by covalent method and thus prevented the protein unfolding and denaturation at higher temperature ranges [81]. The shift in temperature optimum was observed in case of α-amylase immobilization onto the acidic and base form of polyaniline [62]. The similar trend was reported by Chang et al. for the immobilization of α-amylase on chitosan-clay composite. Here the immobilized enzyme on support protected the tertiary structure of enzyme which leads to the reduction in its conformational flexibility and hence attained higher stability [82].

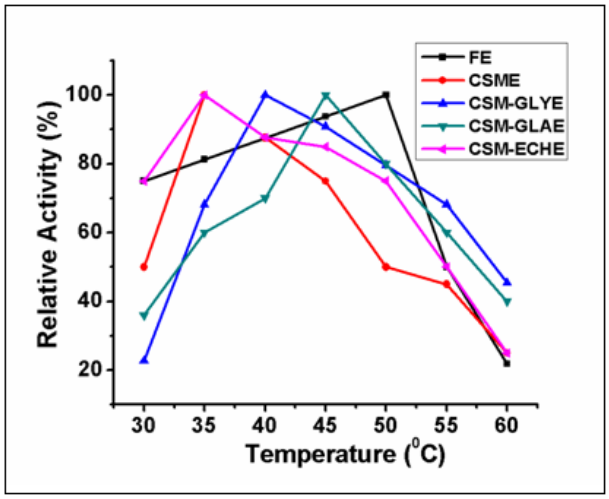

Figure: 2.27 Effect of temperature on the relative activity of free and immobilized α-amylase on magnetic chitosan and its cross-linked forms

2.4.3.4 Activation energy

The figure 2.28 showed the Arrhenius plots of free and immobilized enzymes from which the activation energy can be evaluated. The calculated Ea values are presented in the table 2.10 and it was found that all immobilized enzymes have attained higher Ea values when compared to free enzyme. The values for CSME, CSM-GLYE, CSM-GLAE and CSM-ECHE were calculated as 28.23 KJ mol^{-1}, 16.382 KJ mol^{-1}, 18.13 KJ mol^{-1} and 22.81 KJ mol^{-1} respectively. Here we observed that the covalently immobilized enzymes have shown lesser Ea values than that of adsorbed enzyme systems and this indicated that only shorter period of time was required for the attack of substrate molecule to the active site of respective immobilized enzyme. The covalent binding of enzyme molecules with support provided more rigidity to the enzyme structure and hence the denaturing effect by temperature has become negligible on these immobilized enzymes [83]. The lowering of Ea values of enzyme by

covalent immobilization resulted in higher catalytic efficiency than by adsorption method. Dorra Driss et al. reported that *Penicilliumoccitanis* Pol6 xylanase on covalent immobilization with nickel-chelate Eupergit C has attained higher catalytic efficiency by lowering the Ea values from 17.8 8 kJ mol^{-1} to 8.8 kJ mol^{-1} [84].

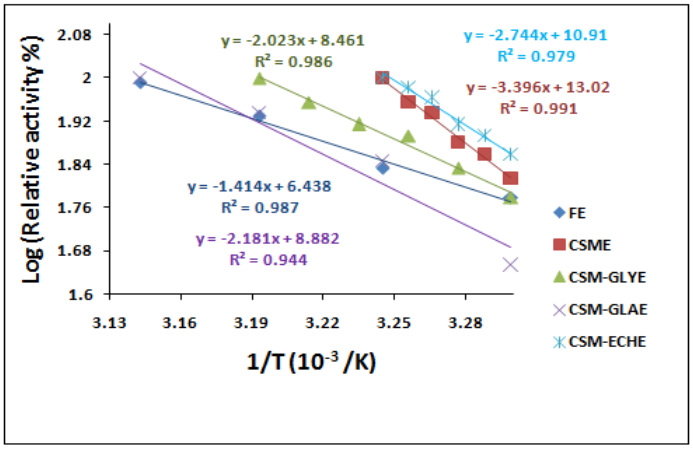

Figure: 2.28 Arrhenius plot to calculate the activation energy (Ea) for free and immobilized α-Amylase

Table 2.10 Activation energy of free and immobilized α-amylase

Immobilized enzyme	Activation energy (KJ mol^{-1})
FE	11.75
CSME	28.23
CSM-GLYE	16.82
CSM-GLAE	18.13
CSM-ECHE	22.81

2.4.3.5 Thermal stability of the free and immobilized enzymes

The thermal stability study was conducted for free and immobilized enzymes at the temperatures ranging 30-70 °C after 60 min. of pre-

incubation. The results are illustrated in the figure 2.29 and it showed the high stability of immobilized enzymes that retained better enzyme activity even at higher temperatures than that of free enzyme. The study at 70 °C showed that the free enzyme retained only 10 % of activity, whereas the immobilize enzymes acquired about 50 % of initial activity for adsorbed enzymes and around 75 % of activity for covalently immobilized enzymes. The higher activity and stability of these immobilized enzymes could be as a result of their increased rigidity and hence they protected from thermal denaturation at higher temperatures. The restricted interactions with the substrate molecules that resulted from the reduced conformational flexibility of covalently immobilized enzyme also have a major role for acquiring an increased enzyme activity. The high stability of amylase was reported by Nwagu et al. when immobilized on polyglutaraldehyde activated chitosan beads by multi point covalent binding [85].

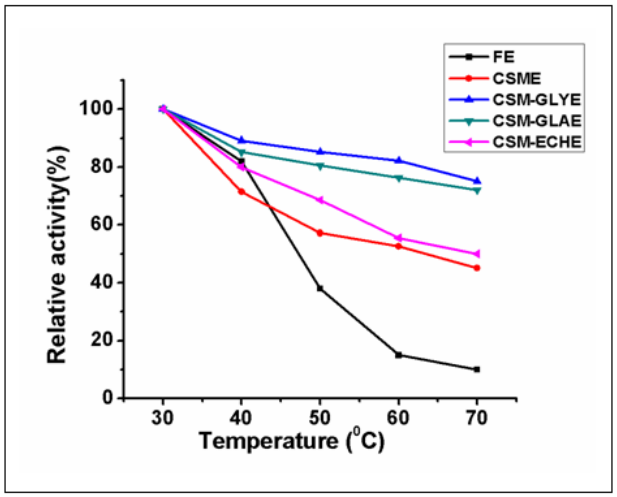

Figure: 2.29 Thermal stability of free and immobilized α-amylase on magnetic chitosan and its cross-linked forms

The effect of pre-incubation time on enzyme activity was studied at optimum conditions and results are plotted in the figure 2.30. The

immobilized enzymes exhibited slow rate of thermal inactivation, but free enzyme has shown sudden drop in activity with increase of incubation time and lost 90 % of activity after 120 min. of pre-incubation. CSME and CSM-ECHE retained above 60 % of activity, while CSM-GLYE and CSM-GLAE attained about 90 % of activity after the end period of study. The thermal inactivation curves for covalently immobilized enzymes were very stable on comparison with free and adsorbed enzymes. The slow rate of inactivation might be due to the strong covalent attachment with the enzyme molecules on the support and this imparted very stable microenvironment to the immobilized enzyme systems by providing stabilizing forces and rigidity to it. The enhancement in thermal stability of α-amylase was also observed when it was immobilized on silica coated magnetite nanoparticles [86] and poly (2-hydroxyethyl methacrylate) [87] by covalent method.

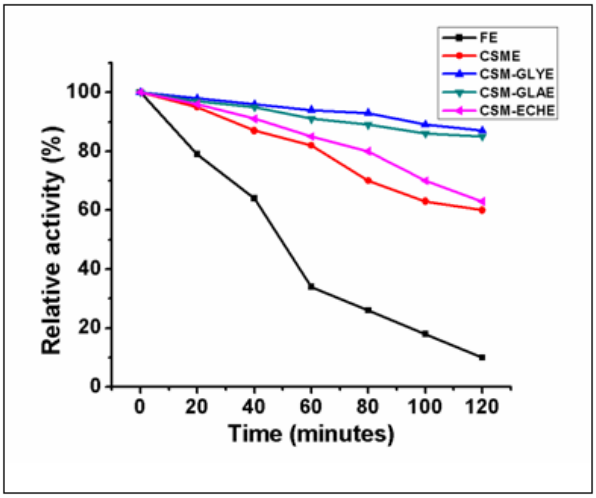

Figure: 2.30 Variation of pre-incubation time on activity of free and immobilized α-amylase on magnetic chitosan and its cross-linked forms

2.4.3.6 Determination of kinetic parameters

The kinetic parameters, K_m and V_{max} were determined from Lineweaver-Burk and Hanes-Woolf plots which were shown in the figure 2.31 and the table 2.11 presented the calculated kinetic parameters, turnover number (K_{cat}) and catalytic efficiency (K_{cat}/K_m) of free and immobilized enzymes. The immobilized α-amylases have shown higher K_m values and lower V_{max} values when compared with free enzyme. The K_m values for immobilized enzymes were 0.525± 0.04 mg mL^{-1}, 0.57±0.06 mg $mL^{-1}$and 1.03±0.03 mg mL^{-1} for CSM-GLYE, CSM-GLAE and CSM-ECHE respectively and their corresponding V_{max} values were 25±0.06 μmol mg^{-1} min^{-1}, 19.6±0.02 μmol mg^{-1} min^{-1}, 15.38±0.05 μmol $mg^{-}min^{-1}$. The increased K_m values of immobilized enzymes indicated their lower affinity towards the substrate molecules which could be due to their structural conformations as a result of immobilization. The extent of structural conformations was greatly influenced on the method of immobilization. The excess adsorption of enzymes on to the support leads to the increased conformational changes in to the enzyme structure and thus caused lower accessibility of substrate molecules towards the active site of the enzyme. The immobilized enzymes have shown lower V_{max} values and this decrease was found to be more with adsorbed enzyme. This lower V_{max} value could be due to the mass transfer limitations as a result of loss of substrate molecules due to its lower accessibility and the blockage of enzyme active site by the overloading of enzyme. Similar observation was reported by Tavano et al. for the amylase immobilization using gluteraldehyde-agarose support [88].

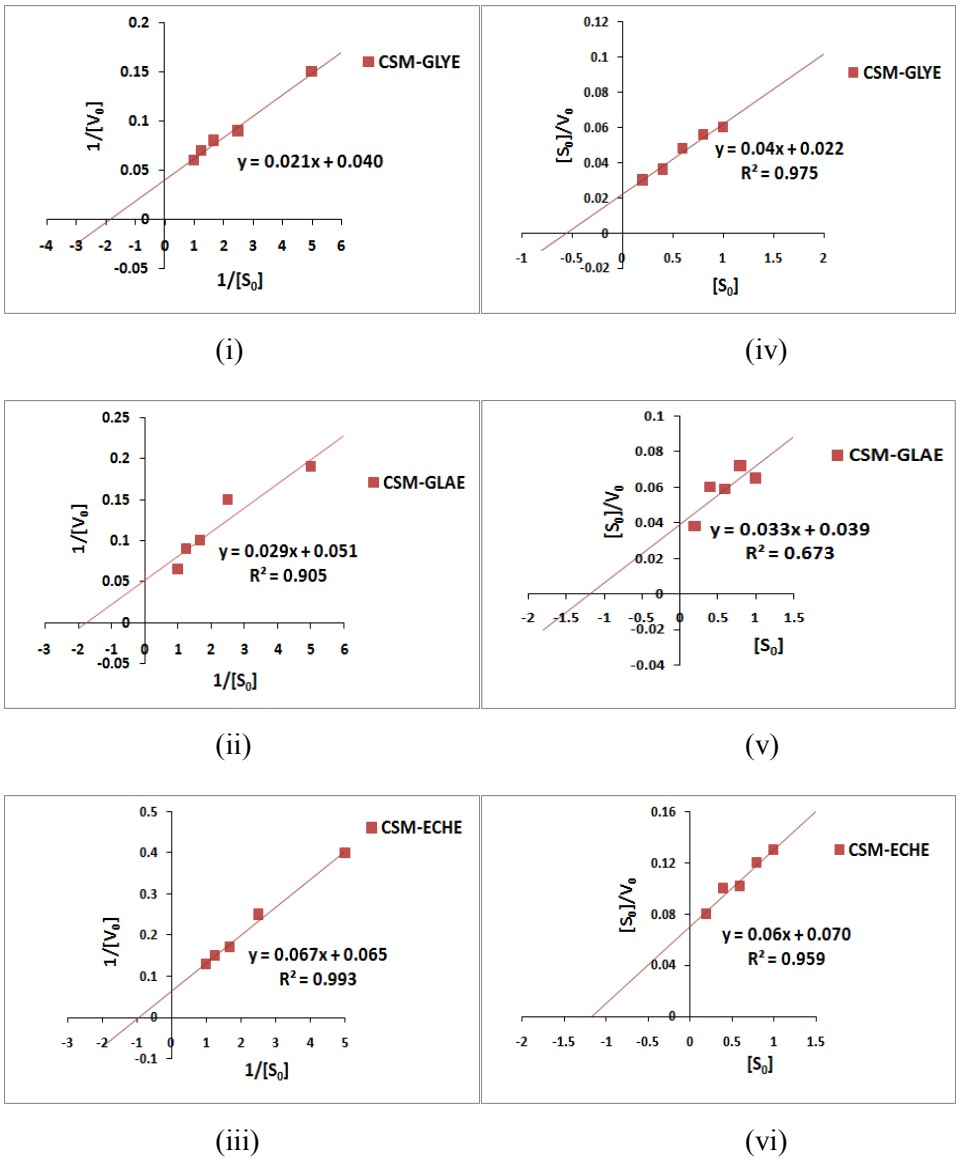

Figure: 2.31 Lineweaver-Burk plots for (i) CSM-GLYE (ii) CSM-GLAE (iii) CSM-ECHE andHanes-Woolf plots for (iv) CSM-GLYE (v) CSM-GLAE (vi) CSM-ECHE

The K_{cat} values of immobilized enzymes CSM-GLYE, CSM-GLAE and CSM-ECHE were 27.49 %, 43.15 % and 55.39 % lesser than that of free enzyme. The turn over number disclosed the time needed for the

conversion of one substrate molecule in to product which was 43.33, 55.28 and 70.42 milliseconds for CSM-GLYE, CSM-GLAE and CSM-ECHE respectively. Their catalytic efficiencies (K_{cat}/K_m) were found to be 37.85 %, 55.12 % and 80.51 % lower than that of free enzyme.

Table 2.11 Kinetic parameters for free and immobilized α-amylase on cross-linked composites

Immobilized enzyme	K_m (mg mL^{-1})	V_{max} (µmol mg^{-1} min^{-1})	K_{cat} (min^{-1})	K_{cat}/K_m (mL$mg^{-1}min^{-1}$)
Free enzyme	0.45± 0.02	34.48±0.05	1910.19	4244.87
CSM-GLYE	0.525± 0.04	25± 0.06	1385	2638.09
CSM-GLAE	0.57±0.06	19.6± 0.02	1085.84	1904.98
CSM- ECHE	1.03±0.03	15.38± 0.05	852.05	827.23

2.4.3.7 Storage stability of Immobilized α-amylase

The storage stability of immobilized enzymes was investigated for 90 days of storage and the observations are illustrated in the figure 2.32. Here we observed that covalently immobilized enzymes were retained more activity than that of adsorbed enzymes. After 90 days of storage CSM-GLYE and CSM-GLAE gained 65 % and 60 % of their initial activities respectively, whereas CSME and CSM-ECHE retained only about 40 % and 45 %. The covalent attachment between the enzyme and aldehyde groups on activated composites imparted higher conformational stability to the immobilized enzyme systems since it caused higher rigidity to the enzyme structure. Arpana Kumari et al. reported the improved storage stability of covalently immobilized α-amylase on chitosan and amberlite MB150 beads in which they retained 40 % and 55 % of initial activity after 100 days of storage [89].

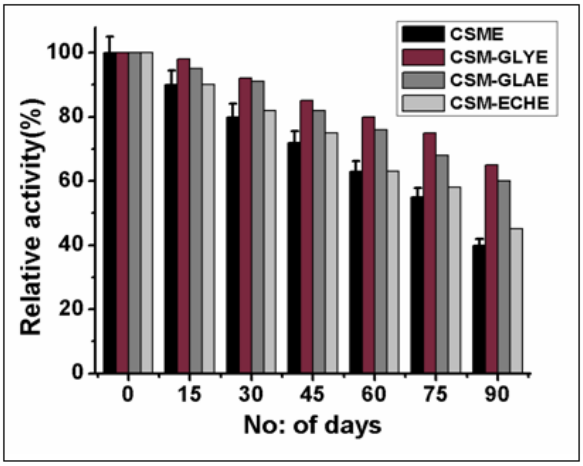

Figure: 2.32 Storage stability of immobilized α-amylase on magnetic chitosan and its cross-linked forms

2.4.3.8 Reusability

The reusability of immobilized enzymes was examined by ten repetitive batch reactions in which they have washed with desired buffer after the completion of each cycle and measured the enzyme activity for corresponding catalytic reaction. The figure 2.33 showed the relative activities of immobilized enzymes on repeated uses.

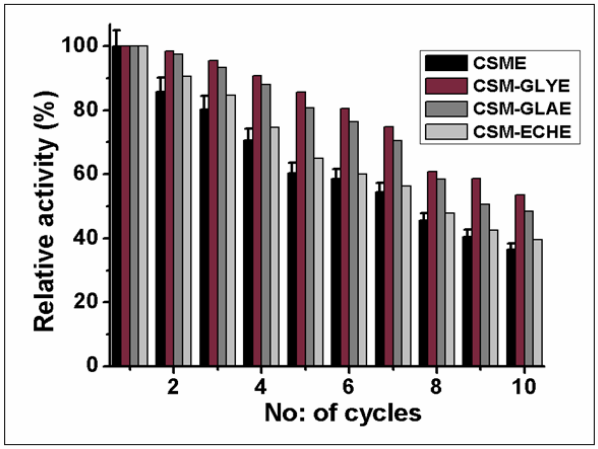

Figure: 2.33 Reusability of immobilized α-amylase on magnetic chitosan and its cross- linked forms

CSM-GLYE and CSM-GLAE retained more than 80 % of activity after five runs and they have acquired about 49 % and 53 % of activity after ten runs. But CSME and CSM-ECHE retained only 38 % and 40 % of their initial activity after ten cycles of uses. The decrease in enzyme activity could be due to the enzyme loss that has occurred by enzyme denaturaion or by enzyme leaching caused by weakening of bonds between enzyme and support. The recurrent encountering of substrate molecules towards the active site of the enzyme also caused loss of enzyme activity due to the distortion of enzyme conformation. For covalently immobilized enzymes, the strong bond between enzyme and bifunctional agents in support provide enough rigidity to the enzyme structure through intermolecular forces and thus minimized the enzyme loss due to the leakage or denaturation [90]. Shukla et al. observed that the immobilized amylase on nylon by covalent method could be reused with 50 % of activity after ten cycles of enzymatic reactions [91].

2.5 Conclusion

The details of various physico-chemical characterizations and experimental methods implemented in the study were described in this chapter. Chitosan-metal oxide composites CSM, CSZ and CST were synthesized, characterized and successfully subjected to α-amylase immobilization. The enzyme loading capacity of CSZ composite was found to be more than that of other composites which is attributed to its higher surface area. Due to the magnetic property, the CSM has been considered as the best support which resulted in high speed and gentle separation in the presence of an external magnetic field. The CSM was chemically modified by three types of cross-linking agents; CSM-GLY and CSM-GLA provided covalent immobilization of α-amylase and CSM-ECH leads to the

adsorption immobilization. The kinetic studies showed that the catalytic efficiencies of the covalently immobilized enzymes were much close to the free enzyme. The excellent immobilization efficiency, thermal stability, storage stability and reusability of the covalently immobilized enzyme systems make good candidates for industrial applications.

References

[1] X.G. Chen, C.S. Liu, C.G. Liu, X.H. Meng, C.M. Lee, H.J. Park, Preparation and biocompatibility of chitosan microcarriers as biomaterial, Biochemical Engineering Journal 27(3) (2006) 269-274.

[2] M.N. Ravi Kumar, A review of chitin and chitosan applications, Reactive and Functional Polymers 46(1) (2000) 1-27.

[3] B. Krajewska, Application of chitin-and chitosan-based materials for enzyme immobilizations: a review, Enzyme and Microbial Technology 35(2-3) (2004) 126-139.

[4] G. Spagna, F. Andreani, E. Salatelli, D. Romagnoli, P.G. Pifferi, Immobilization of α-L-arabinofuranosidase on chitin and chitosan, Process Biochemistry 33(1) (1998) 57-62.

[5] G. Spagna, R.N. Barbagallo, E. Greco, I. Manenti, P.G. Pifferi, A mixture of purified glycosidases from Aspergillus niger for oenological application immobilised by inclusion in chitosan gels, Enzyme and Microbial Technology 30(1) (2002) 80-89.

[6] M. Portaccio, S. Stellato, S. Rossi, U. Bencivenga, M. S. Mohy Eldin, F. S. Gaeta, D. Mita, Galactose competitive inhbition of β-galactosidase (A. oryzae) immobilized on chitosan and nylon supports, Enzyme and Microbial Technology 23(1) (1998) 101-106.

[7] S. Heon Lee, Y. Ha, B. Young Kim, B.S. Kim, Properties of cellulase immobilized on chitosan beads, Korean Society for Biotechnology and Bioengineering Journal 29(4) (2014) 239-243 (2014).

[8] C.M. Almeida, J.N. de Jesus, R.D. Ferreira, V.S. Varandas, P.A. Cavalcante, D.F. Coelho, J.R. Rodrigues, R.R. de Souza, T.S. de Oliveira, Immobilization of amylase using chitosan beads as support, Scientia Plena 13(11) (2017).

[9] L. Dong, G. Wang, Y. Xiao, Y. Xu, X. Zhou, H. Jiang, Q. Luo, Immobilization of glucose oxidase on a novel crosslinked chitosan support grafted with L-lysine spacers, Chemical and Biochemical Engineering Quarterly 25(3) (2011) 395-402.

[10] A. Ghanem, D. Skonberg, Effect of preparation method on the capture and release of biologically active molecules in chitosan gel beads, Journal of Applied Polymer Science 84(2) (2002) 405-413.

[11] R.S. Juang, F.C. Wu, R.L. Tseng, Use of chemically modified chitosan beads for sorption and enzyme immobilization, Advances in Environmental Research 6(2) (2002) 171-177.

[12] R.S. Juang, F.C. Wu, R.L. Tseng, Solute adsorption and enzyme immobilization on chitosan beads prepared from shrimp shell wastes, Bioresource Technology 80(3) (2001) 187-193.

[13] M. Kamburov, I. Lalov, Preparation of chitosan beads for trypsin immobilization, Biotechnology & Biotechnological Equipment 26 (2012) 156-163.

[14] S.H. Chiou, T.C. Hung, R. Giridhar, W.T. Wu, Immobilization of lipase to chitosan beads using a natural cross-linker, Preparative Biochemistry & Biotechnology 37(3) (2007) 265-275.

[15] S. Davis, L. Illum, Sustained release chitosan microspheres prepared by novel spray drying methods, Journal of Microencapsulation 16(3) (1999) 343-355.

[16] J. Filipovic-Grcic, B. Perissutti, M. Moneghini, D. Voinovich, A. Martinac, I. Jalsenjak, Spray-dried carbamazepine-loaded chitosan and HPMC microspheres: preparation and characterisation, Journal of Pharmacy and Pharmacology 55(7) (2003) 921-931.

[17] S.A. Agnihotri, N.N. Mallikarjuna, T.M. Aminabhavi, Recent advances on chitosan-based micro and nanoparticles in drug delivery, Journal of Controlled Release 100(1) (2004) 5-28.

[18] Z. Guo, S. Bai, Y. Sun, Preparation and characterization of immobilized lipase on magnetic hydrophobic microspheres, Enzyme and Microbial Technology 32(7) (2003) 776-782.

[19] S. Budriene, N. Gorochovceva, T. Romaskevic, L. Yugova, A. Miezeliene, G. Dienys, A. Zubriene, β-Galactosidase from Penicillium canescens. Properties and immobilization, Open Chemistry 3(1) (2005) 95-105.

[20] J. Shentu, J. Wu, W. Song, Z. Jia, Chitosan microspheres as immobilized dye affinity support for catalase adsorption, International Journal of Biological Macromolecules 37(1-2) (2005) 42-46.

[21] Z. Xianfang, E. Ruckenstein, Supported chitosan-dye affinity membranes and their protein adsorption, Journal of Membrane Science 117(1) (1996) 271-278.

[22] X. Zeng, E. Ruckenstein, Control of pore sizes in macroporous chitosan and chitin membranes, Industrial & Engineering Chemistry Research 35(11) (1996) 4169-4175.

[23] X. Zeng, E. Ruckenstein, Cross-linked macroporous chitosan anion-exchange membranes for protein separations, Journal of Membrane Science 148(2) (1998) 195-205.

[24] W.Y. Yang, M. Thirumavalavan, M. Malini, G. Annadurai, J.F. Lee, Development of silica gel-supported modified macroporous chitosan membranes for enzyme immobilization and their characterization analyses, The Journal of Membrane Biology 247(7) (2014) 549-559.

[25] R. Khan, A. Kaushik, P.R. Solanki, A.A. Ansari, M.K. Pandey, B. Malhotra, Zinc oxide nanoparticles-chitosan composite film for cholesterol biosensor, Analytica Chimica Acta 616(2) (2008) 207-213.

[26] A. Kaushik, R. Khan, P.R. Solanki, P. Pandey, J. Alam, S. Ahmad, B. Malhotra, Iron oxide nanoparticles–chitosan composite based glucose biosensor, Biosensors and Bioelectronics 24(4) (2008) 676-683.

[27] A. Kaushik, S. Arya, A. Vasudev, S. Bhansali, Nanocomposites based on chitosan- metal/metal oxides hybrids for biosensors applications, Journal of Nanoscience Letters 3 (2013) 32.

[28] R. Khan, M. Dhayal, Electrochemical studies of novel chitosan/TiO_2 bioactive electrode for biosensing application, Electrochemistry Communications 10(2) (2008) 263-267.

[29] M.Y. Chang, R.S. Juang, Stability and reactivity of acid phosphatase immobilized on composite beads of chitosan and ZrO_2 powders, International Journal of Biological Macromolecules 40(3) (2007) 224-31.

[30] I. Deveci, Y.I. Dogac, M. Teke, B. Mercimek, Synthesis and characterization of chitosan/TiO_2 composite beads for improving stability of porcine pancreatic lipase, Applied Biochemistry and Biotechnology 175(2) (2015) 1052-1068.

[31] J. Long, A. Jiao, B. Wei, Z. Wu, Y. Zhang, X. Xu, Z. Jin, A novel method for pullulanase immobilized onto magnetic chitosan/Fe_3O_4 composite nanoparticles by in situ preparation and evaluation of the enzyme stability, Journal of Molecular Catalysis B: Enzymatic 109 (2014) 53-61.

[32] C.H. Kuo, Y.C. Liu, C.M.J. Chang, J.H. Chen, C. Chang, C.J. Shieh, Optimum conditions for lipase immobilization on chitosan-coated Fe_3O_4 nanoparticles, Carbohydrate Polymers 87(4) (2012) 2538-2545.

[33] L. Zuluaga, O. Giraldo, C. Orrego, Immobilization of mannanase on magnetic chitosan microspheres, Revista Mexicana de Fisica 58(2) (2012) 39-43.

[34] L. Zang, J. Qiu, X. Wu, W. Zhang, E. Sakai, Y. Wei, Preparation of magnetic chitosan nanoparticles as support for cellulase immobilization, Industrial & Engineering Chemistry Research 53(9) (2014) 3448-3454.

[35] H. Fang, J. Huang, L. Ding, M. Li, Z. Chen, Preparation of magnetic chitosan nanoparticles and immobilization of laccase, Journal of Wuhan University of Technology-Mater. Sci. Ed. 24(1) (2009) 42-47.

[36] T.A. Costa-Silva, P.S. Marques, C.R.F. Souza, S. Said, W.P. Oliveira, Enzyme encapsulation in magnetic chitosan-Fe_3O_4 microparticles, Journal of Microencapsulation 32(1) (2015) 16-21.

[37] M. Ziegler-Borowska, D. Chelminiak-Dudkiewicz, T. Siodmiak, A. Sikora, K. Wegrzynowska-Drzymalska, J. Skopinska-Wisniewska, H. Kaczmarek, M. Marszall, Chitosan–collagen coated magnetic nanoparticles for lipase immobilization—new type of "enzyme friendly" polymer shell crosslinking with squaric acid, Catalysts 7(1) (2017) 26.

[38] O.A. Monteiro, C. Airoldi, Some studies of crosslinking chitosan–glutaraldehyde interaction in a homogeneous system, International Journal of Biological Macromolecules 26(2) (1999) 119-128.

[39] U. Filipkowska, T. Jozwiak, Application of chemically-cross-linked chitosan for the removal of reactive black 5 and reactive yellow 84 dyes from aqueous solutions, Journal of Polymer Engineering 33(8) (2013) 735-747.

[40] C. Pan, B. Hu, W. Li, Y. Sun, H. Ye, X. Zeng, Novel and efficient method for immobilization and stabilization of β-D-galactosidase by covalent attachment onto magnetic Fe_3O_4–chitosan nanoparticles, Journal of Molecular Catalysis B: Enzymatic 61(3) (2009) 208-215.

[41] D. Gambetta, A. Mendes, W. S. Adriano, L. Gonçalves, R. L.C. Giordano, Multipoint covalent immobilization of microbial lipase on chitosan and agarose activated by different methods, Journal of Molecular Catalysis B Enzymatic 51(3-4) (2008)100-109.

[42] O.H. Lowry, N.J. Rosebrough, A.L. Farr, R.J. Randall, Protein measurement with the folin phenol reagent, Journal of Biological Chemistry 193(1) (1951) 265-275.

[43] P. Bernfeld, Amylases, α and β, Methods in Enzymology 1 (1955) 149-158.

[44] C. Cao, L. Xiao, C. Chen, X. Shi, Q. Cao, L. Gao, In situ preparation of magnetic Fe_3O_4/chitosan nanoparticles via a novel reduction–precipitation method and their application in adsorption of reactive azo dye, Powder Technology 260 (2014) 90-97.

[45] S. Talam, S.R. Karumuri, N. Gunnam, Synthesis, characterization, and spectroscopic properties of ZnO nanoparticles, International Scholarly Research Network Nanotechnology 2012 (2012) 1-6.

[46] M. AbdElhady, Preparation and characterization of chitosan/zinc oxide nanoparticles for imparting antimicrobial and UV protection to cotton fabric, International Journal of Carbohydrate Chemistry 2012 (2012) 1-6.

[47] K. Thangavelu, R. Annamalai, D. Arulnandhi, Preparation and characterization of nanosized TiO_2 powder by sol-gel precipitation route, International Journal of Emerging Technology and Advanced Engineering 3(1) (2013) 636-639.

[48] D. Zvezdova, Synthesis and characterization of chitosan from marine sources in Black Sea, Association for the Advancement of Automotive Medicine 49 (2010) 65-69.

[49] G.Y. Li, Y.R. Jiang, K.L. Huang, P. Ding, L.L. Yao, Kinetics of adsorption of Saccharomyces cerevisiae mandelated dehydrogenase on magnetic Fe_3O_4-chitosan nanoparticles, Colloids and Surfaces A: Physicochemical and Engineering Aspects 320(1) (2008) 11-18.

[50] Z. Li, Y. Du, Z. Zhang, D. Pang, Preparation and characterization of CdS quantum dots chitosan biocomposite, Reactive and Functional Polymers 55(1) (2003) 35-43.

[51] C. Cao, L. Xiao, L. Liu, H. Zhu, C. Chen, L. Gao, Visible-light photocatalytic decolorization of reactive brilliant red X-3B on Cu_2O/crosslinked-chitosan nanocomposites prepared via one step process, Applied Surface Science 271 (2013) 105-112.

[52] S. Dhanavel, E. Nivethaa, V. Narayanan, A. Stephen, Photocatalytic activity of Chitosan/ZnO nanocomposites for degrading methylene blue, International Journal of ChemTech Research 6(3) (2014)1880-1882.

[53] P. Norranattrakul, K. Siralertmukul, R. Nuisin, Fabrication of chitosan/titanium dioxide composites film for the photocatalytic degradation of dye, Journal of Metals, Materials and Minerals 23(2) (2013).

[54] M. Zhang, D. Lei, X. Yin, L. Chen, Q. Li, Y. Wang, T. Wang, Magnetite/graphene composites: microwave irradiation synthesis and enhanced cycling and rate performances for lithium ion batteries, Journal of Materials Chemistry 20(26) (2010) 5538-5543.

[55] T. Theivasanthi, M. Alagar, Titanium dioxide (TiO_2) nanoparticles XRD analyses: An insight, arxiv Materials Science (2013).

[56] W. Li, L. Xiao, C. Qin, The characterization and thermal investigation of chitosan-Fe_3O_4 nanoparticles synthesized via a novel one-step modifying process, Journal of Macromolecular Science, Part A 48(1) (2010) 57-64.

[57] D.T.K. Dung, T.H. Hai, B.D. Long, P.N. Truc, Preparation and characterization of magnetic nanoparticles with chitosan coating, Journal of Physics: Conference Series, IOP Publishing, 2009, p. 012036.

[58] J. Nilsen-Nygaard, S.P. Strand, K.M. Varum, K.I. Draget, C.T. Nordgard, Chitosan: Gels and interfacial properties, Polymers 7(3) (2015) 552-579.

[59] H. Gustafsson, Enzyme immobilization in mesoporous silica, a doctoral dissertation, Chalmers University of Technology, 2013.

[60] D. Ningsih, D. Kartika, A. Fatoni, A. Zuliana, Bacillus thuringiensis HCB6 Amylase Immobilization by Chitosan Beads, IOP Conference Series: Materials Science and Engineering, IOP Publishing, 2017, p. 012068.

[61] E. Egwim, A.A. Adesina, O. Oyewole, I.N. Okoliegbe, Optimization of lipase immobilized on chitosan beads for biodiesel production, Global Research Journal of Microbiology 2(2) (2012)103-112.

[62] P. Ashly, M. Joseph, P. Mohanan, Activity of diastase α-amylase immobilized on polyanilines (PANIs), Food Chemistry 127(4) (2011) 1808-1813.

[63] Y. Zhou, L. Wang, T. Wu, X. Tang, S. Pan, Optimal immobilization of β-glucosidase into chitosan beads using response surface methodology, Electronic Journal of Biotechnology 16(6) (2013) 6-6.

[64] M.A. Abdel-Naby, A.M. Hashem, M.A. Esawy, A.F. Abdel-Fattah, Immobilization of Bacillus subtilis α-amylase and characterization of its enzymatic properties, Microbiological Research 153(4) (1999) 319-325.

[65] Yandri, P. Amalia, T. Suhartati, S. Hadi, Effect of immobilization towards thermal stability of α-amylase isolated from locale bacteria isolate Bacillus subtilis ITBCCB148 with calcium alginate, Asian Journal of Chemistry 25(12) (2013) 6897-6899.

[66] M.Y. Chang, R.S. Juang, Activities, stabilities, and reaction kinetics of three free and chitosan-clay composite immobilized enzymes, Enzyme and Microbial Technology 36(1) (2005) 75-82.

[67] S.A. Ahmed, O.K. Hassan, Studies on the activity and stability of immobilized bacillus acidocaldarius alpha-amylase, Australian Journal of Basic and Applied Sciences 2(3) (2008) 466-474.

[68] A. Kara, B. Osman, H. Yavuz, N. Besirli, A. Denizli, Immobilization of α-amylase on Cu^{2+} chelated poly (ethylene glycol dimethacrylate-n-vinyl imidazole) matrix via adsorption, Reactive and Functional Polymers 62(1) (2005) 61-68.

[69] A. El-Batal, K. Atia, M. Eid, Stabilization of α-amylase by using anionic surfactant during the immobilization process, Radiation Physics and Chemistry 74(2) (2005) 96-101.

[70] F. Eslamipour, P. Hejazi, Evaluating effective factors on the activity and loading of immobilized α-amylase onto magnetic nanoparticles using a response surface-desirability approach, RSC Advances 6(24) (2016) 20187-20197.

[71] K. Singh, A.M. Kayastha, Optimal immobilization of α-amylase from wheat (Triticum aestivum) onto DEAE-cellulose using response surface methodology and its characterization, Journal of Molecular Catalysis B: Enzymatic 104 (2014) 75-81.

[72] O. Danis, S. Demir, Y. Mulazim, M.V. Kahraman, Alpha-amylase immobilization on epoxy containing thiol-ene photocurable materials, Journal of Microbiology and Biotechnology 23(2) (2013) 205-210.

[73] G. Bayramoglu, M. Yilmaz, M.Y. Arica, Immobilization of a thermostable α-amylase onto reactive membranes: kinetics characterization and application to continuous starch hydrolysis, Food Chemistry 84(4) (2004) 591-599.

[74] M. Defaei, A. Taheri-Kafrani, M. Miroliaei, P. Yaghmaei, Improvement of stability and reusability of α-amylase immobilized on naringin functionalized magnetic nanoparticles: A robust nanobiocatalyst, International Journal of Biological Macromolecules 113 (2018) 354-360.

[75] M. Jahir Khan, Q. Husain, A. Azam, Immobilization of porcine pancreatic α-amylase on magnetic Fe_2O_3 nanoparticles: Applications to the hydrolysis of starch, Biotechnology and Bioprocess Engineering 17 (2) (2012) 377-384.

[76] S. Talekar, S. Chavare, Optimization of immobilization of alpha amylase in alginate gel and it's comparative biochemical studies with free alpha amylase, Recent Research in Science and Technology 4(2) (2012) 1-5.

[77] Zusfahair, D. R Ningsih, D. Kartika, A. Fatoni, A. L Zuliana, Bacillus thuringiensis HCB6 amylase immobilization by chitosan beads, Materials Science and Engineering 172 (2017) 012068.

[78] H. Guo, Y. Tang, Y. Yu, L. Xue, J.Q. Qian, Covalent immobilization of α-amylase on magnetic particles as catalyst for hydrolysis of high-amylose starch, International Journal of Biological Macromolecules 87 (2016) 537-544.

[79] O. Prakash, N. Jaiswal, Immobilization of a thermostable-amylase on agarose and agar matrices and its application in starch stain removal, World Applied Sciences Journal 13(3) (2011) 572-577.

[80] P. Tripathi, L.L. Leggio, J. Mansfeld, R. Ulbrich-Hofmann, A.M. Kayastha, α-amylase from mung beans (Vigna radiata)-Correlation of biochemical properties and tertiary structure by homology modelling, Phytochemistry 68(12) (2007) 1623-1631.

[81] U. Hanefeld, L. Gardossi, E. Magner, Understanding enzyme immobilization, Chemical Society Reviews 38(2) (2009) 453-468.

[82] M.Y. Chang, R.S. Juang, Activities, stabilities, and reaction kinetics of three free and chitosan-clay composite immobilized enzymes, Enzyme and Microbial Technology 36(1) (2005) 75-82.

[83] M.T. Martin, M. Alcalde, F.J. Plou, L. Dijkhuizen, A. Ballesteros, Synthesis of malto-oligosaccharides via the acceptor reaction catalyzed by cyclodextrin glycosyltransferases, Biocatalysis and Biotransformation 19(1) (2001) 21-35.

[84] D. Driss, Z. Driss, F. Chaari, S.E. Chaabouni, Immobilization of His-tagged recombinant xylanase from Penicillium occitanis on nickel-chelate Eupergit C for increasing digestibility of poultry feed, Bioengineered 5(4) (2014) 274-279.

[85] T.N. Nwagu, B. Okolo, H. Aoyagi, S. Yoshida, Improved yield and stability of amylase by multipoint covalent binding on polyglutaraldehyde activated chitosan beads: Activation of denatured enzyme molecules by calcium ions, Process Biochemistry 48(7) (2013) 1031-1038.

[86] N. Sohrabi, N. Rasouli, M. Torkzadeh, Enhanced stability and catalytic activity of immobilized α-amylase on modified Fe_3O_4 nanoparticles, Chemical Engineering Journal 240 (2014) 426-433.

[87] M.Y. Arica, V. Hasirci, N.G. Alaeddinoğlu, Covalent immobilization of α-amylase onto pHEMA microspheres: preparation and application to fixed bed reactor, Biomaterials 16(10) (1995) 761-768.

[88] O.L. Tavano, R. Fernandez-Lafuente, A.J. Goulart, R. Monti, Optimization of the immobilization of sweet potato amylase using glutaraldehyde-agarose support. Characterization of the immobilized enzyme, Process Biochemistry 48(7) (2013) 1054-1058.

[89] A. Kumari, A.M. Kayastha, Immobilization of soybean (Glycine max) α-amylase onto Chitosan and Amberlite MB-150 beads: Optimization and characterization, Journal of Molecular Catalysis B: Enzymatic 69(1) (2011) 8-14.

[90] T.N. Nwagu, B.N. Okolo, H. Aoyagi, Stabilization of a raw-starch-digesting amylase by multipoint covalent attachment on glutaraldehyde-activated amberlite beads, Journal of Microbiology and Biotechnology 22(5) (2012) 628-636.

[91] S. Shukla, L. Jajpura, Immobilisation of amylase by various techniques, Indian Journal of Fibre & Textile Research 30 (2005) 75-81.

Chapter 3

Modified forms of magnetic chitosan by synthetic polymers as α-amylase carriers

Contents

3.1 Introduction

Synthetic polymers have been firstly recognized as attractive carriers for biologically active materials by Isliker and coworkers in 1950's, and were extended to the field of enzyme immobilization over the period of next decades. Monomers that form the polymeric chain can be selected based on the nature of enzyme and the immobilization process. The nature and quantity of the monomers determine the chemical structure and properties of the polymer. The functional groups present on the polymer structure promote the enzyme binding [1, 2] and have important role in deciding the method by which the immobilization process has been occurred. These functional groups also influence the hydrophilic or hydrophobic interactions of support with the enzyme [3]. The polymeric supports also determine the length of enzyme-support spacer; the longer spacer maintain increased conformational flexibility to the enzyme and the shorter to prevent the thermal inactivation of enzyme molecules which causes the reduction in enzyme leaching [4]. The polymer materials as effective enzyme carrier can

improve the stability of immobilized enzyme by protecting the active site of the enzyme from the adverse effect of experimental conditions and reaction system [5].

The conducting polymers have gained much attention in the field of enzyme immobilization because of their environmental stability and promising electrochemical properties [6]. The polymeric support materials such as polyaniline (PANI) and polypyrrole (PPY) have been widely used for enzyme immobilization as they provide suitable environment for immobilization of enzymes.

PANI has become very attractive due to its simple method of synthesis, low-cost, biocompatibility, environmental stability, higher temperature and pH stability, stable chemical properties and favorable electrical and optical properties [7-9]. Many enzymes such as amylase, glucoamylase, urease, horseradish peroxidase, and glucose oxidase have been successfully immobilized on PANI [10-13]. In many literatures, it is reported that PANI has been incorporated into flexible matrices in order to overcome its limitations in solubility and mechanical properties. Tiwari et al. reported that chitosan along with PANI turned to be an efficient carrier for immobilization of creatine amidinohydrolase by covalent method [14]. Here the composite achieved the combining properties of good processability of the matrix and the electrical conductivity of the conducting polymer. PPY performs as an efficient carrier due to high electrical conductivity, biocompatibility and its facile synthesis at low cost compared to other polymers [15, 16]. The poor mechanical and thermal stability are the major drawbacks of PPY in the field of enzyme immobilization and these can be

overcome by its composites. Many reports are available regarding the nanocomposites of PPY and their application in the field of biosensors. The enzymes cytochrome c, glucose oxidase and polyphenol oxidase were successfully immobilized on gold polypyrrole (Au–PPY) nanocomposite [17]. The electrically conductive nanocomposite polypyrrole–titanium (IV) phosphate (PPY–TiP) by facile in situ chemical oxidative polymerization was immobilized on yeast alcohol dehydrogenase [18]. Yi Fang et al. have developed polypyrrole-chitosan nanocomposite by combining the conductivity of polypyrrole and biocompatibility of chitosan for immobilization of glucose oxidase and constructed a novel glucose biosensor [19].

Another important movement for the utilization of polymers in the enzyme immobilization field is the arrival of copolymers from the suitable monomers and comonomers. Many copolymers are produced typically on the basis of acrylic and methacrylic acid derivatives. The grafted copolymers were effectively used as the carriers for enzyme immobilization. They provide various functionalities corresponding to the main chain and also to the introduced grafted chains [20]. The grafted copolymerization offers increased number of reactive groups which can be controlled and hence the microenvironment of the enzyme can also be changed. The enzyme immobilization by graft copolymerization onto polysaccharides was reported by D'Angiuro et al. where the enzyme was bound to the support by keeping the ratio of one enzymatic macromolecule for one polysaccharide macromolecule and thus imparting the immobilized enzyme system with good kinetic properties [21].

Polyacrylonitriles (PAN) are excellent candidates for enzyme immobilization due to their mechanical and chemical stability [22, 23]. Introducing functional groups into the PAN backbone facilitate the enzyme immobilization process since its chemical inertness and hydrophobicity have been reduced as a result of functionalization. Xiao-yan et al. has reported the modified form of PAN membrane grafted with acrylamide and its use in enzyme immobilization of cellulase [24, 25]. The incorporation of PAN with a natural polymer makes it biocompatible which is very essential for enzyme immobilization since this property favor more activity to the enzyme by providing specific microenvironment [26]. PAN membrane was treated with biocompatible chitosan for the effective immobilization of acetylcholinesterase [27]. Polymethyl methacrylate (PMMA) can be considered as suitable enzyme carrier with appropriate mechanical strength and PMMA grafted chitosan copolymer as new polymeric support with good mechanical and biocompatibility properties [28]. Abd El-Ghaffar et al. observed the continuous catalytic reaction of α-chymotripsin immobilized on to chitosan grafted PMMA without loss of its activity [29].

The present chapter deals with the surface modification of magnetic chitosan with the synthetic polymers, polyaniline and polypyrrole. This also comprises the graft copolymerization of magnetic chitosan with methyl methacrylate and acrylonitrile. α-amylase was immobilized on all the modified forms of magnetic chitosan and the efficiencies of enzyme carriers were compared with each other.

3.2 Materials Used

Aniline, pyrrole, methyl methacrylate, acrylonitrile and ceric ammonium nitrate were purchased from Sigma Aldrich. Ammonium per sulphate, sodium hydroxide and ferric chloride were obtained from S.d. Fine Chemicals Ltd. The materials used for synthesis of magnetic chitosan and the chemicals for protein estimation and activity assay are presented in the chapter 2.

3.3 Magnetic chitosan-synthetic polymer composites as α-amylase carriers

3.3.1 Synthesis of magnetic chitosan-polyaniline (CSM-PANI) composite

The synthesis of CSM-PANI involves two steps. The first step consists of synthesis of magnetic chitosan suspension as described in the earlier chapter. The second step involves the addition of APS oxidant (0.25 M in 50 mL of 1.0 M HCl) into aniline solution (0.9 mL in 80 mL of 1.0 M HCl). The reaction vessel was kept in an ice bath for 5 h under magnetic stirring. The solution changed from colorless to dark green and the precipitate was washed three times with distilled water, in which magnetic chitosan suspension was mixed together in a single beaker. After that the solution stirred vigorously for 30 min. and then kept for 24 h without any disturbance. The product was filtered and washed with distilled water until the filtrate became colorless, then washed with ethanol and dried in vacuum oven at 80 °C for 12 h.

The reaction can be depicted as shown in the scheme 3.1.

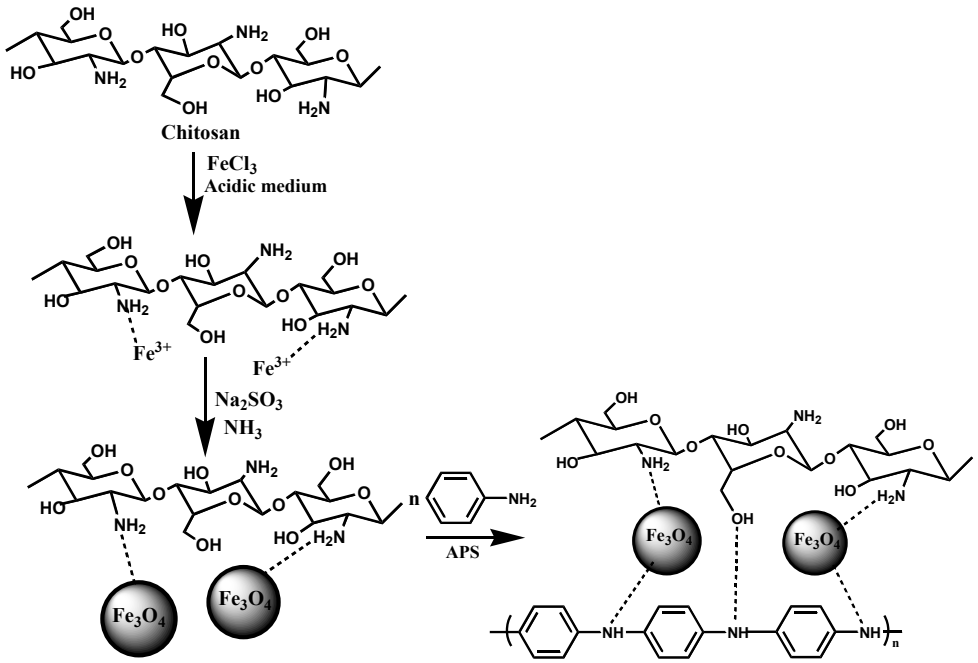

Scheme 3.1 Composite formation of magnetic chitosan with polyaniline

3.3.2 Synthesis of magnetic chitosan-polypyrrole (CSM-PPY) composite

The modified magnetic chitosan by polypyrrole (CSM-PPY) was synthesized in accordance with the already reported procedure with slight modification [30]. About 0.5 mL pyrrole was added into the chitosan solution (1 g in 100 mL of 2 % acetic acid) and the resulting solution was stirred for 45 min. Then 2.82 g anhydrous $FeCl_3$ was added to the solution in an ice bath, keeping $FeCl_3$/pyrrole ratio, 2.45:1. The mixture was stirred overnight and then sodium hydroxide solution was added slowly to the resulting solution. The obtained composite was washed with distilled water several times, followed by ethanol and collected by centrifugation and it was dried in an oven at 50 ºC for 2 days.

The reaction can be depicted as shown in the scheme 3.2.

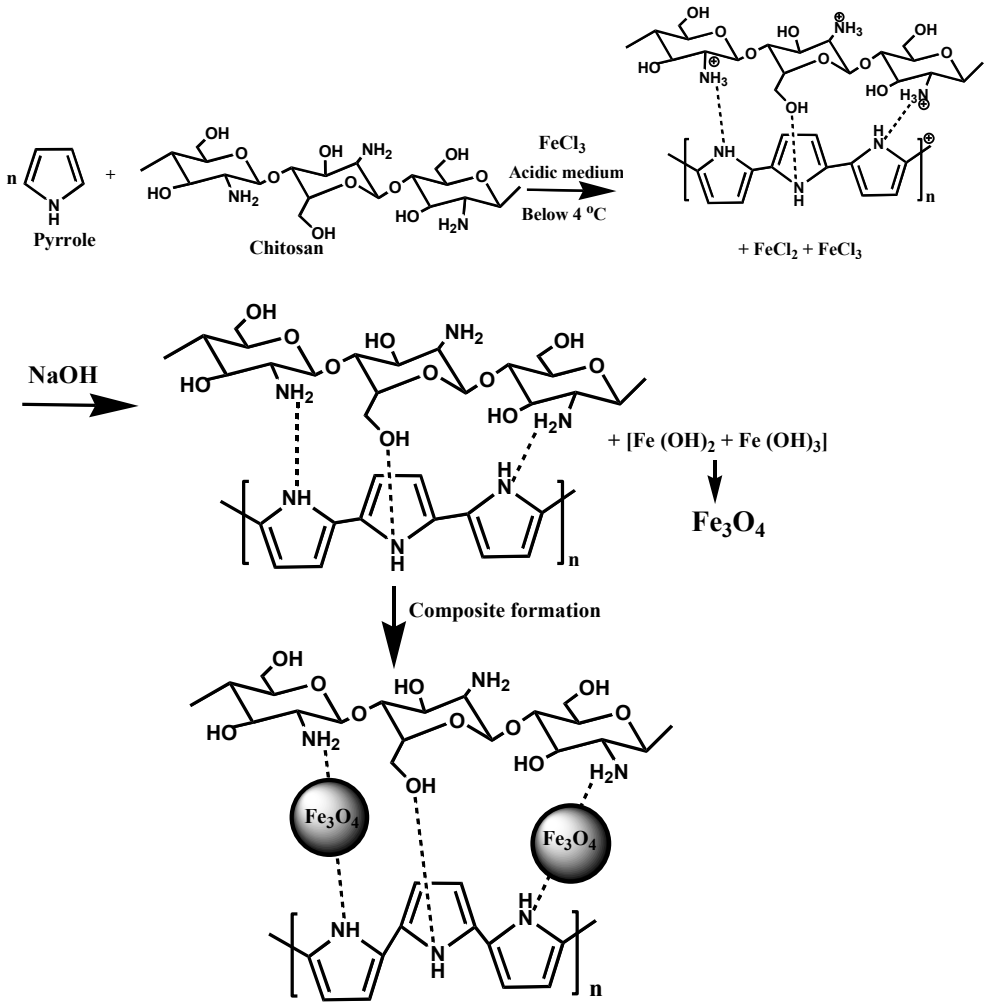

Scheme 3.2 Composite formation of magnetic chitosan with polypyrrole

3.3.3 Physico-chemical characterization

3.3.3.1 Infrared spectra

The IR spectra recorded for modified forms of magnetic chitosan with synthetic polymers are shown in the figure 3.1 and their peak assignments are given in the table 3.1. In case of CSM-PANI composite, the broad peak observed at 3435 cm^{-1} indicates the combined N–H stretching

vibration of PANI and O–H stretching vibration of chitosan. The absorption band at 1078 cm^{-1} is ascribed to the C–O stretching vibration of primary alcoholic group of chitosan and the peak at 610 cm^{-1} to the deformation of benzene ring of polyaniline. The peak at 1472 cm^{-1} and 1571 cm^{-1} corresponds to the C=C and C=N stretching vibrations of benzenoid and quinoid rings. This results showed that the polyaniline is in emeraldine salt form [31, 32]. There was C–N stretching vibration for aromatic secondary amines at 1260 cm^{-1} and the peak at 1121cm^{-1} was assigned to the C–H in plane bending vibration. All the peaks corresponding to polyaniline confirmed the high degree of delocalization of electrons and good electrical conductivity of the composite [33, 34].

For CSM-PPY, the broad peak at 3430 cm^{-1}corresponds to the combined N–H stretching vibration of PPY and O–H stretching vibration of chitosan. The absorption peaks at 1546 cm^{-1} and 1628 cm^{-1} were assigned to C=C stretching of benzenoid and quinoid rings of poypyrrole respectively and the peak at 1315 cm^{-1} to C–N stretching vibration of the ring. The peak at 1166 cm^{-1} indicated the C–H plane deformation and 780 cm^{-1} for C–H out of plane ring deformation. All these vibrations evidence towards the conductivity of the composite and the results are good agreement with the previous reports [35, 36].

The main chitosan peaks (3429 cm^{-1}, 1074 cm^{-1}) shifted to higher frequencies in case of both of the composites, for instance due to the effective interaction between chitosan and polymers. Similar observations are reported in many studies [37, 38].

For both of the polymer composites, the existence of Fe–O bond which could be occurred in the range 500-600 cm^{-1}; for CSM-PANI it was

found to be at 577 cm^{-1} and that appeared at 570 for CSM-PPY. The peak corresponding to Fe–O bond vibration of pure magnetite (580 cm^{-1}-584 cm^{-1}) was shifted to lower vibrational frequencies, which might be as a result of electrostatic interaction between the negatively charged magnetite surface and the positively protonated amino groups of chitosan and the polymers [39, 40].

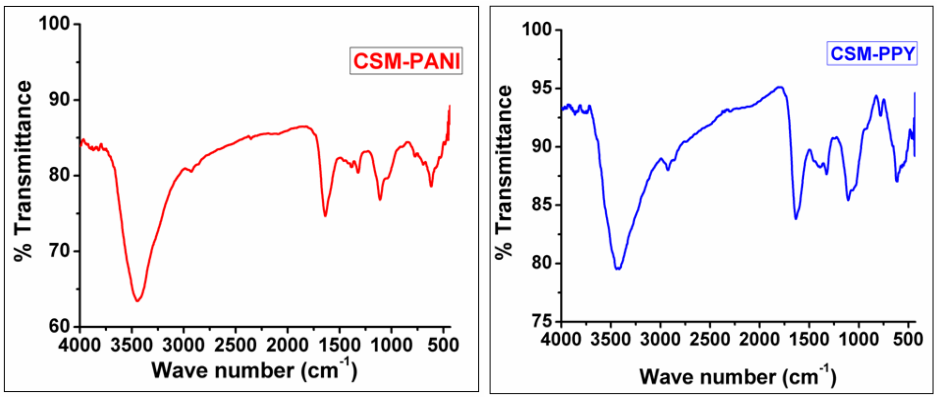

(i) (ii)

Figure: 3.1 IR Spectra of (i) CSM-PANI and (ii) CSM-PPY

Table 3.1 Peak assignments for polymers modified magnetic chitosan

Peak assignment (cm^{-1})	CSM-PANI	CSM-PPY
N–H and O–H stretching vibration	3435	3430
C=C stretching vibration of benzenoid ring	1472	1546
C=C stretching vibration of quinoid ring	-	1628
C=N stretching vibration of quinoid ring	1571	-
C-N stretching vibration of secondary aromatic amines	1260	1315
C-H in plane bending vibration	1121	1166
C-H out of plane ring deformation	510	780
C-O stretching vibration of alcoholic group	1078	1074
Fe-O bond vibration	577	570

3.3.3.2 X-ray powder diffraction spectra

In the case of CSM-PANI the diffraction peak corresponding to PANI at 25º indicates some degree of crystallinity in its emeraldine salt

form [41, 42]. The other diffraction peaks at 2θ = 29.9°, 35°, 43.1°, 53.5°, 57.2° and 63°, corresponding to (220), (311), (400), (422), (511), and (440) of the crystalline Fe_3O_4 phase are also observed in the spectra.

There is a broad peak at 24º for CSM-PPY composite indicates the amorphous form of PPY. The other diffraction peaks observed at 2θ = 30°, 35°, 43°, 54°, 57° and 63° can be indexed with crystallographic planes to (220), (311), (400), (422), (511), and (440) respectively which are related to crystalline Fe_3O_4 phase.

The diffraction peak for chitosan at 2θ=20º has become very weak and broad which indicates the reduction in its crystallinity. This confirms the interaction of chitosan with polymer through the plenty of functional groups present on them during the composite formation [43, 44].

The average particle size of the composites was evaluated using the Debye–Scherrer equation. The particle size of CSM-PANI composite was found to be 39.44 nm and that of CSM-PPY composite was about 36.48 nm.

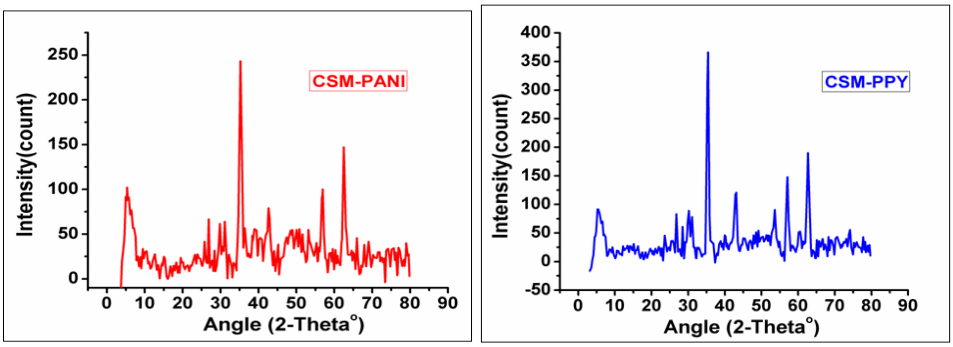

(i) (ii)

Figure: 3.2 XRD spectra of (i) CSM-PANI and (ii) CSM-PPY

3.3.3.3 Thermal analysis

Both of the composites exhibited three step weight losses. In case of CSM-PANI, the first stage of weight loss, found to be below 150 °C, attributed to the loss of physically adsorbed water from the polymer structure. The second weight loss was observed in the range of 200-350 °C might be due to the degradation of chitosan and the third major weight loss between 620-700 °C assigned to the decomposition of PANI main chain. The composite exhibited about 60 % of weight loss at 700 °C, was attributed to the high thermal stability of magnetic chitosan due to its modification by polyaniline. Similar trend is reported by Ayse et al. for chitosan/polyaniline composite which showed better final degradation temperature than chitosan itself [45].

In case of CSM-PPY, the loss of moisture can be observed in the range of 40-150 °C and the second major weight loss between 200 ºC to 350 ºC represents the degradation of chitosan. The rapid weight loss from 600 ºC to 700 ºC attributed to the decomposition of PPY backbone and this confirms the composite formation of magnetic chitosan with polypyrrole [46].

The results showed that the synthesized composites have exhibited better thermal stabilities compared to magnetic chitosan and the TGA-DTG curves of both composites are given in the figure 3.3.

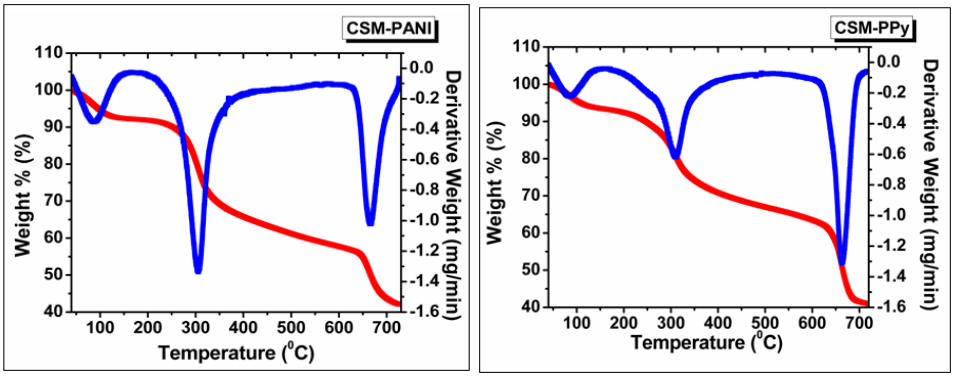

(i) (ii)

Figure: 3.3 TGA-DTG curves of (i) CSM-PANI and (ii) CSM-PPY

3.3.3.4 Scanning electron microscopy

The surface morphologies of the composites were analyzed by SEM micrographs and they are depicted in the figure 3.4.

The SEM image of CSM-PANI composite displayed plate-like structure which indicated that theaniliniumions were adsorbed on the surface of dispersed CSM particles and then undergone oxidative polymerization in a highly acidic condition. The delocalization of charge between the alternative benzenoid rings and imino groups with flat configuration was possible in order to attain the stability and the system having internal chain ordering with plate-like structure. This plate-like morphology has some influence on electrical conductivity and electrochemical properties [47].

For SEM image of CSM-PPY, the composite has exhibited in spherical shape. The formation of coarse particles with spherical shape as a result of polymerization of pyrrole was also reported by Bhaumik et al. in which the reaction has taken place with anhydrous $FeCl_3$ in acidic medium [48].

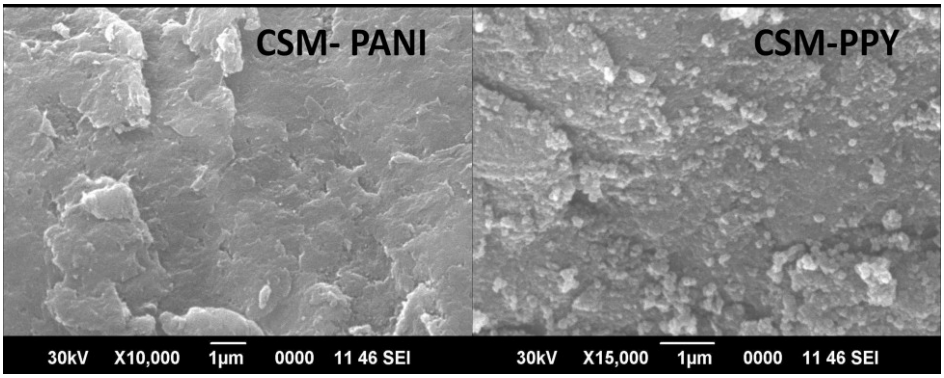

Figure: 3.4 SEM images of CSM-PANI and CSM-PPY

3.3.3.5 Surface area analysis

The surface area obtained for CSM-PANI and CSM-PPY are 7.76 m^2 g^{-1} and 19.36 m^2 g^{-1} respectively. Both of the composites have shown higher surface area compared to magnetic chitosan. The decrease of surface area of CSM-PANI could be due to the presence of agglomerated polymer particles incorporated with the magnetic chitosan.

3.3.3.6 Vibrating sample magnetometry

The magnetization curves obtained for both composites are presented in the figure 3.5. The magnetic saturation values calculatedwas 11.51 emu g^{-1} for CSM-PANI and 16.77 emu g^{-1} for CSM-PPY. These composites have shown decreased Ms values when compared to magnetic chitosan that may be due to the existence of non magnetic polymer layer coating [49].

Among these composites, CSM-PPY exhibited more Ms value than CSM-PANI. The high Ms value can be originated from the larger loading of magnetite particles which make the composite to be a promising adsorbent for enzymes as the immobilized systems can be easily separated by applying an external magnetic field.

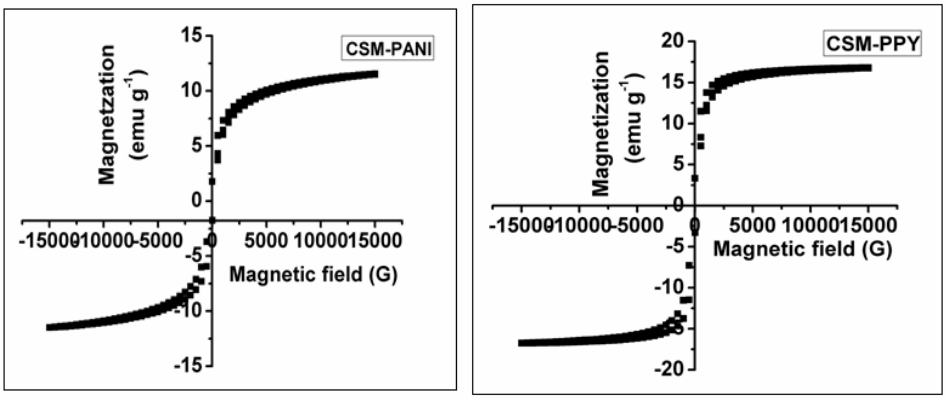

(i) (ii)

Figure: 3.5 Magnetization curves of (i) CSM-PANI and (ii) CSM-PPY

3.3.3.7 CHN analysis

The CHN analysis has provided the carbon, hydrogen and nitrogen contents of CSM, CSM-PANI and CSM-PPY composites and the data are given in the table 3.2. The percentage compositions for C, N and H are found to be higher for polymer composites compared to CSM confirmed its surface modification.

Table 3.2 CHN analytical data of CSM, CSM-PANI and CSM-PPY

composite	N (%)	C (%)	H (%)
CSM	2.33	11.28	2.25
CSM-PANI	5.84	31.64	4.94
CSM-PPY	5.64	24.22	3.75

3.3.3.8 Energy dispersive X-ray analysis

Elemental data of the modified composites gained from this analysis are compared with that of CSM composite and are presented in the table 3.3. The corresponding EDX spectra are shown in the figure 3.6. The increased amount of C and N, decreased amount of O and Fe in CSM-PANI and CSM-PPY stand for the clear evidences for the modification of CSM composite.

Table 3.3 Elemental data of (i) CSM, (ii) CSM-PANI and (iii) CSM-PPY

Element	Weight %	Atomic %
O	42.23	41.93
C	24.04	31.79
N	19.64	22.27
Fe	14.09	4.01

(i)

Element	Weight %	Atomic %
O	42.23	41.93
C	24.04	31.79
N	19.64	22.27
Fe	14.09	4.01

(ii)

Element	Weight %	Atomic %
O	38.67	36.50
C	28.06	37.15
N	21.26	22.35
Fe	10.15	2.85

(iii)

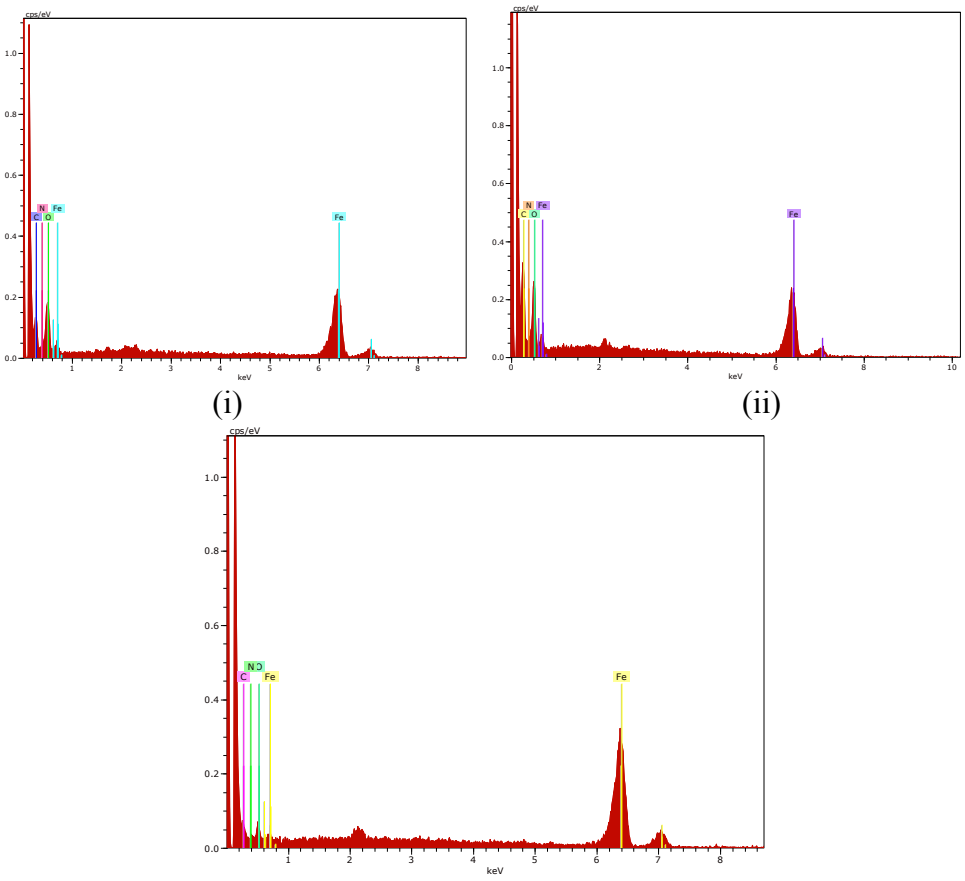

(i) (ii)

(iii)

Figure: 3.6 EDX spectra of (i) CSM, (ii) CSM-PANI and (iii) CSM-PPY

3.3.4 Immobilization of α-amylase on magnetic chitosan-synthetic polymer composites

3.3.4.1 Optimization of α-amylase immobilization conditions

The influence of various immobilization conditions such as pH of the medium, incubation time and enzyme concentration on enzyme activity was determined to get the optimum results.

3.3.4.1.1 Effect of immobilization pH on α-amylase activity

The variation of immobilization pH in the range of 4-9 on relative activity is given in the figure 3.7. The figure showed that CSM-PANI composite exhibited maximum activity at pH 7 and for CSM-PPY it was at pH 6. The decreased activity above and below the optimum values may be due to the unfavorable charge distribution on enzyme and the supports, that result in the conformational changes in the enzyme structure.

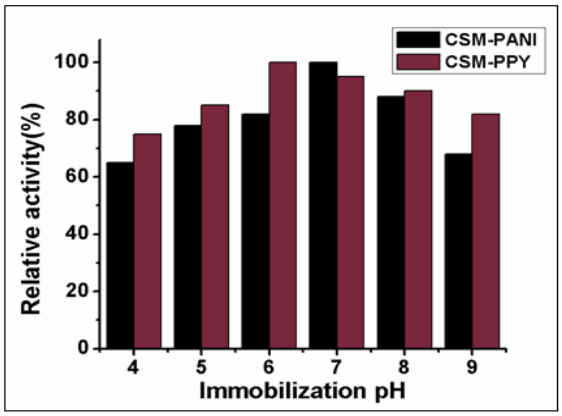

Figure: 3.72 Effect of immobilization pH on the relative activity of α-amylase

The isoelectric points of polyaniline (Ip ~7.6) and polypyrrole (Ip ~7) have great influence on the interaction of enzyme with the support since the Ip of the composites depend on that of chitosan, magnetite and the polymers [50, 51].

In case of CSM-PANI, at pH 7 the composite may attain slightly positive charge and hence it electrostatically interacts with negatively charged α-amylase (Ip ~ 4.6). It is a common phenomenon that the shift in optimum pH of enzyme is observed as a result of immobilization. The microenvironment of the enzyme molecule depends on the surface charges on the solid support and the nature of the bound enzyme due to the immobilization which results in the shift in optimum pH of the enzyme.

As the α-amylase exhibited maximum activity at pH range 5-5.5, it is seemed to denature at higher pH ranges and here we observed that the cationic environment of the composite tend to shift the pH optimum to alkaline region. As the support exhibited increased positive charge on the amino groups, the concentration of H^+ ions in the microenvironment of the immobilized system decreases which leads to the shift in optimum pH to more alkaline region. For CSM-PPY at pH 6, it can interact electrostatically with the enzyme as it acquired positive charges at that region. As going to higher pH, the enzyme activity is found to be decreased for both of the supports, since the enzyme and the supports carrying net negative charge which leads to electrostatic repulsion [52].

3.3.4.1.2 Effect of contact time on α-amylase activity

The contact time required for the enzyme onto the composites in order to obtain maximum activity is shown in the figure 3.8.

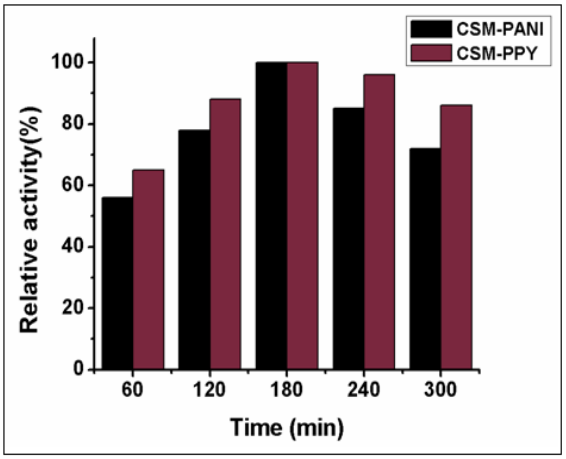

Figure: 3.8 Effect of contact time on immobilized α-amylase activity

It was found that for both of the composites, relative enzyme activities are increased up to 180 min. giving optimum contact time for immobilization. After that the activity is found to be decreased which may be due to the lower accessibility of the substrate towards the enzyme. This can be as a result of multilayer adsorption of the enzyme that leads to the active site to get blocked and hence become deformed. Similar trend was reported when the composite of alginate polymer with magnetic chitosan immobilized on lipase [53].

3.3.4.1.3 Effect of initial amount of protein on protein loading on to composites

The variation of enzyme concentration on immobilization was optimized as the loaded amount of protein play a significant role in the activity of enzyme. The figure 3.9 showed the variation of loaded protein with respect to the initial protein concentration.

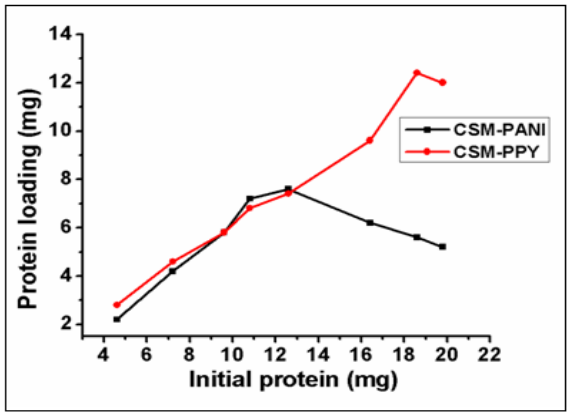

Figure: 3.9 Effect of initial protein amount on protein loading

Here we observed that as the initial protein taken for the immobilization process increases the amount of loaded protein reaches to the maximum value and thereafter no significant increase in protein loading.

In case of CSM-PANI, the maximum protein loading of 7.6 mg g^{-1} support is obtained at the initial amount of 12.6 mg enzyme. For CSM-PPY, the high protein loading of 12.4 mg g^{-1} support was found to be at initial protein amount of 18.6 mg. After these initial enzyme concentrations, the loaded protein on the support get decreases and this saturation point depends on the nature of support and the immobilization method. The adsorption immobilization of the enzyme mainly depends on the surface area of the support. Here the CSM-PPY showed higher surface area than CSM-PANI and correspondingly showed higher loading of enzyme on its surface.

3.3.4.1.4 Effect of initial protein amount on immobilized enzyme activity

A study on variation of enzyme activity with respect to initial protein concentration was carried out and the results are shown in the figure 3.10.

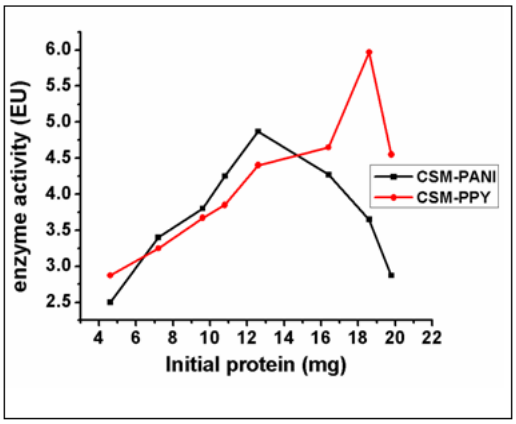

Figure: 3.10 Effect of initial protein amount on immobilized enzyme activity

For CSM-PANI, the optimum enzyme activity of 4.87 EU was obtained at the initial amount of 12.6 mg enzyme and the immobilized enzyme on CSM-PPY exhibited 5.97 EU at initial amount of 18.6 mg enzyme. For both of the immobilized enzymes, the enzyme activity gets reached to maximum value as the initial enzyme concentration increases. The decrease in enzyme activity beyond this saturation value may be due to the multilayer adsorption of the enzyme molecules on the surface of the supports. It was supposed that this may leads to the lower diffusion of the substrate as a result of the higher initial enzyme concentration and at this higher concentration the protein-protein interactions lead to the deformation of their active site which results in the decline of enzyme activity. Furthermore the steric hindrance exists between the large substrate molecule and the extra loaded enzyme which in turn decreased the activity of enzyme.

The immobilization yield, activity yield and immobilization efficiency of the enzyme on the two supports are tabulated in the table 3.4. CSM-PANI and CSM-PPY have shown immobilization yield of 60.32 % and 66.67 % respectively. The immobilization efficiency was higher for CSM-PPY than CSM-PANI which was 56.25 % and 45.82 % respectively.

Table 3.4 Immobilization efficiency of α-amylase on polymers modified magnetic chitosan

Support	Initial protein (mg)	Immobilized protein mg/g support	IY (%)	Initial activity (EU)	Immobilized enzyme activity (EU)	AY (%)	IE (%)
CSM-PANI	12.6	7.6	60.32	17.62	4.87	27.64	45.82
CSM-PPY	18.6	12.4	66.67	15.92	5.97	37.5	56.25

3.3.4.2 Effect of pH on α-amylase activity

The effect of reaction pH on activity of free and immobilized enzymes was examined and the results are shown in the figure 3.11.

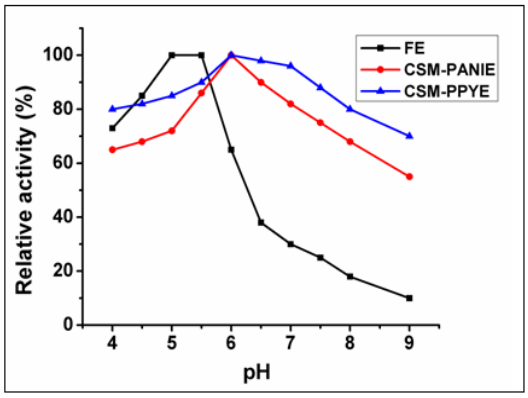

Figure: 3.11 Effect of pH on the relative activity of free and immobilized α-amylase on modified forms of magnetic chitosan

Both of the immobilized enzymes have shown the shift of optimum pH to alkaline region. The unequal partitioning as a result of electrostatic interaction exists between the microenvironment of the immobilized enzyme and the bulk solution that often lead to the shift of optimum reaction pH [54, 55]. Hence the extent of pH displacement depends on the surface charge density on the supports. The positive charges present on the amine groups of both of the composites leads to the decrease of H^+ concentration on the microenvironment of the immobilized enzyme. As a result of this the pH of the immobilized enzyme systems became more alkaline with respect to the

external region. They have shown very broad pH profile and the broadening confirmed the very high loading of the enzyme through the immobilization process [56, 57]. This immobilization method maintained high pH stability in a wider pH range which might be due to the multipoint attachment of the enzyme on the support surfaces.

3.3.4.3 Effect of temperature on α-amylase activity

The temperature dependent activities of free and immobilized enzymes were investigated by conducting the enzymatic reactions in the range of 30-60 ºC and the results are shown in the figure 3.12.

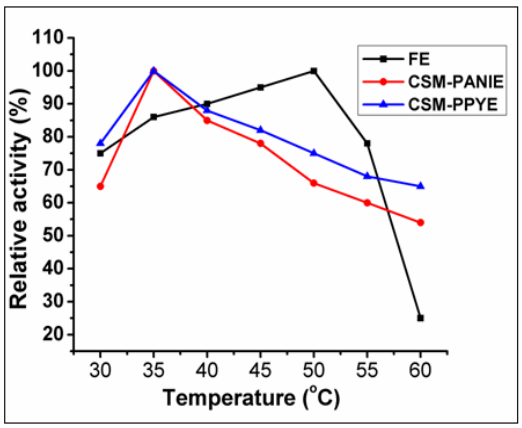

Figure: 3.12 Effect of temperature on the relative activity of free and immobilized α-amylase on modified forms of magnetic chitosan

The immobilized systems have shown broad and stable temperature profile compared to the free enzyme. Both of them exhibited maximum activity at 35 ºC and this lower optimal temperature may be attributed to the changes in physico-chemical properties as a result of immobilization. There might be required less activation energy for the enzyme molecule to allow and reach proper conformation in order to retain its activity. The decrease in optimum temperature was also observed when α-amylase immobilized on

the polymers such as, poly (o-toluidine), polyaniline and polyacrylonitrile [58-60].

They have retained more activity than free enzyme at 60 ºC, CSM-PANIE retained 55 % of relative activity and for CSM-PPYE it was about 65 %. The increased activity of immobilized enzymes might be due to the high rigidity of the enzyme as a result of immobilization and the support had the protection effect at higher temperatures at which the enzyme denaturation taken place [61, 62].

3.3.4.4 Activation energy

Arrhenius plot shown in the figure 3.13 is used for the determination of activation energy (Ea) for the hydrolysis of starch substrate. According to this plot there was decline in the rate of the reaction after the optimum temperature reached. The activation energy calculated for the immobilized enzymes are tabulated in the table 3.5 and the values are found to be higher than that of free enzyme. CSM-PANIE and CSM-PPYE have gained activation energies of 20.76 KJ mol^{-1} and 17.89 KJ mol^{-1} respectively.

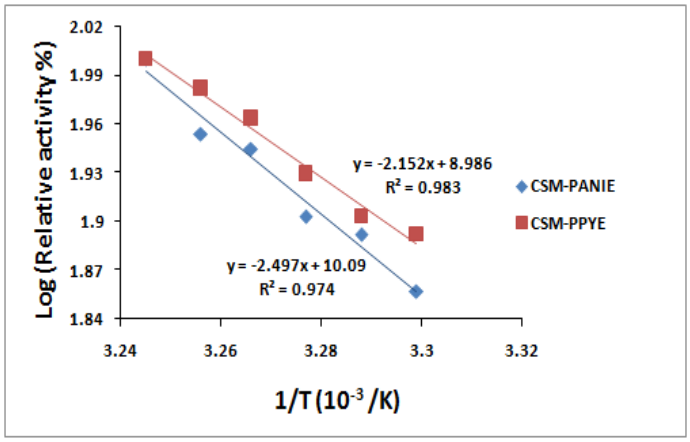

Figure: 3.13 Arrhenius plot to calculate the activation energy (Ea) of immobilized α-amylase on modified forms of magnetic chitosan

Table 3.5 Activation energy of immobilized α-amylase on modified forms of magnetic chitosan

Immobilized enzyme	Activation energy ($KJ\ mol^{-1}$)
CSM-PANIE	20.76
CSM-PPYE	17.89

The higher activation energy for the immobilized enzymes can be due to the fact that the time required for the enzyme and substrate contact prolonged as a result of immobilization and hence decreases their catalytic activity. The Similar finding was reported by Karam et al. when Aspergillus awamori amylase immobilized on a novel carrier Ca^{+2} alginate (Alg) starch (St)/polyethyleneimine (PEI)/glutaraldehyde (GA) [63]. The changes in the structural conformation of the enzyme molecule due to the immobilization process hindered the enzyme catalyzed reaction and caused the higher values for activation energy [64, 65].

3.3.4.5 Thermal stability of the free and immobilized enzymes

Thermal stability study for free and immobilized enzymes was carried out at temperature ranging from 30-70 ºC and the results are presented in the figure 3.14.

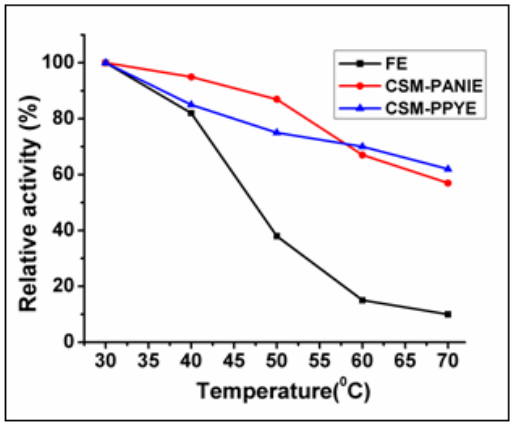

Figure:3.14 Thermal stability of free and immobilized α-amylase on modified forms of magnetic chitosan

At the starting temperature of the study both free and immobilized enzymes have shown maximum activity which is taken as relative to other subsequent studies. At 40 ºC for 1hr incubation they have retained 80-95 % of their initial activity. As the temperature moved to higher region the immobilized enzymes are found to be inactivated at much slower rate than that of free enzyme. At 50 ºC the free enzyme lost above 60 % of its activity while the immobilized enzymes retained about 75-90 % of their activity. At 70 ºC the free enzyme lost about 90 % of its activity whereas, the immobilized enzymes lost only 38-45 % of their activity. These results have shown that the immobilized systems are more resistant to heat than the free form. Immobilization makes the enzyme more rigid and protects it from physical effect which creates enzyme denaturation.

The effect of pre-incubation time on activity of free and immobilized enzymes is shown in the figure 3.15. In this study the free enzyme lost 90 % of its activity and both of the immobilized enzymes lost 45-55 % of their activity when subjected to 120 minutes of pre-incubation time at corresponding optimum temperatures. The results indicated that the multipoint attachment of the enzyme due to immobilization process provide improved heat resistance towards denaturation to the immobilized enzymes [66]. Similar trend in thermal stability was observed by Manu Sharma et al. when α-amylase was immobilized in agar beads by entrapment method [67]. The improvement in thermal stability of α-amylase was also reported by Kritika Singh et al. when immobilized onto functionalized graphene nanosheets as scaffolds [68] and by Usman et al. when immobilized on mesoporous Silica KIT-6 and Palm Wood Chips [69]. The stability of α-amylase increased considerably as a result of immobilization which provides molecular rigidity and protected microenvironment [70-72].

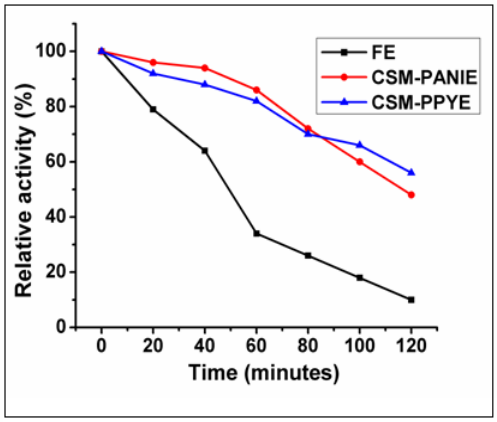

Figure: 3.15 Variation of pre-incubation time on activity of free and immobilized α-amylase on modified forms of magnetic chitosan

3.3.4.6 Determination of kinetic parameters

Lineweaver-Burk plots and Hanes-Woolf plots for free and immobilized enzymes are presented in the figure 3.16 and the kinetic parameters, turnover number (K_{cat}) and catalytic efficiency (K_{cat}/K_m) are exhibited in the table 3.6. Both of the immobilized enzymes exhibited higher K_m and lower V_{max} compared to free enzyme. Since K_m value showed the affinity of the enzyme towards the substrate, the immobilized enzymes with high K_m values indicated their low affinity for substrate. This could be due to the lower accessibility of the substrate towards the active site of the immobilized enzyme. Similar observations are reported in many literatures [73]. As the higher K_m value of the immobilized enzyme indicated its lower affinity for substrate, there should be higher substrate concentration is needed in order to reach a high enzyme activity [74]. Diffusional limitations and steric effects may leads to the lower accessibility of substrate to the enzyme active site which in turn causes the increase of K_m. The structural and conformational changes in the enzyme as a result of immobilization can imparts lower affinity for the substrate molecule which leads to the high K_m as reported by Arica et al. [75].

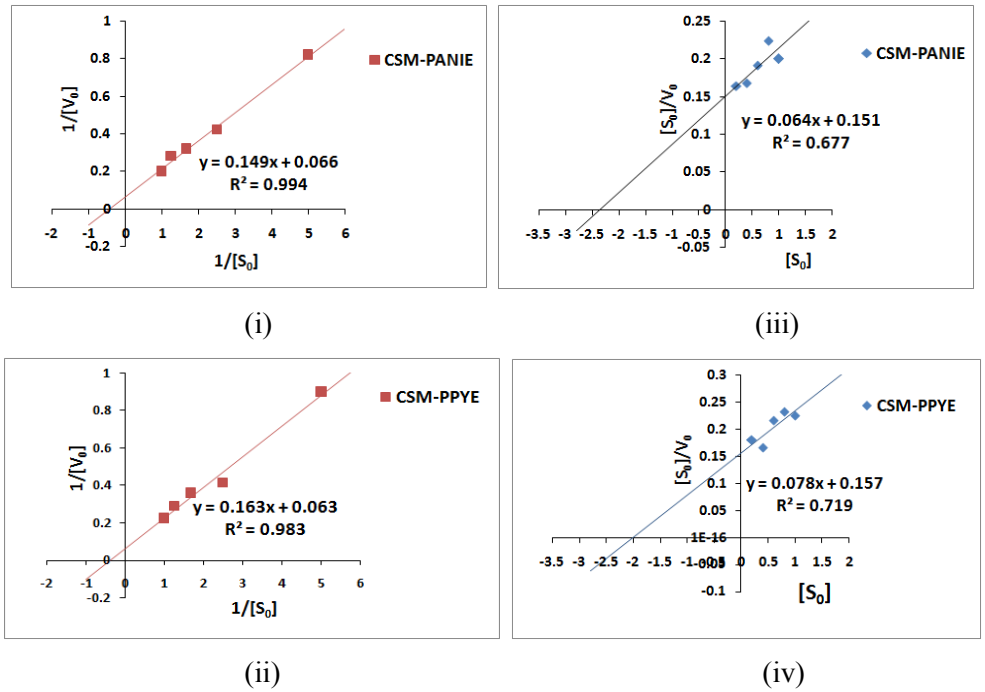

Figure: 3.16 Lineweaver-Burk plots for (i) CSM-PANIE (ii) CSM-PPYE and Hanes-Woolf plots for (iii) CSM-PANIE (iv) CSM-PPYE.

The V_{max} for both of the immobilized enzymes are found to be decreased to almost half of the value for free enzyme. The K_{cat} value of free enzyme was calculated as 1910.19 min^{-1}. The immobilized enzymes, CSM-PANIE and CSM-PPYE are exhibited these values 56.06 % and 53.97 % lower than that of free enzyme. This turn over number revealed their decreased enzyme activity as one molecule of them require 71.48 and 68.26 milliseconds respectively but one molecule of free enzyme take only 31.41 milliseconds for the conversion of one substrate molecule into product. The K_{cat}/K_m values which describe the catalytic efficiency of the enzyme are found to be 4244.87, 371.38 and 339.46 mL mg^{-1} min^{-1} for free enzyme, CSM-PANIE and CSM-PPYE respectively. The results showed that the catalytic efficiency of the enzyme decreased as a result of immobilization.

Table 3.6 Kinetic parameters for free and immobilized α-amylase on modified forms of magnetic chitosan

Immobilized enzyme	K_m (mg mL^{-1})	V_{max} (µmol mg^{-1} min^{-1})	K_{cat} (min^{-1})	K_{cat}/K_m (mL mg^{-1} min^{-1})
Free enzyme	0.45± 0.02	34.48±0.05	1910.19	4244.87
CSM-PANIE	2.26± 0.03	15.15± 0.02	839.31	371.38
CSM-PPYE	2.59± 0.01	15.87±0.03	879.20	339.46

3.3.4.7 Storage stability of immobilized α-amylase

The storage stability of the immobilized enzymes is the important condition for their practical use in industrial sectors. The stability of immobilized enzymes stored at 4 ºC in buffer was determined for regular intervals of time over six months and the results are shown in the figure 3.17.

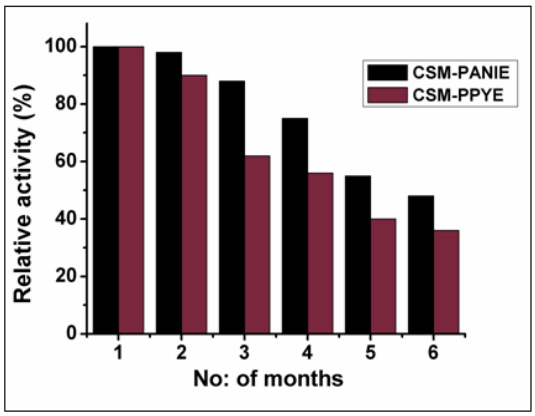

Figure: 3.17 Storage stability of CSM-PANIE and CSM-PPYE

After six months of storage CSM-PANIE retained about 50 % and CSM-PPYE about 40 % of its initial activity. The decline in activity with respect to the shelf time depends on the conformational changes in the immobilized systems and the decrease may be as a result of the time dependent natural loss in enzyme activity [76]. The immobilization process has provided the stability to the enzyme and maintained it for long time storage. Many reports are there in which α-amylase has retained appreciable

activity when immobilized on polymeric supports [77, 78]. The stability of the immobilized enzyme also depends on the attachment of enzyme on the support surface. The multipoint ionic interaction between the enzyme and the support provide much conformational stability to the immobilized enzyme. There exists a difference in enzyme activity in case of both of the immobilized enzymes. The weak interaction between the enzyme and the support may cause the decrease of activity for CSM-PPYE after six months of storage [79-81].

3.3.4.8 Reusability

Reusing the enzyme is very advantageous for their cost effective industrial use. The reusability of the immobilized enzymes was carried out up to 10 cycles and the study was easily conducted by magnetic separation. The plots of the number of cycles and relative activity are shown in the figure 3.18.

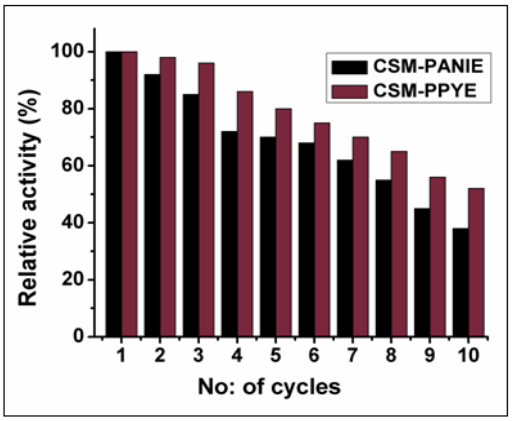

Figure: 3.18 Reusability of CSM-PANIE and CSM-PPYE

After ten cycles of reuses the activity of CSM-PANIE and CSM-PPYE decreased to about 50 % and 40 % respectively of its initial activity. As a result of the repeated uses the interactive forces holding the enzyme on

support become very weak which leads to the enzyme leaching and causes the loss in activity. Furthermore the repeated action of substrate with the active site of the enzyme causes its deformation and ultimately leads to the decrease in activity [82]. The leaching of enzyme from CSM-PPY could be the reason for the low retained activity after ten cycles in case of CSM-PPYE. The deactivation of α-amylase as a result of enzyme leaching was also reported by Radovanovic et al. when immobilized on magnetic particles coated with polyaniline via adsorption [83].

3.4 Magnetic chitosan grafted polymer composites as α-amylase carriers

3.4.1 Synthesis of magnetic chitosan grafted polymethyl methacrylate (CSM-g-PMMA) composite

A solution of 2 % (w/v) chitosan was prepared in 1 % aqueous hydrochloric acid. Then about 140 mL $FeCl_3$ solution (0.13 M in 0.13 M HCl) was added in to the above prepared solution followed by the slow addition of 0.1 M Na_2SO_3 solution under continuous stirring. A solution of 0.1 M CAN in 10 mL of 1 N nitric acid was added in to the resultant colloidal solution and thereafter a known amount of methyl methacrylate monomer was added drop by drop with constant stirring. The precipitate was found to be formed after this solution poured quickly into 12 % ammonia solution with vigorous stirring. The product was collected by using an external magnet after washed several times with distilled water and dried in a vacuum oven at 60 °C.

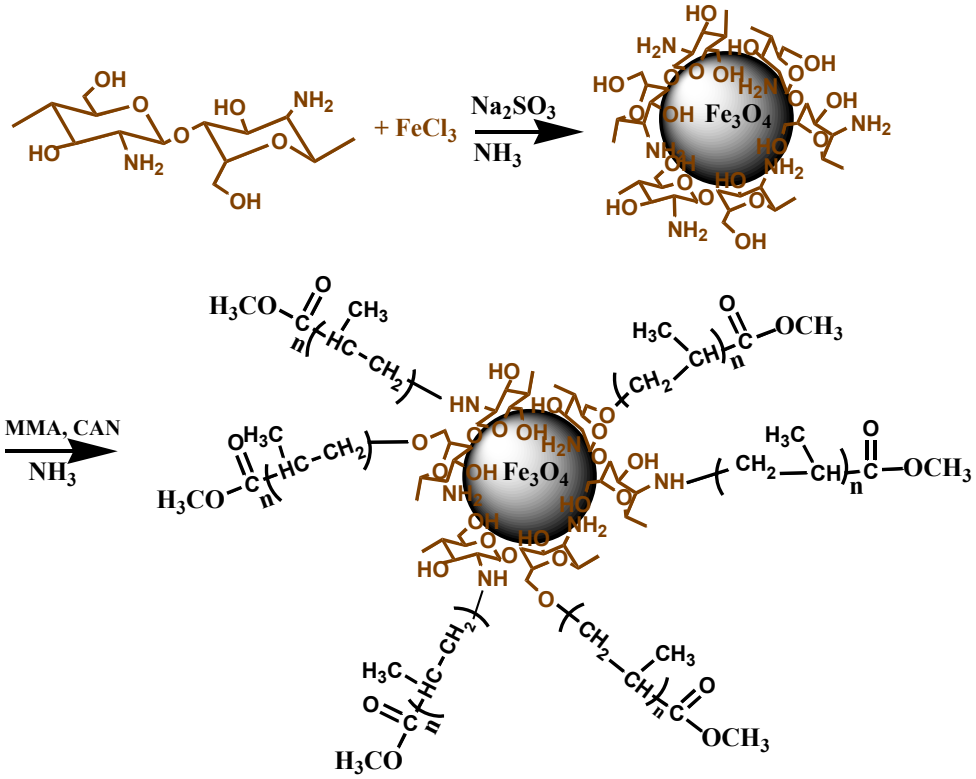

Scheme 3.3 Graft copolymerization of magnetic chitosan with methyl methacrylate

3.4.2 Synthesis of magnetic chitosan grafted poly acrylonitrile (CSM-g-PAN) composite

The CSM-g-PAN was synthesized by adopting the same procedure as that of CSM-g-PMMA in which acrylonitrile is used as the monomer. The initiator CAN (0.1 M in 10 mL of 1 N nitric acid) was added into the magnetic chitosan suspension and then the monomer was added slowly into the resultant solution under constant stirring. The precipitate formed under the vigorous stirring with ammonia solution was separated by using an external magnet and dried in vacuum oven at 60 °C. The procedure was depicted as follows:

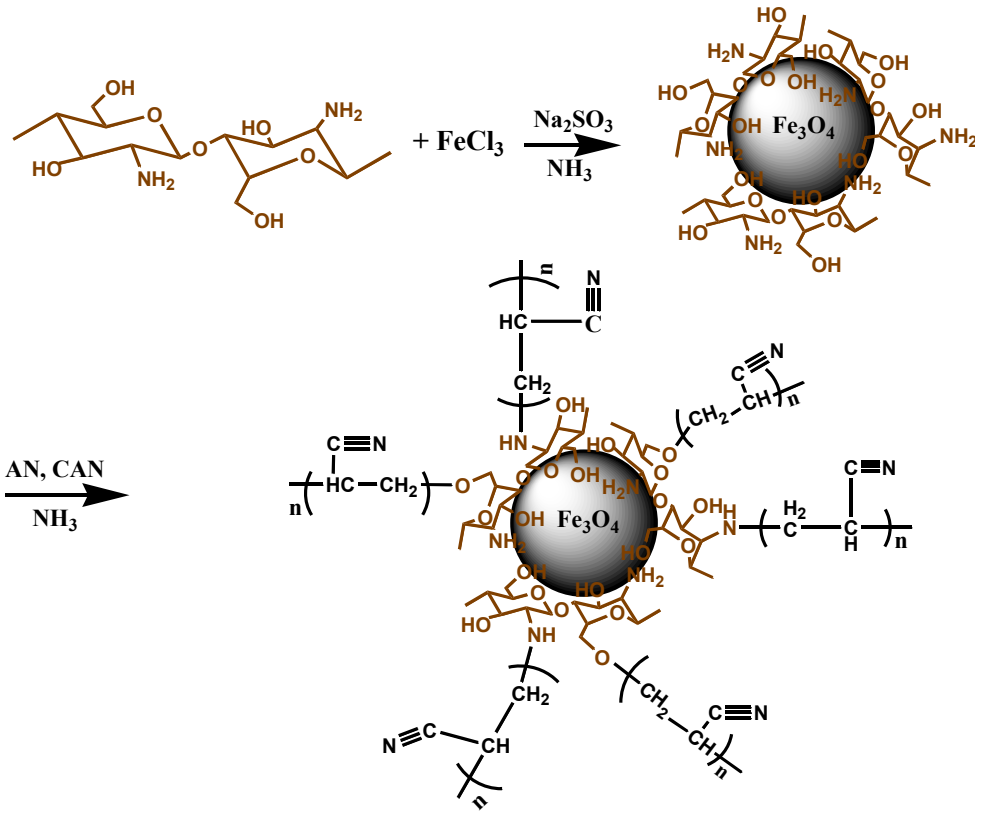

Scheme 3.4 Graft copolymerization of magnetic chitosan with acrylonitrile

3.4.3 Physico-chemical characterization

3.4.3.1 Infrared spectra of magnetic chitosan grafted polymer composites

The IR spectra for magnetic chitosan grafted copolymers are shown in the figure 3.19 and this stands as the promising tool to detect the grafting of polymers on magnetic chitosan.

Magnetic chitosan grafted poly methyl methacrylate copolymer

For CSM-g-PMMA copolymer a broad peak is observed at 3435 cm^{-1} due to N–H and O–H stretching vibrations and the peak corresponding to N–H bending vibration can also be seen around 1640 cm^{-1}. These peaks indicated

the presence of chitosan in the grafted copolymers. But these peaks were shifted to higher frequency region compared to pure chitosan indicating an increased ordered structure [84]. The spectrum showed additional sharp peaks at 1735 cm^{-1} attributed to the ester carbonyl stretching vibrations of PMMA. The weak bands at 2952 cm^{-1} and 2997 cm^{-1} are assigned to symmetrical and asymmetrical stretching vibrations of methyl groups respectively. The peak at 985 cm^{-1} indicates the C–N stretching vibration and the peaks present at 754 cm^{-1} and 843 cm^{-1} attributed to the C–H out of plane bending and C–H_2 rocking [85]. The –O–C–C stretching vibrations in grafted copolymers are observed in the region 1095-1100 cm^{-1} [86]. These characteristic peaks provided sufficient evidences for the grafting of PMMA onto magnetic chitosan.

Magnetic chitosan grafted poly acrylonitrile copolymer

CSM-g-PAN showed C≡N absorption at 2245 cm^{-1} and CH_2 deformation vibration at 1456 cm^{-1} which are confirmed the grafting of PAN with magnetic chitosan. The broad peak at 3450 cm^{-1} corresponds to N–H and O–H stretching vibrations and 1076 cm^{-1} to the C–O stretching vibration of primary alcoholic group indicated the existence of chitosan in the grafted copolymer. The shift of these peaks to slightly higher frequency compared to chitosan confirmed the appreciable grafting at these sites. The grafted copolymer exhibited intense peak at 1260 cm^{-1} assigned to C–N stretching vibrations and the C–H stretching bands of –CH_2–CN, –CH_2– and –CH– groups are presented at the frequencies 2850, 2925 and 2714 cm^{-1} respectively [87]. These peaks stand for the evidences for grafting of PAN with magnetic chitosan. The C–H bending vibration at 1362 cm^{-1} again confirms the grafting.

Both of the grafted copolymers confirmed the presence of magnetite by giving the Fe–O bond vibrations which are found to be 562 cm^{-1} for CSM-g-PMMA and 570 cm^{-1} for CSM-g-PAN. The peak assignments for the modified forms are given in the table 3.7.

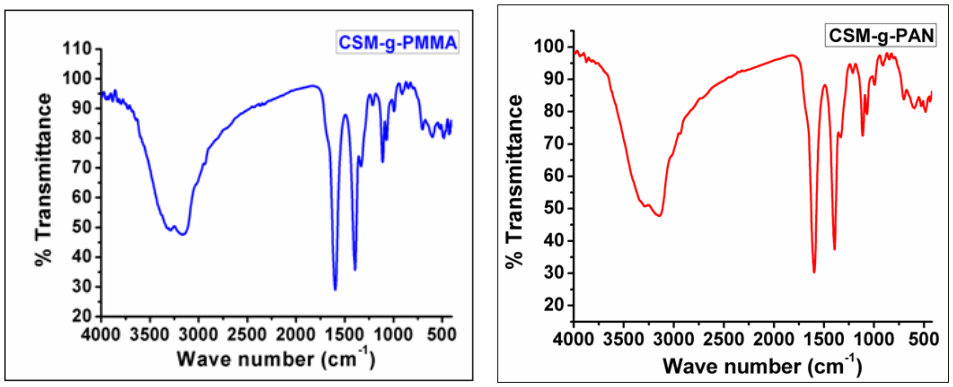

(i) (ii)

Figure: 3.19 IR Spectra of (i) CSM-g-PMMA and (ii) CSM-g-PAN

Table 3.7 Peak assignments for (i) CSM-g-PMMA and (ii) CSM-g-PAN

Peak assignment (cm^{-1})	CSM-g-PMMA
N–H and O–H stretching vibration	3435
N–H bending vibration	1640
C=O stretching vibration	1735
C–O stretching vibration of alcoholic group	1072
Symmetrical stretching of $–CH_3$	2952
Assymmetrical stretching of $–CH_3$	2997
C–N stretching vibration	985
C–H out of plane bending	754
$C–H_2$ rocking	843
O–C–C stretching vibrations	1095-1100
Fe–O bond vibration	562

(i)

Peak assignment (cm^{-1})	CSM-g-PAN
N–H and O–H stretching vibration	3450
C–O stretching vibration of alcoholic group	1076
C-N stretching vibration	1260
C≡ N absorption	2245
CH_2 deformation vibration	1456
C–H stretching in $–CH_2$ CN, $–CH_2$, –CH	2830,2925,2714
Methylene C–H bending	1362
Fe–O bond vibration	570

(ii)

3.4.3.2 X-ray powder diffraction spectra of magnetic chitosan grafted polymer composites

The X-ray diffractograms of both grafted copolymers are shown in the figure 3.20. They have shown specific crystalline peaks as in pure chitosan. In both cases the typical crystalline peak of chitosan that appeared at 2θ=20° has been shifted to around 41° evidenced the grafting of polymers onto the chitosan. The other prominent diffraction peaks are corresponding to the crystalline planes of Fe_3O_4 presented in the composite.

In case of CSM-g-PMMA we observed that the diffraction peaks characteristics to the chitosan and magnetite are distinguishable and so we can say the grafting of magnetic chitosan with PMMA does not much reduce their crystallinity. On the other hand CSM-g-PAN has shown broad peak in the diffraction pattern in which the chitosan peak shifted to more crystalline areas due to the grafted polyacrylonitrile chains [88] and still keep the crystallinity of magnetite by giving corresponding weak diffraction peaks.

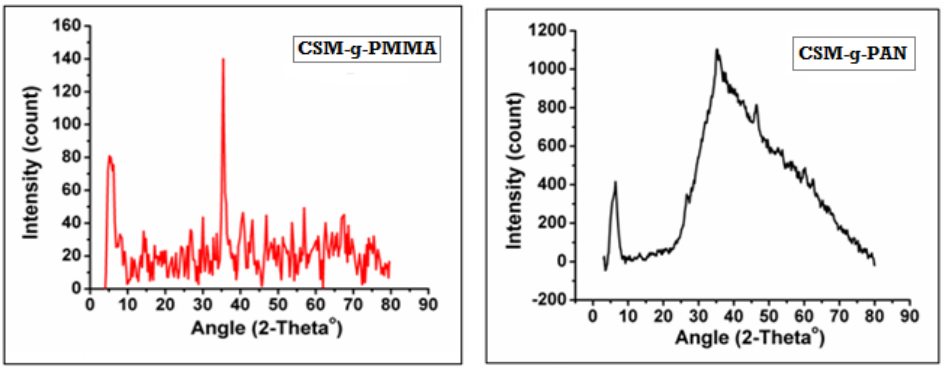

(i) (ii)

Figure: 3.20 XRD spectra of (i) CSM-g-PMMA and (ii) CSM-g-PAN

3.4.3.3 Thermal analysis of magnetic chitosan grafted polymer composites

Thermogram of both grafted copolymers showed weight loss in three stages and are depicted in the figure 3.21. In case of CSM-g-PMMA the first stage of weight loss ranges between 50-130 °C and showed about 8 % of weight loss. This weight loss may correspond to the loss of physically adsorbed water. The second stage of major weight loss can be seen that begins from 220 °C and ends at 450 °C with 40 % loss in weight. This may be due to the degradation of ungrafted chitosan. The third stage of weight loss occurred between 630-700 °C which may be contributed to the decomposition of grafted polymer. At 700 °C we observed that only 60 % of weight loss happened and this indicated the high degree of thermal stability of grafted copolymer. Hence the grafting of methyl methacrylate on to magnetic chitosan supplements more stability to it.

For CSM-g-PAN the weight loss corresponding to adsorbed water can be observed in the region 50-110 °C. The second and third stages of major weight loss observed at 300 °C and 660 °C might be due to the

degradation of ungrafted chitosan and grafted polymer respectively. This thermogram reveals the evidence for the higher thermal stability of the acrylonitrile grafted magnetic chitosan compared to magnetic chitosan itself. The polymer may enfold the chitosan surface and form a physically cross-linked type of network which inhibit the thermal degradation and thus enhance the overall thermal stability of the grafted magnetic chitosan [89].

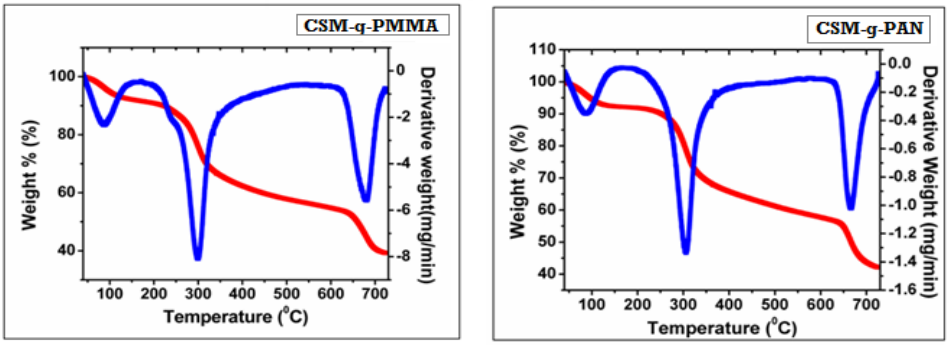

(i) (ii)

Figure: 3.21 TGA-DTG curves of (i) CSM-g-PMMA and (ii) CSM-g-PAN

3.4.3.4 Scanning electron microscopy

The rough surface morphology of the magnetic chitosan grafted copolymers revealed that the surface of the magnetic chitosan was almost covered by the polymers after the grafting process. It is assumed that the polymers are strongly attached to the magnetic chitosan surface. The SEM images are appeared as clustered irregular shape which might be due to the aggregation of the particles and hence leads to the lack of uniformity of the surface structure.

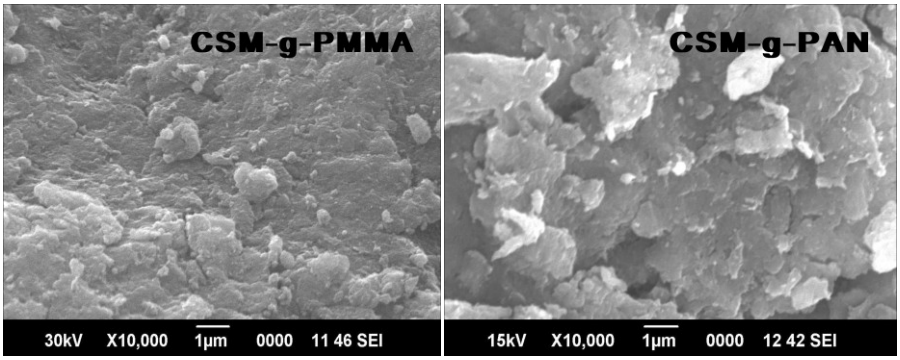

Figure: 3.22 SEM images of CSM-g-PMMA and CSM-g-PAN

3.4.3.5 Surface area analysis

Surface area acquired for CSM-g-PMMA and CSM-g-PAN are 15.67 $m^2\ g^{-1}$ and 21 $m^2\ g^{-1}$ respectively. The CSM-g-PMMA has shown reduced surface area when compared to the other and this might be due to the presence of grafted PMMA with bulky methyl groups on the surface of magnetic chitosan causes the reduction in the surface area.

3.4.3.6 Vibrating sample magnetometry

The magnetization curves for both grafted copolymers are shown in the figure 3.23. The magnetization saturation values are found to be 7.8 emu g^{-1} for CSM-g-PMMA and for CSM-g-PAN is 8.06 emu g^{-1}. They have attained reduced Ms values as compared to that of magnetic chitosan. This might be due to the presence of polymer layers that cover the surface of magnetic chitosan through grafting which reduces its magnetic property and leads to the reduction in the values of magnetic saturation. However these values were much enough in order to meet the need for magnetic separation.

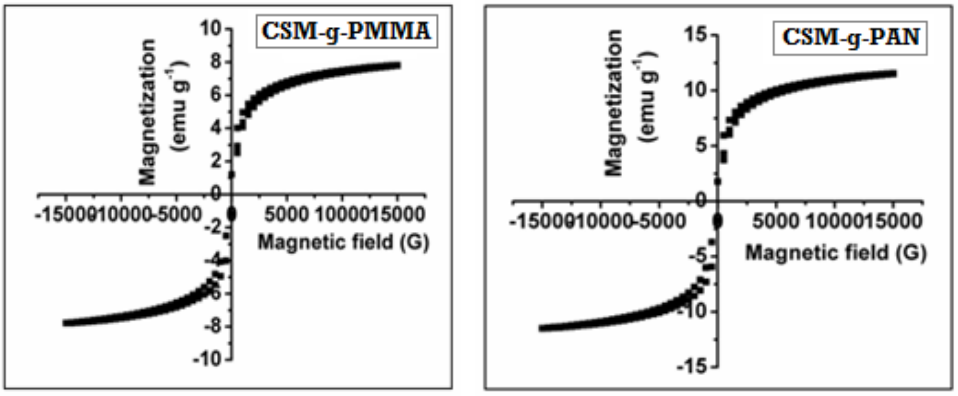

(i) (ii)

Figure: 3.23 Magnetization curves of (i) CSM-g-PMMA and (ii) CSM-g-PAN

3.4.3.7 Energy dispersive X-ray analysis

The elemental composition obtained from EDX spectra of CSM-g-PMMA and CSM-g-PAN are given in the table 3.8 and the spectra are presented in the figure 3.24. Compared to CSM, the former one has shown higher content of C and O, but decreased amount of N and Fe. However, CSM-PAN has shown decreased amount of O and Fe, but has exhibited slight increase of C and N content. All these information confirmed the composite modification.

Table 3.8 Elemental data of (i) CSM-g-PMMA and (ii) CSM-g-PAN

Element	Weight %	Atomic %
O	43.18	42.03
C	26.72	34.64
N	17.93	19.93
Fe	12.17	3.39

(i)

Element	Weight %	Atomic %
O	40.22	39.61
C	24.64	31.80
N	19.84	22.88
Fe	13.30	3.72

(ii)

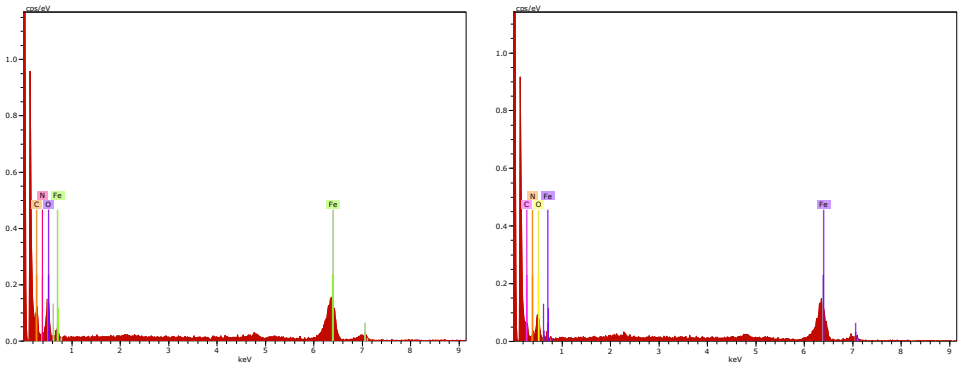

(i) (ii)

Figure: 3.24 EDX spectra of (i) CSM-g-PMMA and (ii) CSM-g-PAN

3.4.4 Immobilization of α-amylase on magnetic chitosan grafted polymer composites

3.4.4.1 Optimization of α-amylase immobilization conditions

The immobilization efficiency can be optimized for α-amylase on both grafted copolymers by varying the immobilization conditions such as immobilization pH, incubation time and enzyme concentration.

3.4.4.1.1Effect of immobilization pH on α-amylase activity

Usually binding between PMMA and enzyme exist via hydrophobic interactions, whereas contributions of electrostatic interactions are seemed to be very little. Palocci and coworkers have immobilized lipolytic enzymes on PMMA through hydrophobic interactive forces [90]. PAN has relatively hydrophobic surface and hence the driving force for enzyme interaction is mainly ascribed to hydrophobicity [91]. For CSM-g-PMMA and CSM-g-PAN the electrostatic interactions that are favored by amino groups also possible in addition with hydrophobic interactions.

The isoelectric point of grafted copolymers depends on that of PMMA and PAN besides that of chitosan and magnetite. The isoelectric

point of PMMA is at pH 6 and that of PAN is around pH 3.96. The strong electrostatic interaction is possible which can be described by the isoelectric point of the grafted polymer and α-amylase.

The levels of enzyme adsorption on both of the supports at different pH ranging 4-9 are compared at 30 °C. The activity of the immobilized enzymes on pH of the immobilization medium was evaluated and is presented in the figure 3.25.

The maximum enzyme activity was obtained at pH 5.5 for CSM-g-PMMA and at pH 4.5 for CSM-g-PAN. In case of CSM-g-PMMA, at pH 5.5 it may retain positively charged and can be interact with the α-amylase through electrostatic interaction as the enzyme is negatively charged at that pH.

For CSM-g-PAN, at pH 4.5 the enzyme gets slightly positively charged and the support surface may exist as negatively charged. This leads to the appreciable electrostatic interaction between the enzyme and the support. Here the immobilized enzyme CSM-g-PAN has shown comparatively lower relative activity than CSM-g-PMMA which might be due to its less interaction with the enzyme and leads to the enzyme leakage. At the pH above and below the optimum value there can be electrostatic repulsion occurs between the enzyme and the support since they carry same charges. The lower enzyme adsorption at these pH ranges might be as a result of hydrophobic interactions of the support with the enzyme. The similar observations are reported when α-amylase immobilized on poly (methyl methacrylate-acrylic acid) microspheres [92] and granular polyacrylonitrile [60].

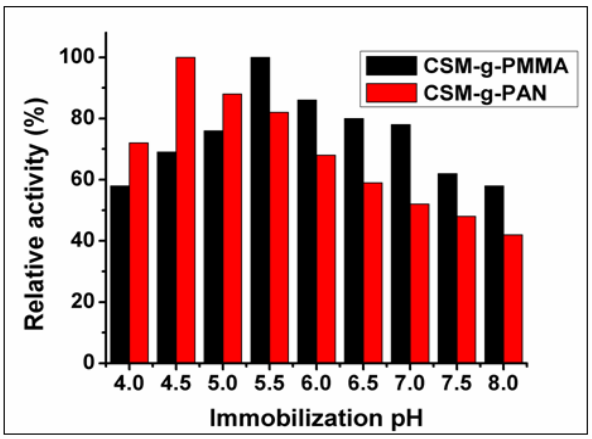

Figure: 3.25 Effect of immobilization pH on the relative activity of immobilized α-amylase on modified forms of magnetic chitosan

3.4.4.1.2 Effect of incubation time on activity of α-amylase

The period of incubation required for the maximum adsorption of enzyme on the grafted polymers were studied and are depicted in the figure 3.26.

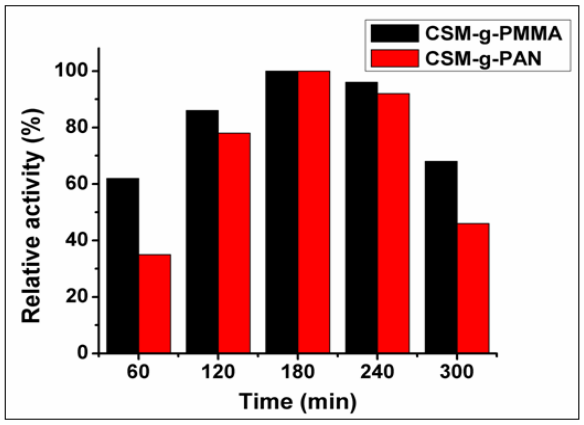

Figure: 3.26 Effect of incubation time on immobilized α-amylase activity

Here α-amylase was immobilized on both supports at different incubation time and for both supports 180 min. was sufficient for maximum enzyme loading. After this optimum incubation time the enzyme activity

was found to be declined which might be due to the leakage of enzyme. The subsequent addition of enzyme on the support surface leads to the repulsive interaction between the enzymes with similar charges which results in desorption of enzyme. So there is no further enzyme loading taken place and correspondingly no more enhancements in enzyme activity was noticed. The similar decline in activity was reported by David et al. when α-amylase immobilized on polyethylene films [93].

3.4.4.1.3 Effect of initial amount of protein on protein loading onto composites

The protein loading on grafted copolymers was estimated by varying the initial protein amount and the results are shown in the figure 3.27.

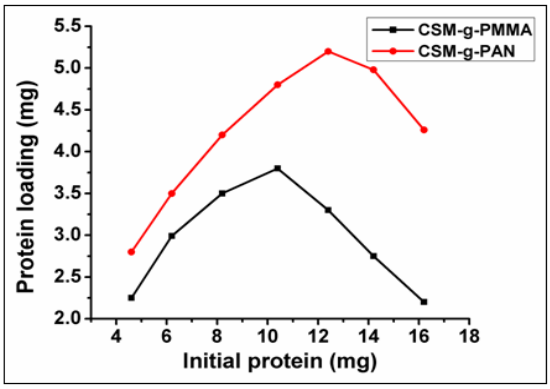

Figure: 3.27 Effect of initial protein amount on protein loading onto modified forms of magnetic chitosan

Here we observed that the protein loading onto the supports increased to a saturation point as the amount of initial protein increases and after that it was found to be decreased. The desorption of enzyme was taken place over this saturation point as it was loaded excessively which may due to the less interaction with the support. The enzyme loading on the support surface can be varied with respect to the nature of the support. From the figure it is clear that CSM-g-PMMA attained enzyme loading of 3.8 mg g^{-1}

support at the initial protein amount of 10.4 mg. The loaded enzyme for CSM-g-PAN at the initial amount of 12.4 mg enzyme was 5.2 mg g^{-1} support. Here CSM-g-PAN has got much more loaded enzyme than the other which could be due to its high surface area. The increase in surface area of CSM-g-PAN was already confirmed by the BET analysis.

3.4.4.1.4 Effect of initial protein amount on immobilized enzyme activity

The variations of immobilized enzyme activity with respect to the initial protein used are shown in the figure 3.28. The α-amylase immobilized on CSM-g-PMMA has shown high activity of 2.92 EU with initial protein of 10.4 mg. But for CSM-g-PAN the maximum immobilized enzyme activity is found to be at 3.58 EU with initial amount of 12.4 mg enzyme.

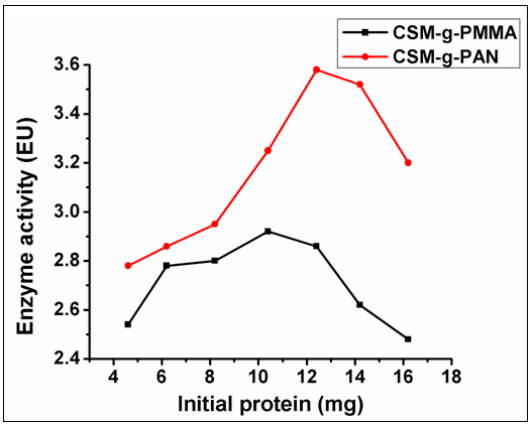

Figure: 3.28 Effect of initial protein amount on immobilized enzyme activity

They have retained the corresponding immobilization yield of 36.54 % at initial protein amount of 10.4 mg and 41.93 % at initial protein amount of 12.4 mg respectively. Comparatively lower immobilization yield of CSM-g-PMMA can be attributed to the multilayer adsorption of enzyme which leads to the weak enzyme substrate interaction and subsequently results in enzyme leaching.

The activity yield and immobilization efficiency for enzyme on both supports are presented in the table 3.9. The activity yield of CSM-g-PMMA was 28.08 % with high value of immobilization efficiency of 76.85 % and the CSM-g-PAN has shown activity yield of 22.48 % with 53.61 % of immobilization efficiency. The lower activity yield of α-amylase immobilized on CSM-g-PAN may be due to its conformational changes in the three dimensional structure that causes less enzyme-substrate affinity which also be affected in its immobilization efficiency.

Table 3.9 Immobilization efficiency of α-amylase on modified forms of magnetic chitosan

Support	Initial protein (mg)	Immobilized protein mg/g support	IY (%)	Initial activity (EU)	Immobilized enzyme activity (EU)	AY (%)	IE (%)
CSM-g-PMMA	10.4	3.8	36.54	10.4	2.92	28.08	76.85
CSM-g-PAN	12.4	5.2	41.93	15.92	3.58	22.48	53.61

3.4.4.2 Effect of pH on α-amylase activity

The pH profile of free and immobilized enzymes with respect to their activity was evaluated and the results are shown in the figure 3.29.

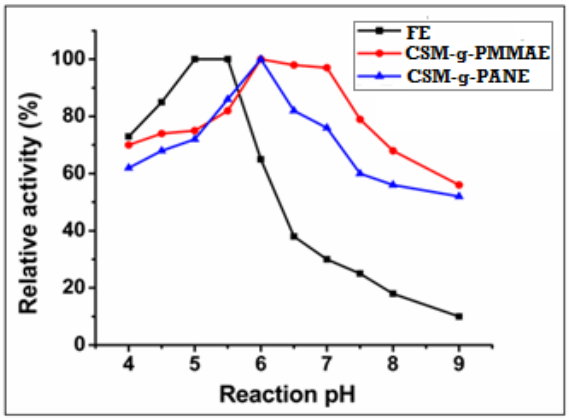

Figure: 3.29 Effect of pH on the relative activity of free and immobilized α-amylase on modified forms of magnetic chitosan

The maximum activity for free enzyme lies in the range of pH 5-5.5 while that for CSM-g-PMMA and CSM-g-PAN are found to be at pH 6. For both of the immobilized enzymes the optimum value shifted to the alkaline region. This shift may probably due to the changes in its microenvironment as a result of the immobilization process. The strong electrostatic interaction between the enzyme and the support results in the changes in ionization of acidic and basic amino acid side chains in the microenvironment leads to the shift in optimum pH value [94]. An increase of optimum pH was reported by Ningsih et al. when *Bacillus thuringiensis* HCB6 Amylase was immobilized on chitosan beads [95].

The enzyme activities are expressed in terms of relative activities by taking the optimum value as 100 %. The immobilized enzymes retained about 58-70 % and 52-58 % of relative activities at pH 8 and 9 respectively whereas the free enzyme lost almost 90 % of its activity at pH 9. Hence the immobilized enzymes have shown broader pH profile than free enzyme which attributed to their high pH stability. The increased stability of the immobilized enzymes over these pH ranges indicated their less susceptibility towards the conformational changes as a result of the changes in the environmental pH.

3.4.4.3 Effect of temperature on α-amylase activity

The influence of reaction temperature on the catalytic activity of free and immobilized enzymes was presented in the figure 3.30.

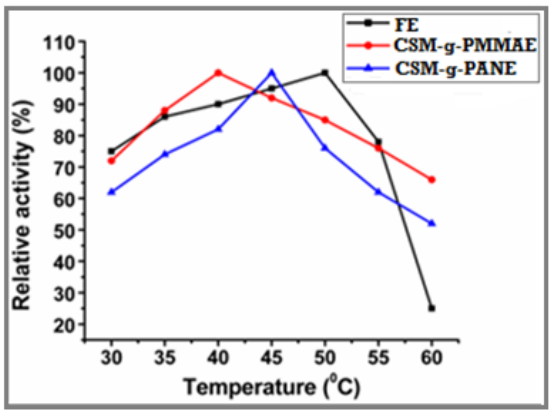

Figure: 3.30 Effect of temperature on the relative activity of free and immobilized α-amylase on modified forms of magnetic chitosan

Both of the immobilized enzymes have shown optimum temperature in lower region compared to free enzyme. This might be because of the conformational changes caused by the enzyme upon immobilization. Furthermore they have shown higher relative activities and slightly broader temperature profile in comparison with free enzyme. It was observed that the immobilized enzymes have retained 52-68 % of their relative activity but the free enzyme possessed only 25 % of activity at 60 °C. The results showed that the immobilization process considerably preserved the activity of enzyme. As the three dimensional structure of the enzyme changed as a result of immobilization on to the support there exists an alteration in enzyme substrate affinity that eventually leads to the decrease of activity at higher temperatures [75, 96].

3.4.4.4 Activation energy

The plot of logarithm of enzyme activity as a function of inverse of temperature was depicted in the figure 3.31 and the activation energy was calculated from the slope of the plot. The activation energy for immobilized enzymes CSM-g-PMMAE and CSM-g-PANE are found to be 13.57 KJ mol^{-1}

and 12.89 KJ mol^{-1} respectively (table 3.10). These values are higher than that of free enzyme and the increased values of activation energies of immobilized enzymes may be due to the changes in the structure of enzyme molecule as a result of immobilization which hinder the enzymatic reaction [65, 96]. Similar findings were reported by Abdel Naby et al. when *Bacillus subtilis* α-amylase immobilized on amino alkyl silane-alumina, DEAE-cellulose, chitin and polyacrylamide [97].

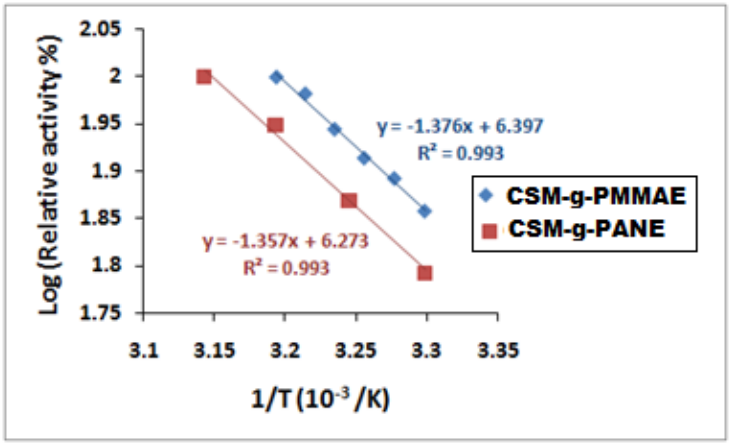

Figure: 3.31 Arrhenius plot to calculate the activation energy (Ea) for immobilized α-amylase on CSM-g-PMMA and CSM-g-PAN

Table 3.10 Activation energy of immobilized α-amylase on CSM-g-PMMA and CSM-g-PAN

Immobilized enzyme	Activation energy (KJ mol^{-1})
CSM-g-PMMAE	13.57
CSM-g-PANE	12.89

3.4.4.5 Thermal stability of the free and immobilized enzymes

Thermal stability curves of both free and immobilized α-amylases were shown in the figure 3.32 and the results showed that the immobilized enzymes performed differently from that of free enzyme. At 40 °C the free

enzyme retained 80 % of its relative activity while the immobilized enzymes gained 97-99 % of activity at that temperature. As the temperature raised to higher region it was found that both the immobilized enzymes denatured at slower rate than that of free enzyme. The relative activity of the free enzyme after heating at 70 °C for 1hour decreased to 10 % which was very lower than that of immobilized enzymes. The immobilization process protected the enzyme from the physical effect that leads to the enzyme denaturation. The multipoint attachment of the support with enzyme as a result of the immobilization process can cause the resistance towards the thermal denaturation. Hence the immobilized enzymes have shown higher heat resistance than free enzyme and prevent the thermal denaturation of the enzyme. The loss in activity at higher temperatures might be as a result of unfolding of protein structure due to the weak interaction between the enzyme and support.

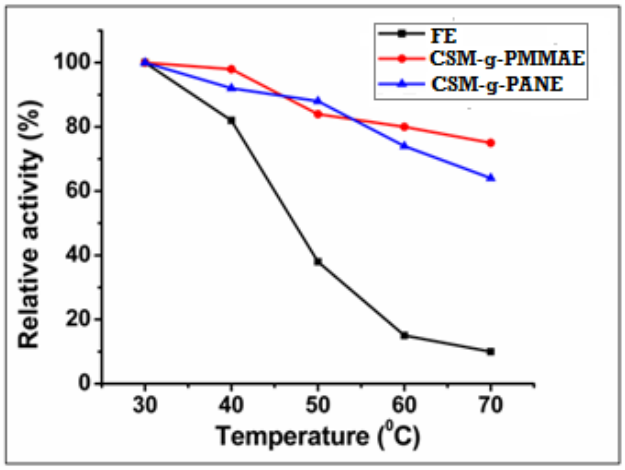

Figure:3.32 Thermal stability of free and immobilized α-amylase on modified forms of magnetic chitosan

The increased thermal stability of α-amylase via immobilization process was further confirmed in terms of their pre-incubation time that

applied in the thermal stability study. The free and immobilized enzymes were pre-incubated up to 120 min. at their optimum temperatures and the inactivation curves are presented in the figure 3.33.

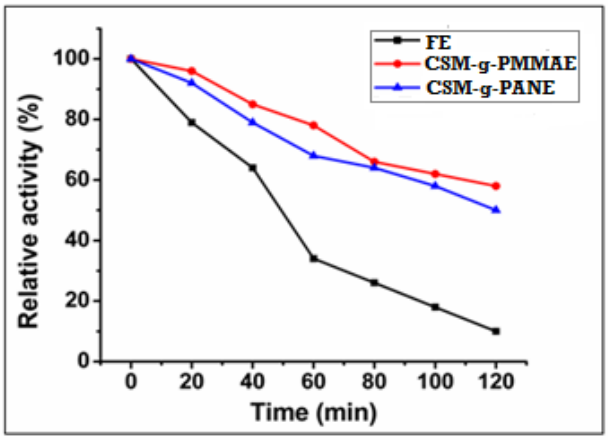

Figure: 3.33 Variation of pre-incubation time on activity of free and immobilized α-amylase on modified forms of magnetic chitosan

After 120 minutes of their pre-incubation at optimum temperature the free enzyme exhibited about 90 % of loss in activity whereas the immobilized enzymes lost only 42-46 % of their initial activity. The plausible reason for the differences in thermal stabilities of free and immobilized enzymes can be due to the changes in the microenvironment of the enzyme by the presence of support. It is possible to modify the molecular conformation in order to reorganize due to the changes in the macro environment like temperature changes [98]. The rigidification of the protein structure as a result of the multipoint attachment and thus reduction in the dissociation difficulties through the immobilization also contribute to these changes in thermal stability [99].

3.4.4.6 Determination of kinetic parameters

The Lineweaver-Burk plots and Hanes-Woolf plots shown in the figure 3.34 are used to determine the kinetic parameters K_m and V_{max}.

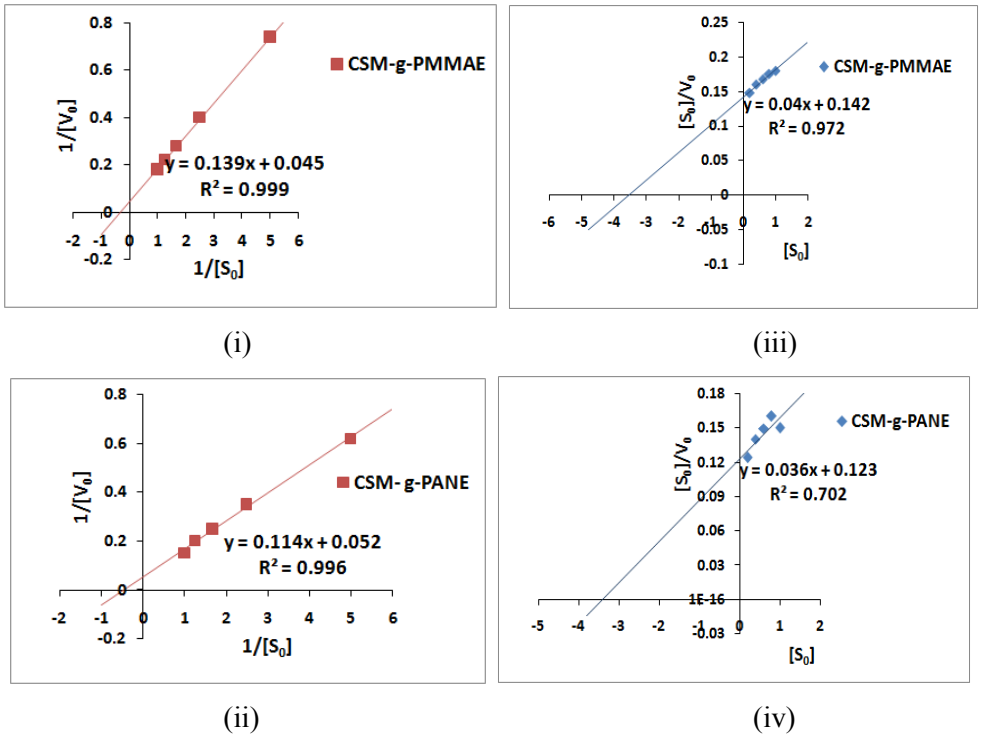

Figure: 3.34 Lineweaver-Burk plots for (i) CSM-g-PMMAE (ii) CSM-g-PANE and Hanes-Woolf plots for (iii) CSM-g-PMMAE (iv) CSM-g-PANE.

The kinetics of the enzymatic reaction changed as a result of the immobilization since the binding of enzyme onto the support leads to changes in enzyme conformation, microenvironment of the support and then the bulk and diffusional effects. The kinetic parameters (K_m and V_{max}), turnover number (K_{cat}) and catalytic efficiency (K_{cat}/K_m) of free and immobilized enzymes are tabulated in the table 3.11.

Both of the immobilized enzymes exhibited higher K_m values in comparison to free enzyme indicated that the substrate affinity of the α-

amylase was decreased after immobilization [100, 101]. Immobilization can alter the shape of enzyme and it could diminish the accessibility of active site of the enzyme for substrate. The high K_m value of the immobilized enzymes could be attributed to their diffusional limitations, ionic and steric effect via immobilization process [102]. The immobilized enzyme activity depends on the particle size of the support and the enzyme loading that influence the effect of diffusional limitations [103, 104]. The immobilized enzymes have shown reduced V_{max} values compared to the free enzyme. This might be due to the substrate diffusion to the active site of the enzyme with an increase of K_m value. The blocking of active sites of enzyme on immobilization can also be decrease the V_{max} value. The increase in K_m and decrease in V_{max} of amylase was reported by Roy et al. when immobilized on polystyrene cation exchange resin equilibrated with Al^{3+} ions [105]. Similar trend in variation of kinetic parameters was reported by D'Angiuro for enzymes immobilized by graft copolymerization to different polysaccharides [21].

The K_{cat} values of CSM-g-PMMAE and CSM-g-PANE are 1230.99 and 1065.34 min^{-1} respectively. The analyzed data assigned that turnover number of both immobilized α-amylases were lower than that of free enzyme which were found to be 35.56 % lesser for CSM-g-PMMAE and 44.23 % lesser for CSM-g-PANE. This indicated that one free enzyme molecule requires 31.41 milliseconds to convert one substrate molecule into product whereas one molecule of immobilized enzymes needs 48.73 and 56.34 milliseconds of time. These results showed that the immobilization leads to the decrease in enzymatic activity of α-amylase.

The K_{cat}/K_m values revealed that immobilized enzymes have exhibited 90.61 % and 88.54 % of lesser catalytic efficiency than that of free

enzyme and this indicated that the immobilization process reduces the catalytic efficiency of the enzyme.

Table 3.11 Kinetic parameters for free and immobilized α-amylase on modified forms of magnetic chitosan

Immobilized enzyme	K_m (mg mL^{-1})	V_{max} (μmol mg^{-1} min^{-1})	K_{cat} (min^{-1})	K_{cat}/K_m ($mlmg^{-1}min^{-1}$)
Free enzyme	0.45± 0.02	34.48±0.05	1910.19	4244.87
CSM-g-PMMAE	3.09± 0.02	22.22± 0.03	1230.99	398.38
CSM-g-PANE	2.19±0.04	19.23± 0.02	1065.34	486.46

3.4.4.7 Storage stability of Immobilized α-amylase

The storage stability of the immobilized enzymes has assessed by storing them at 4 ºC and their activities were evaluated for a period of 6 months. The results are exhibited in the figure 3.35 and it revealed that CSM-g-PMMAE retained about 45 % of its initial activity while that of CSM-g-PANE was only about 25 % of its activity after 6 months. As the storage stability is an intrinsic property of the enzyme and the attachment of enzyme with suitable support can enhance this property. Here we observed that the immobilization process improved the storage stability of the α-amylase as the free enzyme lost all of its activity within 7 days (not shown in the figure). Among the immobilized enzymes CSM-g-PMMAE has shown better storage stability in comparison to the other one. The activity of the immobilized enzymes depends upon the nature and adsorption capacity of the support to bind with the enzyme in a proper orientation for long time. Thus immobilization provides stability to the enzyme conformation which preserves the activity longer. The retained activities of α-amylase were observed previously when immobilized on different polymeric supports [92, 106, 107].

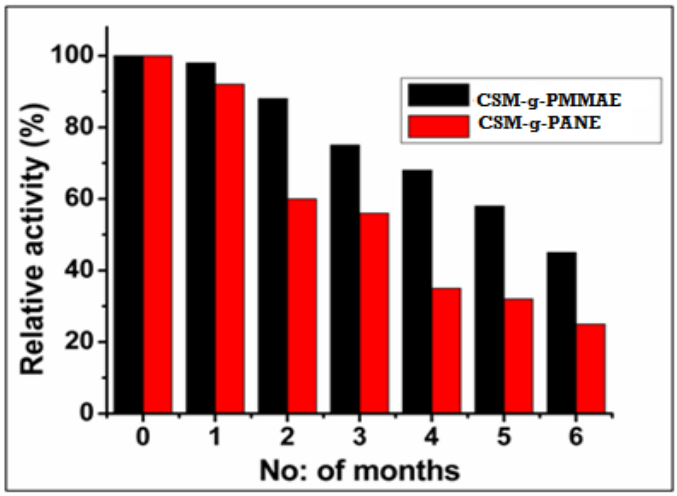

Figure: 3.35 Storage stability CSM-g-PMMAE and CSM-g-PANE

3.4.4.8 Reusability

The α-amylase immobilized supports were easily recovered for the iterative uses due to their magnetic property. The reusability of the immobilized enzymes was examined for 10 cycles of continuous uses by determining their relative activities and is depicted in the figure 3.36.

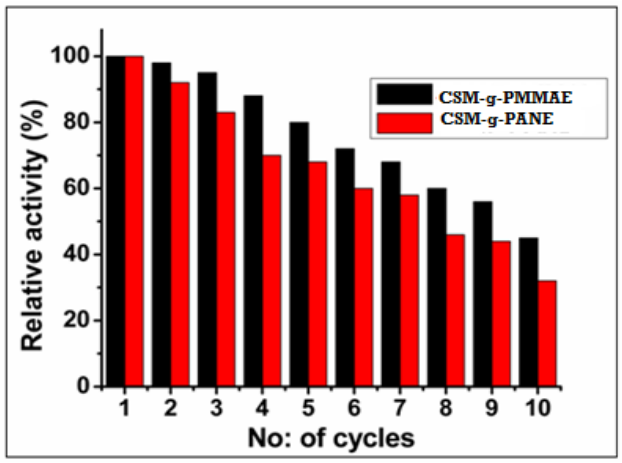

Figure: 3.36 Reusability of CSM-g-PMMAE and CSM-g-PANE

They have exhibited significant activity after 10 continuous cycles of enzyme catalyzed reaction. The repeated uses of immobilized enzymes diminish the interaction between the enzyme and the support which leads to the enzyme leakage from the support surface and consequently reduce the enzyme activity. As a result of this the relative activity was found to be decreased with the increase in number of uses. Furthermore, the denaturation of the enzyme as a result of continuous usage also leads to the loss in activity of the immobilized enzymes [108]. For CSM-g-PMMAE the relative activity was found to be about 45 % at the tenth cycle of iterative enzymatic reaction and CSM-g-PANE retained around 35 % of its initial activity. Cakmakci et al. studied the reuse capability of α-amylase and observed the loss in activity on repeated uses when immobilized on aminated polyimide membrane [109]. Similar trend was observed in other literatures [110, 111].

3.5 Conclusion

Magnetic chitosan was modified with synthetic polymers polyaniline and polypyrrole, also by graft copolymerization of methyl methacrylate and acrylonitrile. All the modified forms were characterized by FT-IR, XRD, TGA-DTG, SEM, VSM, BET, EDX and CHN analysis. The α-amylase immobilized onto the modified magnetic chitosan exhibited increased activity and stability when compared to the free enzyme. The immobilization conditions were optimized and all the immobilized enzymes showed broader pH and temperature profile indicated their higher stability towards the immobilization conditions. The optimum temperature of enzyme gets shifted to pH 6 in case of all immobilized enzymes. For CSM-PANI and CSM-PPY the optimum temperature was shifted to 35 °C, whereas CSM-g-PMMA and CSM-g-PAN exhibited their optimum

temperatures at 40 °C and 45 °C respectively. CSM-PPY has attained highest immobilization yield due to its increased surface area but the immobilization efficiency was highest for CSM-g-PMMA. The CSM-PANIE has showed highest activation energy of 20.76 KJ mol^{-1}. The kinetic parameters, K_m, V_{max} and K_{cat}/K_m were evaluated and compared with that of free enzyme. CSM-PANIE, CSM-PPYE, CSM-PMMAE and CSM-PANE have retained 50 %, 40 %, 45 % and 35 % of activity after 10 cycles of uses and 50 %, 40 %, 45 % and 25 % of initial activity after six months of storage.

References

[1] V. Ferrario, C. Ebert, L. Knapic, D. Fattor, A. Basso, P. Spizzo, L. Gardossi, Conformational changes of lipases in aqueous media: A comparative computational study and experimental implications, Advanced Synthesis & Catalysis 353(13) (2011) 2466-2480.

[2] O. Kirk, M.W. Christensen, Lipases from Candida antarctica: unique biocatalysts from a unique origin, Organic Process Research & Development 6(4) (2002) 446-451.

[3] A. Basso, P. Braiuca, S. Cantone, C. Ebert, P. Linda, P. Spizzo, P. Caimi, U. Hanefeld, G. Degrassi, L. Gardossi, In silico analysis of enzyme surface and glycosylation effect as a tool for efficient covalent immobilisation of CalB and PGA on sepabeads, Advanced Synthesis & Catalysis 349(6) (2007) 877-886.

[4] S. Cantone, V. Ferrario, L. Corici, C. Ebert, D. Fattor, P. Spizzo, L. Gardossi, Efficient immobilisation of industrial biocatalysts: criteria and constraints for the selection of organic polymeric carriers and immobilisation methods, Chemical Society Reviews 42(15) (2013) 6262-6276.

[5] J. Zdarta, A. Meyer, T. Jesionowski, M. Pinelo, A general overview of support materials for enzyme immobilization: Characteristics, properties, practical utility, Catalysts 8(2) (2018) 92.

[6] S.A. Othman, S. Radiman, K.S. Khoo, I. A Rahman, Immobilization of horseradish peroxidase onto polyaniline nanoparticle monolayer, World Applied Sciences Journal 9 (2010) 23-25.

[7] J. Anand, S. Palaniappan, D. N Sathyanarayana, Conducting polyaniline blends and composites, Progress in Polymer Science 23(6) (1998) 993-1018.

[8] G. Gustafsson, Y. Cao, G. Treacy, F. Klavetter, N. Colaneri, A. Heeger, Flexible light-emitting diodes made from soluble conducting polymers, Nature 357(6378) (1992) 477.

[9] S. Virji, J. Huang, R.B. Kaner, B.H. Weiller, Polyaniline nanofiber gas sensors: examination of response mechanisms, Nano letters 4(3) (2004) 491-496.

[10] G. Bayramoglu, A.U. Metin, B. Altintas, M.Y. Arıca, Reversible immobilization of glucose oxidase on polyaniline grafted polyacrylonitrile conductive composite membrane, Bioresource Technology 101(18) (2010) 6881-6887.

[11] R.N. Silva, E.R. Asquieri, K.F. Fernandes, Immobilization of Aspergillus niger glucoamylase onto a polyaniline polymer, Process Biochemistry 40(3) (2005) 1155-1159.

[12] J. Laska, J. Włodarczyk, W. Zaborska, Polyaniline as a support for urease immobilization, Journal of Molecular Catalysis B: Enzymatic 6(6) (1999) 549-553.

[13] K.F. Fernandes, C.S. Lima, H. Pinho, C.H. Collins, Immobilization of horseradish peroxidase onto polyaniline polymers, Process Biochemistry 38(9) (2003) 1379-1384.

[14] A. Tiwari, S. Shukla, Chitosan-g-polyaniline: a creatine amidinohydrolase immobilization matrix for creatine biosensor, eXPRESS Polymer Letters 3 (2009) 553–559.

[15] A. Arslan, S. Kiralp, L. Toppare, Y. Yagci, Immobilization of tyrosinase in polysiloxane/polypyrrole copolymer matrices, International Journal of Biological Macromolecules 35(3-4) (2005) 163-167.

[16] W. Schuhmann, R. Lammert, B. Uhe, H.L. Schmidt, Polypyrrole, a new possibility for covalent binding of oxidoreductases to electrode surfaces as a base for stable biosensors, Sensors and Actuators B: Chemical 1(1-6) (1990) 537-541.

[17] J. Njagi, S. Andreescu, Stable enzyme biosensors based on chemically synthesized Au–polypyrrole nanocomposites, Biosensors and Bioelectronics 23(2) (2007) 168-175.

[18] U. Baig, M.A. Gondal, M.F. Alam, A.A. Laskar, M. Alam, H. Younus, Enzyme immobilization and molecular modeling studies on an organic–inorganic polypyrrole–titanium (IV) phosphate nanocomposite, New Journal of Chemistry 39(9) (2015) 6976-6986.

[19] Y. Fang, Y. Ni, G. Zhang, C. Mao, X. Huang, J. Shen, Biocompatibility of CS–PPY nanocomposites and their application to glucose biosensor, Bioelectrochemistry 88 (2012) 1-7.

[20] S. Takeuchi, I. Omodaka, K. Hasegawa, Y. Maeda, H. Kitano, Temperature-responsive graft copolymers for immobilization of enzymes, Macromolecular Chemistry and Physics 194(7) (1993) 1991-1999.

[21] L. D'Angiuro, P. Cremonesi, G. Mazzola, B. Focher, G. Vecchio, Preparation and characterization of enzymes immobilized by graft copolymerization to different polysaccharides, Biotechnology and Bioengineering 22(11) (1980) 2251-2272.

[22] M. Ulbricht, Advanced functional polymer membranes, Polymer 47(7) (2006) 2217-2262.

[23] K. Gabrovska, A. Georgieva, T. Godjevargova, O. Stoilova, N. Manolova, Poly (acrylonitrile) chitosan composite membranes for urease immobilization, Journal of Biotechnology 129(4) (2007) 674-680.

[24] X. Yuan, J. Sheng, F. He, X. Lu, N. Shen, Surface modification of acrylonitrile copolymer membranes by grafting acrylamide. I. Initiation by ceric ions, Journal of Applied Polymer Science 66(8) (1997) 1521-1529.

[25] X.Y. Yuan, N.X. Shen, J. Sheng, X. Wei, Immobilization of cellulase using acrylamide grafted acrylonitrile copolymer membranes, Journal of Membrane Science 155(1) (1999) 101-106.

[26] A. Sadana, Protein adsorption and inactivation on surfaces. Influence of heterogeneities, Chemical Reviews 92(8) (1992) 1799-1818.

[27] K. Gabrovska, T. Nedelcheva, T. Godjevargova, O. Stoilova, N. Manolova, I. Rashkov, Immobilization of acetylcholinesterase on new modified acrylonitrile copolymer membranes, Journal of Molecular Catalysis B: Enzymatic 55(3) (2008) 169-176.

[28] B. Krajewska, Application of chitin-and chitosan-based materials for enzyme immobilizations: a review, Enzyme and Microbial Technology 35(2-3) (2004) 126-139.

[29] M.A. Abd El-Ghaffar, M.S. Hashem, Calcium alginate beads encapsulated PMMA-g-CS nano-particles for α-chymotrypsin immobilization, Carbohydrate Polymers 92(2) (2013) 2095-2102.

[30] N.S. Mohamad Ayad, A. Fayed, B.P. Bastakoti, N. Suzukic, Y. Yamauchi, Chemical design of a smart chitosan–polypyrrole–magnetite nanocomposite toward efficient water treatment, Physical Chemistry Chemical Physics 16 (2014) 21812-21819.

[31] X.G. Li, A. Li, M.R. Huang, Facile High-Yield Synthesis of polyaniline nanosticks with intrinsic stability and electrical conductivity, Chemistry-A European Journal 14(33) (2008) 10309-10317.

[32] K. Pandiselvi, S. Thambidurai, Chitosan-ZnO/polyaniline ternary nanocomposite for high-performance supercapacitor, Ionics 20(4) (2014) 551-561.

[33] A.G. Yavuz, A. Uygun, V.R. Bhethanabotla, Substituted polyaniline/chitosan composites: Synthesis and characterization, Carbohydrate Polymers 75(3) (2009) 448-453.

[34] E.Y. Rosova, N. Belnikevich, Z. Zoolshoev, N. Saprykina, G. Elyashevich, New polyaniline/chitosan composite systems: Synthesis, structure, and functional properties, Russian Journal of Applied Chemistry 88(11) (2015) 1788-1792.

[35] M.M. Abdi, H.E. Mahmud, A. Kassim, W.M.M. Yunus, Z.A. Talib, M.J. Haron, Synthesis and characterization of a new conducting polymer composite, Polymer Science Series B 52(11-12) (2010) 662-669.

[36] S.S. Tarimsal Gulmen, E.S. Guvel, K. Nilgun, Preparation and characterization of chitosan/polypyrrole/sepiolite nanocomposites, Procedia-Social and Behavioral Sciences 195 (2015) 1623-1632.

[37] T. Thanpitcha, A. Sirivat, A.M. Jamieson, R. Rujiravanit, Preparation and characterization of polyaniline/chitosan blend film, Carbohydrate Polymers 64(4) (2006) 560-568.

[38] E. Khor, J.L. Whey, Interaction of chitosan with polypyrrole in the formation of hybrid biomaterials, Carbohydrate polymers 26(3) (1995) 183-187.

[39] K.Z. Elwakeel, A.A. Atia, A.M. Donia, Removal of Mo(VI) as oxoanions from aqueous solutions using chemically modified magnetic chitosan resins, Hydrometallurgy 97(1) (2009) 21-28.

[40] J. Sun, S. Zhou, P. Hou, Y. Yang, J. Weng, X. Li, M. Li, Synthesis and characterization of biocompatible Fe_3O_4 nanoparticles, Journal of Biomedical Materials Research Part A 80(2) (2007) 333-341.

[41] I. Gawri, S. Khatta, K. Singh, S. Tripathi, Synthesis and characterization of polyaniline as emeraldine salt, AIP Conference Proceedings, AIP Publishing, 2016, p. 020287.

[42] A. Abdolahi, E. Hamzah, Z. Ibrahim, S. Hashim, Synthesis of uniform polyaniline nanofibers through interfacial polymerization, Materials 5(8) (2012) 1487-1494.

[43] S. Govindan, E.A.K. Nivethaa, R. Saravanan, V. Narayanan, A. Stephen, Synthesis and characterization of chitosan–silver nanocomposite, Applied Nanoscience 2(3) (2012) 299-303.

[44] R. Ramya, P. Sudha, J. Mahalakshmi, Preparation and characterization of chitosan binary blend, International Journal of Scientific and Research Publications 2 (10) (2012) 1-9.

[45] A.U. Ayse Gul Yavuz, Venkat R. Bhethanabotla, Substituted polyaniline/chitosan composites: Synthesis and characterization, Carbohydrate Polymers 75 (2009) 448–453.

[46] H. Bagheri, A. Roostaie, M.Y. Baktash, A chitosan-polypyrrole magnetic nanocomposite as μ-sorbent for isolation of naproxen, Analytica chimica acta 816 (2014) 1-7.

[47] Z.D. Zujovic, C. Laslau, J.T. Sejdic, Lamellar-structured nanoflakes comprised of stacked oligoaniline nanosheets, Chemistry-An Asian Journal 6(3) (2011) 701-701.

[48] M. Bhaumik, T.Y. Leswifi, A. Maity, V. Srinivasu, M.S. Onyango, Removal of fluoride from aqueous solution by polypyrrole/Fe_3O_4 magnetic nanocomposite, Journal of Hazardous Materials 186(1) (2011) 150-159.

[49] X.N. Pham, T.P. Nguyen, T.N. Pham, T.T. Nga Tran, T.V. Thi Tran, Synthesis and characterization of chitosan-coated magnetite nanoparticles and their application in curcumin drug delivery, Advances in Natural Sciences: Nanoscience and Nanotechnology 7(4) (2016) 045010.

[50] X. Jiang, J. Cheng, H. Zhou, F. Li, W. Wu, K. Ding, Polyaniline-coated chitosan-functionalized magnetic nanoparticles: preparation for the extraction and analysis of endocrine-disrupting phenols in environmental water and juice samples, Talanta 141 (2015) 239-246.

[51] H. Bagheri, A. Roostaie, M.Y. Baktash, A chitosan–polypyrrole magnetic nanocomposite as μ-sorbent for isolation of naproxen, Analytica Chimica Acta 816 (2014) 1-7.

[52] Z. Baysal, Y. Bulut, M. Yavuz, C. Aytekin, Immobilization of α-amylase via adsorption onto bentonite/chitosan composite: Determination of equilibrium, kinetics, and thermodynamic parameters, Starch-Starke 66(5-6) (2014) 484-490.

[53] X. Liu, X. Chen, Y. Li, X. Wang, X. Peng, W. Zhu, Preparation of superparamagnetic Fe_3O_4@alginate/chitosan nanospheres for candida rugosa lipase immobilization and utilization of layer-by-layer assembly to enhance the stability of immobilized lipase, ACS Applied Materials & Interfaces 4(10) (2012) 5169-5178.

[54] J. Abdullah, M. Ahmad, L.Y. Heng, N. Karuppiah, H. Sidek, An optical biosensor based on immobilization of laccase and MBTH in stacked films for the detection of catechol, Sensors 7(10) (2007) 2238-2250.

[55] S.Z. Mazlan, S.A. Hanifah, Effects of temperature and pH on immobilized laccase activity in conjugated methacrylate-acrylate microspheres, International Journal of Polymer Science 2017 (2017) 8.

[56] E. Fatarella, D. Spinelli, M. Ruzzante, R. Pogni, Nylon 6 film and nanofiber carriers: preparation and laccase immobilization performance, Journal of Molecular Catalysis B: Enzymatic 102 (2014) 41-47.

[57] M. Sevilla, P. Valle-Vigón, P. Tartaj, A.B. Fuertes, Magnetically separable bimodal mesoporous carbons with a large capacity for the immobilization of biomolecules, Carbon 47(10) (2009) 2519-2527.

[58] P.C. Ashly, P.V. Mohanan, Preparation and characterization of Rhizopus amyloglucosidase immobilized on poly(o-toluidine), Process Biochemistry 45(8) (2010) 1422-1426.

[59] P.C. Ashly, M. Joseph, P. Mohanan, Activity of diastase α-amylase immobilized on polyanilines (PANIs), Food Chemistry 127(4) (2011) 1808-1813.

[60] T. Handa, A. Hirose, T. Akino, K. Watanabe, H. Tsuchiya, Preparation of immobilized α-amylase covalently attached to granular polyacrylonitrile, Biotechnology and Bioengineering 25(12) (1983) 2957-2967.

[61] Y. Zhou, L. Wang, T. Wu, X. Tang, S. Pan, Optimal immobilization of β-glucosidase into chitosan beads using response surface methodology, Electronic Journal of Biotechnology 16(6) (2013) 6-6.

[62] S. Yodoya, T. Takagi, M. Kurotani, T. Hayashi, M. Furuta, M. Oka, T. Hayashi, Immobilization of bromelain onto porous copoly(γ-methyl-l-glutamate/l-leucine) beads, European Polymer Journal 39(1) (2003) 173-180.

[63] E.A. Karam, W.A. Abdel Wahab, S.A.A. Saleh, M.E. Hassan, A.L. Kansoh, M.A. Esawy, Production, immobilization and thermodynamic studies of free and immobilized Aspergillus awamori amylase, International Journal of Biological Macromolecules 102 (2017) 694-703.

[64] M.A. Abdel-Naby, A.M. Hashem, M.A. Esawy, A.F. Abdel-Fattah, Immobilization of Bacillus s ubtilis of its enzymatic properties, Microbiological Research 153 (1998) 1-7.

[65] B. Krajewska, M. Leszko, W. Zaborska, Urease immobilized on chitosan membrane: preparation and properties, Journal of Chemical Technology & Biotechnology 48(3) (1990) 337-350.

[66] M. Talebi, S. Vaezifar, F. Jafary, M. Fazilati, S. Motamedi, Stability improvement of immobilized α-amylase using nano pore zeolite, Iranian Journal of Biotechnology 14(1) (2016) 33.

[67] M. Sharma, V. Sharma, D.K. Majumdar, Entrapment of -Amylase in Agar Beads for Biocatalysis of Macromolecular Substrate, International Scholarly Research Notices 2014 (2014) 8.

[68] K. Singh, G. Srivastava, M. Talat, O.N. Srivastava, A.M. Kayastha, α-Amylase immobilization onto functionalized graphene nanosheets as scaffolds: Its characterization, kinetics and potential applications in starch based industries, Biochemistry and biophysics reports 3 (2015) 18-25.

[69] M. Usman, V. Ekwueme, T. Alaje, M. Afolabi, S. Bolakale, Immobilization of α-Amylase on mesoporous silica KIT-6 and palm wood chips for starch hydrolysis, Chemical and Process Engineering Research 9 (2013) 7-13.

[70] M. Amid, Y. Manap, N.K. Zohdi, Microencapsulation of purified Amylase enzyme from Pitaya (Hylocereus polyrhizus) peel in Arabic Gum-Chitosan using freeze drying, Molecules 19(3) (2014) 3731-3743.

[71] Y. Zhang, J. Ge, Z. Liu, Enhanced activity of immobilized or chemically modified enzymes, ACS Catalysis 5(8) (2015) 4503-4513.

[72] P.C. Ashly, A study on the immobilization of enzymes on polymeric supports, a doctoral dissertation, Cochin University of Science and Technology, India, 2009.

[73] S.A. Ahmed, O.K. Hassan, Studies on the Activity and Stability of Immobilized Bacillus acidocaldarius alpha-amylase, Australian Journal of Basic and Applied Sciences 2(3) (2008) 466-474.

[74] B.L. Tee, G. Kaletunc, Immobilization of a thermostable α-amylase by covalent binding to an alginate matrix increases high temperature usability, Biotechnology Progress 25(2) (2009) 436-445.

[75] M. Arica, V. Hasirci, N. Alaeddinoglu, Covalent immobilization of α-amylase onto pHEMA microspheres: preparation and application to fixed bed reactor, Biomaterials 16(10) (1995) 761-768.

[76] G. Bayramoglu, M. Yilmaz, M.Y. Arica, Immobilization of a thermostable α-amylase onto reactive membranes: kinetics characterization and application to continuous starch hydrolysis, Food Chemistry 84(4) (2004) 591-599.

[77] M.V. Kahraman, N. Kayaman-Apohan, A.E. Ogan, A. Gungor, Soybean oil based resin: A new tool for improved immobilization of α-amylase, Journal of Applied Polymer Science 100(6) (2006) 4757-4761.

[78] H. Tumturk, S. Aksoy, N. Hasirci, Covalent immobilization of α-amylase onto poly (2-hydroxyethyl methacrylate) and poly (styrene-2-hydroxyethyl methacrylate) microspheres and the effect of Ca^{2+} ions on the enzyme activity, Food Chemistry 68(3) (2000) 259-266.

[79] D. Gangadharan, K.M. Nampoothiri, S. Sivaramakrishnan, A. Pandey, Immobilized bacterial α-amylase for effective hydrolysis of raw and soluble starch, Food Research International 42(4) (2009) 436-442.

[80] L. Cao, Immobilised enzymes: science or art?, Current Opinion in Chemical Biology 9(2) (2005) 217-226.

[81] C. Mateo, J.M. Palomo, G. Fernandez-Lorente, J.M. Guisan, R. Fernandez-Lafuente, Improvement of enzyme activity, stability and selectivity via immobilization techniques, Enzyme and Microbial Technology 40(6) (2007) 1451-1463.

[82] A. Kumari, A.M. Kayastha, Immobilization of soybean (Glycine max) α-amylase onto Chitosan and Amberlite MB-150 beads: Optimization and characterization, Journal of Molecular Catalysis B: Enzymatic 69(1) (2011) 8-14.

[83] M. Radovanovic, B. Jugovic, M. Gvozdenovic, B. Jokic, B. Grgur, B. Bugarski, Z. Knezevic-Jugovic, Immobilization of α-amylase via adsorption on magnetic particles coated with polyaniline, Starch-Starke 68(5-6) (2016) 427-435.

[84] K.V.Harish Prashanth, R.N. Tharanathan, Studies on graft copolymerization of chitosan with synthetic monomers, Carbohydrate Polymers 54(3) (2003) 343-351.

[85] P. Redoks, Synthesis of chitosan-grafted-poly (methyl methacrylate) with fenton's reagent (Fe_{2+}-H_2O_2) as a redox initiator, Malaysian Journal of Analytical Sciences 18(2) (2014) 415-422.

[86] A.T. Paulino, J.I. Simionato, J.C. Garcia, J. Nozaki, Characterization of chitosan and chitin produced from silkworm crysalides, Carbohydrate Polymers 64(1) (2006) 98-103.

[87] V. Singh, D.N. Tripathi, A. Tiwari, R. Sanghi, Microwave promoted synthesis of chitosan-graft-poly(acrylonitrile), Journal of Applied Polymer Science 95(4) (2005) 820-825.

[88] V. Singh, D.N. Tripathi, A. Tiwari, R. Sanghi, Microwave promoted synthesis of chitosan-graft-poly (acrylonitrile), Journal of Applied Polymer Science 95(4) (2005) 820-825.

[89] R.K. Das, D. Basu, A. Banerjee, Study of methyl-methacrylate -viscose fiber graft copolymerization and the effect of grafting on thermal properties, Journal of Applied Polymer Science 72(1) (1999) 135-140.

[90] C. Palocci, L. Chronopoulou, I. Venditti, E. Cernia, M. Diociaiuti, I. Fratoddi, M.V. Russo, Lipolytic enzymes with improved activity and selectivity upon adsorption on polymeric nanoparticles, Biomacromolecules 8(10) (2007) 3047-3053.

[91] Z.G. Wang, L.S. Wan, Z.K. Xu, Surface engineerings of polyacrylonitrile-based asymmetric membranes towards biomedical applications: An overview, Journal of Membrane Science 304(1-2) (2007) 8-23.

[92] S. Aksoy, H. Tumturk, N. Hasirci, Stability of α-amylase immobilized on poly (methyl methacrylate-acrylic acid) microspheres, Journal of Biotechnology 60(1-2) (1998) 37-46.

[93] G.A. Meridor David, Preparation of enzyme nanoparticles and studying the catalytic activity of the immobilized nanoparticles on polyethylene films, Ultrasonics Sonochemistry 20(1) (2013) 425-431.

[94] F. Kara, G. Demirel, H. Tumturk, Immobilization of urease by using chitosan-alginate and poly (acrylamide-co-acrylic acid)/κ-carrageenan supports, Bioprocess and Biosystems Engineering 29(3) (2006) 207-211.

[95] D. Ningsih, D. Kartika, A. Fatoni, A. Zuliana, Bacillus thuringiensis HCB6 Amylase Immobilization by Chitosan Beads, IOP Conference Series: Materials Science and Engineering, IOP Publishing, 2017, p. 012068.

[96] R. Reshmi, G. Sanjay, S. Sugunan, Enhanced activity and stability of α-amylase immobilized on alumina, Catalysis Communications 7(7) (2006) 460-465.

[97] M.A. Abdel-Naby, A.M. Hashem, M.A. Esawy, A.F. Abdel-Fattah, Immobilization of Bacillus subtilis α-amylase and characterization of its enzymatic properties, Microbiological research 153(4) (1999) 319-325.

[98] E. Aguiar-Oliveira, F. Maugeri, Thermal stability of the immobilized fructosyltransferase from Rhodotorula sp, Brazilian Journal of Chemical Engineering 28(3) (2011) 363-372.

[99] O.L. Tavano, R. Fernandez-Lafuente, A.J. Goulart, R. Monti, Optimization of the immobilization of sweet potato amylase using glutaraldehyde-agarose support. Characterization of the immobilized enzyme, Process Biochemistry 48(7) (2013) 1054-1058.

[100] S. Talekar, S. Chavare, Optimization of immobilization of α-amylase in alginate gel and its comparative biochemical studies with free α-amylase, Recent Research in Science and Technology 4(2) (2012).

[101] D. Kumar, M. Muthukumar, N. Garg, Kinetics of fungal extracellular α-amylase from Fusarium solani immobilized in calcium alginate beads, Journal of Environmental Biology 33(6) (2012) 1021.

[102] G.P. Lopez, B.D. Ratner, R.J. Rapoza, T.A. Horbett, Plasma deposition of ultrathin films of poly (2-hydroxyethyl methacrylate): surface analysis and protein adsorption measurements, Macromolecules 26(13) (1993) 3247-3253.

[103] C. Garcia-Galan, A. Berenguer-Murcia, R. Fernandez-Lafuente, R.C. Rodrigues, Potential of different enzyme immobilization strategies to improve enzyme performance, Advanced Synthesis & Catalysis 353(16) (2011) 2885-2904.

[104] R.C. Rodrigues, C. Ortiz, A. Berenguer-Murcia, R. Torres, R. Fernandez-Lafuente, Modifying enzyme activity and selectivity by immobilization, Chemical Society Reviews 42(15) (2013) 6290-6307.

[105] F. Roy, M.V. Hegde, Immobilization of β-amylase on polystyrene cation exchange resin equilibrated with Al^{3+}ions (IR-120 Al^{3+}), Enzyme and Microbial Technology 9(9) (1987) 550-552.

[106] T. Hayrettin, A. Serpil, H. Nesrin, Covalent Immobilization of a α-Amylase onto poly (methyl methacrylate-2-hydroxyethyl methacrylate) microspheres and the effect of Ca^{2+} ions on the enzyme activity, Starch-Starke 51(6) (1999) 211-217.

[107] H. Tumturk, S. Aksoy, N. Hasirci, Covalent immobilization of α-amylase onto poly(2-hydroxyethyl methacrylate) and poly(styrene-2-hydroxyethyl methacrylate) microspheres and the effect of Ca^{2+} ions on the enzyme activity, Food Chemistry 68(3) (2000) 259-266.

[108] [108] R. Zhai, B. Zhang, L. Liu, Y. Xie, H. Zhang, J. Liu, Immobilization of enzyme biocatalyst on natural halloysite nanotubes, Catalysis Communications 12(4) (2010) 259-263.

[109] E. Cakmakci, A.B. Cigil, O. Danıs, S. Demir, M.V. Kahraman, Immobilization of alpha-amylase on aminated polyimide membrane: Preparation, characterization, and properties, Starch-Starke 66(3-4) (2014) 274-280.

[110] D. Serap, G.S. Burcu, K.M. Vezir, α-Amylase immobilization on functionalized nano $CaCO_3$ by covalent attachment, Starch-Starke 64(1) (2012) 3-9.

[111] M.V. Kahraman, N. Kayaman-Apohan, A.E. Ogan, A. Gungor, Soybean oil based resin: A new tool for improved immobilization of α-amylase, Journal of Applied Polymer Science 100(6) (2006) 4757-4761.

Chapter 4

Modified forms of magnetic chitosan by inorganic layered solids as α-amylase carriers

Contents

4.1 Introduction

The layered solids comprised of stacked arrangement of two dimensional layers with high characteristic ratio one above the other to form three dimensional macro molecular structures. Here the adjacent layers hold together by van der Waals forces and the atoms of the same layer experiencing covalent bond between them. Hence the bonding between the atoms of the same layer constitutes much stronger than the bonding between the atoms of adjacent layers [1]. The guest species can be accommodated into the spaces between the layers with respect to their charges.

The important layered solids such as smectic clays and layered oxides consist of negatively charged layers with positively charged ions occupied in the interlayer. The cationic biomolecules have been introduced into the interlayer spaces of smectites [2-4] and the amino groups of enzyme can be interacted with these types of layered solids through electrostatic interaction.

The graphite oxide (GO) has layered structure and can act as an adsorbent to remove biomaterials [5]. The multiple oxygen containing

functional groups of GO are covalently bonded to its layers and form negatively charged surface on to it. The exfoliation of graphite oxide gives graphene oxide on which many studies were reported as efficient enzyme carrier. This layered material can be dispersed into the polymer matrix in order to provide enhanced mechanical and thermal properties and hence impart biocompatibility to the resultant composite. Many attempts have been done in order to improve the electrical properties of chitosan by the dispersion of super paramagnetic Fe_3O_4 nanoparticles for biosensor applications [6]. The dispersion of Fe_3O_4 and graphene oxide into chitosan matrix was also reported in which the mechanical and electrical properties of graphene oxide and Fe_3O_4 was combined with scaffold forming properties of chitosan [7]. The various surface functional groups on graphene oxide such as –OH, –O–, C=O and –COOH contribute hydrophilic nature to it which favor the adsorption of enzyme and due to the presence of these functional groups, the enzymes can also be covalently immobilized on it without any cross-linkers. There are many reports in which the enzyme successfully immobilized on the surface of graphene oxide layer without getting any pretreatment [8, 9]. Pavlidis et al. observed that the amine functionalized graphene oxide layer has been performed as effective carrier for enzyme immobilization of industrially important enzymes such as lipase and esterase [10]. The improvement in thermal stability, reusability and storage stability of immobilized enzymes has also observed when gluteraldehyde was used as cross-linker in the covalent immobilization method [11, 12].

Montmorillonite is a layered silicate structure showing intercalation properties and have certain characteristics such as chemically inert and higher temperature resistance [13] . The clays are aluminosilicates which consists of acidic sites and can be interact with the amino groups of enzyme.

As this interaction is much stronger than the physical adsorption, the enzyme leaching from the support can be much reduced [14]. The hydrophobic character of the clay can be changed through organo modification that could increase the strength of enzyme adsorption and hence the catalytic activity of the enzyme [15]. The intercalation of MMT with chitosan showed improvement in their stability and mechanical properties. The polycationic nature of chitosan provides excellent intercalation with MMT [16, 17]. The improved properties of the composite may be due to the stronger interfacial interaction between layered MMT and the polymer matrix. The improvement in mechanical properties of the composite could be due to the electrostatic interaction between the hydroxyl and amino groups of chitosan and the clay surface. The chitosan-clay composite attained enhanced thermal stability due to the superior insulation property of the clay mineral which provided mass transport barrier against thermal degradation of the polymer matrix [18]. Sanjay et al. reported the effective immobilization of α-amylase on to montmorillonite by adsorption and covalent method [19]. The author observed that as the entire enzyme backbone was on the periphery of the clay surface the enzyme as a whole is not intercalated. Tohid Mardani et al. noticed that chitosan-montmorillonite nanocomposite beads were found to be suitable carrier for α-amylase immobilization [20]. A study on interactions of clay rich in montmorillonite with enzymes were reported by azzouz et al. and they declared that the clay-enzyme interactions were mainly due to the cations presented at the surface of clay which determined by their acid base properties [21].

The current chapter deals with the effectiveness of modified magnetic chitosan by graphite oxide and montmorillonite as enzyme carrier for α-amylase immobilization. This describes the adsorption and covalent

immobilization methods for α-amylase on CSM-GO composite. The variation of MMT concentration in CSM-MMT composite on enzyme immobilization is also investigated in this chapter.

4.2 Materials Used

Ferrous sulphate, ferric chloride and ammonium hydroxide were purchased from S.d. Fine Chemicals Ltd. Mumbai. Graphite powder, montmorillonite, potassium permanganate and hydrogen peroxide solution were procured from Sigma Aldrich Chemicals. Gluteraldehyde was acquired from LOBA CHEMIE Pvt. Ltd. Mumbai. Chitosan (95% degree of deacylation) was obtained from Meron marine chemicals, Cochin. The details of materials used for protein estimation and activity assay were given in the chapter 2.

4.3 Graphite oxide modified magnetic chitosan as α-amylase carrier

4.3.1 Synthesis of graphite oxide modified magnetic chitosan

Synthesis of magnetic particles

The co-precipitation method was adopted for the preparation of magnetic particles in which the precursors used are the aqueous mixture of ferrous sulphate ($FeSO_4.7H_2O$) and ferric chloride ($FeCl_3.6H_2O$) keeping their molar concentration in the proportion of Fe^{2+}:Fe^{3+} = 1:2 [22]. A volume of 125 mL of the precursors with molar concentration of aqueous solutions 2M Fe^{3+} and 1M Fe^{2+} was mixed and agitated thoroughly. Afterwards, NH_4OH added to the above solution drop by drop under constant stirring at room temperature until the pH reaches 9. The resulting black precipitated suspension was heated at 80 ºC for 30 minutes, then the

precipitate filtered and washed with distilled water. The precipitate was dried in vacuum oven at 70 ºC and ground to fine powder.

Synthesis of graphite oxide (GO)

Graphite oxide (GO) was synthesized by utilizing the altered form of Hummers' method [23]. About 1g graphite powder was stirred in 23 mL conc.H_2SO_4 at 0 °C. Then 3g potassium permanganate was added gradually in to the resultant suspension, maintaining the temperature less than 20 °C. After taken from the ice bath, the reaction mixture was agitated at room temperature for about 30 min. About 23 mL of distilled water slowly added into the suspension by keeping the temperature less than 98 °C. The suspension was kept for 10 min. agitation and again diluted with 140 mL of distilled water. About 10 mL of hydrogen peroxide solution (30 wt %) was added in to the reaction mixture and then kept for overnight. The precipitate formed was decanted and then dried.

Synthesis of magnetic chitosan-graphite oxide composite

Chitosan solution was prepared by dissolving 2 g chitosan in 100ml of 2 % acetic acid (v/v) and then the mixture was stirred for 30 min. of sonication. The prepared chitosan solution was stirred continuously for 2 h with 0.75 g of magnetite. After that 5 mL of gluteraldehyde (25 %) was mixed with the resultant solution and then about 1.5 g of graphite oxide was successively added in to it. The pH of the solution was maintained between 9 and 10 and kept stirred for 1 h at 80 °C. The precipitate formed was separated by applying an external magnetic field, washed with ethanol and distilled water and then dried in a vacuum oven at 50 °C.

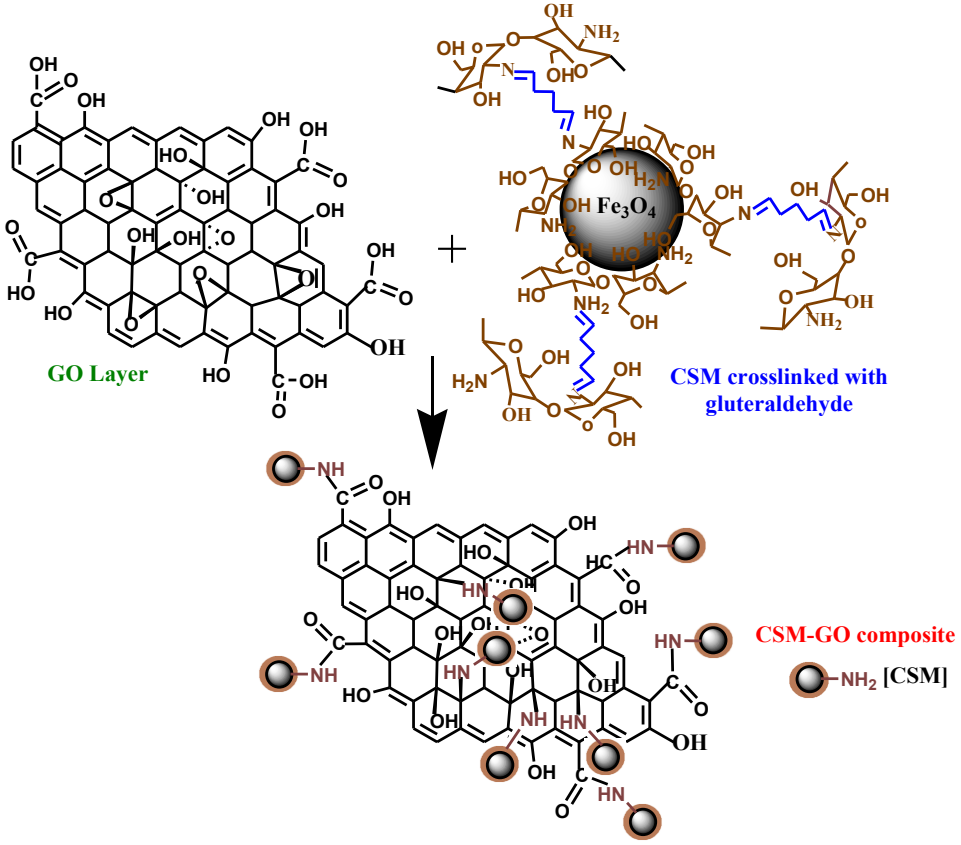

Scheme 4.1 Composite formation of magnetic chitosan with graphite oxide

4.3.2 Physico-chemical characterization

4.3.2.1 Infrared spectra

The IR spectra of GO, CSM and CSM-GO are shown in the figure 4.1 and the peak informations are detailed in the table 4.1. The spectrum of GO exhibited the vibrational bands at 1750 cm^{-1} corresponding to the carboxyl groups. The peak at 1055 cm^{-1} assigned to the presence of epoxy groups and the band at 1200 cm^{-1} might be due to the C–O group vibrations in epoxides [24, 25]. The peak at 1600 cm^{-1} indicated the C=C stretching vibrations and the broad peak at 1350 cm^{-1} attributed to the C–OH stretching vibrations.

For CSM-GO the broad peak that observed at 3400 cm^{-1} assigned to the combined stretching vibrations of NH_2 and OH groups. The peak of GO at 1750 cm^{-1} corresponding to the carboxyl groups was found to be disappeared in case of CSM-GO indicated that the composite formation has taken place due to the reaction of carboxyl group of GO with amino group of chitosan to form amides. As a result of this the intensity of the amide peak of CSM presented at 1614 cm^{-1} was found to be broadened and shifted to 1636 cm^{-1} in case of CSM-GO. The intensity of the NH_2 vibrational bands is more in case of CSM-GO which appeared at 1597 cm^{-1} than that of CSM which confirmed the composite formation. The amino groups of chitosan react with epoxy groups of GO through the nucleophilic substitution reaction. The Fe–O bond vibrations are noticed in the range of 575 cm^{-1} indicated the presence of magnetite in the composite. The peak at 1450 cm^{-1} was attributed to the symmetric deformations of methyl and methylene groups and the band at 1025 cm^{-1} assigned to C–O–C stretching vibration [26, 27].

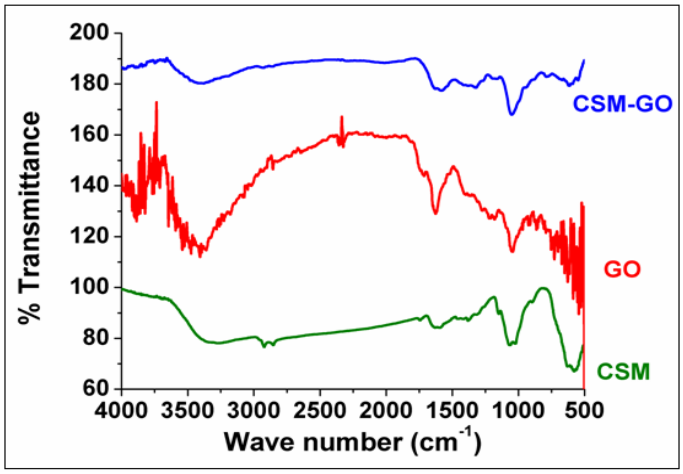

Figure: 4.1 IR Spectra of CSM, GO and CSM-GO

Table 4.1 Peak assignments for GO modified magnetic chitosan

Peak assignment (cm^{-1})	CSM	GO	CSM-GO
N–H and O–H stretching vibration	3310	-	3400
C=O stretching vibration in carboxylic acid	-	1750	-
NH_2 bending	1514	-	1597
C=O stretching of amide	1614	-	1636
C–O group stretching vibrations	1056	1200	1078
C–O–C stretching vibration	1028	1055	1025
Fe–O bond vibration	577	-	570

4.3.2.2 X-ray powder diffraction spectra

The XRD spectra of CSM-GO exhibited broad peak around 2θ = 20° corresponds to the chitosan presented in the composite. The GO peak at 2θ = 9° can be seen in case of CSM-GO with lesser intensity which may be due to the structural disorder of the graphite oxide layer as it was reduced when reacted with chitosan during the composite formation [28]. The introduction of amino groups of magnetic chitosan in to the graphite oxide layer leads to the changes in its interlayer spacing.

The other peaks at 2θ=30.5°, 35.2°, 43°, 54.1°, 57.1° and 62.8° are assigned to the indices (220), (311), (400), (422), (511) and (440) respectively characteristics to the crystalline phases of Fe_3O_4 with cubic inverse spinel structure [29]. This indicated that composite formation of CSM with GO provides little changes in the crystalline phases of magnetite. The average crystallite size was calculated as 38.08 nm from Debye–Scherrer equation.

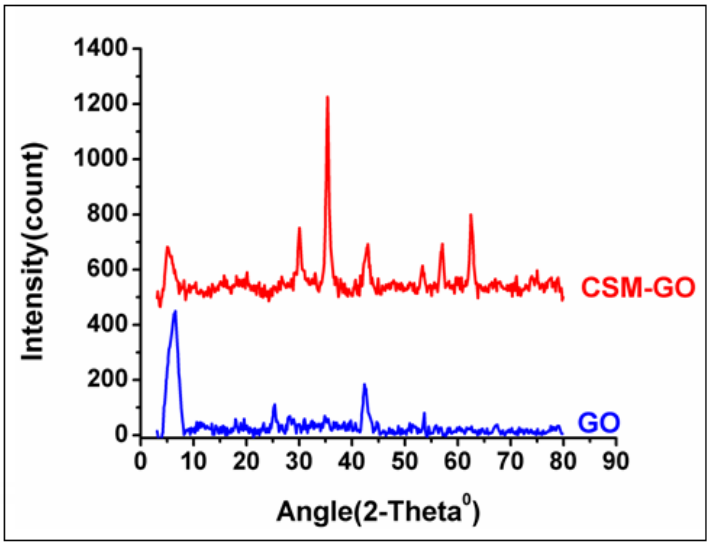

Figure: 4.2 XRD Spectra of GO and CSM-GO

4.3.2.3 Thermal analysis

The TGA-DTG curves of CSM-GO was compared with that of GO and are depicted in the figure 4.3. For CSM-GO the first peak presented at 100 °C was due to the evaporation of physically adsorbed water. The second major weight loss observed at 150-250 °C was associated with the decomposition of surface functional groups of GO such as epoxy and carboxyl groups [24]. The intensity of the peak was found to be less when compared to that of GO. This fact also confirms the composite formation of CSM with GO as the reaction during the composite formation leads to the structural disorder of the GO layer due to its reduction. The third weight loss at 250-350 °C attributed to the decomposition of chitosan with hydroxyl and amino functional groups. The other minor peaks observed above 400 °C might be related to the further degradation of chitosan residues [30].

The TGA curves revealed the better thermal stability of CSM-GO composite. For GO 40 % weight loss was obtained up to 200 °C whereas

CSM-GO showed only 20 % of weight loss at the same temperature range. At 600 °C, GO exhibited almost 100 % degradation while for CSM-GO only 70 % of weight loss occurred and this accounts for its better thermal stability.

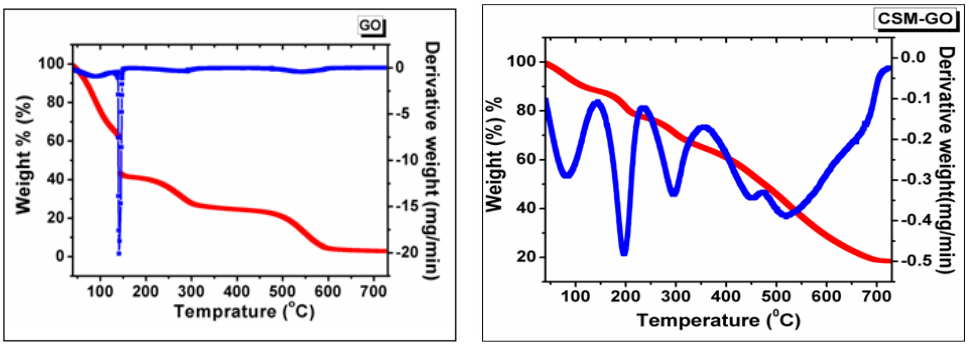

(i) (ii)

Figure: 4.3 TGA-DTG curves of (i) GO and (ii) CSM-GO

4.3.2.4 Surface area analysis

BET analysis was implemented for the evaluation of the surface area of CSM-GO composite and it was acquired an appreciable value of 5.4 m^2g^{-1}. Surface area of the support plays an important role in enzyme immobilization; one with large surface area should be acquired best loading capacity towards enzyme. Here the surface area of CSM was improvised considerably due to the introduction of GO particles which in turn results in an efficient enzyme carrier.

4.3.2.5 Energy dispersive X-ray analysis

The EDX spectrum of CSM-GO is given in the figure 4.4 and the elemental data obtained are presented in the table 4.2. The acquired data were compared with that of magnetic chitosan and the structural modification of CSM was confirmed by the presence of increased amount of O and C and decreased amount of N and Fe in CSM-GO.

Table 4.2 Elemental data of CSM-GO

Element	Weight %	Atomic %
O	46.07	45.21
C	30.98	40.28
N	18.30	20.41
Fe	13.65	3.9

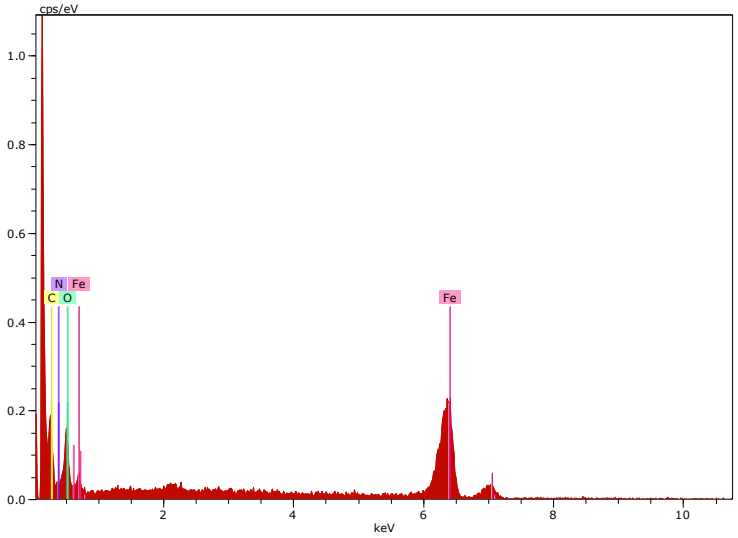

Figure: 4.4 EDX spectra of CSM-GO

4.3.2.6 Magnetic properties

The magnetic property of CSM-GO composite was studied by using VSM analysis and the magnetization curve was shown in the figure 4.5. The plot gives the saturation magnetization value of 5.33 emu g^{-1} and this decreased value compared to CSM may be as a result of the low loading of magnetite on CSM-GO composite [31, 32]. The modification of magnetic chitosan with GO reduces its overall magnetic property due to the presence of non magnetic GO particles.

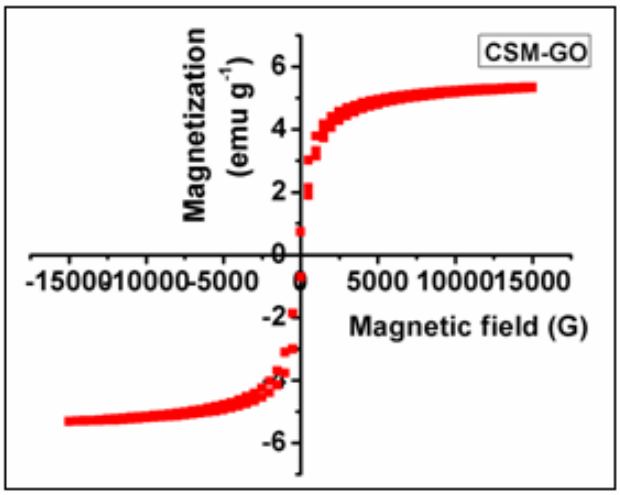

Figure: 4.5 Magnetization curve of CSM-GO composite

4.3.3 Immobilization of α-amylase on GO modified magnetic chitosan

Adsorption and covalent binding methods were adopted for the α-amylase immobilization on CSM-GO composite.

Adsorption method

A definite volume of enzyme in desired buffer was added in to 1g support and incubated in a water bath shaker for 2 h at room temperature. Then the immobilized enzyme has undergone magnetic separation and washed several times with the same buffer in order to remove the unbound enzyme.

Covalent method

In this method 1 mL of 25 % gluteraldehyde solution was mixed with 1 g support in basic medium and the mixture was allowed to stir for 3 h at room temperature. After the time period the modified support magnetically separated and washed with the same buffer in order to remove the excess gluteraldehyde. The support was dried in air, immersed in the enzyme

solution in buffer and incubated in a shaking water bath under constant stirring for 2 h at room temperature. The immobilized enzyme thus formed was separated by external magnetic field and washing was performed three times with the same buffer for the removal of unbound enzyme.

4.3.3.1 Optimization of α-amylase immobilization conditions

4.3.3.1.1 Effect of immobilization pH on α-amylase activity

In adsorption method, since GO in the support has plenty of surface functional groups such as carboxyl and epoxy groups, its surface can strongly interact with the enzyme molecules via electrostatic interaction. The gluteraldehyde activated CSM-GO promotes multipoint covalent binding with the enzyme, through their aldehyde groups and free amino groups of enzyme.

The optimum pH of the enzyme may shift towards the acidic or alkaline region as a result of immobilization. The immobilized enzyme formed through both of the methods has shown the optimum pH at 6. But the activity of covalently immobilized enzyme at either side of this optimum pH was found to be high and it has shown broader pH profile compared to the other. This increased activity might be as a result of more active conformation of enzyme which attained through the strong interaction between the enzyme and the support during covalent immobilization [33]. These covalent interactions are much more affected the intra molecular forces of enzyme than that caused by adsorption in order to maintain the active conformation of enzyme.

The adsorption immobilization of enzyme should be strongly influenced by the electrostatic interaction between enzyme and the support. α-amylase (pI=4.6) has a net positive charge at pH below 4.6 and a net

negative charge at pH above 4.6. The multiple oxygen containing functional groups in CSM-GO can provide negatively charged surfaces and can interact with the positively charged enzyme. The amino groups of CSM-GO established after the cleavage of epoxy groups of GO through the nucleophilic attack of the lone pair of amino groups of CSM and the amido groups of CSM-GO that originated after the interaction of carboxyl groups of GO with the amino groups of CSM form the cationic sites at acidic pH values, which can make electrostatic interaction with the negatively charged enzyme [34, 35].

As the pH varied from 5 to 6 the relative enzyme activity was found to be increased which might be due to the strong interaction of negatively charged enzyme with the positively charged support. Here the enzyme interaction with cationic sites of the support predominates over the interaction with negatively charged surfaces of support which results in strong interaction between them and leads to the increase of enzyme activity.

At pH above the optimum value, the enzyme activities are likely to be decreased which could be as a result of the repulsive interaction between the enzyme and the negatively charged surfaces of the support. The other interactive forces such as hydrogen bonding between oxygen containing functional groups of support and amino acid residues of enzyme may contribute to the resultant enzyme activity. Jiali et al. argued that strong electrostatic interaction and hydrogen bonding contribute to the high loading of horseradish peroxidase on GO [8].

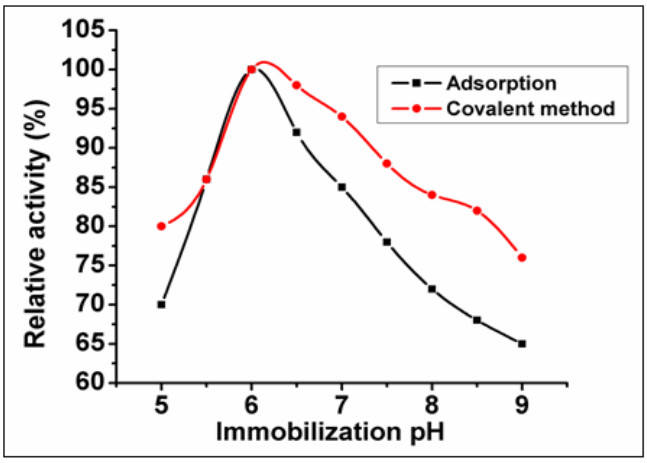

Figure: 4.6 Effect of immobilization pH on the relative activity of immobilized α-amylase by adsorption and covalent methods

4.3.3.1.2 Effect of incubation time on α-amylase activity

The incubation time course was checked for both of the immobilization methods from 60 to 300 min. and the results are depicted in the figure 4.7. For adsorption and covalent methods as the incubation time prolonged from 60 to 180 min. the relative activity of the enzyme was found to be gradually increased and then reached a plateau. As the time was further continued to increase, the activity decreased to lower values and this might be due to the reduction in the availability of the active site of the enzyme for the substrate molecule as a result of multilayer adsorption of enzyme on support. The similar trend in incubation period of immobilization process was reported by Jian et al. when cellulase was immobilized on to graphene oxide with hydrophobic spacer [36].

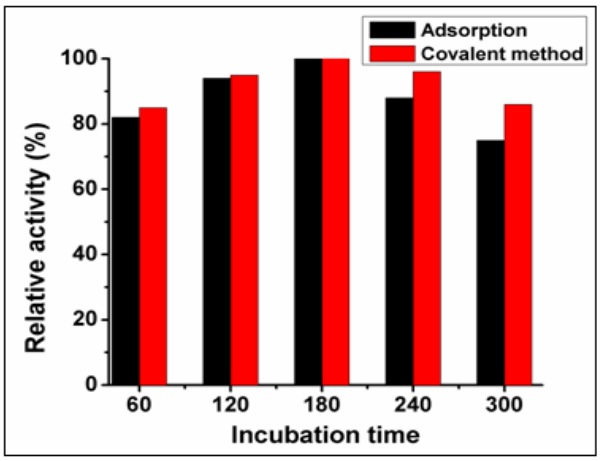

Figure: 4.7 Effect of incubation time on activity of immobilized α-amylase by adsorption and covalent methods

4.3.3.1.3 Effect of initial amount of protein on protein loading onto modified magnetic chitosan

The variations of loaded protein on CSM-GO with respect to different initial protein concentration by two different immobilization methods are shown in the figure 4.8. On comparing adsorption and covalent binding methods of immobilization, the former one has given high loaded protein on support which was 9.6 mg g^{-1} support at the initial protein amount of 12.4 mg. For covalent immobilization method the protein loaded was 5.8 mg g^{-1} support at 8.6 mg of initial protein. These initial enzyme concentrations are taken for the further studies as the optimum enzyme concentration for enzyme immobilization. The lesser amount of loaded protein in case of covalent immobilization method may be due to the reduced sites for immobilization on the surface of support as it was activated with gluteraldehyde cross-linking agents.

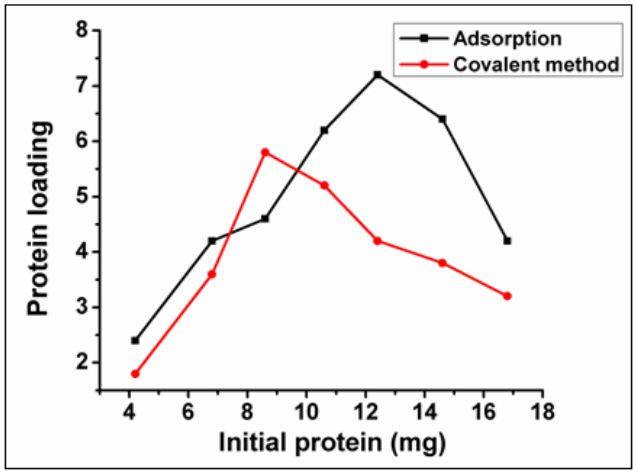

Figure: 4.8 Effect of initial protein amount on protein loading onto CSM-GO by adsorption and covalent methods

4.3.3.1.4 Effect of initial protein amount on immobilized enzyme activity

The enzyme activity of immobilized enzyme by adsorption and covalent method was plotted against the variation of initial protein amount and the figure 4.9 showed that the immobilized enzyme by adsorption method acquired higher enzyme activity, which was about 13.37 EU with initial protein of 12.4 mg. The covalently immobilized enzyme gained only the activity of 11.16 EU when 8.6 mg of enzyme was used for immobilization.

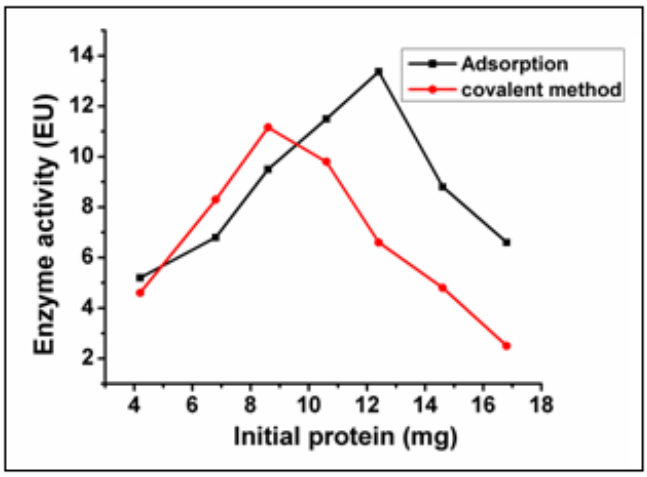

Figure: 4.9 Effect of initial protein amount on activity of immobilized α-amylase by adsorption and covalent methods

The loss in activity of covalently immobilized enzyme could be as a consequence of the changes in the structural conformation of the active site of enzyme due its multipoint covalent binding with the support. But in case of adsorption immobilization of enzyme on support only electrostatic interactions contribute to the binding forces between them. As a result of this the changes of structural conformation of enzyme should be negligible due to these weak interactive forces and hence acquired insignificant loss of enzyme activity compared to the other one.

The immobilization yield was found to be more for the immobilized enzyme by adsorption method and it was 77.42 %. This can be due to the presence of multiple oxygen containing functional groups on support provide several binding sites for enzyme and so the enzyme adsorption capacity become enhanced. The lower immobilization yield for the covalently immobilized enzyme might be due to the lesser number of gluteraldehyde activated ends as the enzyme binding sites and subsequently decreased the enzyme binding capacity.

The activity yield and immobilization efficiency were also evaluated for the immobilized enzyme by two methods and are shown in the table 4.3. The immobilized enzyme by adsorption has shown higher activity yield than covalent method and it was 63.95 %. The same has shown better immobilization efficiency than the other one. For covalently immobilized enzyme the gluteraldehyde linkages between the enzyme and support affected the structural conformation of the active site of the enzyme. This causes to slow down the starch hydrolysis reaction due to the less affinity of enzyme active site towards the substrate molecules and eventually has shown low activity yield and immobilization efficiency.

Table 4.3 Immobilization efficiency of α-amylase on CSM-GO by adsorption and covalent methods

Support	Initial protein (mg)	Immobilized protein mg/g support	IY (%)	Initial activity (EU)	Immobilized enzyme activity (EU)	AY (%)	IE (%)
CSM-GO (Adsorption)	12.4	9.6	77.42	20.89	13.37	63.95	82.6
CSM-GO (Covalent method)	8.6	5.8	67.44	25.82	11.16	43.22	64.09

4.3.3.2 Effect of pH on α-amylase activity

The pH effect on the activity of free and immobilized α-amylase by adsorption and covalent methods was investigated in the pH range 4-9 and the results are illustrated in the figure 4.10.

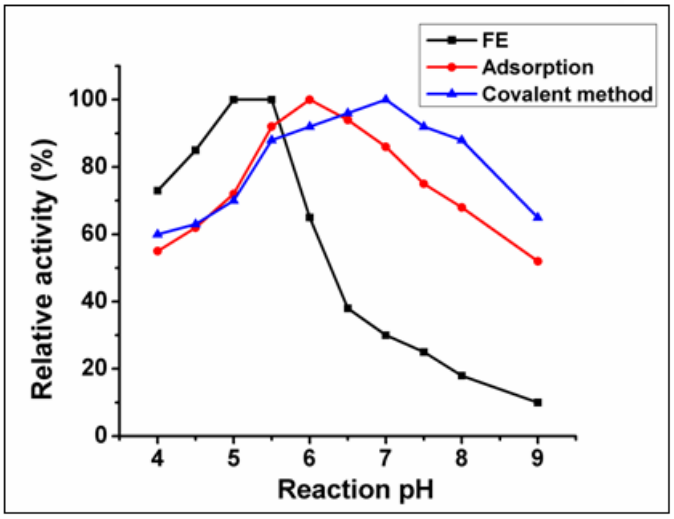

Figure: 4.10 Effect of pH on the relative activity of free and immobilized α-amylase by adsorption and covalent methods

Both of the immobilized enzymes have shown broader pH profile and their optimum pH have shifted to more alkaline region compared to free enzyme, which are at pH 6 and 7 respectively. This shift of optimum pH of enzyme depends on the method of immobilization adopted and also on the nature of the support selected. Here we observed that the covalently immobilized enzyme has retained more activity in the alkaline region than that of free and adsorbed enzyme. This could be due to the fact that the covalent binding of amino groups of enzyme with gluteraldehyde has taken place in the alkaline medium and the Schiff bases formed are stable at this region, hence the immobilized system preserved more activities [37]. But there was decrease of enzyme activities at acidic regions can be noticed which might be due to the instability of the Schiff bases at this region and subsequently enzyme desorption taken place.

For the immobilized enzyme by adsorption method, the surface functional groups on the support influence its pH stability as the

immobilization of the enzyme has been taken place by direct contact with the support. At lower pH the –COOH and $–NH_2$ functional groups present on the support get protonated and so there exists a lower H^+ concentration in the microenvironment of the immobilized enzyme compared to bulk solution which results in the pH of the immobilized enzyme more alkaline than external region. At higher pH ranges these surface functional groups became deprotonated and generated an electrostatic repulsion between the enzyme and the support which leads to the decrease of activity [38]. The similar trend was reported by Hermanova et al. when lipase immobilized on graphene oxide by physical adsorption and covalent attachment [39].

4.3.3.3 Effect of temperature on α-amylase activity

The effect of temperature on activity of free and immobilized α-amylase was analyzed in the temperature ranges from 30-60 °C. Both of the immobilized enzymes have shown optimum temperature at 40 °C.

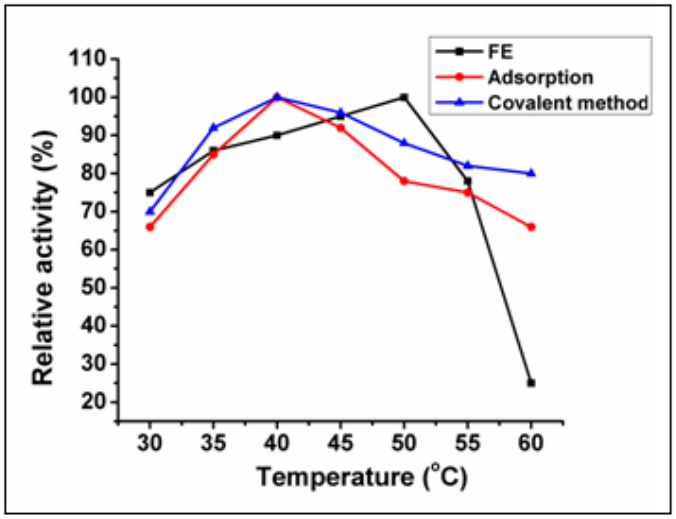

Figure: 4.11 Effect of temperature on the relative activity of free and immobilized α-amylase by adsorption and covalent methods

The immobilized enzymes have shown broader temperature profile and have retained the activity about 65 % for adsorption method and 80 % for covalent method. The enhanced activity of α-amylase on covalent immobilization provides effectual protection from heat inactivation of enzyme by structural denaturation. This confirmed that the covalent immobilization protected the α-amylase activity to a great extent than that by adsorption method. The increased activity of α-amylase was observed in many literatures where the enzyme was undergone covalent immobilization [40-42].

4.3.3.4 Activation energy

The activation energy (Ea) of enzyme catalysis reaction for CSM-GOE by both methods was calculated from Arrhenius plot shown in the figure 4.12 and the values are presented in the table 4.4. They have shown increased activation energies compared to free enzyme and out of which the covalent immobilization of α-amylase has shown lower activation energy than that of by adsorption immobilization. This described the higher catalytic efficiency of covalently immobilized enzyme and showed that the covalent immobilization conserved more energy which results in economically favorable immobilized system [43]. This observation was also associated with the mass transfer control for covalently immobilized α-amylase preferably than kinetic control.

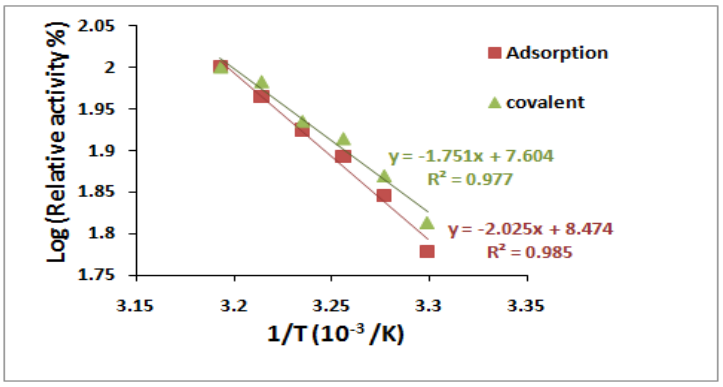

Figure: 4.12 Arrhenius plot to calculate the activation energy (Ea) of immobilized α-amylase by adsorption and covalent methods

Table 4.4 Activation energy of CSM-GOE by adsorption and covalent methods

Immobilization method	Activation energy (KJ mol^{-1})
Adsorption	16.83
Covalent method	14.56

4.3.3.5 Thermal stability of the free and immobilized enzymes

Thermal stability of free and immobilized α-amylase by adsorption and covalent methods was studied and the results are illustrated in the figure 4.13.

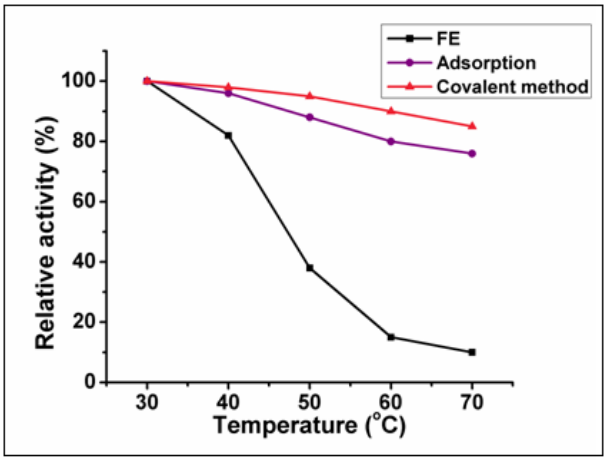

Figure:4.13 Thermal stability of free and immobilized α-amylase by adsorption and covalent methods

The free α-amylase retained 80 % of its initial activity at 40 °C while both of the immobilized enzymes preserved around 99 % of their activity at the same temperature. After this temperature the relative activity of the free enzyme decreased significantly and it has shown only 35 % of activity at 50 °C. The immobilized enzyme by adsorption method lost only 10 % of its activity at this temperature and for covalently immobilized enzyme it was about 5 % loss in activity. Both immobilization methods contribute increased thermal stability to α-amylase and prevent the denaturation of enzyme at elevated temperatures [44, 45]. But the loss in activity for covalently immobilized enzyme was found to be at slower rate compared to other one which might be due to the covalent attachment of enzyme with the support. The covalent binding of enzyme with gluteraldehyde activated support provides enhanced rigidity to the enzyme structure and hence restricted conformational flexibility was achieved by the enzyme. As a result of this the covalently immobilized enzyme has shown more activity at higher temperatures. At 70 °C the immobilized enzyme retained activity of 75 % and 85 % respectively for adsorption and covalent method. This improvement in thermal stability of α-amylase as a result of immobilization will be reflected in its catalytic performance and so can be utilized in many industrial sectors where the high temperature conditions needed.

The thermal inactivation curves for free and immobilized enzymes were plotted in figure 4.14 which describes the effect of pre-incubation time on their activity. At the end period of study the free enzyme lost 90 % of its activity while the immobilized enzymes retained about 70 % of activity for adsorption method and 80 % of activity for covalent method. As a result of thermal inactivation the conformation changes occurred in enzyme structure due to the destruction of intermolecular forces that maintained the three

dimensional structure. Here we noticed that covalently immobilized enzyme retained more activity than others due to the existence of covalent interaction between the enzyme and support which imparts stability to it. The covalent binding between the aldehyde group of support and amino group of enzyme leads to the protected microenvironment to the immobilized system by providing stabilizing forces and hence molecular rigidity [46, 47]. The increase in thermal stability of α-amylase was also observed by Maedeh et al. when it was immobilized on nano pore zeolite [48]. The denaturation resistance of immobilized α-amylase was found to be improved by its multipoint attachment acquired through the covalent immobilization.

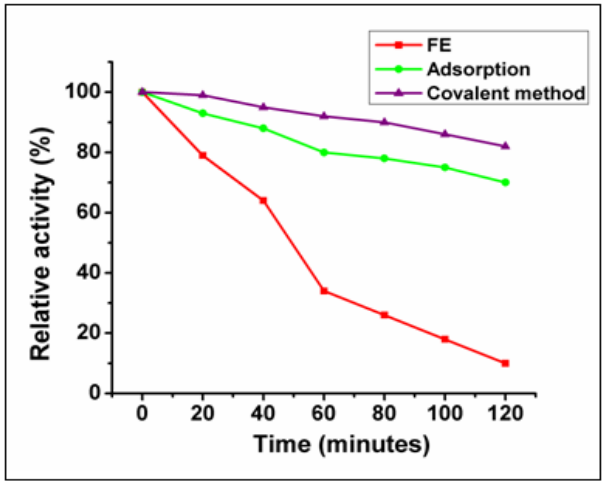

Figure: 4.14 Variation of pre-incubation time on activity of free and immobilized α-amylase by adsorption and covalent methods

4.3.3.6 Determination of kinetic parameters

The kinetic parameters for free enzyme, CSM-GOE by adsorption and covalent method were determined by evaluating the activity of enzyme towards starch hydrolysis reaction. The K_m and V_{max} values were calculated from the Lineweaver-Burk plots and Hanes-Woolf plots, shown in the figure 4.15 and are presented in the table 4.5. The immobilized enzymes by both

methods have shown slightly higher K_m values compared to that of free enzyme which indicated their low affinity towards the substrate molecule. They have shown lower V_{max} values which could be due to the loss of substrate molecules from their microenvironment as a result of the diffusional limitations or might be as a result of partial inactivation of the active sites of enzyme [49]. Tatah et al. reported the difference in kinetic parameters of α-amylase as a result of immobilization process [50]. Similar results are reported when α-amylase immobilized covalently on plastic supports [51].

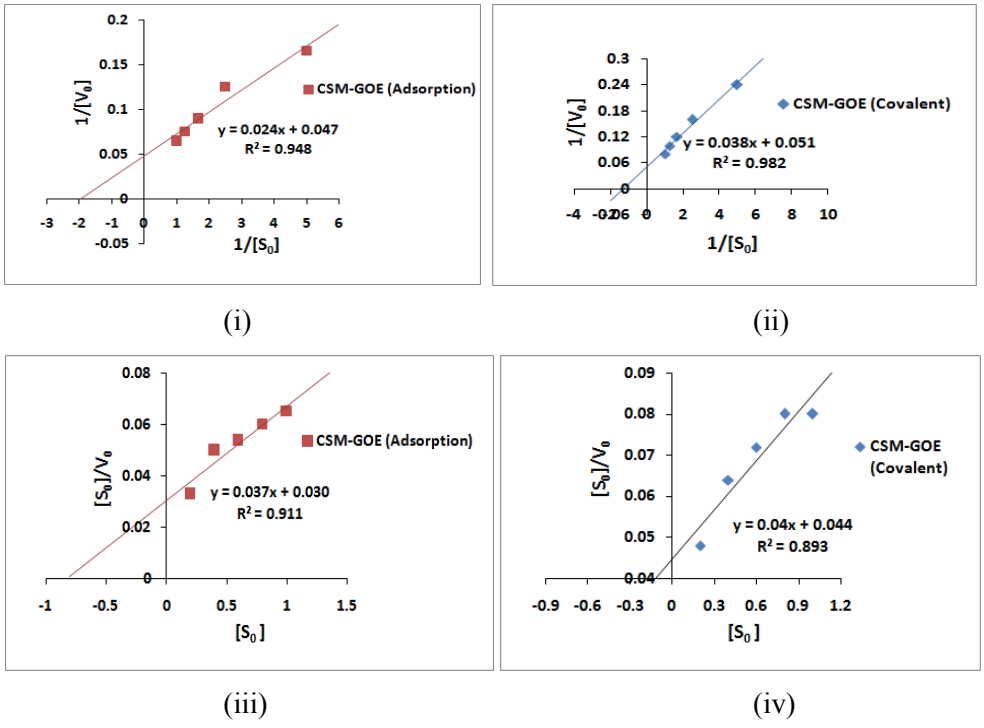

(i) (ii)

(iii) (iv)

Figure: 4.15 Lineweaver-Burk plots for CSM-GOE by (i) adsorption method (ii) covalent method and Hanes-Woolf plots for CSM-GOE by (iii) adsorption method (iv) covalent method.

Table 4.5 Kinetic parameters for free and immobilized α-amylase by adsorption and covalent methods

Immobilized enzyme	K_m (mg mL^{-1})	V_{max} (µmol mg^{-1} min^{-1})	K_{cat} (min^{-1})	K_{cat}/K_m ($mLmg^{-1}min^{-1}$)
Free enzyme	0.45± 0.02	34.48±0.05	1910.19	4244.87
CSM-GOE (Adsorption)	0.51± 0.03	21.28± 0.04	1178.91	2311.59
CSM-GOE (Covalent method)	0.5±0.04	23.81± 0.02	1638.73	3277.46

By knowing the values of K_m and V_{max}, we have calculated the turnover number (K_{cat}) and catalytic efficiency (K_{cat}/K_m) for free and immobilized enzymes. The K_{cat} values evaluated for CSM-GOE by adsorption and covalent method are 1178.91 min^{-1} and 1638.73 min^{-1} respectively which were 38.28 % and 14.21 % lesser than that of free enzyme. These results showed that one molecule of each immobilized enzymes have taken 50.89 and 36.62 milliseconds of time for the conversion of one substrate molecule into product. The respective catalytic efficiencies of immobilized enzymes calculated were 45.54 % and 22.79 % lower than that of free enzyme.

4.3.3.7 Storage stability of immobilized α-amylase

The stability of enzyme during storage is the important feature for its applicability in the industrial field. The effect of immobilization method on storage stability was investigated at 4 ºC for six months of duration and the results are depicted in the figure 4.16.

After six months of storage CSM-GOE by adsorption method retained 50 % of its initial activity whereas that by covalent binding method acquired 70 % of activity. The multipoint covalent attachment between the enzyme and support should bring the higher conformational stability to the

immobilized enzyme and eventually leads to the higher activity. Nwagu et al. observed the improved stability of immobilized raw starch digesting amylase on gluteraldehyde activated amberlite beads through multipoint covalent attachment for longer period of time [52]. The activation of the resin by cross-linking with gluteraldehyde improved the binding stability of immobilized enzyme by rigidification of protein structure via intermolecular forces between the enzyme and support.

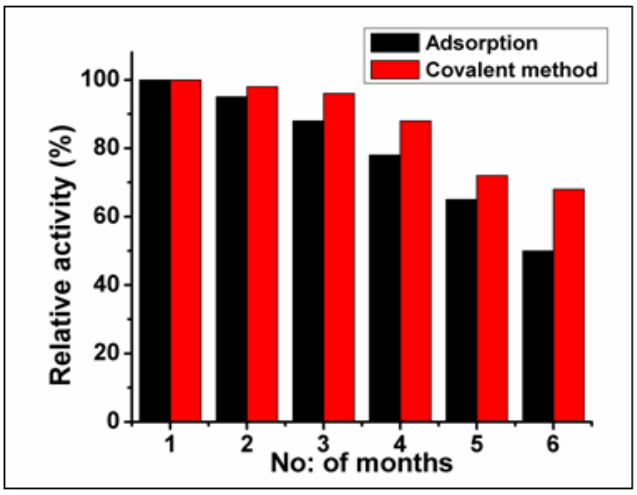

Figure:4.16 Storage stability of immobilized α-amylase by adsorption and covalent method

4.3.3.8 Reusability

Enzymatic reactions for both immobilized preparations were repeated for ten cycles. At the end of each cycle the relative enzyme activities were determined and the results are presented in the figure 4.17. The relative activities are found to be declined for subsequent cycles in case of both immobilized enzymes.

On repeated uses the interaction between the enzyme and support become weak and also causes the distortion of active site of enzyme, ultimately leads to the loss in activity. At the end of tenth cycle, CSM-GOE by adsorption method gained 50 % of its initial activity whereas for that by covalent binding method the activity was about 70 %. Due to the weak interaction with support, the adsorbed enzyme may leach out form the surface of support on repeated use and consequently leads to the decrease of enzyme activity. But for covalent binding method the aldehyde groups of gluteraldehyde activated support formed strong covalent bond with the enzyme to create stable and protective environment for enzyme immobilized system. This provides better reusability for CSM-GOE by covalent method. Similarly Garima et al. reported that β-amylase on covalent immobilization with gluteraldehyde functionalized graphene sheets showed more than 76 % of activity after ten repeated cycles of uses [44].

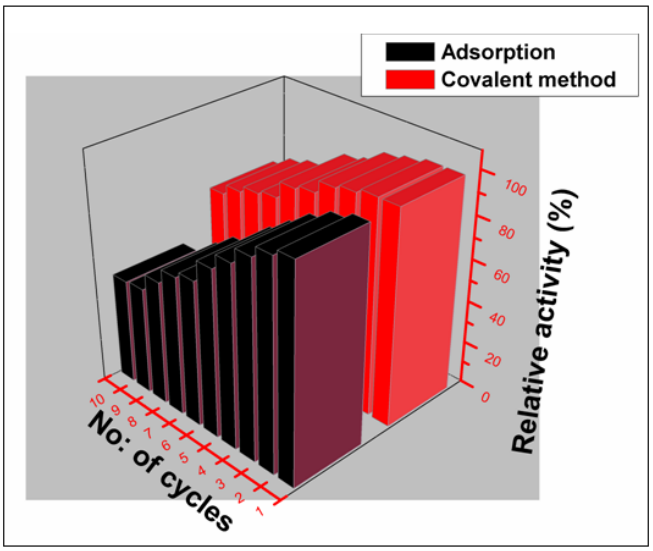

Figure: 4.17 Reusability of immobilized α-amylase by adsorption and covalent method

4.4 Montmorillonite modified magnetic chitosan as α-amylase carrier

4.4.1 Synthesis of montmorillonite modified magnetic chitosan

A solution of 2 wt % chitosan was prepared in a 2 % (v/v) acetic acid under constant stirring. Then 0.1M $FeCl_3$ solution was added into the resultant solution and thereafter 0.1 M Na_2SO_3 solution slowly mixed with the yellow colloidal solution. The MMT was added in to the solution with varied concentrations such as 2.5 %, 5 % and 10 % and then the solution was poured in to ammonia solution under vigorous stirring. The black precipitated suspension washed with distilled water to get the colorless filtrate by applying the external magnetic field and after that the precipitate dried in vacuum oven at 60 ^{0}C.

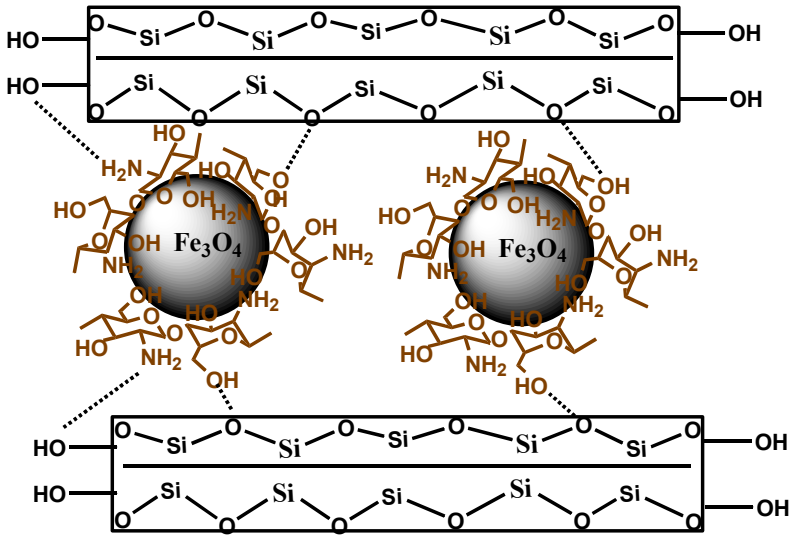

Scheme 4.2 Formation of montmorillonite modified magnetic chitosan

4.4.2 Physico-chemical characterization

4.4.2.1 Infrared spectra

The IR spectra for CSM-MMT composites are shown in the figure 4.18 and the peak assignments are presented in the table 4.6.

The vibrational bands corresponding to both CSM and MMT are observed in the spectra of composites. A broad band that range from 3000 cm^{-1} -3750 cm^{-1} might be attributed to the N–H and O–H stretching vibrations in chitosan and O–H stretching frequencies (Al, Mg (OH)) of silicates in MMT. The vibrations at 2920 cm^{-1} and 2860 cm^{-1} corresponds to C–H stretching vibrations of methylene and methyl groups. The C–H bending vibrations of $–CH_2$ and $–CH_3$ could be seen at 1370 cm^{-1} and 1450 cm^{-1} respectively [53]. The sharp peak at 1652 cm^{-1} was related to the NH–CO stretching of amide group [54]. The absorption band in the range from 790 cm^{-1}-1150 cm^{-1} was ascribed to the C–O stretching vibrations of C–OH, C–O–C and CH_2–OH groups of chitosan, also related to the Si–O vibrational frequencies of Si–O–Si bonds in MMT [55, 56]. This confirms the overlapping of Si–O–Si bands of MMT with C–O–C bands of chitosan and this absorption band became more intense due to the addition of increased concentration of MMT. The peak corresponding to N–H bending vibration found to be shifted to lower frequency region, which is at 1500 cm^{-1} can be due to the electrostatic interaction with the negatively charged sites of MMT structure. There was no new peak appeared in the spectra of composite, indicated that no covalent bond existed between CSM and MMT. The spectra showed characteristic peak at 674 cm^{-1} ascribed to the Si–O–Al stretching vibrations of added MMT [57]. All composites have shown the Fe–O bond vibration in the range of 550 cm^{-1}-570 cm^{-1} confirmed the presence of magnetite in the composite.

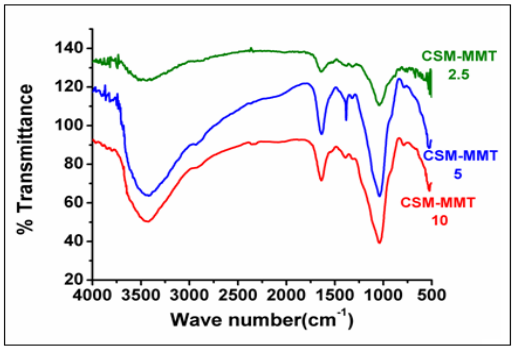

Figure: 4.18 IR Spectra of CSM-MMT 2.5, CSM-MMT 5 and CSM-MMT 10

Table 4.6 Peak assignments for CSM-MMT 2.5, CSM-MMT 5 and CSM-MMT 10

Peak assignment (cm^{-1})	CSM-MMT 2.5	CSM-MMT 5	CSM-MMT 10
N–H and O–H stretching vibration	3485	3488	3490
C–H stretching vibration of CH_2 and CH_3 groups	2920	2917	2915
C–H bending vibration of CH_2 and CH_3 groups	2860	2858	2855
N–H bending vibration	1510	1506	1500
C=O stretching vibration in amide	1690	1660	1652
C–O stretching vibration of alcoholic group	1070	1062	1056
C–O stretching vibration of C–O–C	1242	1246	1250
Si–O vibrations in Si–O–Si bond	782	785	790
Si–O–Al stretching vibration	670	672	674
Fe–O bond vibration	562	560	558

4.4.2.2 X-ray powder diffraction spectra

The XRD spectra for CSM-MMT composites were shown in the figure 4.19. Due to the incorporation of MMT into CSM the characteristic crystalline peaks of chitosan around 2θ =10° become disappeared and 2θ =20° found to be diminished. This might be due to the rupturing of intermolecular bonds in CSM and confirmed its modification by MMT [58]. Literatures revealed the peak of MMT observed at 2θ =7.1° [16], but here this peak was shifted to lower angle of 2θ ≈ 6° and became broadened, which could be as a result of formation of intercalated structure. The other

peaks observed in the diffraction patterns of modified composites attributed to the crystalline planes of Fe_3O_4. All these data showed that the introduction of MMT into CSM has little change in the crystallinity of chitosan and magnetite as the modified form still keep their distinctive diffraction peaks in the spectra.

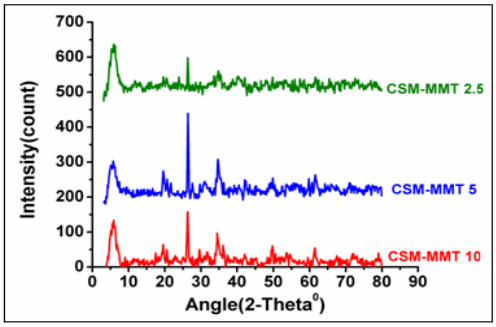

Figure: 4.19 XRD Spectra of CSM-MMT 2.5, CSM-MMT 5 and CSM-MMT 10

4.4.2.3 Thermal analysis

Thermal stability of CSM-MMT composites were evaluated by TGA analysis and their TGA-DTG curves were illustrated in the figure 4.20. All the composites exhibited the thermogram with two major weight losses. The first stage of weight loss in the range of 50-150 °C was associated with loss of adsorbed water around 8 % and the second major weight loss ranges between 200-450 °C was attributed to the degradation of chitosan. The weight loss obtained for CSM-MMT 2.5, CSM-MMT 5 and CSM-MMT 10 at this region was found to be 30 %, 25 % and 20 % respectively. As the concentration of MMT added into the composite increased, the degradation of chitosan found to be decreased. This indicated the high thermal stability of the composite due to the incorporation of MMT into it. After that there was no significant weight loss observed for all the three composites. The high temperature of heating provide the formation of char with multilayered carbonaceous silicate structure from the composite and this structure can

withstand stable at this region without any degradation to polymer [59]. Hence this multilayered structure imparted better protection to the polymer matrix from the thermal degradation. As the concentration of MMT in the CSM composite increases the rate of thermal degradation found to be decreased since it supplement more char on the polymer surface [18, 60]. This indicated that thermal stability of modified composite gets improved with increase of MMT concentration and the thermogram of composites showed that at 700 °C the weight losses evaluated for CSM-MMT 2.5, CSM-MMT 5 and CSM-MMT 10 were 40 %, 30 % and 25 % respectively. Here the thermal stabilities of composites found to be increased as the MMT addition enriched from 2.5 % to 10 %.

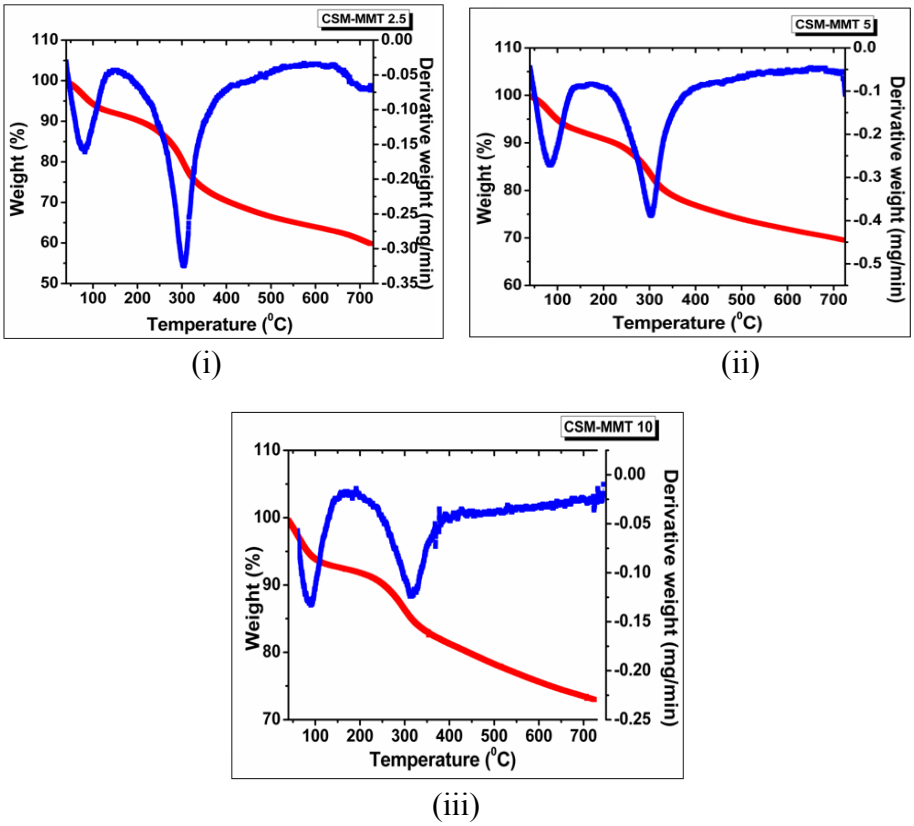

Figure: 4.20 TGA-DTG curves of (i) CSM-MMT 2.5 (ii) CSM-MT 5 and (iii) CSM-MMT 10

4.4.2.4 Scanning electron microscopy

The surface morphologies of CSM-MMT composites were studied by SEM images and are given in the figure 4.21. The increase of MMT content in the composite leads to the changes in their surface morphology and the MMT layers are found to be assembled to get the flocculated structures. This structure might be appeared as a result of the hydroxylated edge to edge interactions in the silicate layers towards the polymer matrix. The hydroxyl and amino functional groups presented in CSM composite can be interacted with the hydroxylated edge groups of silicate layers via hydrogen bonding [61]. Tan et al. also observed flocculated structure for the synthesized chitosan/hydroxy-aluminum pillared montmorillonite nanocomposites [62].

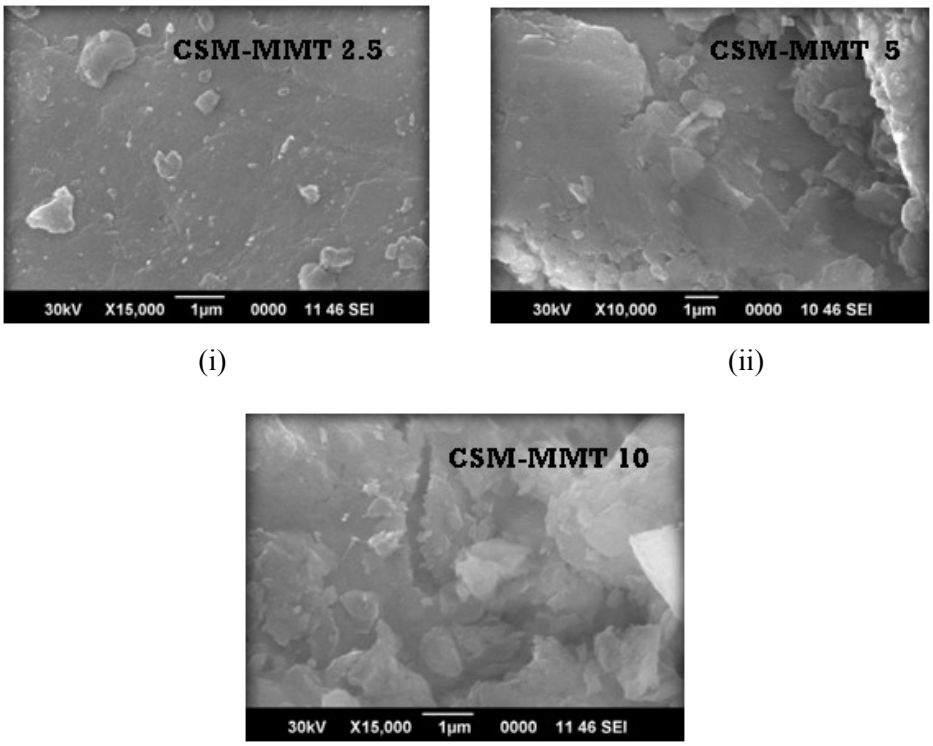

(i) (ii)

(iii)

Figure:4.21 SEM images of (i) CSM-MMT 2.5, (ii) CSM-MMT 5 and (iii) CSM-MMT 10

4.4.2.5 Surface area analysis

BET surface area values for CSM-MMT composites are given in the table 4.7 and observed that all the modified composites acquired larger surface area compared to CSM. This can be due to the incorporation of the MMT layers with high surface area into the CSM composite. As the concentration of MMT increased from 2.5 % to 5 %, the surface area of the composite was found to be also doubled and the values are 27.13 $m^2 g^{-1}$ and 54.88 $m^2 g^{-1}$ for CSM-MMT 2.5 and CSM-MMT 5 respectively. As the MMT concentration increased to 10 %, the surface area of the composite again found to be increased around twice compared to CSM-MMT 5, which was calculated as 96.56 $m^2 g^{-1}$. Since the surface area of the composite depends on the MMT concentration, it will be also reflected in its adsorption capacity towards biomolecules.

Table 4.7 Surface area of CSM-MMT composites with varying MMT concentration

Composite	Surface area ($m^2 g^{-1}$)
CSM-MMT 2.5	27.13
CSM-MMT 5	54.88
CSM-MMT 10	96.56

4.4.2.6 Magnetic properties

Magnetization curves for CSM-MMT composites with varied MMT concentrations were recorded by VSM analysis and are illustrated in the figure 4.22.

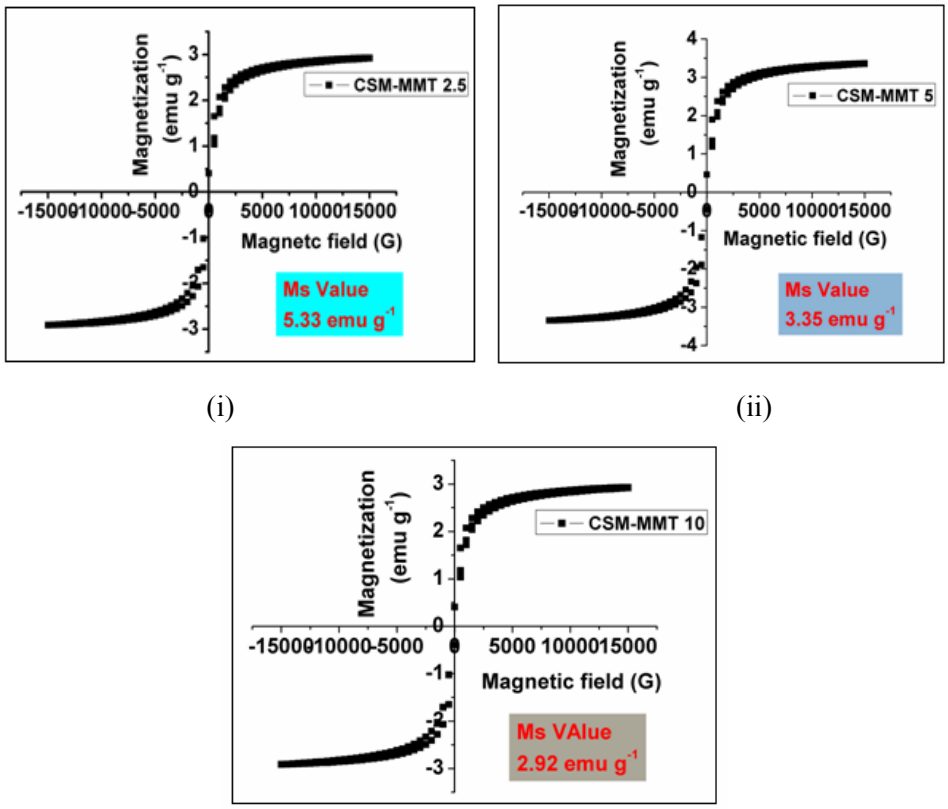

Figure: 4.22 Ms values of (i) CSM-MMT 2.5 (ii) CSM-MMT 5 and (iii) CSM-MMT 10

All the composites have shown a narrow hysteresis loop and the magnetization found to be reached saturation when the magnetic field increased to 15000 G. They have exhibited lower saturation magnetization values compared to CSM and the values calculated are 5.33 emu g^{-1}, 3.35 emu g^{-1} and 2.92 emu g^{-1} for CSM-MMT 2.5, CSM-MMT 5 and CSM-MMT 10 respectively. The Ms values for the modified composites are decreased with the increase of MMT concentration and this lower values attributed to the larger incorporation of the MMT layer. The incorporated MMT layer on the surface of CSM leads to the reduction in its magnetic

moment due to the quenching of surface moments attained and the increased concentration of the added MMT leads to the more quenching of surface moments as a result of decrease in uniformity and causes the reduction in magnetic moment.

4.4.2.7 Energy dispersive X-ray analysis

The EDX spectra of MMT modified magnetic chitosan are exhibited in the figure 4.23 and spectral data are presented in the table 4.8. All the composites have shown decreased amount of C, N and Fe content. They have shown new compositions of Si, Na, Al and increased percentage of O content. All these data confirmed the modification of magnetic chitosan by MMT.

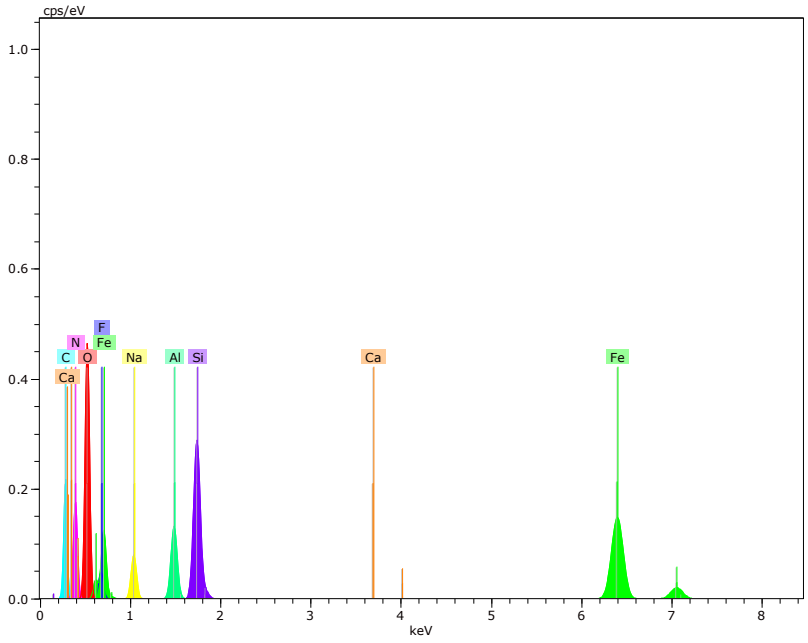

(i)

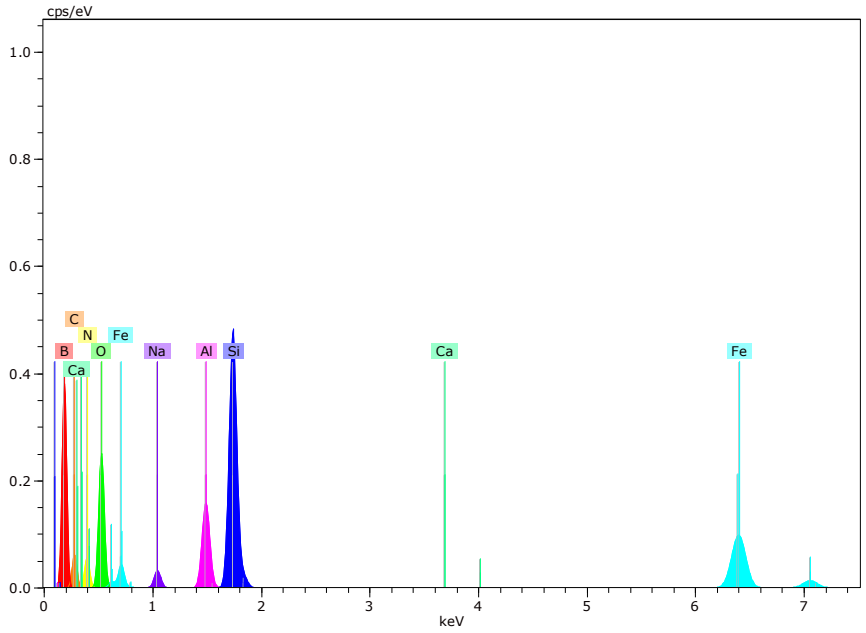

(ii)

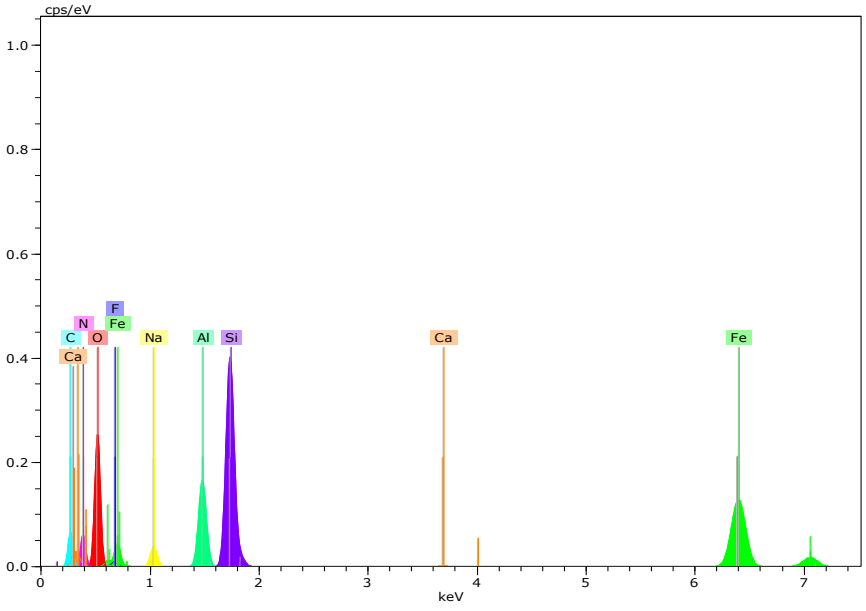

(iii)

Figure: 4.23 EDX spectra of (i) CSM-MMT 2.5 (ii) CSM-MMT 5 and (iii) CSM-MMT 10

Table 4.8 Elemental data of (i) CSM-MMT 2.5 (ii) CSM-MMT 5 and (iii) CSM-MMT 10

Element	Weight %	Atomic %
O	42.50	40.12
C	23.82	27.33
N	19.45	24.18
Fe	6.59	3.25
Si	2.82	1.65
Na	1.93	1.28
Al	1.14	0.69

(i)

Element	Weight %	Atomic %
O	43.76	41.43
C	22.50	25.06
N	18.28	23.74
Fe	4.47	1.25
Si	3.04	1.69
Na	2.31	1.57
Al	1.65	0.97

(ii)

Element	Weight %	Atomic %
O	44.17	43.22
C	20.22	23.89
N	17.17	22.26
Fe	3.62	1.09
Si	5.25	3.09
Na	4.18	2.78
Al	3.23	1.9

(iii)

4.4.3 Immobilization of α-amylase on montmorillonite modified magnetic chitosan

4.4.3.1 Optimization of enzyme immobilization conditions

Optimization of various immobilization conditions were performed by varying only one factor under study and the others maintained at constant level. The immobilization conditions such as pH of the medium, incubation time and enzyme concentration are optimized in order to achieve maximum immobilization efficiency.

4.4.3.1.1 Effect of immobilization pH on α-amylase activity

The charges on MMT surface have great influence on immobilization of enzyme in addition to surface functional groups on chitosan. Enzyme adsorption on clay surface has taken place through electrostatic and hydrophobic interactions. The surface charges on MMT exerted electrostatic forces towards enzyme molecule and regarded as pH modifying support for enzyme immobilization. The planar surface of MMT usually carries negative charges while the charges on edge surface depend on its isoelectric point (pH~7). These surface charges provide appreciable enzyme interaction based on the pH environment.

The figure 4.24 showed that for all composites the maximum activity was observed at pH 6 and beyond this pH the activities are found to be decreased. At pH 6, the edge surface of the MMT has shown positive charges whereas the α-amylase was negatively charged as its isoelectric point is 4.6. These opposite charges generate strong electrostatic interaction between them and so the enzyme could adsorbed on the edge surface of MMT. The enzyme could not be adsorbed on planar surfaces of MMT at pH 6 as the surface always carries negative charges which results in electrostatic repulsion towards the negatively charged enzyme.

At pH 7 the edge surface of MMT did not contain any charges and the negatively charged planar surface results in electrostatic repulsion with enzyme. The observed enzyme activity at this pH might be as a result of the enzyme adsorption by hydrophobic interaction. Above pH 7 both edge and planar surfaces become negatively charged and so experiencing the electrostatic repulsion with enzyme. The lower loading of enzyme at these pH ranges could be due to the hydrophobic interaction between the support

and enzyme. The higher activity exhibited by the immobilized enzyme at these higher pH can be attributed to the increased amount of MMT in the composite. As the surface area of the composite increased due to the presence of increased amount of MMT, the enzyme adsorption has taken place in the higher range and exhibited higher activity. Hence CSM-MMT 10 showed higher activity at these pH region than that of the others.

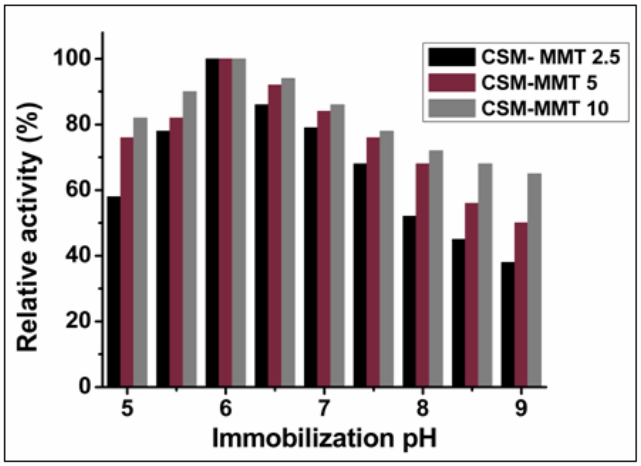

Figure: 4.24 Effect of immobilization pH on relative activity of α-amylase on modified forms of magnetic chitosan

4.4.3.1.2 Effect of contact time on α-amylase activity

The time required for the immobilization has an important role in the industrial application as it influence the production and profit-making. The variations of relative activity with respect to the incubation time are presented in the figure 4.25.

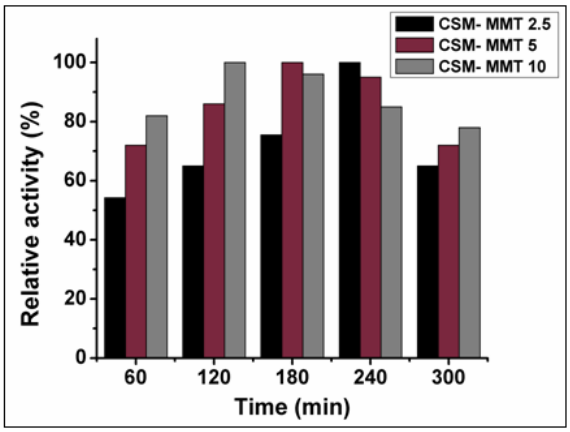

Figure: 4.25 Effect of contact time on relative activity of α-amylase on modified forms of magnetic chitosan

The maximum activity exhibited by CSM-MMT 2.5, CSM-MMT 5 and CSM-MMT 10 were at 240 min., 180 min. and 120 min. respectively. The MMT presented in the composite can adsorb more enzymes onto it and found that the composite with high MMT concentration attained maximum enzyme activity rapidly compared to the others. After reached this saturation level it was observed that the enzyme activity decreased gradually as the immobilization time further prolonged. This could be as a result of desorption of enzyme from the surface of composite as it loaded excessively on it which results in decrease of electrostatic interaction between them [63].

4.4.3.1.3 Effect of initial amount of protein on protein loading on to supports

The optimum enzyme concentration needed for the immobilization process can be observed from the figure 4.26 and the maximum protein adsorbed was 4.2 mg g^{-1} support, 6.2 mg g^{-1} support and 9.4 mg g^{-1} support at 12.8 mg, 16.4 mg and 16.8 mg of initial enzymes. Here we have noticed that the loaded protein onto the support increased with increase of MMT

concentration in it. The immobilization yield of α-amylase on the three supports is given in the table 4.9 and the value is more with CSM-MMT 10. This might be due to the increased surface area of the composite with high MMT concentration which results in improved protein loading. After this optimum loading the protein desorption has taken place which results in decrease of loading.

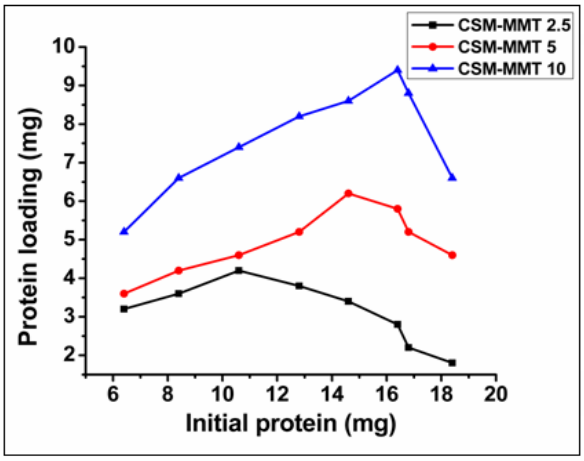

Figure: 4.26 Effect of initial protein amount on protein loading onto modified forms of magnetic chitosan

4.4.3.1.4 Effect of initial protein amount on immobilized enzyme activity

The enzyme activity change with respect to the amount of initial enzyme used in the immobilization was studied and the results are depicted in the figure 4.27. The optimum enzyme activities for CSM-MMT 2.5, CSM-MMT 5 and CSM-MMT 10 were at 4.85 EU, 5.37 EU and 9.84 EU respectively and after these values enzyme activity found to be decreased. This could be due to the lower diffusion of substrate molecules into the active site of enzyme as the increased enzyme concentration results in multilayer enzyme adsorption. The steric hindrance at the active site of

enzyme can also be the reason for the decreased enzyme activity since it lowers the chances for enzymatic reaction. The activity yield for immobilized enzymes were found to be increased as the MMT concentration in the support goes to higher percentage. Consequently immobilization efficiencies were varied in the same manner and calculated as 68.18 %, 69.95 % and 79.95 % for CSM-MMT 2.5, CSM-MMT 5 and CSM-MMT 10 respectively. This trend in immobilization efficiency could be as a result of increased binding sites between enzyme and the support.

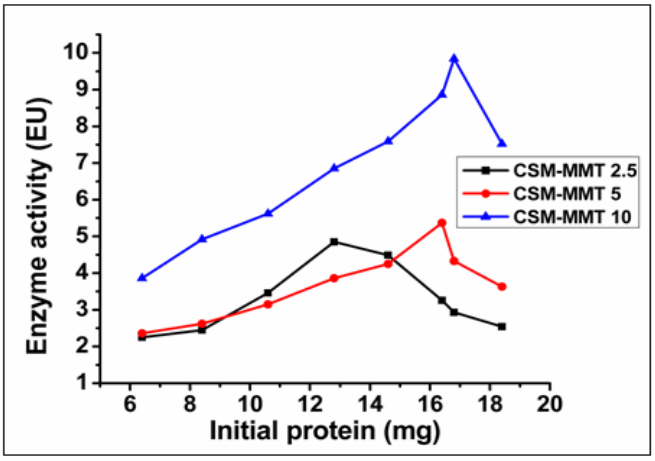

Figure: 4.27 Effect of initial protein amount on immobilized enzyme activity

Table 4.9 Immobilization efficiency of α-amylase on modified forms of magnetic chitosan

Support	Initial protein (mg)	Immobilized protein mg/g support	IY (%)	Initial activity (EU)	Immobilized enzyme activity (EU)	AY (%)	IE (%)
CSM-MMT 2.5	12.8	4.2	32.81	21.68	4.85	22.37	68.18
CSM-MMT 5	16.4	6.2	37.80	20.31	5.37	26.44	69.95
CSM-MMT 10	16.8	9.4	55.95	22.03	9.84	44.73	79.95

4.4.3.2 Effect of pH on α-amylase activity

The pH of the reaction medium influences the conformational structure of enzyme as it changes the intra molecular hydrogen bonding within the enzyme structure. When the pH of the medium changes, the protein structure tends to contract or expand and this leads to the conformational changes in its structure and subsequently affect the enzyme activity.

The pH stability of free and immobilized enzymes was estimated in the pH range of 4-9 and the stability diagram illustrated in the figure 4.28. All the immobilized enzymes have shown broad pH profile and attained high enzyme activity at all pH compared to free enzyme.

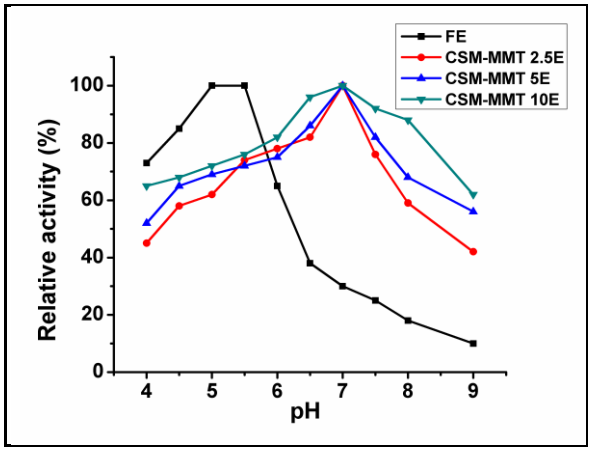

Figure: 4.28 Effect of pH on the relative activity of free and immobilized α-amylase on modified forms of magnetic chitosan

For all the immobilized enzymes optimum pH shifted to alkali region and it was at pH 7. At pH 7, as the clay surface is negatively charged, the microenvironment of the enzyme attained less pH than that of the bulk and so the bulk pH should be shifted to higher values in order to reach the optimum in the microenvironment. The shift to higher pH was also reported in many literatures [64, 65]. After this optimum pH the enzyme activity was

found to be decreased which could be due to the inactivation of enzyme as a result of oxidation of sulphur containing amino acids and deamidation of glutamine residues [66]. The broad pH profile of the immobilized enzymes can be due to the secondary interaction between the α-amylase and clay surface. Sanjay et al. observed a broad pH profile and improved activity for α-amylase when immobilized on K-10 montmorillonite [19].

4.4.3.3 Effect of temperature on α-amylase activity

The effect of temperature on activity of free and immobilized α-amylase on modified forms of magnetic chitosan was determined in the range of 30-70 ºC and the results are shown in the figure 4.29.

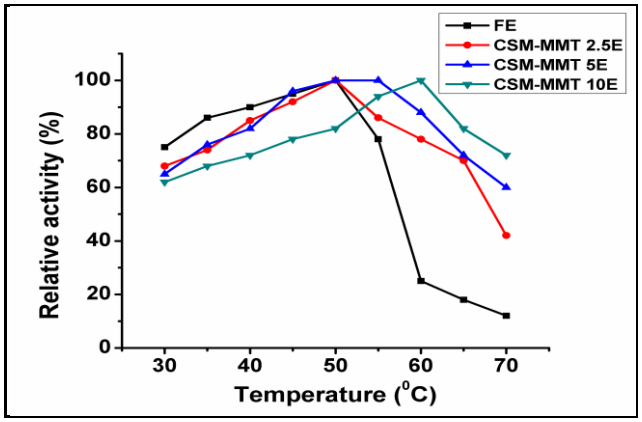

Figure: 4.29 Effect of temperature on the relative activity of free and immobilized α-amylase on modified forms of magnetic chitosan

Here we observed that all the immobilized enzymes have shown broad temperature profile and exhibited high relative activity during the temperature ranges compared to free enzyme. The optimum temperature obtained for CSM-MMT 2.5E, CSM-MMT 5E and CSM-MMT 10E were 50 ºC, 55 ºC and 60 ºC. As the MMT concentration in the support increases the temperature optimum for the enzyme was found to be shifted to high

temperature ranges. Here MMT has the ability to change the temperature activity profile of enzyme due to its insulation and high heat resistance property [67]. Here it provided broader temperature profile to the enzyme and hence the immobilized enzymes keep excellent activity at higher temperature ranges. As the MMT content in the composite increases, the temperature stability of the immobilized enzymes was also found to be increased. At 70 ºC CSM-MMT 2.5E, CSM-MMT 5E and CSM-MMT 10E have retained about 40 %, 60 % and 70 % of their initial activities respectively. Similar trend in increase of enzyme activity was also observed by Sanjay et al. when invertase immobilized on montmorillonite K-10 [68].

4.4.3.4 Activation energy

The activation energies of immobilized systems were calculated from the Arrhenius plot which is presented in the figure 4.30 and the values are tabulated in the table 4.10.

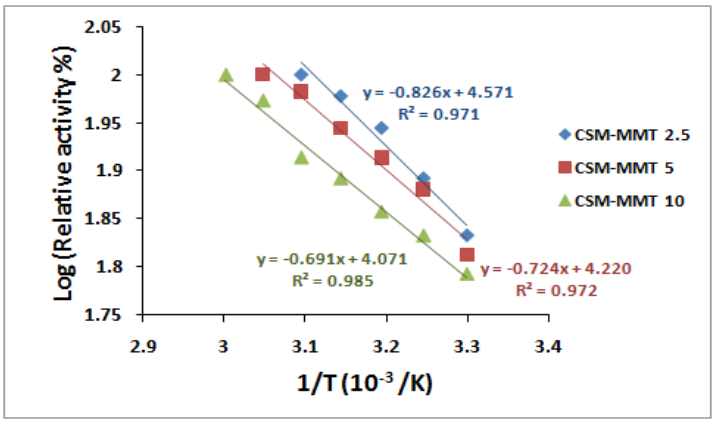

Figure: 4.30 Arrhenius plot to calculate the activation energy (Ea) of immobilized α-amylase on modified forms of magnetic chitosan

Table 4.10 Activation energy of immobilized α-amylase on modified forms of magnetic chitosan

Immobilized enzyme	Activation energy (KJ mol^{-1})
CSM- MMT 2.5E	6.87
CSM- MMT 5E	6.02
CSM- MMT 10E	5.74

The Ea for CSM-MMT 2.5E, CSM-MMT 5E and CSM-MMT 10E were 6.87 KJ mol^{-1}, 6.02 KJ mol^{-1} and 5.74 KJ mol^{-1} respectively and it was confirmed that the activation energy of α-amylase reduced as a result of its immobilization on to MMT modified magnetic chitosan. The decrease of activation energy of free enzyme after immobilization was also noticed when xylanase immobilized on gluteraldehyde activated alginate beads [69]. The results showed that the increase of MMT content in the support decrease the activation energy of the immobilized enzyme systems.

4.4.3.5 Thermal stability of the free and immobilized enzymes

Thermal stability of free and immobilized enzymes was studied and is depicted in the figure 4.31.

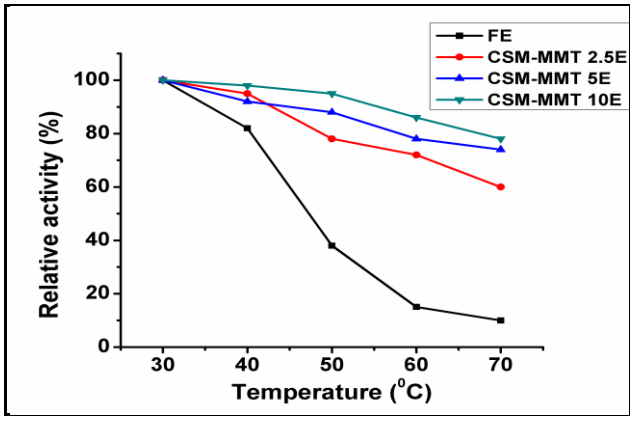

Figure:4.31 Thermal stability of free and immobilized α-amylase on modified forms of magnetic chitosan

The immobilized enzymes have attained better thermal stability compared to free enzyme and retained 60 %, 75 % and 80 % of initial activity for CSM-MMT 2.5E, CSM-MMT 5E and CSM-MMT 10E. As a result of immobilization, enzyme gets restricted mobility and hence diminishes the unfolding of enzyme structure which provides high enzyme activity. The excellent heat resistant capacity of MMT imparted high thermal stability to the immobilized enzymes and it was found that the activity enhanced with respect to the increase of MMT content in the support.

The thermal inactivation of free and immobilized enzymes was investigated by pre-incubating them for 0-120 min. and the results are illustrated in the figure 4.32. The initial activity was taken as 100 % and later activities for corresponding pre-incubation time were determined relative to this initial activity. After 20 min. of pre-incubation free enzyme retained about 80 % of its activity whereas the immobilized enzymes kept above 90 % of their initial activities. After that as the pre-incubation time increases the free enzyme lost its activity very rapidly and reached to 10 % of initial activity at 120 min. of pre-incubation. While the immobilized enzymes gradually lost their activities with respect to the increase of pre-incubation period. The activities attained by immobilized enzymes after 120 min. of pre-incubation were found to be 62 %, 70 % and 90 % of initial activity for CSM-MMT 2.5E, CSM-MMT 5E and CSM-MMT 10E respectively. All the immobilized enzymes have retained much activity since the MMT in the support reduced the rate of thermal inactivation of enzyme and the rate was found to be improved as the MMT concentration increased from 2.5 % to 10 % in the modified magnetic chitosan. The improvement in thermal stability of glucoamylase was observed on immobilization with montmorillonite by adsorption and covalent method [14].

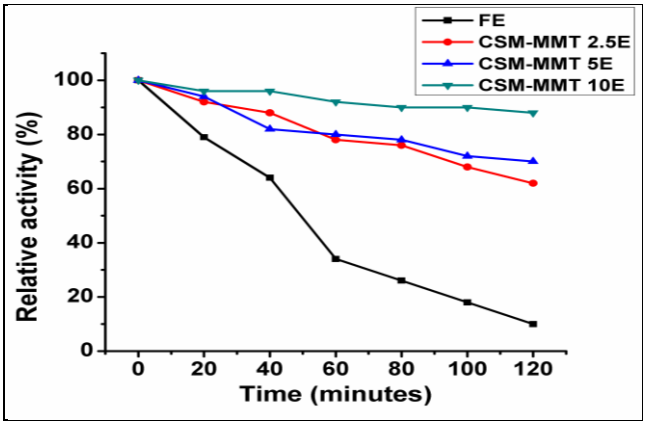

Figure: 4.32 Variation of pre-incubation time on activity of free and immobilized α-amylase on modified forms of magnetic chitosan

4.4.3.6 Determination of kinetic parameters

The evaluation of kinetic parameters imparts the awareness about activity of enzyme in the immobilized condition. The parameters determined from the Lineweaver-Burk plots and Hanes-Woolf plots presented in the figure 4.33 and the results are shown in the table 4.11.

The kinetic parameters of the immobilized enzymes will be different from that of free enzyme due to the occurrence of conformational changes as a result of immobilization process. Here the immobilized enzymes exhibited higher K_m values than the free enzyme indicated the lower enzyme affinity towards substrate molecules generated by diffusional limitations. The reduced conformational flexibility of the protein structure as a result of immobilization also caused the lower affinity and hence higher K_m values for immobilized enzymes [70, 71]. The K_m values for CSM-MMT 2.5E, CSM-MMT 5E and CSM-MMT 10E were found to be 2.93± 0.02 mg mL^{-1}, 2.69±0.04 mg mL^{-1} and 1.81± 0.06 mg mL^{-1} respectively. Here the K_m values for the immobilized enzymes were decreased; that is affinity increased as the MMT content presented in them increased. The lowest K_m for CSM-MMT 10E attributed to the lower diffusional limitations and less

deformation of the protein structure. Many reporters revealed that the enzyme molecules can be located at the edge surface of the clay matrix and the amino acid residues in the enzyme structure penetrate between the layers [67, 72]. The increase of K_m value also leads to the decrease of V_{max} as the active site of the enzyme was distorted by immobilization. However in case of immobilized enzymes, the V_{max} values were found to be increased with corresponding increase in MMT concentration.

The calculated turn over number (K_{cat}) and catalytic efficiency (K_{cat}/K_m) were presented in the above mentioned table. These parameters were lower for all the immobilized enzymes compared to free enzyme, indicated the decrease of enzyme activity and reduction in catalytic efficiency as a result of immobilization process. But these values were found to be increased for immobilized enzyme with high MMT concentration which might be due to its enzyme activity retention ability.

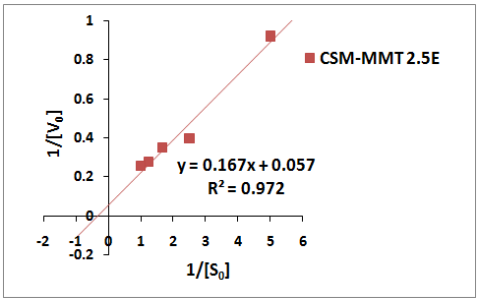

(i)

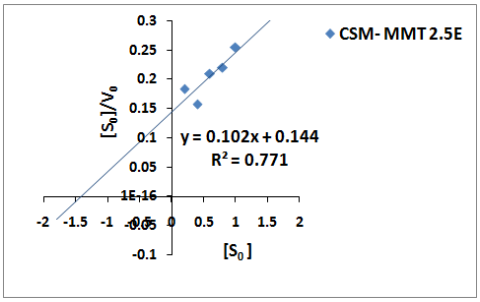

(iv)

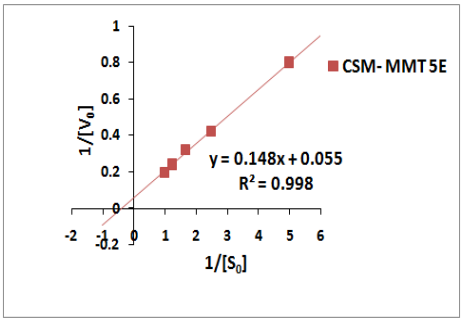

(ii)

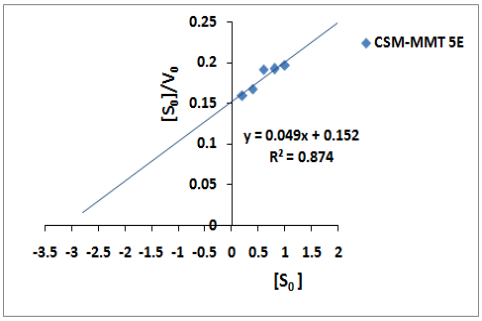

(v)

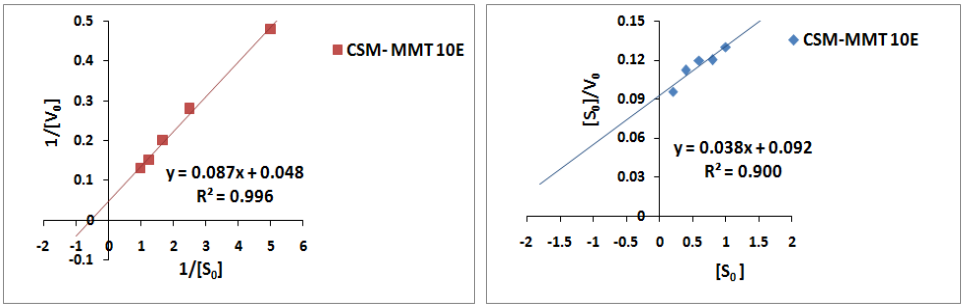

(iii) (vi)

Figure: 4.33 Lineweaver-Burk plots for (i) CSM-MMT 2.5E (ii) CSM-MMT 5E (iii) CSM- MMT 10E and Hanes-Woolf plots for (iv) CSM-MMT 2.5E (v) CSM-MMT 5E (vi) CSM-MMT 10E

Table 4.11 Kinetic parameters for free and immobilized α-amylase on modified forms of magnetic chitosan

Immobilized enzyme	K_m (mg mL^{-1})	V_{max} (µmol mg^{-1} min^{-1})	K_{cat} (min^{-1})	K_{cat}/K_m ($mLmg^{-1}min^{-1}$)
Free enzyme	0.45± 0.02	34.48±0.05	1910.19	4244.87
CSM-MMT 2.5 E	2.93± 0.02	17.54± 0.02	971.72	331.64
CSM-MMT 5 E	2.69±0.04	18.18± 0.03	1007.12	374.39
CSM-MMT 10 E	1.81± 0.06	20.83± 0.02	1153.98	637.56

4.4.3.7 Storage stability of immobilized α-amylase

Storage stability is considered as the important parameter for enzyme immobilization as it affects the activity retention during storage period. The figure 4.34 showed the storage stability of immobilized enzymes and their activity retention after six months were 30 %, 38 % and 52 % for CSM-MMT 2.5E, CSM-MMT 5E and CSM-MMT 10E respectively.

The results indicated that the enzyme immobilized on support containing 10 % MMT has exhibited best storage stability and its high activity could be due to the high enzyme loading capacity and enzyme activity retention of MMT modified support. Here the support effectively prevented the natural loss in enzyme activity during the storage time. The

loss in α-amylase activity of 36 % during 40 days of storage at 4 ºC was reported by Mardani et al. when immobilized on chitosan-montmorillonite nanocomposite beads [20]. But in our case the immobilized enzymes retained about 85-95 % of activity during the same period of storage.

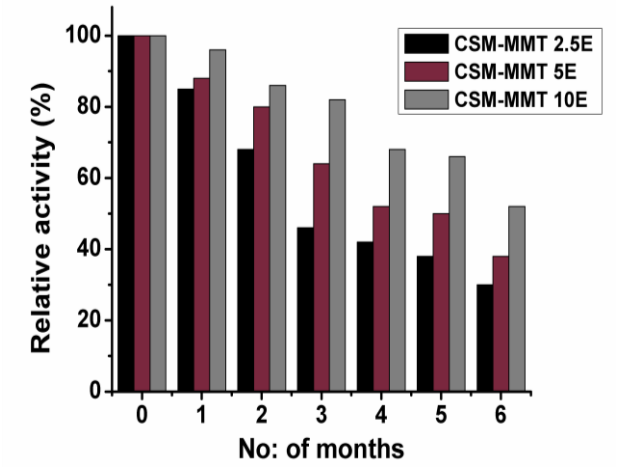

Figure:4.34 Storage stability of immobilized α-amylase on modified forms of magnetic chitosan

4.4.3.8 Reusability of immobilized α-amylase

We have investigated the performance of immobilized enzymes during their reuses as this is the important parameter for potential industrial applications. The relative activities of immobilized enzymes up to 10 cycles are shown in the figure 4.35.

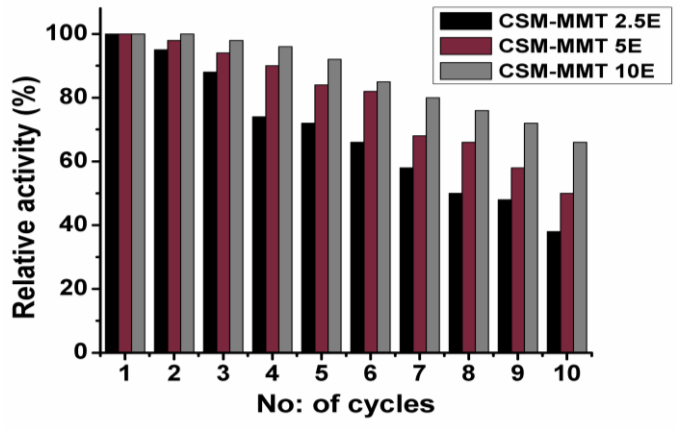

Figure: 4.35 Reusability of immobilized α-amylase on modified forms of magnetic chitosan

When the 10 reuse cycles were completed immobilized enzymes retained 38 %, 52 % and 67 % of activity for CSM-MMT 2.5E, CSM-MMT 5E and CSM-MMT 10E respectively. The decrease in enzyme activity after each cycles of catalytic reaction might be due to the enzyme desorption from the surface of the support. Here we observed that the reduction in relative enzyme activity of immobilized enzymes have taken place at slower rate when the MMT content in the support increased. This indicated that the operational stability of immobilized enzymes enhanced and this could be due to the increased enzyme activity retention capacity of the support with corresponding increase of MMT content in it. Guanghui Zhao et al. reported that the glucoamylase retained 60 % of residual activity after ten cycles of reuses when immobilized on Fe_3O_4@clays nanocomposites [73].

4.5 Conclusion

Magnetic chitosan was modified with graphite oxide and montmorillonite based on the previously reported procedures. α-amylase was successfully immobilized on CSM-GO by adsorption and covalent binding. The immobilization efficiency was about 82.6 % for adsorption and 64.09 % for covalent binding. The optimum pH for immobilized enzymes was shifted to 6 and 7 respectively, but for both of them the optimum temperature was shifted to 40 °C. The activation energy was calculated as 16.83 KJ mol^{-1} and 14.56 KJ mol^{-1}. The catalytic efficiency for covalently immobilized CSM-GOE was higher than that of free and adsorbed one. Thermal stability, reusability and storage stability studies showed that the covalently immobilized enzyme retained more activity than the adsorbed one. In case of CSM-MMT composites the IY % and IE % were found to be increased significantly as the MMT % increases and this is attributed to the increased surface areas of composites. For all the immobilized enzymes the optimum pH gets shifted to 7. The optimum temperature for CSM-MMT 2.5 is same as that of free enzyme, whereas for CSM-MMT 5 and CSM-MMT 10 the optimum temperature shifted to 55 °C and 60 °C respectively. The activation energy calculated for immobilized enzymes were found to be decreased as the MMT concentration increased to higher values. Thermal stability, reusability and storage stability studies confirmed that the immobilized enzymes retained more activity as the MMT % increases.

References

[1] J.M. Lehn, G. Alberti, T. Bein, Comprehensive supramolecular chemistry volume 7, volume 7, Pergamon, Oxford; New York; Tokyo, 1996.

[2] I. Fejer, M. Kata, I. Eros, O. Berkesi, I. Dekany, Release of cationic drugs from loaded clay minerals, Colloid and Polymer Science 279(12) (2001) 1177-1182.

[3] F.H. Lin, Y.H. Lee, C.H. Jian, J.M. Wong, M.-J. Shieh, C.-Y. Wang, A study of purified montmorillonite intercalated with 5-fluorouracil as drug carrier, Biomaterials 23(9) (2002) 1981-1987.

[4] G.V. Joshi, B.D. Kevadiya, H.A. Patel, H.C. Bajaj, R.V. Jasra, Montmorillonite as a drug delivery system: Intercalation and in vitro release of timolol maleate, International Journal of Pharmaceutics 374(1) (2009) 53-57.

[5] W. Ya-Ling, G. Peng, H. Lang-Huan, W. Xiao-Jing, L. Ying-Liang, Graphite Oxide: Preparation and removal ability of cationic dyes, Chinese Journal of Inorganic Chemistry 28 (2) (2012) 391-397.

[6] A. Kaushik, R. Khan, P.R. Solanki, P. Pandey, J. Alam, S. Ahmad, B. Malhotra, Iron oxide nanoparticles–chitosan composite based glucose biosensor, Biosensors and Bioelectronics 24(4) (2008) 676-683.

[7] M. Yadav, K.Y. Rhee, S.J. Park, D. Hui, Mechanical properties of Fe_3O_4/GO/chitosan composites, Composites Part B: Engineering 66 (2014) 89-96.

[8] J. Zhang, F. Zhang, H. Yang, X. Huang, H. Liu, J. Zhang, S. Guo, Graphene oxide as a matrix for enzyme immobilization, Langmuir 26(9) (2010) 6083-6085.

[9] Y. Zhang, J. Zhang, X. Huang, X. Zhou, H. Wu, S. Guo, Assembly of graphene oxide–enzyme conjugates through hydrophobic interaction, Small 8(1) (2012) 154-159.

[10] I.V. Pavlidis, T. Vorhaben, T. Tsoufis, P. Rudolf, U.T. Bornscheuer, D. Gournis, H. Stamatis, Development of effective nanobiocatalytic systems through the immobilization of hydrolases on functionalized carbon-based nanomaterials, Bioresource Technology 115 (2012) 164-171.

[11] R. Su, P. Shi, M. Zhu, F. Hong, D. Li, Studies on the properties of graphene oxide–alkaline protease bio-composites, Bioresource Technology 115 (2012) 136-140.

[12] D. Kishore, M. Talat, O.N. Srivastava, A.M. Kayastha, Immobilization of β-galactosidase onto functionalized graphene nano-sheets using response surface methodology and its analytical applications, Plos One 7(7) (2012) e40708.

[13] M.E. Sedaghat, M. Ghiaci, H. Aghaei, S. Soleimanian-Zad, Enzyme immobilization. Part 3: Immobilization of α-amylase on Na-bentonite and modified bentonite, Applied Clay Science 46 (2) (2009) 125-130.

[14] G. Sanjay, S. Sugunan, Glucoamylase immobilized on montmorillonite: influence of nature of binding on surface properties of clay-support and activity of enzyme, Journal of Porous Materials 14(2) (2007) 127-136.

[15] H. Ozturk, E. Pollet, V. Phalip, Y. Guvenilir, L. Averous, Nanoclays for lipase immobilization: biocatalyst characterization and activity in polyester synthesis, Polymers 8(12) (2016) 416.

[16] S. Wang, L. Shen, Y. Tong, L. Chen, I. Phang, P. Lim, T. Liu, Biopolymer chitosan/montmorillonite nanocomposites: preparation and characterization, Polymer Degradation and Stability 90(1) (2005) 123-131.

[17] M. Darder, M. Colilla, E. Ruiz-Hitzky, Biopolymer−clay nanocomposites based on chitosan intercalated in montmorillonite, Chemistry of Materials 15(20) (2003) 3774-3780.

[18] J.W. Gilman, Flammability and thermal stability studies of polymer layered-silicate (clay) nanocomposites, Applied Clay Science 15(1-2) (1999) 31-49.

[19] G. Sanjay, S. Sugunan, Immobilization of α-amylase onto K-10 montmorillonite: characterization and comparison of activity in a batch and a fixed-bed reactor, Clay Minerals 40(4) (2005) 499-510.

[20] T. Mardani, M.S. Khiabani, R.R. Mokarram, H. Hamishehkar, Immobilization of α-amylase on chitosan-montmorillonite nanocomposite beads, International Journal of Biological Macromolecules 120 (2018) 354-360.

[21] A.N. Azzouz, P, F. Monette, S. Asaftei, R. Hausler, D. Nistor, D. Miron, Acid-base properties of montmorillonite and interactions with enzymes through REM investigations, Sciences & Technologie (22) (2004) 89-96.

[22] W.S. Peternele, V.M. Fuentes, M.L. Fascineli, J.R. Silva, R.C. Silva, C.M. Lucci, R.B. Azevedo, Experimental investigation of the coprecipitation method: an approach to obtain magnetite and maghemite nanoparticles with improved properties, Journal of Nanomaterials 2014 (2014) 94.

[23] W.S. Hummers, R.E. Offeman, Preparation of graphitic oxide, Journal of the American Chemical Society 80(6) (1958) 1339-1339.

[24] S. Mykola, P. Robert, B.T. J, Role of graphite oxide (GO) and polyaniline (PANI) in NO_2 reduction on GO-PANI composites, Industrial & Engineering Chemistry Research 46(21) (2007) 6925-6935.

[25] S. Mykola, T.A. V, B.T. J, Graphite oxides obtained from porous graphite: the role of surface chemistry and texture in ammonia retention at ambient conditions, Advanced Functional Materials 20(10) (2010) 1670-1679.

[26] G.Z. Kyzas, D.N. Bikiaris, N.K. Lazaridis, Low-swelling chitosan derivatives as biosorbents for basic dyes, Langmuir 24(9) (2008) 4791-4799.

[27] K.G. Z, K. Margaritis, L.N. K, Relating interactions of dye molecules with chitosan to adsorption kinetic data, Langmuir 26(12) (2010) 9617-9626.

[28] A.B. Bourlinos, D.Gournis, P. Dimitrios, S. Tamas, S. Anna, D. Imre, Graphite oxide: chemical reduction to graphite and surface modification with primary aliphatic amines and amino acids, Langmuir 19(15) (2003) 6050-6055.

[29] L. Fan, C. Luo, X. Li, F. Lu, H. Qiu, M. Sun, Fabrication of novel magnetic chitosan grafted with graphene oxide to enhance adsorption properties for methyl blue, Journal of Hazardous Materials 215 (2012) 272-279.

[30] N.A. Travlou, G.Z. Kyzas, N.K. Lazaridis, E.A. Deliyanni, Functionalization of graphite oxide with magnetic chitosan for the preparation of a nanocomposite dye adsorbent, Langmuir 29(5) (2013) 1657-1668.

[31] L. Fan, C. Luo, M. Sun, X. Li, F. Lu, H. Qiu, Preparation of novel magnetic chitosan/graphene oxide composite as effective adsorbents toward methylene blue, Bioresource Technology 114 (2012) 703-706.

[32] D. Hritcu, D. Humelnicu, G. Dodi, M.I. Popa, Magnetic chitosan composite particles: evaluation of thorium and uranyl ion adsorption from aqueous solutions, Carbohydrate Polymers 87(2) (2012) 1185-1191.

[33] M. Patila, A. Kouloumpis, D. Gournis, P. Rudolf, H. Stamatis, Laccase-functionalized graphene oxide assemblies as efficient nanobiocatalysts for oxidation reactions, Sensors 16(3) (2016) 287.

[34] J. Li, X. Zeng, T. Ren, E. Van Der Heide, The preparation of graphene oxide and its derivatives and their application in bio-tribological systems, Lubricants 2(3) (2014) 137-161.

[35] M.J. Li, C.M. Liu, H.B. Cao, Y. Zhang, Surface charge research of graphene oxide, chemically reduced graphene oxide and thermally exfoliated graphene oxide, Advanced Materials Research, Trans Tech Publications, 2013, pp. 127-131.

[36] J. Gao, C.L. Lu, Y. Wang, S.S. Wang, J.J. Shen, J.X. Zhang, Y.W. Zhang, Rapid immobilization of cellulase onto graphene oxide with a hydrophobic spacer, Catalysts (2073-4344) 8(5) (2018).

[37] I.D. Yasemin, T. Mustafa, Immobilization of bovine catalase onto magnetic nanoparticles, Preparative Biochemistry & Biotechnology 43(8) (2013) 750-65.

[38] B. Konkena, S. Vasudevan, Understanding aqueous dispersibility of graphene oxide and reduced graphene oxide through pKa measurements, The Journal of Physical Chemistry Letters 3(7) (2012) 867-872.

[39] S. Hermanova, M. Zarevucka, D. Bousa, M. Pumera, Z. Sofer, Graphene oxide immobilized enzymes show high thermal and solvent stability, Nanoscale 7(13) (2015) 5852-5858.

[40] S. Fang, J. Chang, Y.S. Lee, E.-J. Hwang, J.B. Heo, Y.-L. Choi, Immobilization of α-amylase from Exiguobacterium sp. DAU5 on chitosan and chitosan-carbon bead: Its Properties, Journal of Applied Biological Chemistry 59(1) (2016) 75-81.

[41] T.N. Nwagu, B.N. Okolo, H. Aoyagi, Immobilization of raw starch digesting amylase on silica gel: A comparative study, African Journal of Biotechnology 10(71) (2011) 15989-15997.

[42] S.A. Ahmed, F.A. Mostafa, M.A. Ouis, Enhancement stability and catalytic activity of immobilized α-amylase using bioactive phospho-silicate glass as a novel inorganic support, International Journal of Biological Macromolecules 112 (2018) 371-382.

[43] M.A. Esawy, A.A. Gamal, Z. Kamel, A.M. Ismail, A.F. Abdel-Fattah, Evaluation of free and immobilized Aspergillus niger NRC1ami pectinase applicable in industrial processes, Carbohydrate Polymers 92(2) (2013) 1463-1469.

[44] G. Srivastava, K. Singh, M. Talat, O.N. Srivastava, A.M. Kayastha, Functionalized graphene sheets as immobilization matrix for fenugreek β-amylase: enzyme kinetics and stability studies, Plos One 9(11) (2014) e113408.

[45] M.Y. Chang, R.-S. Juang, Use of chitosan–clay composite as immobilization support for improved activity and stability of β-glucosidase, Biochemical Engineering Journal 35(1) (2007) 93-98.

[46] A.A. Mendes, R.C. Giordano, R.d.L.C. Giordano, H.F. de Castro, Immobilization and stabilization of microbial lipases by multipoint covalent attachment on aldehyde-resin affinity: Application of the biocatalysts in biodiesel synthesis, Journal of Molecular Catalysis B: Enzymatic 68(1) (2011) 109-115.

[47] J.M. Palomo, G. Fernandez-Lorente, C. Mateo, M. Fuentes, J.M. Guisan, R. Fernandez-Lafuente, Enzymatic production of (3S,4R)-(−)-4-(4′-fluorophenyl)-6-oxo-piperidin-3-carboxylic acid using a commercial preparation from Candida antarctica A: the role of a contaminant esterase, Tetrahedron: Asymmetry 13(24) (2002) 2653-2659.

[48] M. Talebi, S. Vaezifar, F. Jafary, M. Fazilati, S. Motamedi, Stability improvement of immobilized α-amylase using nano pore zeolite, Iranian Journal of Biotechnology 14(1) (2016) 33.

[49] S. Hermanova, M. Zarevucka, D. Bousa, M. Pumera, Z. Sofer, Graphene oxide immobilized enzymes show high thermal and solvent stability, Nanoscale 7(13) (2015) 5852-5858.

[50] V. Tatah, O. Otitoju, Characterization of immobilized post-carbohydrate meal salivary α-amylase, African Journal of Biotechnology 14(31) (2015) 2472-2477.

[51] M. Roig, A. Slade, J. F Kennedy, α-amylase immobilized on plastic supports: Stabilities, pH and temperature profiles and kinetic parameters, Biomaterials, artificial cells, and immobilization biotechnology: official journal of the International Society for Artificial Cells and Immobilization Biotechnology 21 (4) (1993) 487-525.

[52] T.N. Nwagu, B.N. Okolo, H. Aoyagi, Stabilization of a raw-starch-digesting amylase by multipoint covalent attachment on glutaraldehyde-activated amberlite beads, Journal of Microbiology and Biotechnology 22(5) (2012) 628-636.

[53] J. Mano, D. Koniarova, R. Reis, Thermal properties of thermoplastic starch/synthetic polymer blends with potential biomedical applicability, Journal of Materials Science: Materials in Medicine 14(2) (2003) 127-135.

[54] C. Paluszkiewicz, E. Stodolak, M. Hasik, M. Blazewicz, FT-IR study of montmorillonite–chitosan nanocomposite materials, Spectrochimica Acta Part A: Molecular and Biomolecular Spectroscopy 79(4) (2011) 784-788.

[55] M. Duarte, M. Ferreira, M. Marvao, J. Rocha, An optimised method to determine the degree of acetylation of chitin and chitosan by FTIR spectroscopy, International Journal of Biological Macromolecules 31(1-3) (2002) 1-8.

[56] M. Darder, M. Colilla, E. Ruiz-Hitzky, Biopolymer-clay nanocomposites based on chitosan intercalated in montmorillonite, Chemistry of Materials 15(20) (2003) 3774-3780.

[57] P. Mitra, K. Sarkar, P.P. Kundu, Carboxymethyl chitosan modified montmorillonite for efficient removal of cationic dye from waste water, Defence Science Journal 64(3) (2014) 198-208.

[58] N. Banik, A. Ramteke, T.K. Maji, Carboxymethyl chitosan -montmorillonite nanoparticles for controlled delivery of isoniazid: evaluation of the effect of the glutaraldehyde and montmorillonite, Polymers Advanced Technologies 25 (12) (2014) 1580-1589.

[59] S. Wang, L. Chen, Y. Tong, Structure–property relationship in chitosan-based biopolymer/montmorillonite nanocomposites, Journal of Polymer Science Part A: Polymer Chemistry 44(1) (2006) 686-696.

[60] W. Xie, Z. Gao, W.P. Pan, D. Hunter, A. Singh, R. Vaia, Thermal degradation chemistry of alkyl quaternary ammonium montmorillonite, Chemistry of Materials 13(9) (2001) 2979-2990.

[61] Y. Kasirga, A. Oral, C. Caner, Preparation and characterization of chitosan/montmorillonite-K10 nanocomposites films for food packaging applications, Polymer Composites 33 (11) (2012) 1874-1882.

[62] W. Tan, Y.H. Zhang, Y.S. Szeto, L.B. Liao, Preparation and characterization of chitosan/hdroxy-aluminium pillared montmorillonite nanocomposites, key engineering materials, Trans Tech Publications, 2007, pp. 825-828.

[63] M. Usman, V. Ekwueme, T. Alaje, M. Afolabi, S. Bolakale, Immobilization of α-Amylase on mesoporous silica kit-6 and palm wood chips for Starch Hydrolysis, Chemical and Process Engineering 9 (2013) 7-13.

[64] N. Kizilyar, U. Akbulut, L. Toppare, M.Y. Ozden, Y. Yagci, Immobilization of invertase in conducting polypyrrole/ polytetrahydrofuran graft polymer matrices, Synthetic Metals 104(1) (1999) 45-50.

[65] K. Nakane, T. Ogihara, N. Ogata, Y. Kurokawa, Entrap-immobilization of invertase on composite gel fiber of cellulose acetate and zirconium alkoxide by sol–gel process, Journal of Applied Polymer Science 81(9) (2001) 2084-2088.

[66] J.M. Hess, R.M. Kelly, Influence of polymolecular events on inactivation behavior of xylose isomerase from Thermotoga neapolitana 5068, Biotechnology and Bioengineering 62(5) (1999) 509-517.

[67] Q. Wang, L. Peng, G. Li, P. Zhang, D. Li, F. Huang, Q. Wei, Activity of laccase immobilized on TiO_2-montmorillonite complexes, International Journal of Molecular Sciences 14(6) (2013) 12520-12532.

[68] G. Sanjay, S. Sugunan, Enhanced pH and thermal stabilities of invertase immobilized on montmorillonite K-10, Food Chemistry 94(4) (2006) 573-579.

[69] A. Pal, F. Khanum, Covalent immobilization of xylanase on glutaraldehyde activated alginate beads using response surface methodology: characterization of immobilized enzyme, Process Biochemistry 46(6) (2011) 1315-1322.

[70] L. Lu, M. Zhao, Y. Wang, Immobilization of laccase by alginate–chitosan microcapsules and its use in dye decolorization, World Journal of Microbiology and Biotechnology 23(2) (2007) 159-166.

[71] Y.G. Makas, N.A. Kalkan, S. Aksoy, H. Altinok, N. Hasirci, Immobilization of laccase in κ-carrageenan based semi-interpenetrating polymer networks, Journal of Biotechnology 148(4) (2010) 216-220.

[72] S. Gopinath, S. Sugunan, Enzymes immobilized on montmorillonite K 10: effect of adsorption and grafting on the surface properties and the enzyme activity, Applied Clay Science 35(1-2) (2007) 67-75.

[73] G. Zhao, J. Wang, Y. Li, X. Chen, Y. Liu, Enzymes immobilized on superparamagnetic Fe_3O_4@ clays nanocomposites: preparation, characterization, and a new strategy for the regeneration of supports, The Journal of Physical Chemistry C 115(14) (2011) 6350-6359.

Chapter 5

Modified forms of magnetic chitosan by PAMAM dendrimers as α-amylase carriers

Contents

5.1 Introduction

Dendrimers constitute a new class of polymer family, characterized by well defined structural properties with hyper branched macromolecules in which each unit of symmetric branching get assembled around a linear polymer core [1-3]. Dendrimers have been attained an appreciable attention due to the arrival of enormously branched polymers in 1987 by Tomalia et al. and much researches have focused on them throughout the past decades [4-6]. These are of much interested as they acquired hyper branched structure with central core, internal spaces within the structure and terminal ends with multivalent groups. Polyamidoamine (PAMAM) dendrimers, the principal commercialized category of dentritic polymers were of much attracted towards enzyme immobilization field due to their structural characteristics and biocompatibility [7-9]. The groups presented in the terminal branches provide many reaction sites for attaching biomolecules and also for their structural modifications. These properties made them more advantageous than classic linear polymers as enzyme carrier.

The polymer hydrogels, on enzyme immobilization have faced some limitations because of their swelling properties in organic solvents which caused the entrapment of enzyme inside the polymer gels and thus created some restrictions towards the enzyme catalyzed reaction [10, 11]. Kimura et al. reported the lower enzyme activity of entrapped lipase on hydrophobic photo-cross-linkable resin pre polymer due to the poor immobilization method [12]. These limitations can be overcome by the introduction of PAMAM dendrimer as enzyme carrier. Weiwei Zhu et al. observed that the magnetic nanoparticles modified with PAMAM-dendrimer get performed as a good enzyme carrier for reversible enzyme immobilization and can be used for many biomedical applications [13]. The PAMAM coating on magnetic particles tends to reduce the particles agglomeration. The three dimensional structure of dendrimer imparted high stability to the immobilized enzyme by providing protective effect for the stable structural conformation of enzyme. The high kinetic rates and stability of immobilized laccase was observed by Cardoso et al. and they have assessed that the use of PAMAM dendrimer constituted as an attractive platform for enzyme immobilization [14].

When PAMAM grows into higher generation, there existed an exponential increase in amount of surface amino functional groups and thus provided more adsorption sites for enzyme molecules. Siming Wang et al. reported the high binding capacity and enzymolysis efficiency of cellulase on PAMAM-grafted silica with the increase of PAMAM generations in the carrier. The authors have compared the elevated enzyme activity and better pH and temperature stabilities of immobilized enzymes with the free enzyme [15]. PAMAM dendrimers on polymer surfaces and in polymer blocks were implemented in order to establish novel functional materials

[16, 17]. But there is still no report on polymer grafted dendrimers in enzyme immobilization.

This chapter explains the immobilization of α-amylase on PAMAM modified magnetic chitosan using ethylene diamine and diethylene triamine. This comprises influence of next higher generation of PAMAM modified magnetic chitosan on enzyme immobilization. The comparison of adsorption and covalent immobilization methods on modified carrier is also included in this chapter.

5.2 Materials Used

All chemicals were of analytical grade and used without any previous treatment. Methyl acrylate, ethylene diamine and diethylene triamine were obtained from Sigma Aldrich. The chemicals used for the synthesis of magnetic chitosan, protein estimation and enzyme activity assay were given in the chapter 2.

5.3 PAMAM dendrimer modified magnetic chitosan as α-amylase carrier

5.3.1 Synthesis of magnetic chitosan

The magnetic chitosan was synthesized by reduction precipitation method and the procedure was already described in the chapter 2.

5.3.2 Synthesis of PAMAM dendrimer modified magnetic chitosan (CSM-PAMAM)

The magnetic chitosan was modified with PAMAM dendrimer based on the already reported procedure with slight changes [18]. Here the reaction was conducted by using methanol as solvent instead of ethanol. The

reaction was comprised of two steps; the first step was the Michael addition of amino functional groups of magnetic chitosan to methyl acrylate and the second step involved the amidation of resultant ester with ethylene diamine. The reaction is depicted in scheme 5.1.

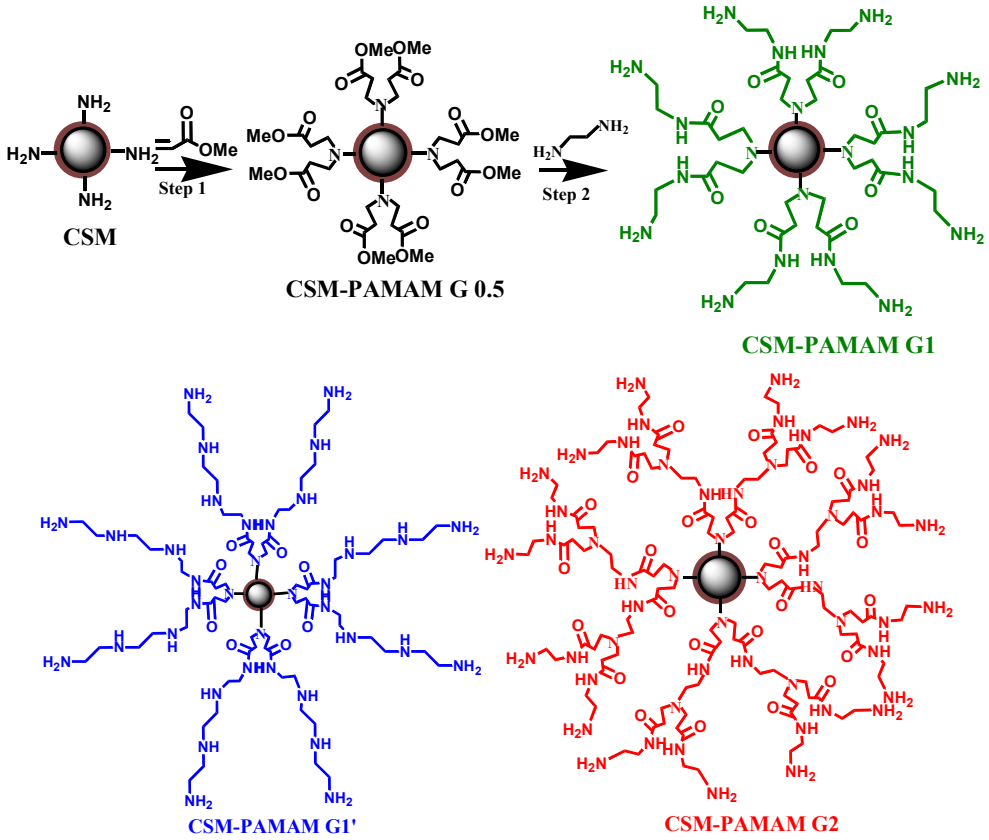

Scheme 5.1 Surface modification of magnetic chitosan by PAMAM dendrimer

For the synthesis of first generation of PAMAM modified magnetic chitosan (CSM-PAMAM G1), about 1 g of magnetic chitosan was refluxed with methyl acrylate solution in methanol (25 mL, 10 % v/v) for three days. Then the resultant product was separated by applying an external magnetic field, after that washed with methanol for three times. The product formed was refluxed with ethylene diamine solution (25 mL, 15 % v/v) for another

three days and at the end of the period the solid substance collected by magnetic separation, washed with the same solvent and further with deionized water. The similar steps were repeated for the formation of second generation of PAMAM modified magnetic chitosan (CSM-PAMAM G2). Another first generation of PAMAM dendrimer was also synthesized by the similar method in which diethylene triamine was used instead of ethylenediamine (CSM-PAMAM G1'). The products formed were dried in vacuum oven at 60 °C for overnight.

5.3.3 Physico-chemical characterization

5.3.3.1 IR spectra of PAMAM modified magnetic chitosan

The IR spectra of PAMAM modified forms of magnetic chitosan were compared with that of magnetic chitosan itself and are depicted in the figure 5.1. The broad peak at 3310 cm^{-1} in CSM attributed to the combined stretching vibrations of $–NH_2$ and –OH functional groups and the absorption at 1320 cm^{-1} assigned to –CN axial deformation of amino groups. The vibrational peaks at 2856 cm^{-1} and 2916 cm^{-1} indicated the asymmetric stretching vibrations of $–CH_2$ and $–CH_3$ groups and the peak at 1036 cm^{-1} corresponds to C–O stretching vibration. The absorption bands at 1428 cm^{-1} and 1372 cm^{-1} were attributed to $–CH_2$ and –CH bending vibrations respectively. The absorption in the region of 1540 cm^{-1} was due to $–NH_2$ bending vibrations and at 1644 cm^{-1} assigned to C=O stretching vibrations. The vibrational peak at 576 cm^{-1} corresponding to the Fe–O bond vibration of Fe_3O_4. All these corresponding absorptions were also noticed in case of all dendritic polymers. The intense peaks at 1657 cm^{-1} and 1447 cm^{-1} for dendritic polymers indicated the presence of –CO–NH– groups, which confirmed the covalent binding of PAMAM with magnetic chitosan. All these vibrational frequencies are agreed to other reports [19].

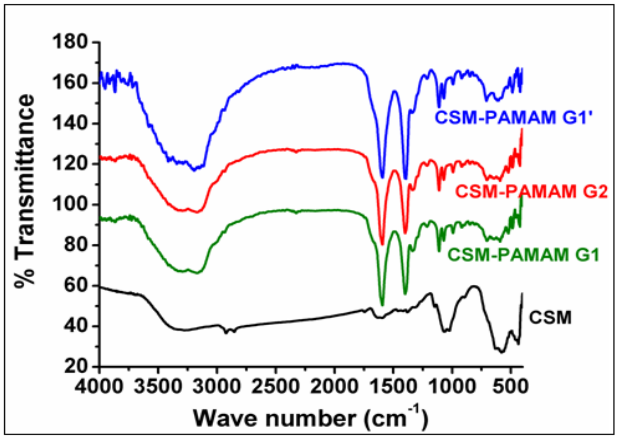

Figure: 5.1 IR Spectra of CSM, CSM-PAMAM G1, CSM-PAMAM G2 and CSM-PAMAM G1'

Table5.1 Peak assignments for PAMAM modified magnetic chitosan

Peak assignment (cm^{-1})	CSM	CSM-PAMAM G1	CSM-PAMAM G2	CSM-PAMAM G1'
N–H and O–H stretching vibration	3310	3305	3301	3306
–CN axial deformation of $–NH_2$ groups	1320	1317	1318	1317
Asymmetric stretching vibrations of $–CH_2$ and $–CH_3$ groups	2856, 2916	2852, 2913	2850, 2911	2853, 2914
C–O stretching vibration	1036	1034	1033	1035
$–NH_2$ bending vibrations	1540	1535	1533	1536
C=O stretching vibrations	1644	16442	1640	1640
Fe–O bond vibration of Fe_3O_4	576	572	570	573
Vibrations of –CO–NH– groups	-	1657,1447	1655,1444	1655, 1445

5.3.3.2 X-ray powder diffraction spectra

The crystal structure of PAMAM modified forms of magnetic chitosan was determined by X-ray diffraction study and their diffractograms were compared with that of magnetic chitosan. All the modified forms have shown diffraction peaks at (220), (311), (400), (422), (511) and (440) indexed to the planes of magnetite with cubic spinel structure (JCPDS File No: 75-0033) and this showed that magnetite was stable during the dendrimerization process. The presence of these diffraction peaks indicated the crystallinity of the

modified forms and this confirmed that the dendrimerization did not affect the crystal phase of magnetic chitosan. The CSM displayed characteristic peak of chitosan at 2θ = 20º as broad and this became more intense for modified forms. This could be due to the fact that the introduction of polar amino groups leads to the increase of crystallinity of chitosan [19].

By using Debye–Scherrer equation the particle sizes of the modified forms were calculated as 32.96 nm, 41.54 nm and 34.25 nm for CSM-PAMAM G1, CSM-PAMAM G2 and CSM-PAMAM G1' respectively.

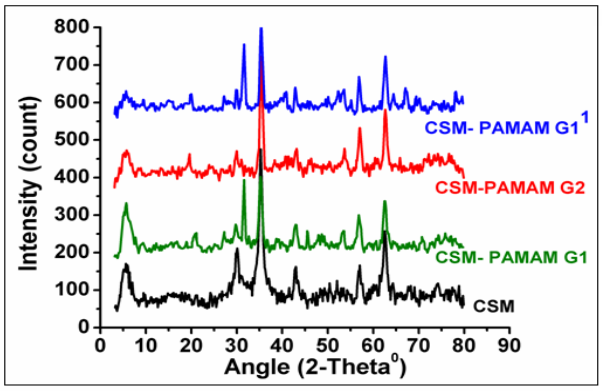

Figure:5.2 XRD Spectra of CSM, CSM-PAMAM G1, CSM-PAMAM G2 and CSM-PAMAM G1'

5.3.3.3 Thermogram of PAMAM modified magnetic chitosan

The TGA-DTG curves of modified forms of magnetic chiotsan by PAMAM dendrimer were illustrated in the figure 5.3. The first stage of weight loss mainly up to 200 ºC for all the modified forms could be due to desorption of physically adsorbed water and they exhibited about 10 % of weight loss. After that they have shown a significant weight loss at 300 ºC which might be as a result of degradation of organic moieties like ethylene diamine and the decomposition of main chain of chitosan polymer [20]. At this stage weight loss were calculated as 20 %, 30 % and 25 % for CSM-

PAMAM G1, CSM-PAMAM G2 and CSM-PAMAM G1' respectively. Here CSM-PAMAM G2 acquired higher percentage of weight loss compared to the others since an increased amount of loss of organic contents have taken place on going from first to second generation. At 500 ºC, PAMAM modified forms exhibited the weight losses of 60 %, 65 % and 57 % respectively and beyond this temperature there was no further degradation can be seen. Similar trend in thermal degradation was observed by Weiwei Zhu et al. where Fe_3O_4-DA showed 25 % of weight loss at 800 ºC, while the weight loss of Fe_3O_4-DA-G3 was around 35 % at the same temperature [13].

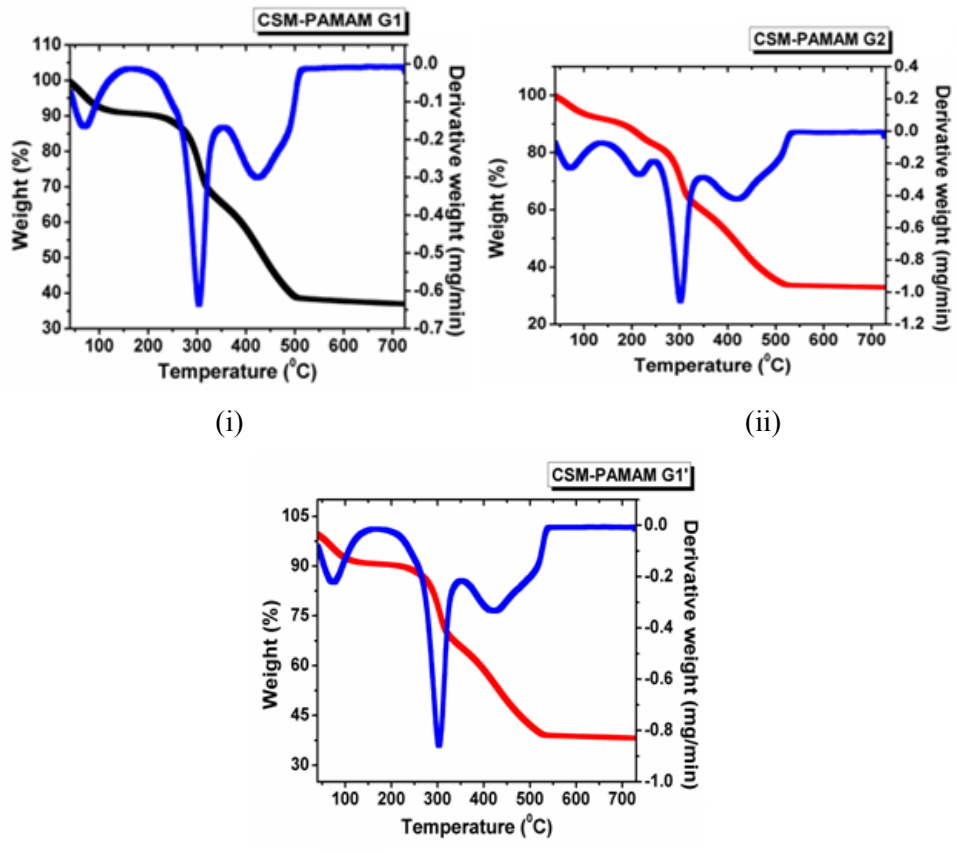

Figure: 5.3 TGA-DTG curves of CSM-PAMAM G1, CSM-PAMAM G2 and CSM-PAMAM G1'

5.3.3.4 Scanning electron microscopy

The surface morphology of modified forms of magnetic chitosan was compared with that of bare form of magnetic chitosan. The SEM images are shown in the figure 5.4 and the morphological changes of magnetic chitosan after the modification can be clearly observed. The modified forms have shown rough and agglomerated surface morphology and this confirmed the surface dendrimerization of magnetic chitosan.

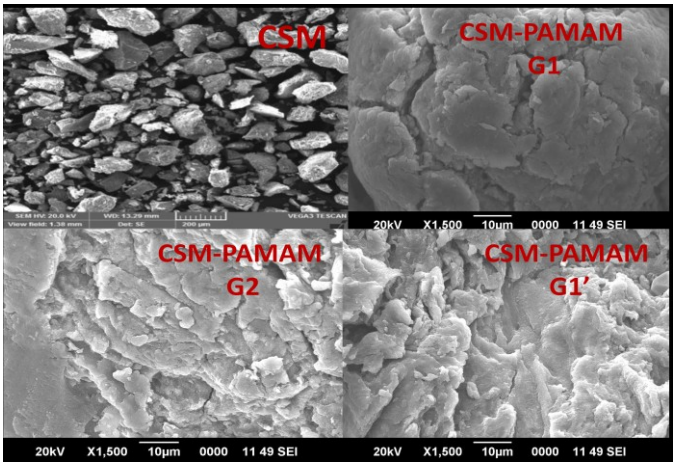

Figure: 5.4 SEM images of CSM, CSM-PAMAM G1, CSM-PAMAM G2 and CSM-PAMAM G1'

5.3.3.5 Surface area analysis

The surface areas of PAMAM modified magnetic chitosan are presented in the table 5.2. The surface area of CSM-PAMAM G1, CSM-PAMAM G2 and CSM-PAMAM G1' are 1.77 $m^2 g^{-1}$, 1.13 $m^2 g^{-1}$ and 1.67 $m^2 g^{-1}$ respectively. Here we noticed that CSM-PAMAM G2 attained lower surface area than that of first generation of dendritic polymers. This could be as a result of agglomeration of the dendritic polymer as it goes to higher generation. This analysis also confirmed the surface dendrimerization of magnetic chitosan.

Table 5.2 Surface area of PAMAM modified magnetic chitosan

Composite	Surface area ($m^2 g^{-1}$)
CSM-PAMAM G1	1.77
CSM-PAMAM G2	1.13
CSM-PAMAM G1'	1.67

5.3.3.6 Magnetic properties

The magnetic properties of the modified forms of magnetic chitosan were examined by VSM analysis and the magnetization curves are plotted in the figure 5.5. All the composites have shown S-like curve that cross the zero point indicated their super paramagnetic behavior. The magnetization values evaluated are 13.85 emu g^{-1}, 11.04 emu g^{-1} and 14.85 emu g^{-1} for CSM-PAMAM G1, CSM-PAMAM G2 and CSM-PAMAM G1'. The results showed that all the modified forms exhibited lower Ms values compared to CSM which indicated the surface dendrimerization of magnetic chitosan. The lowest value of CSM-PAMAM G2 proved that the Ms value of dendritic polymer was again decreased as it reached higher generation. All these explanations revealed that dendritic modification of magnetic chitosan was taken place successfully and the modified forms are capable to response to a magnetic field, thus magnetic separation is possible to it.

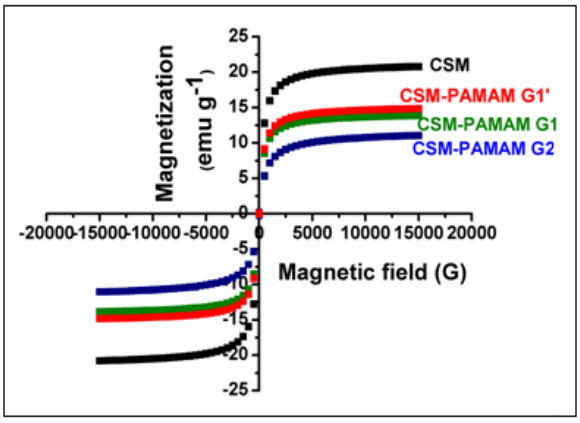

Figure: 5.5 Magnetization curves of CSM, CSM-PAMAM G1, CSM-PAMAM G2 and CSM-PAMAM G1'

5.3.3.7 CHN analysis

The surface dendrimerization on magnetic chitosan was also confirmed by elemental analysis and the percentages of elements are given in the table 5.3. The nitrogen content presented in amino groups of CSM is 2.33 % and in dendritic polymers are 4.52 %, 6.45 % and 4.67 % respectively for CSM-PAMAM G1, CSM-PAMAM G2 and CSM-PAMAM G1' respectively. The increased nitrogen content in the CSM-PAMAM G2 indicated the dendritic growth of polymer to higher generation. It was noticed that when the second generation of dendritic polymer was originated from first generation, the nitrogen content presented in it did not increase exponentially which could be as a result of existence of steric hindrance on the surface of magnetic chitosan.

Table 5.3 CHN analytical data of magnetic chitosan and its PAMAM modified forms

Composite	N (%)	C (%)	H (%)
CSM	2.33	11.28	2.25
CSM-PAMAM G1	4.52	23.21	4.62
CSM-PAMAM G2	6.45	32.69	6.48
CSM-PAMAM G1'	4.67	28.22	4.94

5.3.4 Immobilization of α-amylase on PAMAM modified magnetic chitosan

5.3.4.1 Optimization immobilization conditions

Various conditions for immobilization of α-amylase onto the PAMAM modified magnetic chitosan was optimized for further studies.

5.3.4.1.1 Effect of immobilization pH on α-amylase activity

The immobilization pH greatly influence the activity of enzyme since the activity related to the ionization state of amino acid residues at the active site. The optimum pH for maximum immobilization of enzyme on support was determined by the combined pKa of chitosan and PAMAM dendrimer. The dendrimer maintain different pKa values based on the amino groups presented in the peripheral region and internal cavities. The pKa of PAMAM is 7-9 due to the peripheral $–NH_2$ groups and 3-6 by tertiary amine moieties [21].

The variations of immobilization pH on relative activity of enzyme were studied and are depicted in the figure 5.6. The immobilized enzymes have shown maximum activity at definite pH values where high electrostatic interactions have been taken place. The maximum activity obtained for CSM-PAMAM G1' and CSM-PAMAM G2 was at pH 7 and it was at pH 6 for CSM-PAMAM G1. When the support acquired more number of amino groups, the positive charges presented on them increased since the amino groups existed as positively charged. As a result of this the H^+ ions in the microenvironment of the immobilized system is reduced and hence the optimum pH changed to more basic region. The lowering of enzyme activity below and above this optimum pH might be due to the electrostatic repulsion existed between the enzyme and the support.

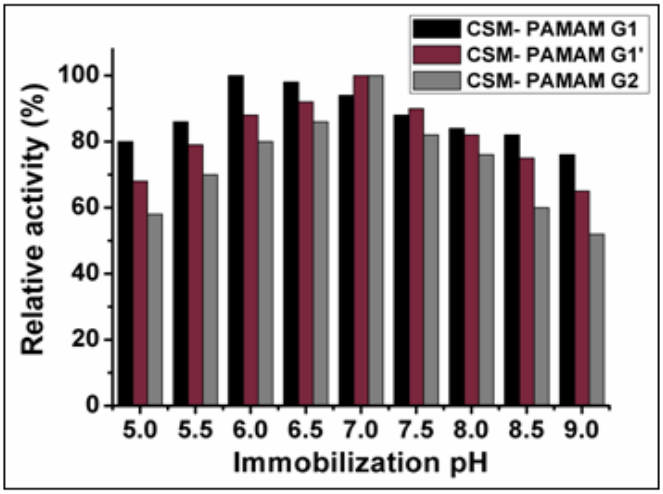

Figure: 5.6 Effect of immobilization pH on the relative activity of immobilized α-amylase on PAMAM modified magnetic chitosan

5.3.4.1.2 Effect of incubation time on α-amylase activity

The incubation time of the immobilization process has great influence on the enzyme activity. The variations of relative activity of enzyme on incubation time were evaluated and are plotted in the figure 5.7. The immobilized enzyme activities were improved with increase of incubation time and reached the maximum activities at 240 min. for CSM-PAMAM G1, 180-240 min. for CSM-PAMAM G1' and 180 min. for CSM-PAMAM G2. The further increase of incubation time declined the relative activities of immobilized enzymes as the immobilization capacity of the supports gets saturated. The prolonged immobilization time enabled the enzyme to bind almost completely with the support and this excessive enzyme adsorption caused the inactivation of immobilized enzyme systems. Chen Hou observed the lipase inactivation after 300 min. of prolonged immobilization on to PAMAM dendrimer modified macroporous polystyrene [22].

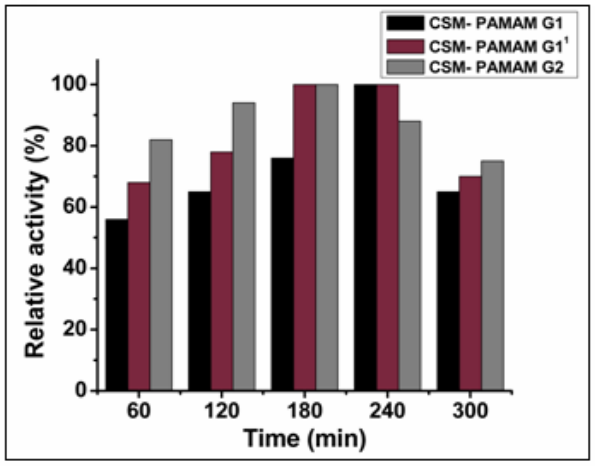

Figure: 5.7 Effect of contact time on activity of immobilized α-amylase on PAMAM modified magnetic chitosan

5.3.4.1.3 Effect of initial amount of protein on protein loading onto supports

The effect of initial amount of α-amylase on protein loading was investigated at optimum temperature and incubation time. The figure 5.8 shows the variations of protein loading with respect to the initial amount of enzyme taken for the immobilization process.

The loaded protein was found to be increased with the rise of initial amount of enzyme until reached 14.4 mg for CSM-PAMAM G1, 16.8 mg for both CSM-PAMAM G1' and CSM-PAMAM G2 and the maximum loaded protein on to these supports was observed to be as 8.5, 10.4 and 12.5 mg/g support respectively. There was no further protein loading observed for all supports as the enzyme concentration increased to higher ranges which could be due to the multilayer adsorption of enzyme that lower the enzyme-support interaction and hence leads to the desorption of enzyme. The percentage of immobilization yield was calculated (table 5.4) and found to be the highest value of 74.4 % for CSM-PAMAM G2. The second

generation of PAMAM modified magnetic chitosan has provided more reactive sites for enzyme binding as it contained increased number of terminal amino groups. However, the IY % of CSM-PAMAM G2 was not exponential that of CSM-PAMAM G1which might be due to the steric hindrance caused by the higher generations of dendritic polymer that prevent the enzyme binding capacity.

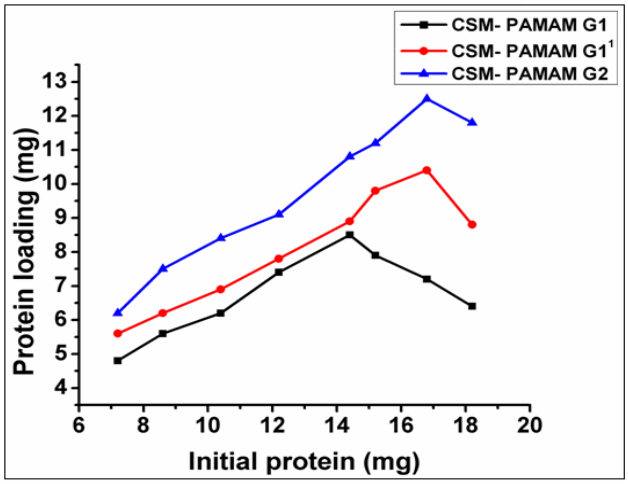

Figure: 5.8 Effect of initial protein amount on protein loading onto PAMAM modified magnetic chitosan

5.3.4.1 .4 Effect of initial protein amount on immobilized enzyme activity

The change in enzyme activity of the immobilized enzymes with respect to the initial protein amount was investigated and the results are depicted in the figure 5.9.

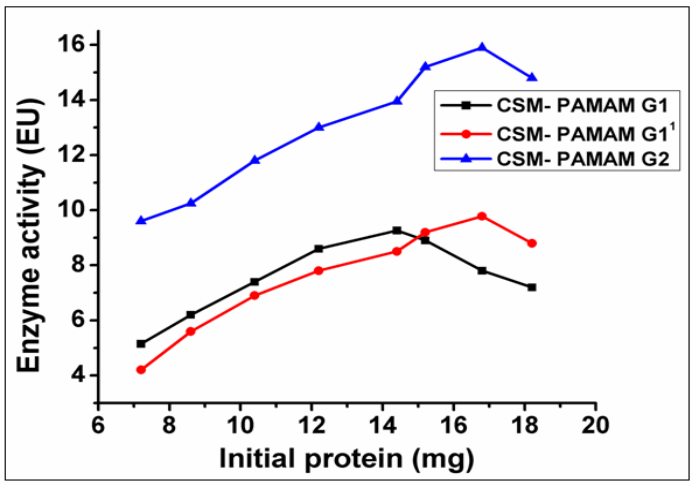

Figure: 5.9 Effect of initial protein concentration on immobilized enzyme activity

For all immobilized enzymes the enzyme activity was found to be increased as the amount of initial protein increases. For CSM-PAMAM G1, the maximum enzyme activity of 9.26 EU was obtained at initial amount of 14.4 mg enzyme. The α-amylase on CSM-PAMAM G1' and CSM-PAMAM G2 attained optimum activity of 9.78 EU and 15.9 EU at 16.8 mg of enzyme. The percentage of activity yield (AY %) was determined using the above results and the highest value of 69.89 % was acquired by CSM-PAMAM G2. This could be arising from the increased availability of desirable active sites on enzyme structure at which the catalytic reaction has taken place. The immobilization efficiency (IE %) evaluated from the corresponding values of IY % and AY % was 67.81 % for CSM-PAMAM G1, 71.71 % for CSM-PAMAM G1'and 93.94 % for CSM-PAMAM G2.

Table 5.4 Immobilization efficiency of α-amylase on PAMAM modified forms of magnetic chitosan

Support	Initial protein (mg)	Immobilized protein mg/g support	IY (%)	Initial activity (EU)	Immobilized enzyme activity (EU)	AY (%)	IE (%)
CSM-PAMAM G1	14.4	8.5	59.03	23.13	9.26	40.03	67.81
CSM-PAMAM G2	16.8	12.5	74.4	22.75	15.9	69.89	93.94
CSM-PAMAM G1[1]	16.8	10.4	61.90	22.03	9.78	44.39	71.71

5.3.4.1.5 Nitrogen content in PAMAM modified forms and α-amylase immobilization Efficiency

The immobilization efficiency of α-amylase on PAMAM modified forms were explained on the basis of percentage of nitrogen content presented in it. The CSM-PAMAM G1' has shown higher IE % compared to CSM-PAMAM G1since it exhibited slight increase of nitrogen content and hence more reactive sites to bind the enzyme. On comparing the first and second generation of PAMAM modified magnetic chitosan the later one attained increased density of terminal amino groups, but there was no exponential increase in binding capacity with enzyme as the large enzyme structure caused drastic steric hindrance with it. Hence there existed slower incremental growth of binding capacity of immobilized enzyme even the generation of PAMAM dendrimer increased to higher states. The slower incremental growth of cellulase binding capacity was reported by Ping Su et al. when immobilized on G0–G3 PAMAM-grafted silica [23].

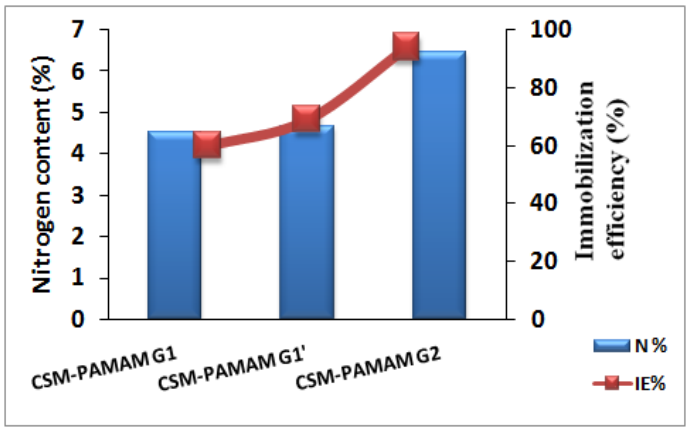

Figure: 5.10 The effect of nitrogen content in PAMAM modified magnetic chitosan on α-amylase immobilization efficiency

5.3.4.2 Effect of pH on α-amylase activity

The effect of pH on activity of free and immobilized enzymes towards starch hydrolysis was determined in the pH range 4-9 and the observations are illustrated in the figure 5.11.

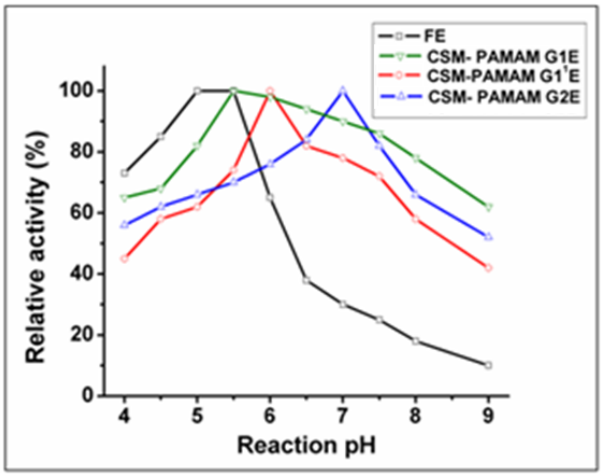

Figure: 5.11 Effect of pH on the relative activity of free and immobilized α-amylase on PAMAM modified magnetic chitosan

The CSM-PAMAM G1E exhibited optimum reaction pH at 5.5, similar to that of free enzyme. The optimum pH of CSM-PAMAM G1'E and CSM-PAMAM G2E were at 6 and 7 respectively. All the immobilized

enzymes have shown broad pH profile compared to free enzyme. After optimum pH the free enzyme lost its activity very sharply and here we noticed that it retained only 10 % of initial activity at pH 9, while the immobilized enzymes retained 42-62 % of activity at the same pH. The increased density of amino groups presented on the surface of support provided more positive charges to it and made the microenvironment of the enzyme with lesser H^+ ions, hence led to the pH of the immobilized systems more basic compared to bulk region. The higher activity of the immobilized enzymes might be due to the reduced diffusional limitations compared to free enzyme. The less diffusional limitations of the enzyme was also observed when lipase immobilized on poly(phenylene sulfide) dendrimers [24].

5.3.4.3 Effect of temperature on α-amylase activity

The temperature of the enzymatic reaction has major role in predicting its application in industrial scale. The effect of temperature on relative activities of free and immobilized enzymes was assessed in the range of 30-70 ºC and the results of the study are presented in the figure 5.12.

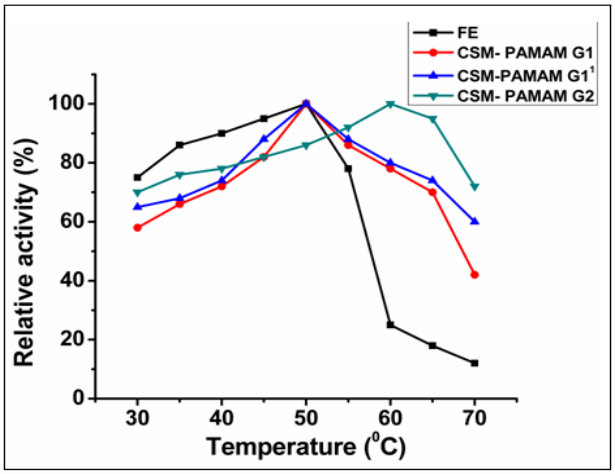

Figure: 5.12 Effect of temperature on the relative activity of free and immobilized α-amylase on PAMAM modified magnetic chitosan

For free enzyme, the activity was first increased with increase of temperature and exhibited maximum at 50 ºC, thereafter a dramatic decrease in enzyme activity was observed as the temperature further increased. The CSM-PAMAM G1E and CSM-PAMAM G1'E have shown optimum temperature similar to that of free enzyme, while for CSM-PAMAM G2E the optimum temperature shifted to 60 ºC. All immobilized enzymes have exhibited broad temperature profile and retained the activity in the range of 40-70 % as the temperature reached 70 ºC. This temperature profile of immobilized enzymes has demonstrated their stable three dimensional conformations and higher stability than that of free enzyme. The shift of optimum temperature of CSM-PAMAM G2E to higher temperature indicated its excellent heat resistance and this might be due to its reduced conformational flexibility as a result of multipoint attachment of enzyme on to the support [25].

5.3.4.4 Activation energy

The Arrhenius plot of free and immobilized enzymes are shown in the figure 5.13 and from the slopes the activation energy, Ea was calculated. The table 5.5 showed the calculated Ea values, 10.42 KJ mol^{-1}, 8.57 KJ mol^{-1} and 4.54 KJ mol^{-1} for CSM-PAMAM G1E, CSM-PAMAM G1'E and CSM-PAMAM G2E respectively.

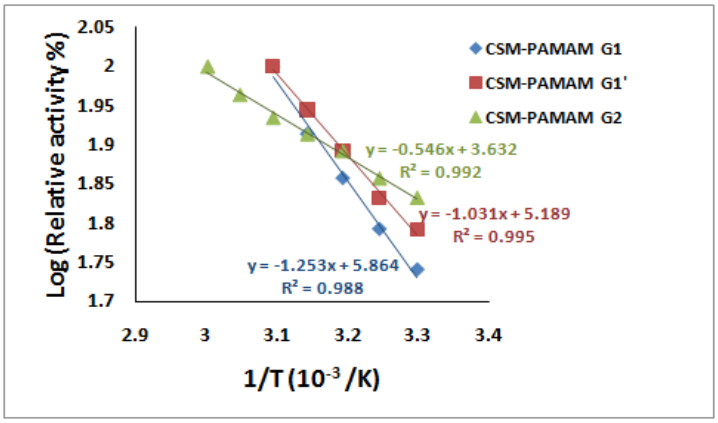

Figure: 5.13 Arrhenius plot to calculate the activation energy (Ea) of immobilized α-amylase on PAMAM modified magnetic chitosan

Table 5.5 Activation energy of immobilized α-amylase on PAMAM modified magnetic chitosan

Immobilized enzyme	Activation energy (KJ mol^{-1})
CSM-PAMAM G1	10.42
CSM-PAMAM G1'	8.57
CSM-PAMAM G2	4.54

All the immobilized enzymes have shown lower values compared to free enzyme and these lower values ascribed to mass transfer limitations for immobilized enzymes [26]. The decrease of activation energy for immobilized enzyme was also reported by Esawy et al. [27], where the shift of optimum pH and temperature affected the chemical bonding within the molecules, led to the change of shape of the active site and hence the activation energy get shifted.

5.3.4.5 Thermal stability of the free and immobilized enzymes

The thermal stability study was carried out with free and immobilized enzymes in which they pre-incubated for 30-70 ºC at optimum

pH in the absence of substrate for 1 h. After that enzymatic reaction was carried out with starch substrate at optimum temperature. The stability curves for free and immobilized enzymes are plotted in the figure 5.14 and all the immobilized enzymes exhibited enhanced thermal stability compared to free enzyme.

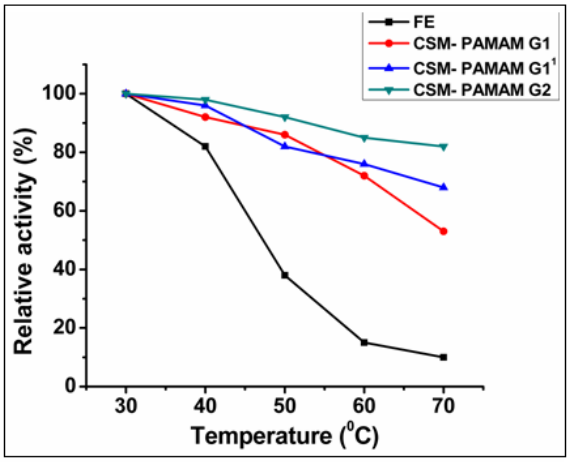

Figure:5.14 Thermal stability of free and immobilized α-amylase on PAMAM modified magnetic chitosan

In all cases the enzyme activity at starting temperature was taken as 100 % and activities corresponding to the increased temperatures were expressed relative to this value. The free enzyme has shown sharp decrease in activity as the temperature increased and at 50 ºC it retained only 38 % of relative activity. However the immobilized enzymes acquired 82-92 % of activity at that temperature indicated their increased thermal resistance. At 70 ºC the free enzyme lost 90 % of its initial activity, whereas the immobilized enzymes lost only 48 % for CSM-PAMAM G1E, 34 % for CSM-PAMAM G1'E and 18 % for CSM-PAMAM G2E. The results were showed that all the immobilized enzymes decreased their activity more slowly than that of their free counterpart and hence they attained enhanced

thermal stability predominantly at higher temperatures. This could be as a result of conformational integrity of the enzyme structure due to the multi point adsorption on PAMAM modified magnetic chitosan.

Thermal stability of free and immobilized enzymes were also studied by pre- incubating them up to 120 min. at their optimum temperature and the enzymatic activities were measured for corresponding incubation time. The figure 5.15 shows that after 120 min. of pre-incubation time the free enzyme lost 90 % of activity, while the immobilized enzymes lost 50 % of activity for CSM-PAMAM G1E, 40 % of activity for CSM-PAMAM G1'E and 25 % of activity for CSM-PAMAM G2E. The similar trend was observed when lipase immobilized on PAMAM modified monodisperse magnetic microspheres [13] and the stability was acquired by multipoint attachment between the enzyme and support which caused the strengthening of intra molecular forces in enzyme structure.

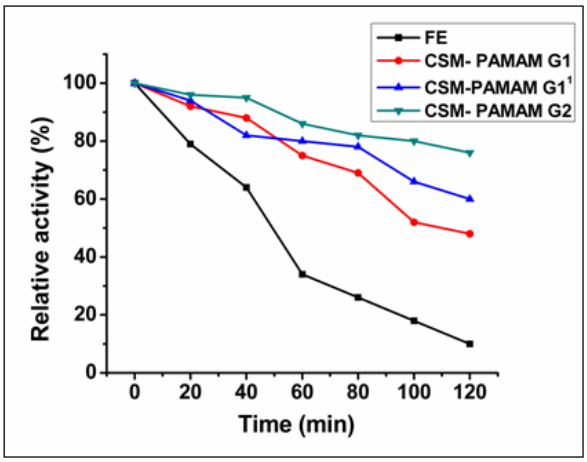

Figure:5.15 Variation of pre-incubation time on activity of free and immobilized α-amylase on PAMAM modified magnetic chitosan

5.3.4.6 Determination of kinetic parameters

The kinetic parameters K_m and V_{max} were determined from Lineweiver-Burk method [28]. The Lineweaver-Burk plots and Hanes-Woolf plots are given in the figure 5.16 and the calculated kinetic parameters are presented in the table 5.6.

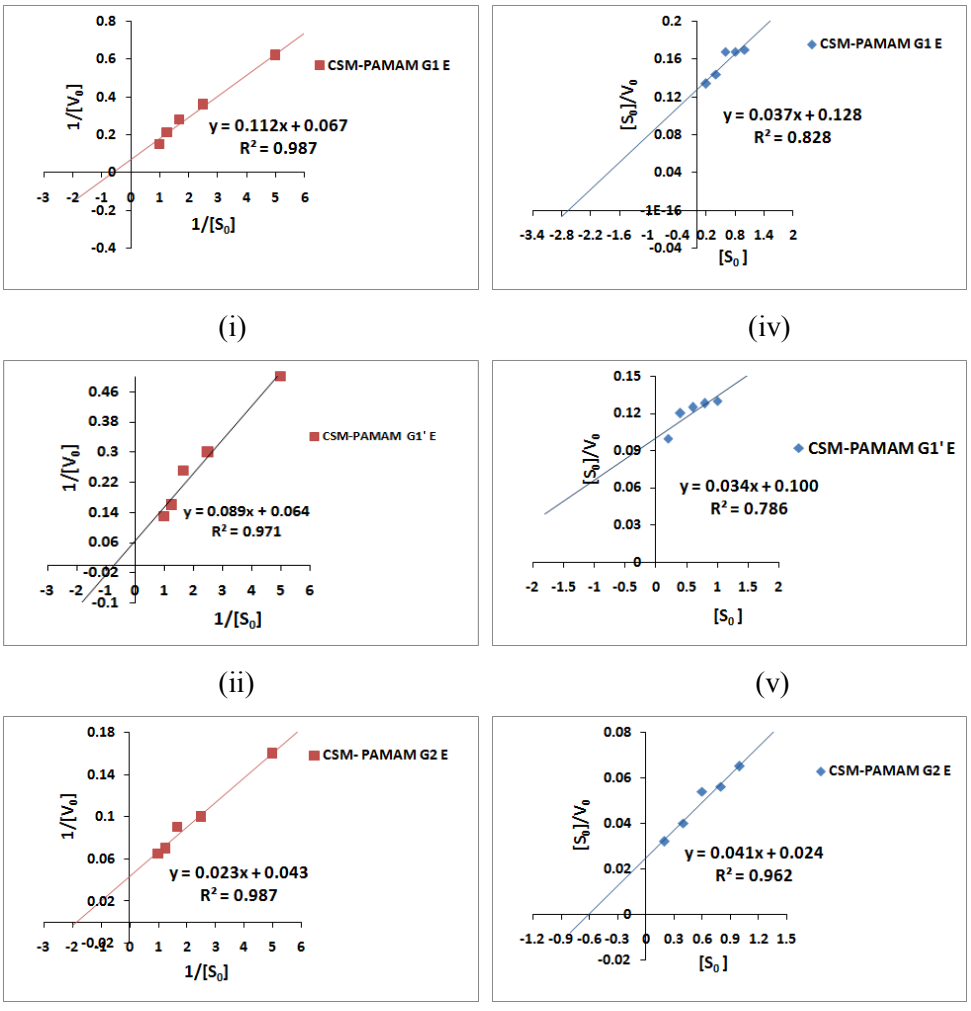

Figure: 5.16 Lineweaver-Burk plots for (i) CSM-PAMAM G1E (ii) CSM-PAMAM G1'E (iii) CSM-PAMAM G2E and Hanes-Woolf plots for (iv) CSM-PAMAM G1E (iv) CSM-PAMAM G1'E (vi) CSM-PAMAM G2E

Table 5.6 Kinetic parameters for free and immobilized α-amylase on PAMAM modified magnetic chitosan

Immobilized enzyme	K_m (mg mL^{-1})	V_{max} (μmol mg^{-1} min^{-1})	K_{cat} (min^{-1})	K_{cat}/K_m (mL$mg^{-1}min^{-1}$)
Free enzyme	0.45± 0.02	34.48±0.05	1910.19	4244.87
CSM-PAMAM G1 E	1.67± 0.03	14.92± 0.05	826.57	494.95
CSM-PAMAM G1' E	0.85±0.03	16.67± 0.02	923.52	1086.49
CSM-PAMAM G2 E	0.53± 0.04	23.25± 0.04	892.49	1683.94

The immobilized enzymes have shown higher K_m and lower V_{max} values compared to free enzyme which indicated their decreased affinity towards substrate molecule. The diffusional limitations can be avoided in case of free enzymes in solution; but for the enzymes immobilized on PAMAM modified magnetic chitosan, the role of mass transfer by diffusional limitations played more effectively. The immobilization of enzyme on to the support caused structural changes in enzyme and leads to the conformational changes in the active site which hinder the substrate affinity. Among the immobilized enzymes, CSM-PAMAM G2E attained K_m and V_{max} values with small changes compared to free enzyme and this showed its increased affinity and activity.

The turn over number (K_{cat}) for immobilized enzymes were calculated and compared with that of free enzyme. The K_{cat} values calculated for CSM-PAMAM G1E, CSM-PAMAM G1'E and CSM-PAMAM G2E were 826.57 min^{-1}, 923.52 min^{-1} and 892.49 min^{-1} respectively which are found to be 56.73 %, 51.65 % and 53.28 % lesser than that of free enzyme. This indicated their decreased enzyme activity since one molecule required 72.57, 64.97 and 67.25 milliseconds of time respectively to convert one substrate molecule in to product, while for free enzyme it was only 31.41 milliseconds.

The catalytic efficiency (K_{cat}/K_m) was also calculated and the immobilized enzymes displayed 88.34 %, 74.40 % and 60.33 % of lesser values compared to free enzyme. The lower catalytic efficiency for immobilized enzymes was also reported when alcohol and aldehyde dehydrogenases immobilized onto carbon platform through PAMAM dendrimer [29].

5.3.4.7 Storage stability of Immobilized α-amylase

The storage stability of immobilized enzymes was studied for six months of period by storing them in buffer at 4 °C. The activities were determined for definite intervals of time and the results are shown in the figure 5.17.

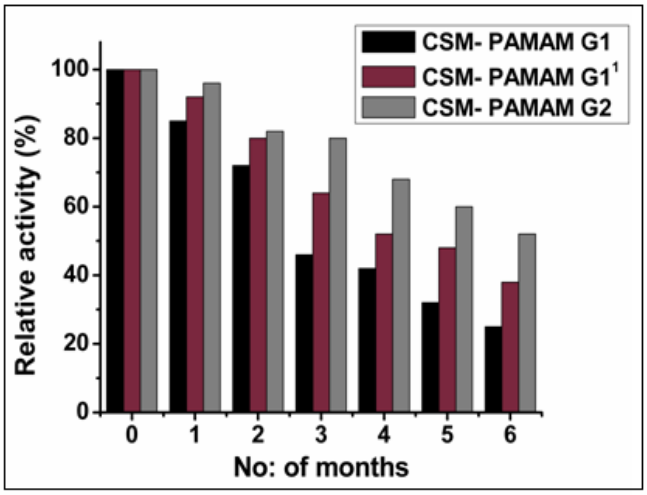

Figure:5.17 Storage stability of immobilized α-amylase on PAMAM modified magnetic chitosan

After six months of storage, the immobilized enzymes retained activity of 25 % for CSM-PAMAM G1E, 38 % for CSM-PAMAM G1'E and 52 % for CSM-PAMAM G2E. The results showed that time dependent natural loss of enzyme activity can be minimized through immobilization process, as it provided rigidity to the enzyme structure and hence conformational stability

to the active site of the enzyme. The multipoint interaction between the enzyme and carrier imparted improved conformational stability to the enzyme and this provided enhanced substrate affinity towards the enzymatic reaction. The improved storage stability of enzyme was also reported where invertase immobilized on PAMAM modified superparamagnetic iron oxide nanoparticles [30], in which the immobilized enzyme lost 22 % of activity when stored at 4 °C over a period of 30 days.

5.3.4.8 Reusability

The reusability study was conducted by subjecting the immobilized enzymes on 10 cycles of continual catalytic reaction and measured the respective enzyme activity. The figure 5.18 showed that after 10^{th} cycles of reuses the immobilized enzymes retained 30 %, 50 % and 83 % activities for CSM-PAMAM G1E, CSM-PAMAM G1'E and CSM-PAMAM G2E respectively. Here CSM-PAMAM G2E has acquired higher activity at the end of the cycle indicated more reduction in enzyme leaching from the support and in enzyme denaturation during the period of uses [31]. The PAMAM dendrimer assisted enzyme immobilization provided multi-interaction between the enzyme and the terminal amino functional groups on support in order to stabilize the three dimensional protein structure and thus enzyme denaturation get diminished. The similar observation was reported when lipase immobilized on PAMAM modified macroporous polystyrene [22], in which the immobilized enzyme for olive oil emulsion hydrolysis retained 85 % of initial activity at the end of 10^{th} recycling process.

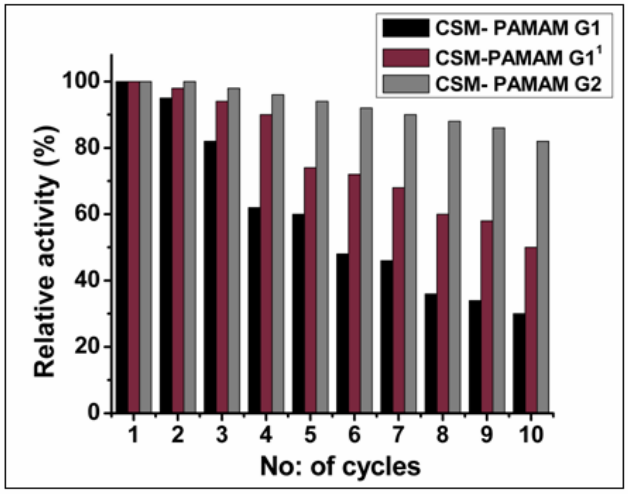

Figure: 5.18 Reusability of immobilized α-amylase on PAMAM modified magnetic chitosan

5.4 Covalent immobilization of α-amylase on CSM-PAMAM G2

5.4.1 Immobilization of α-amylase by covalent method

For covalent immobilization method, the CSM-PAMAM G2 was stirred with 0.4 % (v/v) gluteraldehyde solution for 2 h. The support was then separated by applying an external magnetic field, washed to remove excess of gluteraldehyde and dried in air. Thereafter the support was immersed in enzyme solution in buffer and incubated for 2 h. After the time period the immobilized enzyme formed was undergone magnetic separation by washing with same buffer in order to remove the unbound enzyme. The filtrate was used to estimate the residual enzyme by Lowry's method [32] and the immobilized enzyme was stored at 4 °C for further studies. The schematic diagram representing the covalent immobilization method is given in scheme 5.2.

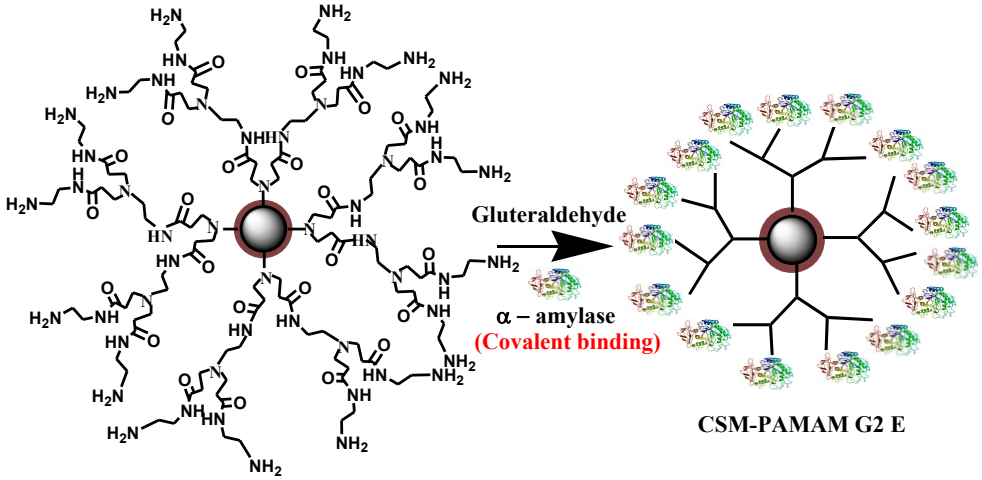

Scheme 5.2 Covalent immobilization of α-amylase on CSM-PAMAM G2

5.4.1.1 Optimization of α-amylase immobilization conditions

The immobilization conditions such as pH of the medium, incubation time, gluteraldehyde concentration and enzyme concentration for covalent immobilization of α-amylase on CSM-PAMAM G2 were optimized in order to get maximum immobilization efficiency and compared with that of adsorption immobilization.

5.4.1.1.1 Effect of immobilization pH on α-amylase activity

The pH of the immobilization medium was optimized in the range of 5-9 for covalent immobilization of α-amylase on CSM-PAMAM G2 and the results were compared with that of adsorption method. The maximum immobilization pH by adsorption method was already observed at pH 7 and here the optimum pH was obtained at pH 7.5 for covalent method. In covalent immobilization, the enzyme was bounded with gluteraldehyde activated carrier through Schiff base reaction. Since this reaction was favored by basic medium, in covalent immobilization method the maximum activity shifted to

at slightly higher pH. Under basic conditions the aldehyde groups of activated carrier are able to allow multipoint covalent immobilization with enzyme having large amount of lysine groups. The increased activities at higher pH were acquired by covalent method might be due to the reduced enzyme leaching as there existed a strong binding between enzyme and the carrier. The shift of optimum pH towards alkaline region was also observed by Shukla et al. when α-amylase immobilized on nylon 6 via covalent method. They observed that maximum immobilized enzyme stability was at pH 6-7 and found to be decreased towards acidic region [33].

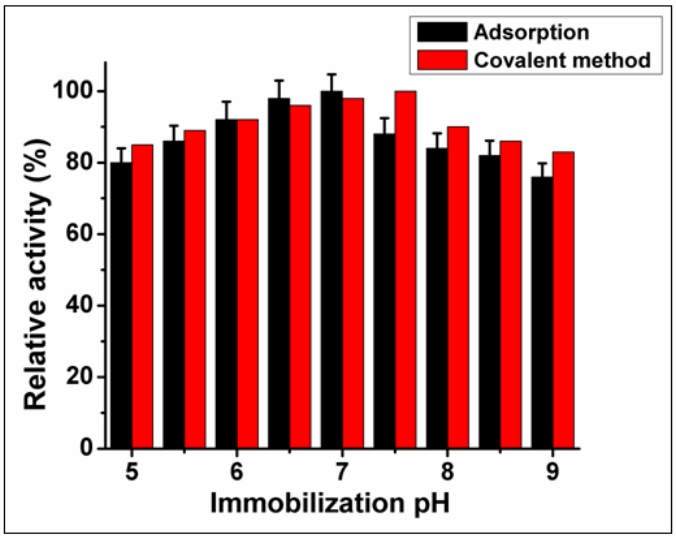

Figure: 5.19 Effect of immobilization pH on the relative activity of immobilized α-amylase on CSM-PAMAM G2 by adsorption and covalent methods

5.4.1.1.2 Effect of incubation time on activity of α-amylase

The incubation time required for covalent immobilization was optimized and compared to that of adsorption method. The figure 5.20 showed that both of the methods for α-amylase immobilization exhibited optimum incubation time of 180 min. In both cases the relative activity of the

immobilized enzyme was found to be decreased beyond this optimum value due to the saturation in loading capacity of the carrier. However, this decrease in enzyme activity was lesser with covalent method since it contributed strong binding of enzyme on to the carrier and hence prevented the enzyme desorption more effectively, which was not possible with adsorption method.

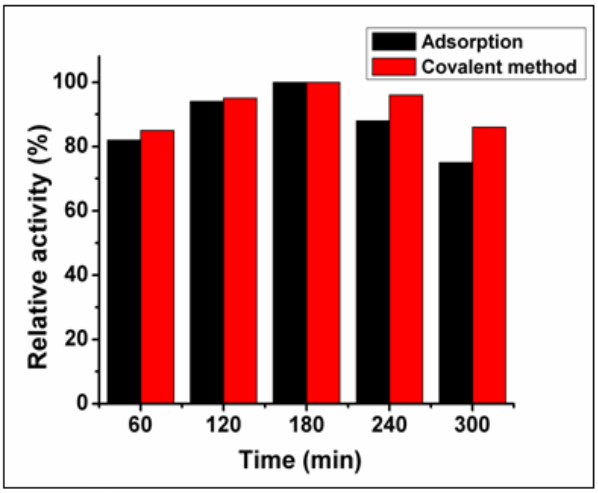

Figure: 5.20 Effect of incubation time on activity of immobilized α-amylase on CSM-PAMAM G2 by adsorption and covalent methods

5.4.1.1.3 Effect of gluteraldehyde concentration on immobilized α-amylase activity

The concentration of cross-linking agent has major role in providing favorable efficiency for α-amylase immobilization. The gluteraldehyde concentration in the activated carrier was varied in the range of 0.1 to 1 % (v/v) and α-amylase immobilization was carried out with support contained each gulteraldehyde concentration. The relative enzyme activities were measured and plotted against corresponding gluteraldehyde concentration taken during the activation of support.

The figure 5.21 showed that maximum enzyme activity was obtained for immobilized enzyme with 0.4 % of gluteraldehyde and this immobilized enzyme with optimum gluteraldehyde concentration was taken for further studies. The lower and higher concentrations of this optimum value resulted in decrease of enzyme activity since the lower gluteraldehyde concentration provided insufficient cross-linking and higher amounts caused intermolecular cross-linking of enzyme molecules and gluteraldehyde polymerization [34].

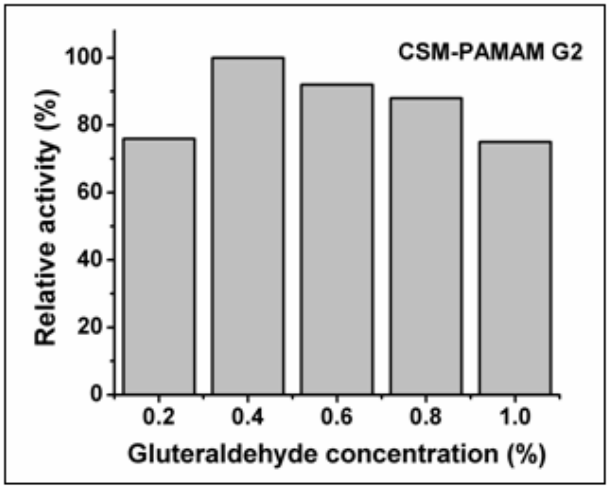

Figure: 5.21 Effect of gluteraldehyde concentration on the relative activity of immobilized α-amylase on CSM-PAMAM G2

5.4.1.1.4 Effect of initial amount of protein on protein loading on to CSM-PAMAM G2

The protein loading on to CSM-PAMAM G2 by adsorption and covalent method was investigated by varying the initial amount of enzyme. The figure 5.22 showed that protein loading onto the support increased with continuous rise of initial amount of enzyme and reached to a saturation point which was 12.5 mg g^{-1} support at 16.8 mg of initial protein for adsorption method and 9.6 mg g^{-1} support at initial protein of 14.4 mg for

covalent method. These respective initial enzyme concentrations were selected for α-amylase immobilization to get maximum enzyme loading by adsorption and covalent methods.

The immobilization yield (IY %) was calculated for the immobilized enzymes by both methods and are presented in the table 5.7. The IY % of α-amylase on CSM-PAMAM G2 by adsorption method was 74.4 % and it was 66.67 % for covalent immobilization method. The support activated with cross-linking agents provides restricted reaction sites for enzyme immobilization and this may lead to lesser protein loading by covalent method compared to adsorption.

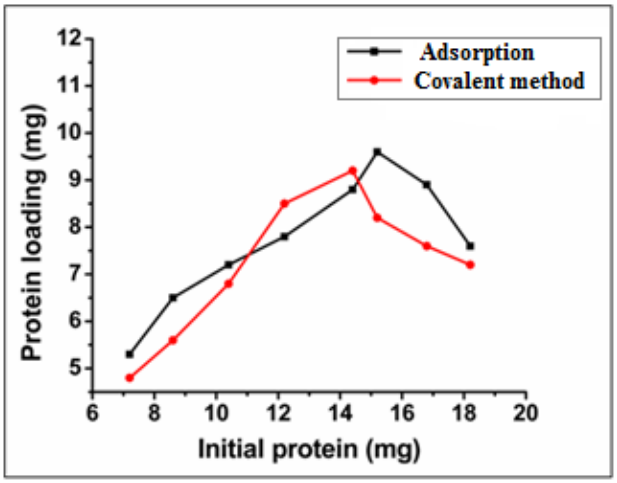

Figure: 5.22 Effect of initial protein amount on protein loading onto CSM-PAMAM G2 by adsorption and covalent methods

5.4.1.1.5 Effect of initial protein amount on immobilized α-amylase activity

The effect of initial amount of α-amylase on immobilized enzyme activity was assayed and is illustrated in the figure 5.23. The immobilized enzyme activity was increased with rise of initial protein amount and reached a maximum activity of 15.9 EU for adsorption method with initial

amount of 16.8 mg enzyme and 13.95 EU for covalent method with initial enzyme of 14.4 mg. In both cases, the further increase of initial protein amount did not enhance the enzyme activity. The activity yield (%) was calculated for the immobilized enzyme by the two methods and the results showed that covalently immobilized enzyme attained only lower value compared to the adsorbed one. This lower activity of immobilized enzyme by covalent method might be due to the effect of immobilization conditions and conformational changes in the three dimensional structure of enzyme [35]. The strong binding of enzyme with the support leads to the reduction in conformational flexibility to the enzyme structure and causes deformation in active site of enzyme molecule which imparts lower substrate affinity towards enzymatic reaction. This could be impossible with adsorption immobilization since there existed only weak interactions between the enzyme and support, hence showed higher activity.

The immobilization efficiency was evaluated and it was found that the immobilized enzyme by adsorption method attained higher IE % than covalently immobilized enzyme which was 93.95 % and 73.42 % respectively.

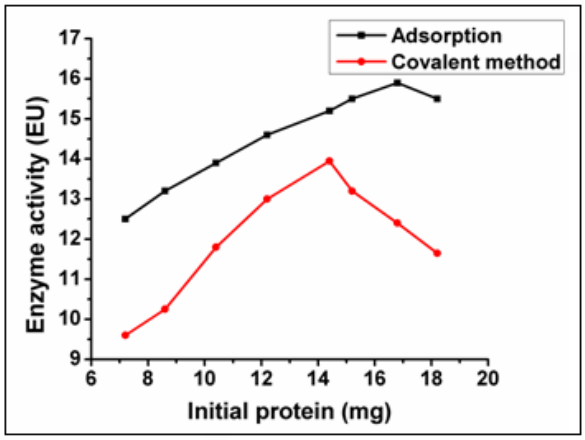

Figure: 5.23 Effect of initial protein concentration on activity of immobilized enzyme by adsorption and covalent methods

Table 5.7 Immobilization efficiency of α-amylase on CSM-PAMAM G2 by adsorption and covalent methods

Support	Initial protein (mg)	Immobilized protein mg/g support	IY (%)	Initial activity (EU)	Immobilized enzyme activity (EU)	AY (%)	IE (%)
CSM- PAMAM G2 (Adsorption)	16.8	12.5	74.4	22.75	15.9	69.89	93.95
CSM- PAMAM G2 (Covalent method)	14.4	9.6	66.67	28.5	13.95	48.95	73.42

5.4.1.2 Effect of pH on α-amylase activity by adsorption and covalent methods

The effect of pH on starch hydrolysis activities of free and immobilized α-amylases by adsorption and covalent methods was investigated and the results are presented in the figure 5.24. The reaction pH greatly influences the enzyme activity since it preserved the actual conformation of enzyme structure by maintaining the ionization state of amino acid residues presented in the active site of enzyme. The figure showed that both free and adsorbed enzymes attained maximum activity at pH 5.5 and after that the activity decreased sharply for free enzyme, while the adsorbed enzyme exhibited better activities at higher pH ranges. Compared to free and adsorbed α-amylase, the covalently immobilized enzyme displayed a broad pH profile and showed maximum activity at pH 6.5. This shift of optimum pH towards basic region could be as a result of strong covalent bond between enzyme and the support which results in rigidity to the enzyme structure and caused the conformational changes in it. The covalent binding of amino groups of enzyme and aldehyde groups of activated support favors the formation of stable Schiff base in the alkaline region that could affect the active site of the enzyme. The similar tendency

in shift of optimum pH towards alkaline region was also reported by Siming Wang et al. when cellulase immobilized on PAMAM grafted silica by covalent method [15].

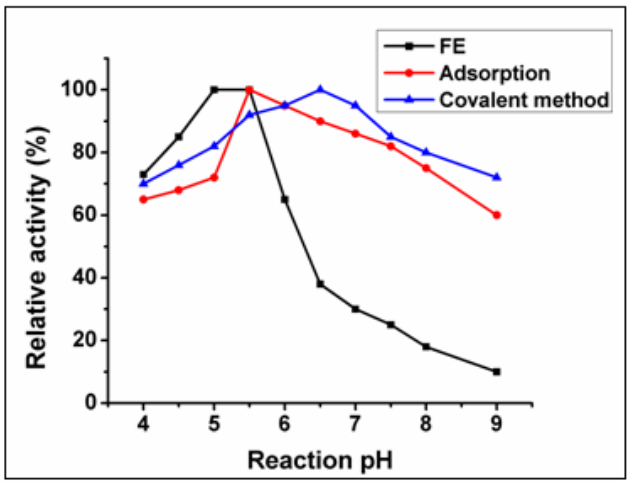

Figure: 5.24 Effect of pH on the relative activity of immobilized α-amylase by adsorption and covalent methods

5.4.1.3 Effect of temperature on α-amylase activity by adsorption and covalent methods

The temperature effect on activity of free and immobilized enzymes were studied in the range between 30-70 °C at corresponding optimum pH and the observations are depicted in the figure 5.25. The free enzyme showed optimum temperature at 50 °C and thereafter a sudden decline in activity was exhibited as the temperature of the reaction system increased to higher ranges. The free enzyme retained only 10 % of relative activity as the temperature reached 70 °C. The immobilized enzyme by both methods acquired maximum activity at same temperature, which was at 60 °C. They have shown very stable temperature profile and at 70 °C, they retained 72 % of activity by adsorption method and 88 % of activity by covalent method.

The increased activity achieved by the covalently immobilized enzyme might be due to its high stable three-dimensional structure. The similar observation was reported by Uzun et al. where covalently immobilized invertase on PAMAM dendrimer modified superparamagnetic nanoparticles showed a shift of optimum temperature from 50 °C to 60 °C. This shift could be as a result of increased activation energy of the enzyme in order to get appropriate structural conformation to bind with substrate molecule [36].

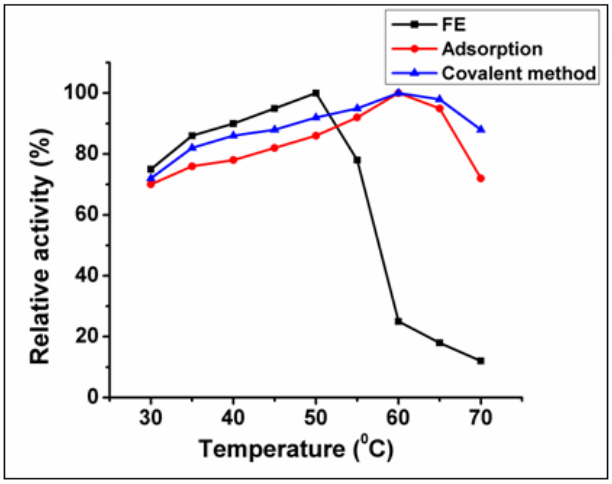

Figure: 5.25 Effect of temperature on the relative activity of immobilized α-amylase by adsorption and covalent methods

5.4.1.4 Activation energy

The activation energy (Ea) required for covalently immobilized enzyme was compared to that of immobilized enzyme by adsorption method. The Arrhenius plot is given in the figure 5.26 and the calculated values are presented in the table 5.8.

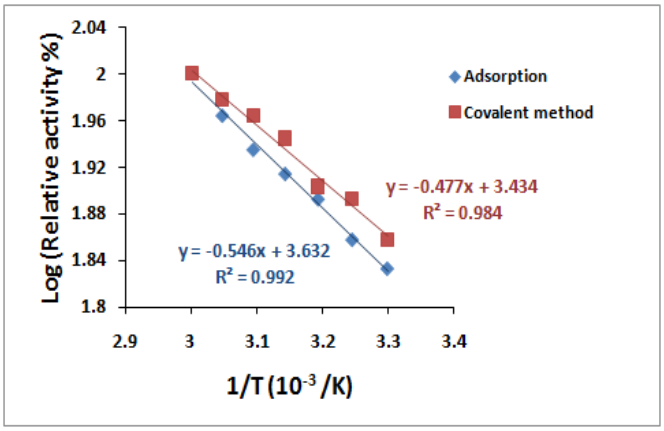

Figure: 5.26 Arrhenius plot to calculate the activation energy (Ea) of immobilized α-amylase by adsorption and covalent methods

Here we noticed that the immobilized enzyme by covalent method attained lower activation energy than that by adsorption method. This lower Ea value of covalently immobilized enzyme indicated its higher catalytic efficiency and this could be due to its increased diffusional resistance towards substrate molecules in the catalytic reaction [37]. This controlled diffusion kept the enzyme not more saturated and so the threshold energy for the activated complex of the enzymatic reaction decreased. The rate of the diffusion controlled reaction showed less sensitivity towards temperature than catalytic activity [38].

Table 5.8 Activation energy of immobilized α-amylase on CSM-PAMAM G2 by adsorption and covalent methods

Immobilized enzyme	Activation energy ($KJ\ mol^{-1}$)
Adsorption	4.54
Covalent method	3.96

5.4.1.5 Thermal stability of the free and immobilized enzymes

Thermal stability of immobilized enzyme by covalent method was investigated and compared with that of free and adsorbed ones. The

experiment was carried out by incubating the enzyme system in buffer at 30 -70 °C in the absence of substrate for 1 h and then the enzymatic reaction was performed with starch substrate.

The figure 5.27 showed that the free enzyme exhibited sudden loss in activity at higher temperatures while the immobilized enzyme by adsorption and covalent method retained higher activities. At 70 °C the immobilized enzyme by adsorption and covalent method attained relative activities of 83 % and 90 % respectively. The higher activity of covalently immobilized enzyme might be due to conformational integrity of the enzyme structure by covalent attachment with the support. The increased stability may arise from stable three dimensional structure of enzyme that established as a result of higher rigidity of the enzyme by covalent binding and hence the conformational changes in enzyme structure from the environment can be neglected by preserving its three dimensional structure.

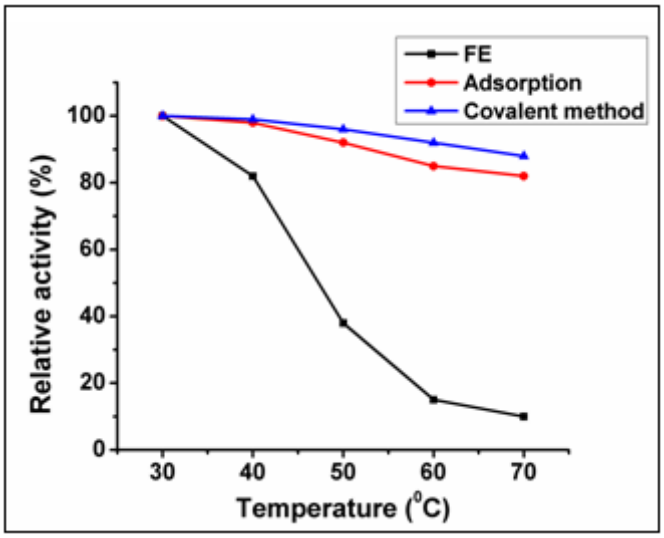

Figure: 5.27 Thermal stability of free and immobilized α-amylase on CSM-PAMAM G2 by adsorption and covalent methods

The thermal stability of immobilized enzymes was again examined by subjecting them to pre-incubation up to 150 min. at their optimum temperatures. The enzyme activity measured at regular intervals of time and the results are shown in the figure 5.28.

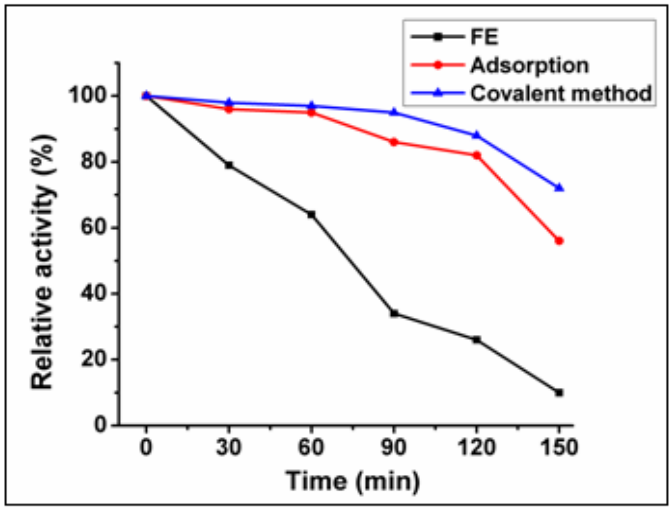

Figure: 5.28 Variation of pre-incubation time on activity of free and immobilized α-amylase on CSM-PAMAM G2 by adsorption and covalent methods

The covalently immobilized enzyme has shown highest stability when compared to free and adsorbed ones. After 150 min. of pre-incubation the free and adsorbed enzyme retained 10 % and 56 % of activity, whereas the immobilized enzyme by covalent method exhibited 72 % of activity. The increased rigidity that attained by covalent immobilization has imparted higher stability to the enzyme and enhanced the resistance towards protein unfolding at higher temperatures. The high thermal stability of immobilized enzyme was also reported by Omprakash et al. when lipase immobilized on poly (phenylene sulfide) dendrimers by covalent method in which the covalent bonded PPS dendrimer preserved the tertiary structure of enzyme from thermal denaturation [24].

5.4.1.6 Determination of kinetic parameters

The Lineweaver-Burk plots and Hanes-Woolf plots for CSM-PAMAM G2E by adsorption and covalent method are depicted in the figure 5.29 and the kinetic parameters compared with that of free enzyme are presented in the table 5.9.

Table 5.9 Kinetic parameters for free and immobilized α-amylase on CSM-PAMAM G2 by adsorption and covalent methods

Immobilized enzyme	K_m (mg mL^{-1})	V_{max} (μmol mg^{-1} min^{-1})	K_{cat} (min^{-1})	K_{cat}/K_m ($mlmg^{-1}min^{-1}$)
Free enzyme	0.45± 0.02	34.48±0.05	1910.19	4244.87
CSM-PAMAM G2 E (Adsorption)	0.53± 0.04	23.25± 0.04	1288.05	2430.28
CSM-PAMAM G2 E (Covalent)	0.85±0.03	16.67± 0.02	923.52	1086.49

The K_m value for covalently immobilized enzyme is found to be higher than that of free and adsorbed enzymes which can be due to its lower affinity towards substrate molecule in the enzymatic reaction. The rigidity attained by the covalently immobilized enzyme leads to the reduction in conformational flexibility of the enzyme structure and hence caused the lower accessibility of the enzyme active site to substrate. The decreased V_{max} value for covalently immobilized enzyme could be as a result of lesser tendency of substrate molecule to approach into the active site of the enzyme structure which may arise from the unfavorable conformational changes of active site by covalent immobilization [39]. The similar trend was observed by Aparna Kumari et al. in case of immobilized soybean α-amylase on chitosan and amberlite MB-150 beads [40].

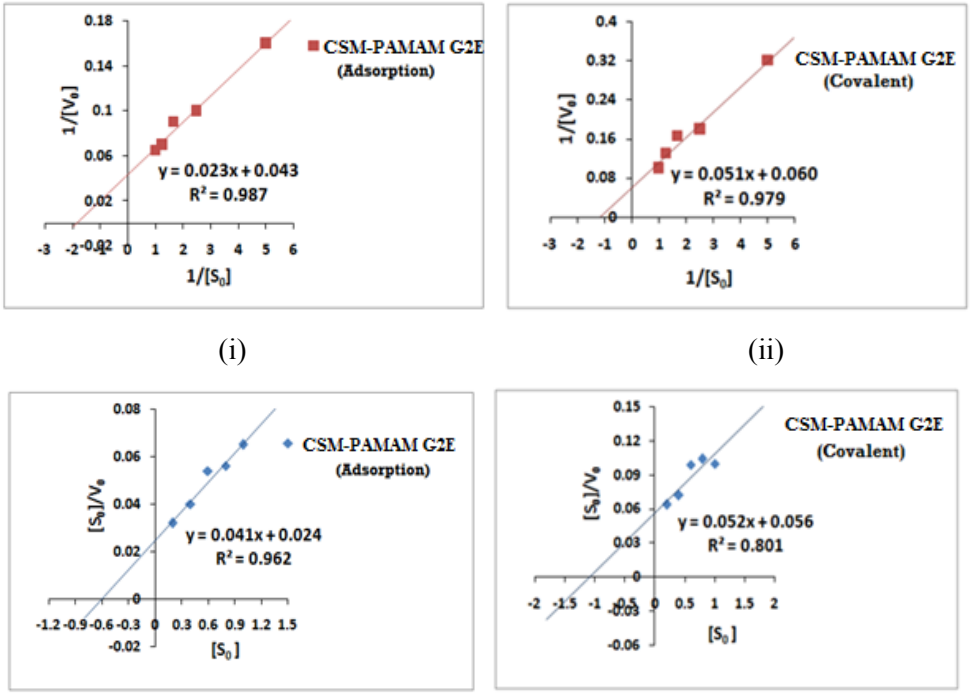

Figure: 5.29 Lineweaver-Burk plots for CSM-PAMAM G2E by (i) adsorption method (ii) covalent method and Hanes-Woolf plots for CSM-PAMAM G2E by (iii) adsorption method (iv) covalent method.

The K_{cat} and K_{cat}/K_m values were evaluated for covalently immobilized enzyme by using the kinetic parameters. Its K_{cat} value was 51.65 % and 28.30 % lesser than that of free and adsorbed enzymes respectively. It has shown decreased catalytic efficiency when compared to free and adsorbed enzymes which was 74.40 % lesser than that of free enzyme and 55.29 % lesser than that of adsorbed enzyme.

5.4.1.7 Storage stability of immobilized α-amylase by adsorption and covalent methods

The storage stability of covalently immobilized α-amylase was compared with that of adsorbed one. The figure 5.30 exhibited the relative activities of immobilized enzymes up to six months of storage. The immobilized enzyme by covalent method retained 62 % of its initial activity at the end of six months of period, while for immobilized enzyme by adsorption method it was only about 52 %. The strong covalent binding between the enzyme and support provided higher conformational stability to the immobilized enzyme and hence increased enzyme activity on comparison with adsorbed enzyme. Seyyedeh et al. reported that covalently immobilized α-amylase on chitosan coated amine functionalized silica-magnetite nanoparticles preserved 78.63 % of activity after 80 days of storage time [41].

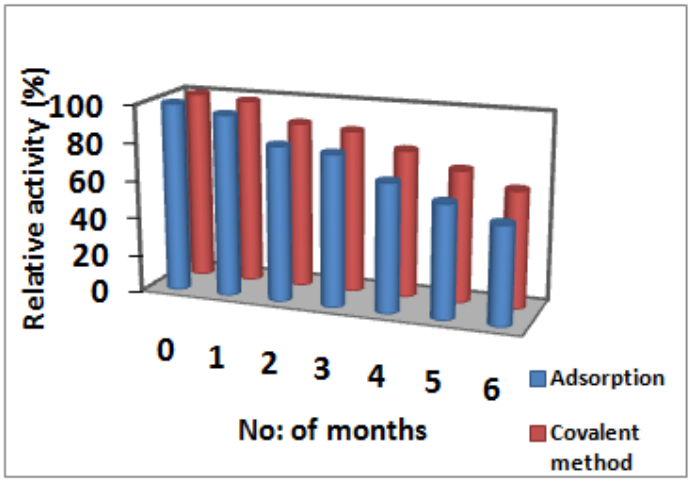

Figure: 5.30 Storage stability of immobilized α-amylase on CSM-PAMAM G2 by adsorption and covalent methods

5.4.1.8 Reusability

The reusability of covalently immobilized enzyme was investigated throughout ten consecutive cycles and figure 5.31 showed the comparison of reusability of covalently immobilized enzyme with adsorbed one. After three successive runs, the adsorbed and covalently immobilized enzymes retained 81 % and 90 % of their activity respectively. At the end of tenth cycles it was about 46 % and 72 %. The higher activity attained by the immobilized enzyme by covalent method might be due to strong binding of enzyme on to the carrier. This strong covalent bond can prevent the enzyme leakage to some extend which caused as a result of successive runs. Shujun Fang et al. observed that the immobilized α-amylase on cross-linked chitosan and chitosan-carbon beads showed about 60 % of activity after ten cycles of reuses [42].

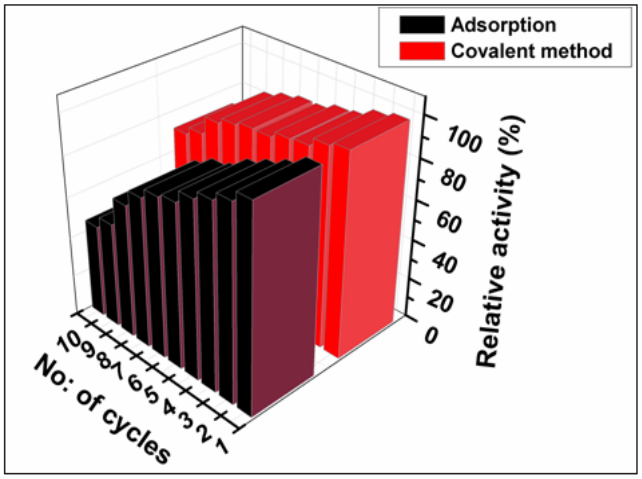

Figure: 5.31 Reusability of immobilized α-amylase on CSM-PAMAM G2 by adsorption and covalent methods

5.5 Conclusion

Surface dendrimerization of magnetic chitosan was successfully conducted in order to obtain the modified forms CSM-PAMAM G1, CSM-PAMAM G1' and CSM-PAMAM G2. These dendritic polymers constitute the new type of carriers for the immobilization of α- amylase and the binding capacity of the enzyme was found to be more with CSM-PAMAM G2. The immobilized enzymes have shown high pH and temperature tolerance compared to their free counterpart and the magnetic separation provided the efficient means of their recovery. The kinetic study revealed that CSM-PAMAM G2E has retained more affinity and activity since the km and Vmax values were only slightly different from that of the free enzyme. As the covalent immobilization provided high rigidity to the enzyme by stabilizing its three dimensional structure, the tendency for denaturation reduced much more and thereby attained improved stability and life time.

References

[1] D.A. Tomalia, J.M. Frechet, Discovery of dendrimers and dendritic polymers: a brief historical perspective, Journal of Polymer Science Part A: Polymer Chemistry 40(16) (2002) 2719-2728.

[2] G.R. Newkome, Z. Yao, G.R. Baker, V.K. Gupta, Micelles. Part 1. Cascade molecules: a new approach to micelles. A [27]-arborol, The Journal of Organic Chemistry 50(11) (1985) 2003-2004.

[3] C.J. Hawker, J.M. Frechet, Preparation of polymers with controlled molecular architecture. A new convergent approach to dendritic macromolecules, Journal of the American Chemical Society 112(21) (1990) 7638-7647.

[4] A.D. Schluter, J.P. Rabe, Dendronized polymers: synthesis, characterization, assembly at interfaces, and manipulation, Angewandte Chemie International Edition 39(5) (2000) 864-883.

[5] F.N. Crespilho, M.E. Ghica, M. Florescu, F.C. Nart, O.N. Oliveira Jr, C.M. Brett, A strategy for enzyme immobilization on layer-by-layer dendrimer–gold nanoparticle electrocatalytic membrane incorporating redox mediator, Electrochemistry Communications 8(10) (2006) 1665-1670.

[6] M. Bagheri, H. Rodríguez, R.P. Swatloski, S.K. Spear, D.T. Daly, R.D. Rogers, Ionic liquid-based preparation of cellulose−dendrimer films as solid supports for enzyme immobilization, Biomacromolecules 9(1) (2007) 381-387.

[7] D.A. Tomalia, H. Baker, J. Dewald, M. Hall, G. Kallos, S. Martin, J. Roeck, J. Ryder, P. Smith, Dendritic macromolecules: synthesis of starburst dendrimers, Macromolecules 19(9) (1986) 2466-2468.

[8] D.A. Tomalia, Birth of a new macromolecular architecture: dendrimers as quantized building blocks for nanoscale synthetic polymer chemistry, Progress in Polymer Science 30(3-4) (2005) 294-324.

[9] Q. Chen, S. Ai, X. Zhu, H. Yin, Q. Ma, Y. Qiu, A nitrite biosensor based on the immobilization of Cytochrome c on multi-walled carbon nanotubes–PAMAM–chitosan nanocomposite modified glass carbon electrode, Biosensors and Bioelectronics 24(10) (2009) 2991-2996.

[10] O. Yemul, T. Imae, Covalent-bonded immobilization of lipase on poly (phenylene sulfide) dendrimers and their hydrolysis ability, Biomacromolecules 6(5) (2005) 2809-2814.

[11] A. Mustranta, P. Forssell, K. Poutanen, Applications of immobilized lipases to transesterification and esterification reactions in nonaqueous systems, Enzyme and microbial technology 15(2) (1993) 133-139.

[12] Y. Kimura, A. Tanaka, K. Sonomoto, T. Nihira, S. Fukui, Application of immobilized lipase to hydrolysis of triacylglyceride, European Journal Of Applied Microbiology And Biotechnology 17(2) (1983) 107-112.

[13] W. Zhu, Y. Zhang, C. Hou, D. Pan, J. He, H. Zhu, Covalent immobilization of lipases on monodisperse magnetic microspheres modified with PAMAM-dendrimer, Journal of Nanoparticle Research 18(2) (2016) 32.

[14] F.P. Cardoso, S.A. Neto, P. Ciancaglini, A.R. de Andrade, The use of PAMAM dendrimers as a platform for laccase immobilization: kinetic characterization of the enzyme, Applied Biochemistry and Biotechnology 167(7) (2012) 1854-1864.

[15] S. Wang, P. Su, F. Ding, Y. Yang, Immobilization of cellulase on polyamidoamine dendrimer-grafted silica, Journal of Molecular Catalysis B: Enzymatic 89 (2013) 35-40.

[16] A. Pfaff, A.H. Mu¨ ller, Hyperbranched glycopolymer grafted microspheres, Macromolecules 44(6) (2011) 1266-1272.

[17] A. Kunzmann, B. Andersson, T. Thurnherr, H. Krug, A. Scheynius, B. Fadeel, Toxicology of engineered nanomaterials: focus on biocompatibility, biodistribution and biodegradation, Biochimica et Biophysica Acta (BBA)-General Subjects 1810(3) (2011) 361-373.

[18] S.C.W. Sakti, Development of magnetic separation using modified magnetic chitosan for removal of pollutants in solution, (2015).

[19] Z. Zarghami, A. Akbari, A.M. Latifi, M.A. Amani, Design of a new integrated chitosan-PAMAM dendrimer biosorbent for heavy metals removing and study of its adsorption kinetics and thermodynamics, Bioresource technology 205 (2016) 230-238.

[20] J. Zawadzki, H. Kaczmarek, Thermal treatment of chitosan in various conditions, Carbohydrate Polymers 80(2) (2010) 394-400.

[21] D.A. Tomalia, H. Baker, J. Dewald, M. Hall, G. Kallos, S. Martin, J. Roeck, J. Ryder, P. Smith, A new class of polymers: starburst-dendritic macromolecules, Polymer Journal 17(1) (1985) 117.

[22] C. Hou, H. Zhu, D. Wu, Y. Li, K. Hou, Y. Jiang, Y. Li, Immobilized lipase on macroporous polystyrene modified by PAMAM-dendrimer and their enzymatic hydrolysis, Process Biochemistry 49(2) (2014) 244-249.

[23] P. Su, S. Wang, Y. Shi, Y. Yang, Application of cellulase-polyamidoamine dendrimer-modified silica for microwave-assisted chitosan enzymolysis, Process Biochemistry 48(4) (2013) 614-619.

[24] O. Yemul, T. Imae, Covalent-bonded immobilization of lipase on poly(phenylene sulfide) dendrimers and their hydrolysis ability, Biomacromolecules 6(5) (2005) 2809-2814.

[25] A.A. Mendes, H.F. de Castro, D.S. Rodrigues, W.S. Adriano, P.W. Tardioli, E.J. Mammarella, R.C. Giordano, R.L. Giordano, Multipoint covalent immobilization of lipase on chitosan hybrid hydrogels: influence of the polyelectrolyte complex type and chemical modification on the catalytic properties of the biocatalysts, Journal of Industrial Microbiology & Biotechnology 38(8) (2011) 1055-1066.

[26] M.A. Abdel-Naby, A.S. Ismail, S. Ahmed, A.F.A. Fattah, Production and immobilization of alkaline protease from Bacillus mycoides, Bioresource Technology 64(3) (1998) 205-210.

[27] M.A. Esawy, A.A. Gamal, Z. Kamel, A.M. Ismail, A.F. Abdel-Fattah, Evaluation of free and immobilized Aspergillus niger NRC1ami pectinase applicable in industrial processes, Carbohydrate Polymers 92(2) (2013) 1463-1469.

[28] H. Lineweaver, D. Burk, The determination of enzyme dissociation constants, Journal of the American Chemical Society 56(3) (1934) 658-666.

[29] S.A. Neto, J.C. Forti, V. Zucolotto, P. Ciancaglini, A.R. De Andrade, The kinetic behavior of dehydrogenase enzymes in solution and immobilized onto nanostructured carbon platforms, Process Biochemistry 46(12) (2011) 2347-2352.

[30] K. Uzun, E. Cevik, M. Senel, H. Sozeri, A. Baykal, M. Abasiyanik, M. Toprak, Covalent immobilization of invertase on PAMAM-dendrimer modified superparamagnetic iron oxide nanoparticles, Journal of Nanoparticle Research 12(8) (2010) 3057-3067.

[31] Y. Yong, Y.X. Bai, Y.F. Li, L. Lin, Y.J. Cui, C.G. Xia, Characterization of Candida rugosa lipase immobilized onto magnetic microspheres with hydrophilicity, Process Biochemistry 43(11) (2008) 1179-1185.

[32] O.H. Lowry, N.J. Rosebrough, A.L. Farr, R.J. Randall, Protein measurement with the folin phenol reagent, Journal of Biological Chemistry 193(1) (1951) 265-275.

[33] S. Shukla, L. Jajpura, Immobilisation of amylase by various techniques, Indian Journal of Fibre & Textile Research 30 (2005) 75-81.

[34] Y. Fan, G. Wu, F. Su, K.a. Li, L.i. Xu, X. Han, Y. Yan, Lipase oriented-immobilized on dendrimer-coated magnetic multi-walled carbon nanotubes toward catalyzing biodiesel production from waste vegetable oil, Fuel 178 (2016) 172-178.

[35] P.S. Borkar, Purification and immobilization of thermostable serine alkaline protease from Bacillus subtilis, The Pharma Innovation Journal 7(5) (2018) 622-626.

[36] K. Uzun, E. Cevik, M. Senel, H. Sozeri, A. Baykal, M. Abasiyanik, M. Toprak, Covalent immobilization of invertase on PAMAM-dendrimer modified superparamagnetic iron oxide nanoparticles, Journal of Nanoparticle Research 12(8) (2010) 3057-3067.

[37] J.M. Engasser, C. Horvath, Diffusion and kinetics with immobilized enzymes, Applied Biochemistry and Bioengineering, 1 (1976) 127-220.

[38] V. Bille, D. Plainchamp, J. Remacle, Affinity and stability modifications of immobilized alcohol dehydrogenase through multipoint copolymerization, Biochimica et Biophysica Acta 915(3) (1987) 393-398.

[39] A.M. Klibanov, Enzyme stabilization by immobilization, Analytical Biochemistry 93 (1979) 1-25.

[40] A. Kumari, A.M. Kayastha, Immobilization of soybean (Glycine max) α-amylase onto Chitosan and Amberlite MB-150 beads: optimization and characterization, Journal of Molecular Catalysis B: Enzymatic 69(1-2) (2011) 8-14.

[41] S.L. Hosseinipour, M.S. Khiabani, H. Hamishehkar, R. Salehi, Enhanced stability and catalytic activity of immobilized α-amylase on modified Fe_3O_4 nanoparticles for potential application in food industries, Journal of Nanoparticle Research 17(9) (2015) 382.

[42] S. Fang, J. Chang, Y.S. Lee, E.J. Hwang, J.B. Heo, Y.L. Choi, Immobilization of α-amylase from Exiguobacterium sp. DAU5 on chitosan and chitosan-carbon bead: Its Properties, Journal of Applied Biological Chemistry 59(1) (2016) 75-81.

Chapter 6

Kinetics and thermodynamics of thermal deactivation of immobilized α-amylase on modified magnetic chitosan

Contents

6.1 Introduction

Thermal stability of the enzyme is one of the major requirements for its employment in industrial applications. The major problem that facing the use of industrial enzymes was the occurrence of thermal deactivation processes under high temperature conditions. The production of thermostable enzymes has become very important as the resistance to thermal deactivation stand for very important for their application in commercial levels. Many researchers focused on the enhancement in thermal stability of α-amylase since Madsen and Saito et al. reported its isolation and distinctive properties [1, 2].

The thermal deactivation process leads to the conformational changes in the protein structure without breaking the covalent bonds [3-5] and these conformational structural changes could adversely affect their specific activity. So understanding of deactivation kinetics and thermodynamic parameters is very necessary for analyzing enzyme stability in order to make it viable for biotechnological processes [6, 7]. The awareness about enzyme

stability encourages the economical growth of industrial enzymes by the prolonged enzymatic processes. The stability of enzyme mainly described about kinetic and thermodynamic stability; in which the former determines the resistance to thermal deactivation and indicated as half life of enzyme ($t_{1/2}$), while the later measures the changes in Gibbs free energy (ΔG^o) between free form and deactivated form of enzyme and the other thermodynamic parameters, change in enthalpy (ΔH^o) and change in entropy (ΔS^o) can be determined from the value of ΔG^o. Assessment of these thermodynamic parameters gives certain clarifications about the enzyme action towards specific substrate molecule. The efficacy of transition state can be explained by ΔH^o value, but ΔS^o value denoted the stability of transition state and thus indicated enzyme-substrate affinity. The ΔG^o value measures the feasibility of enzymatic reaction [8]. Thermodynamic parameters of deactivation study provide the information about the structure of enzyme and also impart the plausible mechanism of deactivation process.

Several studies were reported on the determination of kinetic and thermodynamic parameters of thermal deactivation of free and immobilized enzymes. The higher catalytic efficiency of xylanase was observed by Dorra Driss et al. when immobilized on nickel-chelate Eupergit C, where $t_{1/2}$ of immobilized enzyme was higher than that of free enzyme [9]. The higher kinetic parameters, $t_{1/2}$ and D-values (decimal reduction time) and increased thermodynamic parameters, ΔH^o and ΔG^o were reported by Karam et al. for immobilized *Aspergillus awamori* amylase on Ca^{+2} alginate starch/polyethyleneimine /glutaraldehyde [10]. Here the more negative value of ΔS^o indicated the more ordered state of immobilized enzyme. Ajay Pal et al. observed the thermal deactivation of sorbitol treated xylanase from *A. niger* DFR-5 between 45-70 ºC and expressed as first order kinetics [11].

They observed the thermostabilizing nature of sorbitol as the deactivation rate constant (k_d) decreased in the presence of sorbitol. The increase in $t_{1/2}$ and D-value of sorbitol treated xylanase further confirmed the emergence of thermostable enzyme.

The present chapter deals with the thermal deactivation study on free and immobilized α-amylase on magnetic chitosan and its modified forms at temperature ranges between 50-70 ºC. This includes evaluation of kinetic parameters, $t_{1/2}$, D-value, E_d and z-value for thermal deactivation of free and immobilized enzymes at 50-70 ºC. The estimation of thermodynamic parameters, ΔHº, ΔGº and ΔSº are also embodied in this chapter.

6.2 Materials and methods

6.2.1 Materials

The details of materials used for the preparation of immobilized α-amylase on magnetic chitosan and its modified forms and for enzyme activity assay were given in the earlier chapters.

6.2.2 Thermal deactivation study

The stability of immobilized enzymes was evaluated by conducting thermal deactivation study at different temperatures ranging 50-70 ºC. In this study all the immobilized enzymes in desired buffer taken in test tubes were pre-incubated in a temperature controlled shaking water bath at temperatures which mentioned above by varying the time periods up to $2\frac{1}{2}$ h. Here after each 30 min. intervals of incubation period, aliquots of samples were withdrawn and assayed for residual enzyme activity by DNS method at corresponding optimum temperature. The enzyme activity at 0 min. incubation was taken as 100 % and for subsequent time periods the

activities were taken as relative to this value. The data obtained from the thermal deactivation profile were used to analyze kinetic and thermodynamic parameters related to the α-amylase activity [11].

6.2.2.1 Estimation of kinetic parameters for thermal deactivation of immobilized enzymes

Thermal deactivation study gives the stability profile for each immobilized enzymes in which residual activity expressed in terms of percent of initial enzyme activity for definite time intervals of pre-incubation period. The plots of log relative activities against time were first order kinetics and the deactivation rate constant (k_d) can be calculated from the slope of this plot [12].

The temperature dependence of k_d was described by Arrhenius plot and the deactivation energy (E_d) obtained from the Arrhenius equation,

$$\ln K_d = \ln K_0 - E_d / R(1/T) \qquad (1)$$

Where K_0 is the Arrhenius constant, R the universal gas constant *(R = 8.314 J mol^{-1} K^{-1})*

Slope of the plot gives the E_d which is drawn between ln kd and reciprocal of temperature, 1/T (K) by the equation,

$$Slope = -\frac{E_d}{R} \qquad (2)$$

The apparent half-lives of immobilized enzymes, $t_{1/2}$ the time needed to reach 50 % of residual activity can be derived from the equation,

$$t_{1/2} = \ln(2) / k_d \qquad (3)$$

The D-values represent the decimal reduction time; the pre-incubation time required for the enzyme to preserve 10 % of residual activity and was calculated by the equation,

$$D = \ln(10) / k_d \qquad (4)$$

The temperature sensitivity parameter, z-value is the temperature required to reduce D-value by one logarithmic cycle and calculated from the slope of plot between log D versus T (°C) by,

$$Slope = -\frac{1}{z} \qquad (5)$$

These kd, E_d, $t_{1/2}$, D-values and z-values stand for the kinetic parameters for thermal deactivation of enzyme [9, 13].

6.2.2.2 Estimation of thermodynamic parameters for thermal deactivation of immobilized enzymes

Thermal stability of free and immobilized enzymes was described by the deactivation rate constant, K_d as a function of temperature and the deactivation energy, E_d [3]. These values are used to estimate thermodynamic parameters such as the change in enthalpy (ΔH^o, kJ mol^{-1}), free energy (ΔG^o, kJ mol^{-1}) and entropy (ΔS^o, J mol^{-1} K^{-1}) for thermal deactivation of enzyme by the following equations,

$$\Delta H^\circ = E_d - RT \qquad (6)$$

$$\Delta G^\circ = -RT \ln \frac{kd.h}{k_B.T} \qquad (7)$$

$$\Delta S^\circ = \frac{\Delta H^\circ - \Delta G^\circ}{T} \qquad (8)$$

Here, k_B is the Boltzman constant (1.38 x10^{-23} J K^{-1}) and h is the Planck constant (11.04x10^{-36} J min)

6.3 Results and discussion

6.3.1 Thermal deactivation of immobilized enzymes

Thermal stability of the enzyme infers the capacity of the enzyme to resist thermal denaturation as a result of its unfolding in the absence of substrate molecules [14]. The immobilization provides increased stability to the enzyme at higher temperatures as it imparts enzyme rigidity and so protects the enzyme from thermal deactivation. The stability of the enzyme at higher temperatures indicates its applicability in industrial sectors.

The thermal deactivation rates of immobilized enzymes were investigated at temperatures range between 50-70 ºC and compared with that of free enzyme. The linear plots of log relative activities against time were illustrated in the figures given below, indicating the first order kinetics of thermal deactivation of enzyme.

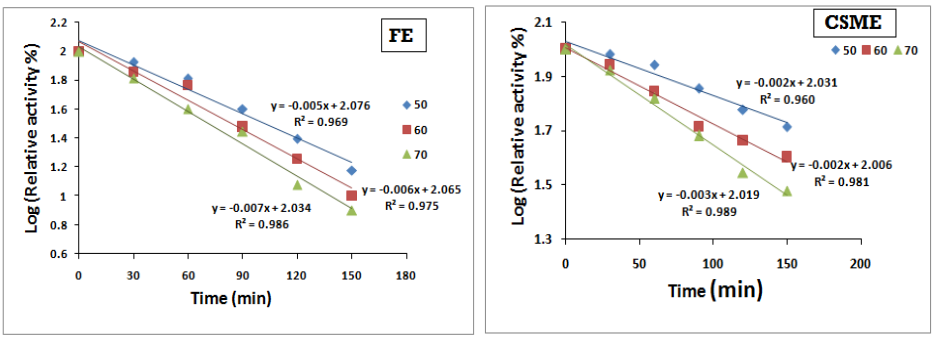

(i) (ii)

Figure 6.1 First order thermal deactivation of (i) free enzyme and (ii) CSME

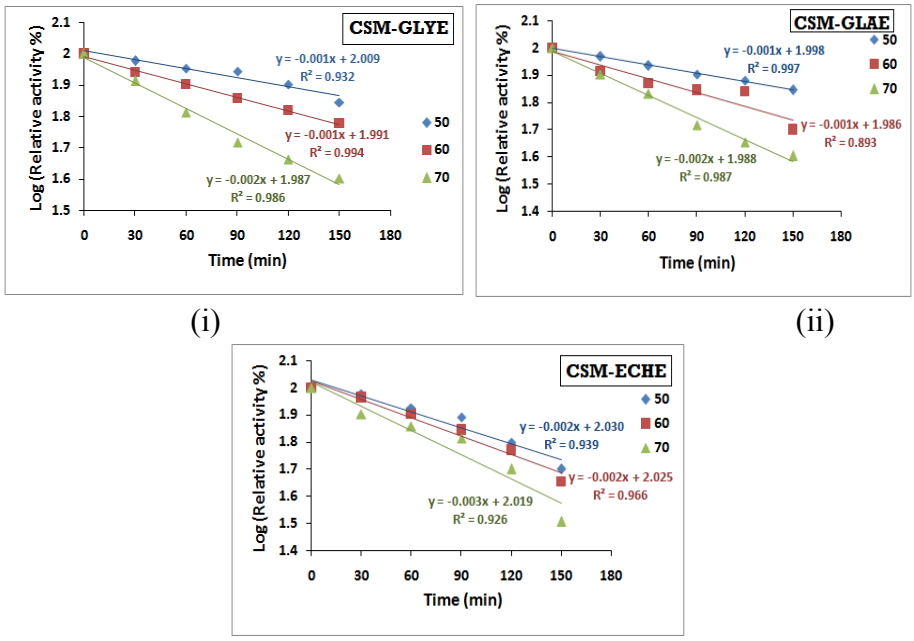

Figure 6.2 First order thermal deactivation of (i) CSM-GLYE (ii) CSM-GLAE and (iii) CSM-ECHE

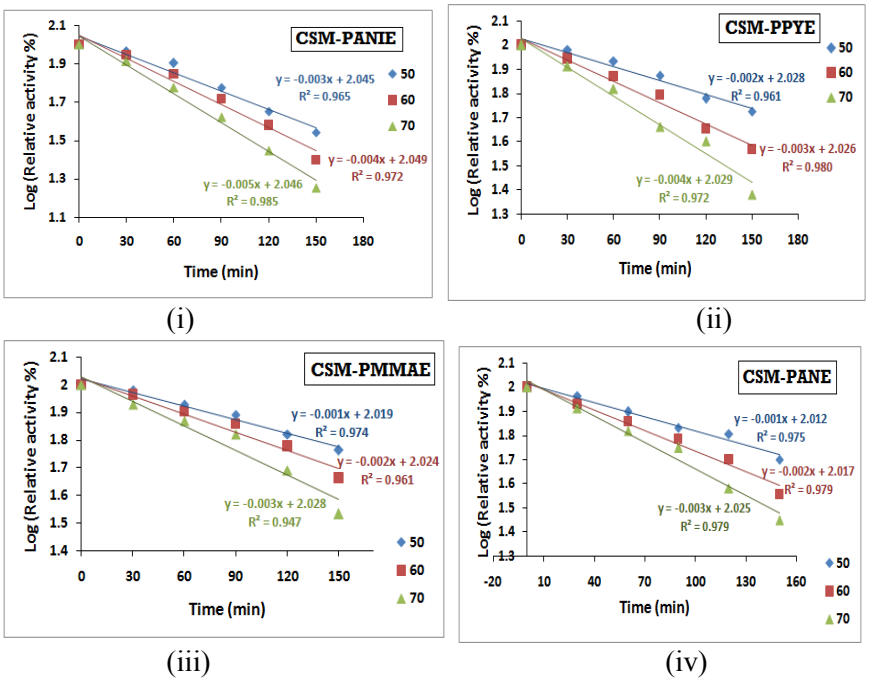

Figure 6.3 First order thermal deactivation of (i) CSM-PANIE (ii) CSM-PPYE (iii) CSM- PMMAE and (iv) CSM-PANE

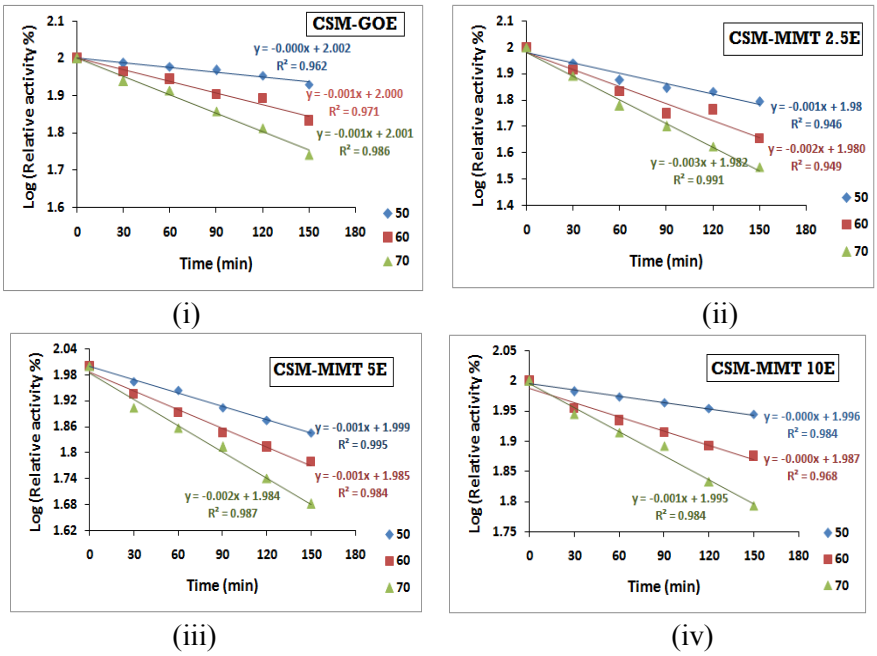

Figure 6.4 First order thermal deactivation of (i) CSM-GOE (ii) CSM-MMT 2.5E (iii) CSM-MMT 5E and (iv) CSM-MMT 10E

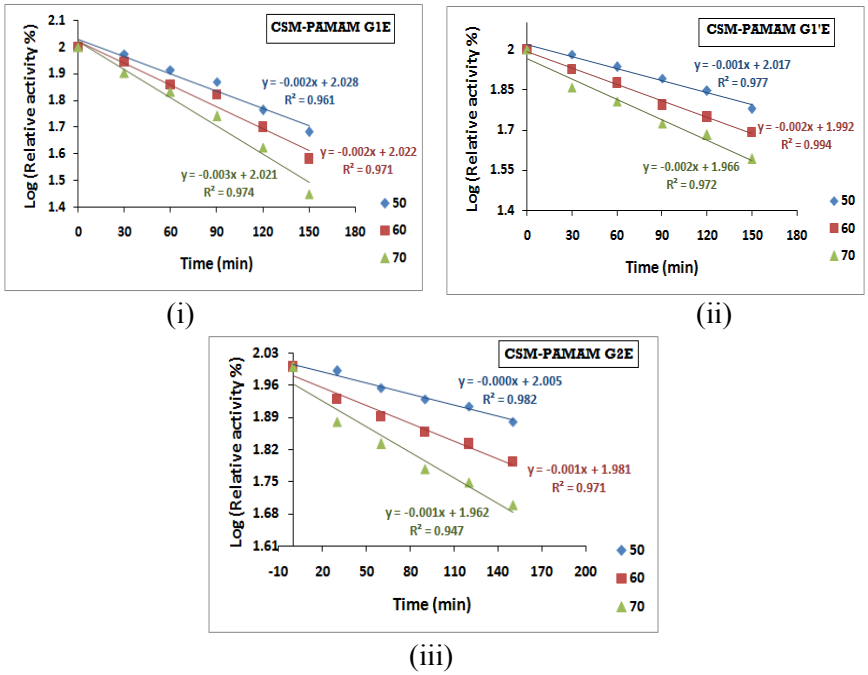

Figure 6.5 First order thermal deactivation of (i) CSM-PAMAM G1E (ii) CSM-PAMAMG1'E and (iii) CSM-PAMAM G2E

6.3.2 Estimation of kinetic parameters for thermal deactivation of immobilized enzymes

The deactivation energy, E_d for thermal denaturation process was calculated from the Arrhenius plot drawn between ln kd and reciprocal of temperature shown in the figures 6.6 to 6.10 and the values are presented in the tables 6.1 to 6.4.

The E_d values for all immobilized enzymes were found to be higher in comparison to free enzyme which indicates their high stability. An immobilized enzyme with high E_d value confirmed that it require more energy for denaturation by heat [15]. As a result of immobilization the enzyme has become compact, more rigid and highly resistant to thermal denaturation. The similar trend was also observed by Mateo et al. for lipase immobilization on hydrophobic supports [16].

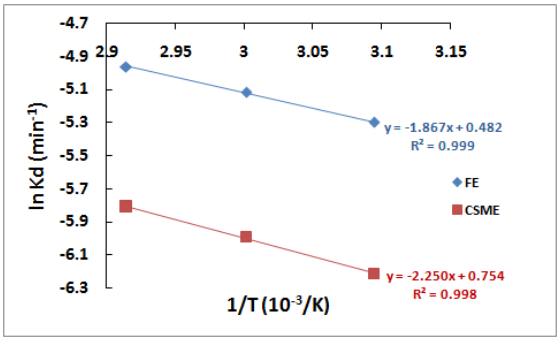

Figure 6.6 Arrhenius plot to calculate deactivation energy (E_d) of free enzyme and CSME

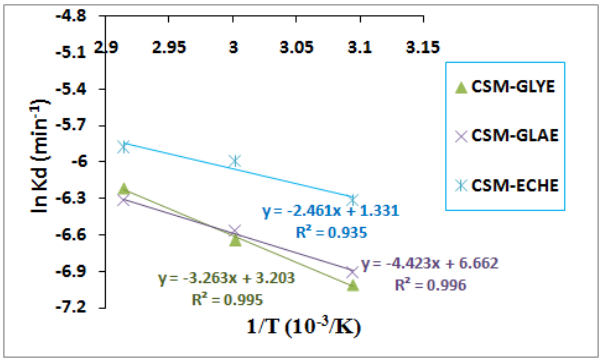

Figure 6.7 Arrhenius plot to calculate deactivation energy (E_d) of CSM-GLYE, CSM-GLAE and CSM-ECHE

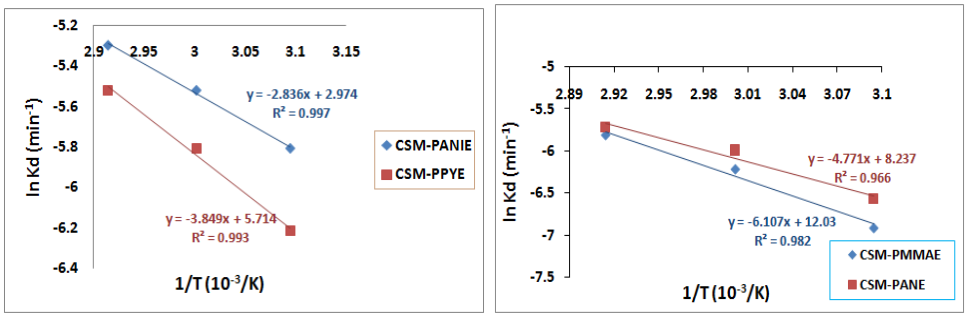

(i) (ii)

Figure 6.8 Arrhenius plot to calculate deactivation energy (E_d) of (i) CSM-PANIE and CSM- PPYE (ii) CSM-PMMAE and CSM-PANE

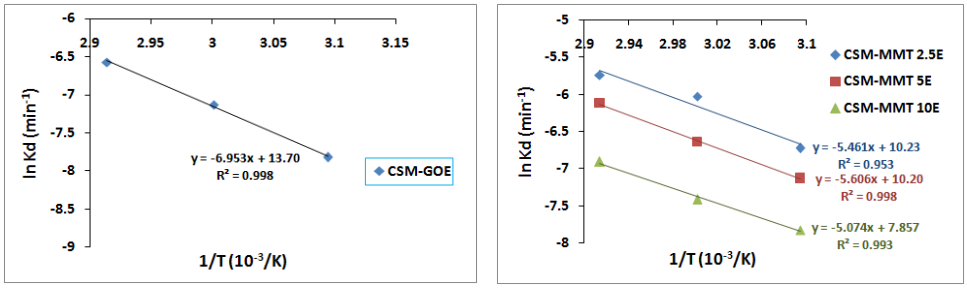

(i) (ii)

Figure 6.9 Arrhenius plot to calculate deactivation energy (E_d) of (i) CSM-GOE (ii) CSM-MMT 2.5E, CSM-MMT 5E and CSM-MMT 10E

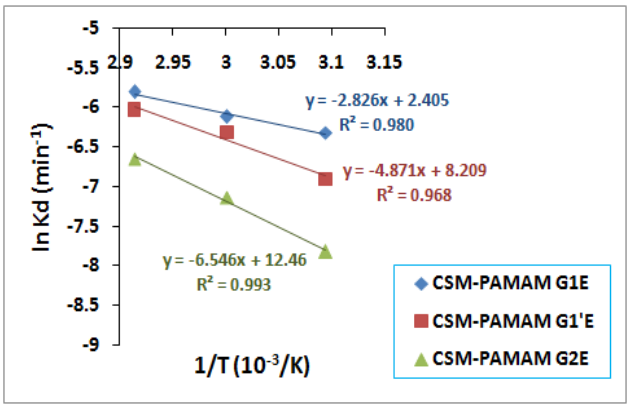

Figure 6.10 Arrhenius plot to calculate deactivation energy (E_d) of CSM-PAMAM G1E, CSM-PAMAM G1'E and CSM-PAMAM G2E

The E_d value for free α-amylase was calculated as 15.52 KJ mol^{-1} and that of CSME was 18.71 KJ mol^{-1} which confirmed the increase of thermal stability of α-amylase upon immobilization with magnetic chitosan. The modified forms of magnetic chitosan have also provided high stability to the enzyme as their immobilized forms exhibited higher E_d values. Among the modified forms of magnetic chitosan with cross-linking agents, CSM-GLYE has shown higher deactivation energy of 36.77 KJ mol^{-1} than CSM-GLAE (27.12 KJ mol^{-1}) and CSM-ECHE (20.46 KJ mol^{-1}). In case of modified forms of CSM with synthetic polymers, the higher E_d value of 50.77 KJ mol^{-1} was shown by CSM-PMMAE and this indicated its higher stability compared to the immobilized enzymes by other synthetic polymers. The layered solids modified magnetic chitosan on α-amylase immobilization have shown high E_d values compared to free enzyme and out of this CSM-GOE exhibited highest value of 57.81 KJ mol^{-1}. In case of α-amylase immobilized on PAMAM modified magnetic chitosan, CSM-PAMAM G2E has attained better energy for thermal deactivation (54.42 KJ mol^{-1}) compared to the other PAMAM modified forms.

The free α-amylase showed a $t_{1/2}$ of 138.63 min. at 50 ºC and it was found that with the increase of temperature the $t_{1/2}$ of enzyme decreased to lower value and reached to 99.02 min. at 70 ºC. Similar trend was observed in case of all the immobilized enzymes and this indicated the decrease of enzyme stability at higher temperatures. However, immobilized enzymes have shown increase in half-life at all temperature ranges confirmed the enhanced thermal stability of enzyme as a result of immobilization. Yagar et al. reported high stability of immobilized α-amylase by *Aspergillus sclerotiorum* in calcium alginate gel beads in terms of their half-lives at different temperatures [17]. The time needed for the enzyme to preserve 10 % of residual activity, D-value found to be higher in case of all immobilized enzymes than that of free enzyme and this further confirmed the protecting effect of magnetic chitosan and its modified forms on α-amylase. The immobilization process protect the enzyme significantly against thermal deactivation [18].

The temperature needed to reduce the D-value by one logarithmic cycle (z-value), of free and immobilized enzymes were calculated from the plot drawn between log D and temperature, shown in the figures 6.11 to 6.15. The inverse of the slope of plot gives the z-value and the tables 6.1 to 6.4 showed that all the immobilized enzymes have attained lower z-values compared to the free enzyme. The free enzyme gained high z-value of 142.86 °C and that of CSME calculated as 125 °C. The enzyme on modified forms of magnetic chitosan showed lower z-values. In case of magnetic chitosan modified with cross-linking agents, CSM-GLYE has shown lowest value of 58.82 °C compared to other cross-linked forms and CSM-PMMAE exhibited smallest value of 43.48 °C among polymer modified forms of CSM. For CSM with inorganic layered solids, CSM-GOE has given lowest

z-value of 37.04 °C and CSM-PAMAM G2E showed the value of 40 °C which was lowest among PAMAM modified forms of CSM.

The z-value with high magnitude indicates more sensitivity to the duration of thermal treatment and lower magnitude stands for more sensitivity to rise in temperature [11]. Hence all the immobilized enzymes with lower z-value compared to free enzyme showed that the magnetic chitosan and its modified forms keep the enzyme more sensitivity to rise in temperature than the duration of heat treatment.

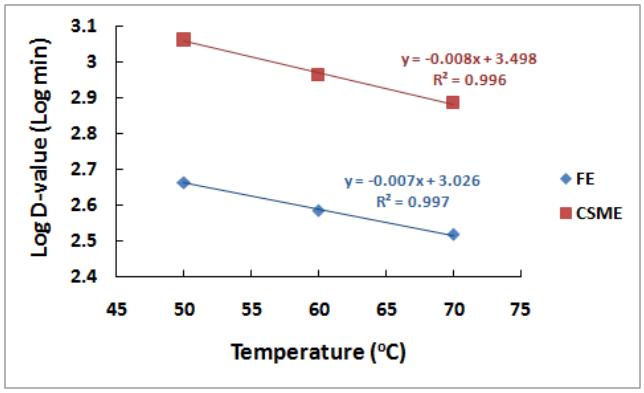

Figure 6.11 Temperature dependence of the decimal reduction of free enzyme and CSME to evaluate z-values.

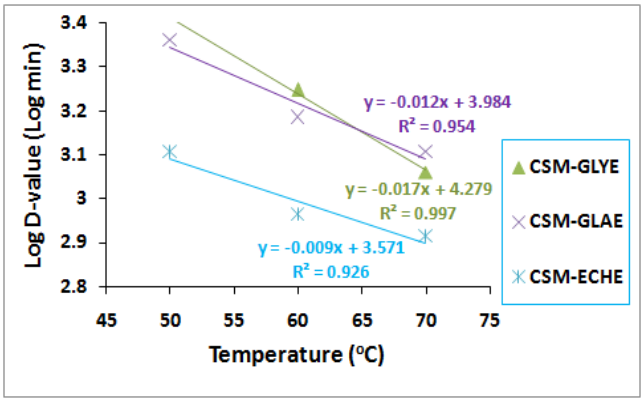

Figure 6.12 Temperature dependence of the decimal reduction of CSM-GLYE, CSM-GLAE and CSM-ECHE to evaluate z-values.

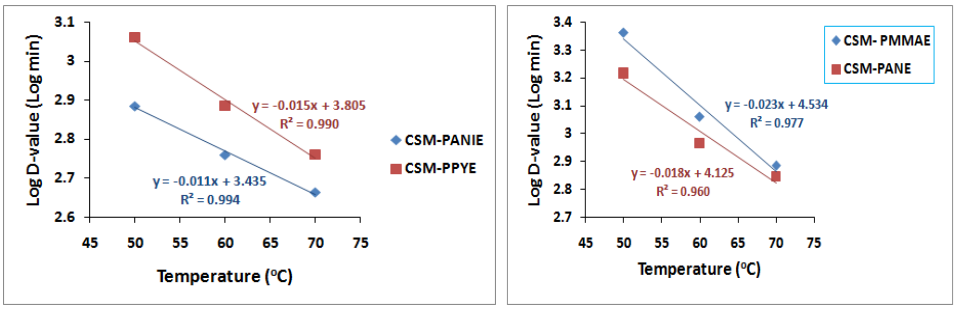

(i) (ii)

Figure 6.13 Temperature dependence of the decimal reduction of (i) CSM-PANIE and CSM-PPYE (ii) CSM-PMMAE and CSM-PANE to evaluate z-values.

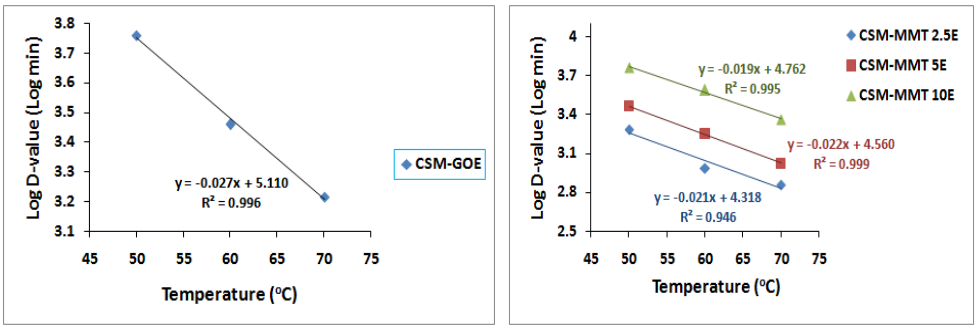

(i) (ii)

Figure 6.14 Temperature dependence of the decimal reduction of (i) CSM-GOE (ii) CSM-MMT 2.5E, CSM-MMT 5E and CSM-MMT 10E to evaluate z-values.

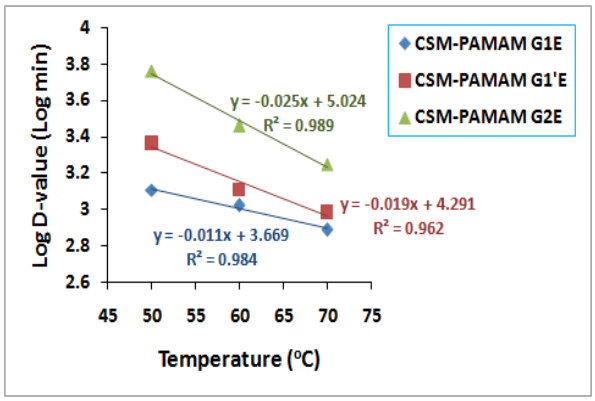

Figure 6.15 Temperature dependence of the decimal reduction of CSM-PAMAM G1E, CSM-PAMAM G1'E and CSM-PAMAM G2E

Table 6.1 Kinetic parameters for thermal deactivation of free enzyme, immobilized enzymes on magnetic chitosan and its modified forms with cross-linking agents

Enzyme	Temperature (^{o} C)	$t_{1/2}$ (min)	D-value (min)	Ed (KJ mol^{-1})	z-value (^{o} C)
FE	50 ^{0}C	138.63	460.52	15.52	142.86
	60 ^{0}C	115.52	383.76		
	70 ^{0}C	99.02	328.94		
CSME	50 ^{0}C	346.57	1151.293	18.71	125
	60 ^{0}C	277.26	921.034		
	70 ^{0}C	231.05	767.5284		
CSM-GLYE	50 ^{0}C	770.16	2558.43	36.77	58.82
	60 ^{0}C	533.19	1771.22		
	70 ^{0}C	346.57	1151.29		
CSM-GLAE	50 ^{o}C	693.15	2302.58	27.12	83.33
	60 ^{o}C	495.10	1644.70		
	70 ^{o}C	385.08	1279.21		
CSM-ECHE	50 ^{o}C	385.08	1279.21	20.46	111.11
	60 ^{o}C	277.26	921.03		
	70 ^{o}C	247.55	822.35		

Table 6.2 Kinetic parameters for thermal deactivation of immobilized enzymes on modified forms of magnetic chitosan with synthetic polymers

Enzyme	Temperature (^{o} C)	$t_{1/2}$ (min)	D-value (min)	Ed (KJ mol^{-1})	z-value (^{o} C)
CSM-PANIE	50 ^{0}C	231.05	767.53	23.58	90.91
	60 ^{0}C	173.29	575.65		
	70 ^{0}C	138.63	460.52		
CSM-PPYE	50 ^{0}C	346.57	1151.29	32	66.67
	60 ^{0}C	231.05	767.53		
	70 ^{0}C	173.28	575.65		
CSM-PMMAE	50 ^{0}C	693.15	2302.58	50.77	43.48
	60 ^{0}C	346.57	1151.29		
	70 ^{0}C	231.05	767.53		
CSM-PANE	50 ^{o}C	495.10	1644.70	39.67	55.55
	60 ^{o}C	277.26	921.03		
	70 ^{o}C	210.04	697.75		

Table 6.3 Kinetic parameters for thermal deactivation of immobilized enzymes on modified forms of magnetic chitosan with inorganic layered solids

Enzyme	Temperature (°C)	$t_{1/2}$ (min)	D-value (min)	Ed (KJ mol^{-1})	z-value (°C)
CSM-GOE	50 °C	1732.868	5756.46	57.81	37.04
	60 °C	866.434	2878.23		
	70 °C	495.1051	1644.70		
CSM-MMT 2.5E	50 °C	577.6227	1918.82	45.40	47.62
	60 °C	288.8113	959.41		
	70 °C	216.6085	719.56		
CSM-MMT 5E	50 °C	866.434	2878.23	46.61	45.45
	60 °C	533.1901	1771.22		
	70 °C	315.0669	1046.63		
CSM-MMT 10E	50 °C	1732.868	5756.46	42.18	55.55
	60 °C	1155.245	3837.64		
	70 °C	693.1472	2302.58		

Table 6.4 Kinetic parameters for thermal deactivation of immobilized enzymes on PAMAM modified forms of magnetic chitosan

Enzyme	Temperature (°C)	$t_{1/2}$ (min)	D-value (min)	Ed (KJ mol^{-1})	z-value (°C)
CSM-PAMAM G1E	50 °C	385.08	1279.21	23.49	90.91
	60 °C	315.06	1046.63		
	70 °C	231.05	767.53		
CSM-PAMAM G1'E	50 °C	693.15	2302.58	40.50	52.63
	60 °C	385.08	1279.21		
	70 °C	288.81	959.41		
CSM-PAMAM G2E	50 °C	1732.87	5756.46	54.42	40
	60 °C	866.43	2878.23		
	70 °C	533.19	1771.22		

6.3.3 Estimation of thermodynamic parameters for thermal deactivation of immobilized enzymes

The thermodynamic parameters for thermal deactivation of free and immobilized enzymes were determined by using their corresponding E_d values and the results are presented in the tables 6.5 to 6.7. The ΔH° values for all the immobilized enzymes were found to be higher than that of free enzyme. This revealed that the immobilization provided high stability to the enzyme and hence the immobilized systems required more energy for thermal deactivation. It was noticed that at higher temperatures, ΔH° values were slightly decreased for both free and immobilized enzymes which indicated that they required lesser amount of energy for their deactivation at higher temperatures and it was confirmed that they undergone significant conformational changes at that temperature ranges [8]. However, the immobilized enzymes still keep their ΔH° values more than that of free enzyme.

The thermal deactivation process was accompanied with unfolding of protein structure that causes the increase of disorder which describe entropy of deactivation, ΔS°. Both free and immobilized enzymes have shown negative values for ΔS° indicated their high ordered state. However the immobilized enzymes have exhibited the entropy values with lesser in magnitude when compared to free enzyme and this could be as a result of interaction between the enzyme and support. This leads to the immobilized enzyme with lesser compaction and resistant towards thermal deactivation that eventually causes increased enzyme stability [19].

The Gibbs free energy (ΔG°) for thermal deactivation of free and immobilized enzymes was increased as the temperature of the process

increased to higher values, yet the values are more with immobilized enzymes. The higher ΔG° values at elevated temperatures confirmed the more stability of the immobilized enzyme and this revealed their resistance towards thermal denaturation at higher temperatures. The ΔG° values that determine the spontaneity of the thermal deactivation process and these are found to be higher than that of ΔH° for both free and immobilized forms. This might be due to the negative entropic contribution of thermal deactivation process [20].

Table 6.5 Thermodynamic parameters of free enzyme, immobilized enzymes on magnetic chitosan and its modified forms on thermal deactivation study at 50 ºC

Temperature (^{0}C)	Enzyme	ΔGº KJ mol^{-1}	ΔHº KJ mol^{-1}	ΔSº KJ mol^{-1} K^{-1}
50 ^{0}C	FE	104.59	12.83	-0.28395
	CSME	107.05	16.01	-0.28172
	CSZE	109.20	20.81	-0.27354
	CSTE	109.52	39.57	-0.21646
	CSM-GLYE	109.29	29.31	-0.2472
	CSM-GLAE	108.92	24.51	-0.2612
	CSM-ECHE	107.34	17.61	-0.2771
	CSM-PANIE	105.97	20.89	-0.2633
	CSM-PPYE	107.05	29.31	-0.2406
	CSM-PMMAE	108.92	48.09	-0.1882
	CSM-PANE	108.01	36.98	-0.2198
	CSM-GOE	111.38	55.12	-0.1741
	CSM-MMT 2.5E	108.43	42.71	-0.2034
	CSM-MMT 5E	109.52	43.92	-0.203
	CSM-MMT 10E	111.38	24.51	-0.2688
	CSM-PAMAM G1E	107.34	20.81	-0.2677
	CSM-PAMAM G1'E	108.92	37.81	-0.22
	CSM-PAMAM G2E	111.38	51.74	-0.1845

Table 6.6 Thermodynamic parameters of free enzyme, immobilized enzymes on magnetic chitosan and its modified forms on thermal deactivation study at 60 ºC

Temperature (^{0}C)	Enzyme	ΔG^o KJ mol^{-1}	ΔH^o KJ mol^{-1}	ΔS^o KJ mol^{-1} K^{-1}
60 ^{0}C	FE	107.41	12.75	-0.28413
	CSME	109.83	15.94	-0.28185
	CSZE	112.11	20.72	-0.2743
	CSTE	111.64	39.49	-0.21657
	CSM-GLYE	111.64	29.23	-0.2473
	CSM-GLAE	111.25	24.42	-0.2606
	CSM-ECHE	109.83	17.69	-0.2766
	CSM-PANIE	108.53	20.81	-0.2637
	CSM-PPYE	109.33	29.23	-0.2404
	CSM-PMMAE	110.45	48	-0.1874
	CSM-PANE	109.83	36.89	-0.2189
	CSM-GOE	112.99	55.04	-0.1739
	CSM-MMT 2.5E	109.95	42.63	-0.2021
	CSM-MMT 5E	111.64	43.84	-0.2035
	CSM-MMT 10E	113.79	24.42	-0.2682
	CSM-PAMAM G1E	110.19	20.72	-0.2685
	CSM-PAMAM G1'E	110.74	37.73	-0.2191
	CSM-PAMAM G2E	112.99	51.65	-0.1841

Table 6.7 Thermodynamic parameters of free enzyme, immobilized enzymes on magnetic chitosan and its modified forms on thermal deactivation study at 60 ºC

Temperature (^{0}C)	Enzyme	ΔG^o KJ mol^{-1}	ΔH^o KJ mol^{-1}	ΔS^o KJ mol^{-1} K^{-1}
70 ^{0}C	FE	110.28	12.67	-0.28444
	CSME	112.69	15.85	-0.28221
	CSZE	114.67	20.64	-0.27402
	CSTE	113.85	39.40	-0.21696
	CSM-GLYE	113.85	29.15	-0.2468
	CSM-GLAE	114.15	24.34	-0.2617
	CSM-ECHE	112.89	17.61	-0.2777
	CSM-PANIE	111.24	20.72	-0.2637
	CSM-PPYE	111.87	29.15	-0.2411
	CSM-PMMAE	112.69	47.92	-0.1887
	CSM-PANE	112.42	36.81	-0.2203
	CSM-GOE	114.87	54.95	-0.1746
	CSM-MMT 2.5E	112.58	42.55	-0.2041
	CSM-MMT 5E	113.58	43.75	-0.2035
	CSM-MMT 10E	115.83	24.34	-0.2661
	CSM-PAMAM G1E	112.69	20.64	-0.2682
	CSM-PAMAM G1'E	113.33	37.64	-0.2205
	CSM-PAMAM G2E	115.07	51.57	-0.1850

6.4 Conclusion

The thermal deactivation energy (E_d) for immobilized α-amylase was found to be higher than that of free enzyme indicated its high stability and increased resistance to heat denaturation. The apparent half-life ($t_{1/2}$) and D-value of immobilized α-amylases were found to be appreciably increased in the temperature range 50–70 ºC. The lower z-value of immobilized enzyme designated that the immobilization provided more sensitivity to enzyme towards the increase of temperature rather than its duration. Based on the obtained thermodynamic parameters ΔH°, ΔS° and ΔG°, it is confirmed that the thermal denaturation of α-amylase was reduced much more as a result of immobilization and the interactive forces between support and enzyme have assigned much stability to it.

References

[1] G. Madsen, B. Norman, S. Slott, A new, heat stable bacterial amylase and its use in high temperature liquefaction, Starch-Starke 25(9) (1973) 304-308.

[2] N. Saito, A thermophilic extracellular α-amylase from Bacillus licheniformis, Archives of Biochemistry and Biophysics 155(2) (1973) 290-298.

[3] G.S. Narayana Naidu, T. Panda, Studies on pH and thermal deactivation of pectolytic enzymes from Aspergillus niger, Biochemical Engineering Journal 16(1) (2003) 57-67.

[4] H.N. Bhatti, M. Asgher, A. Abbas, R. Nawaz, M.A. Sheikh, Studies on kinetics and thermostability of a novel acid invertase from Fusarium solani, Journal of Agricultural and Food Chemistry 54(13) (2006) 4617-4623.

[5] X.Y. Wang, F.G. Meng, H.M. Zhou, Unfolding and inactivation during thermal denaturation of an enzyme that exhibits phytase and acid phosphatase activities, The International Journal of Biochemistry & Cell Biology 36(3) (2004) 447-459.

[6] E. Jurado, F. Camacho, G. Luzon, J. Vicaria, Kinetic models of activity for β-galactosidases: influence of pH, ionic concentration and temperature, Enzyme and Microbial Technology 34(1) (2004) 33-40.

[7] M.P. Klein, L.P. Fallavena, J.d.N. Schöffer, M.A. Ayub, R.C. Rodrigues, J.L. Ninow, P.F. Hertz, High stability of immobilized β-D-galactosidase for lactose hydrolysis and galactooligosaccharides synthesis, Carbohydrate Polymers 95(1) (2013) 465-470.

[8] E. Marin, L. Sanchez, M. Perez, P. Puyol, M. Calvo, Effect of heat treatment on bovine lactoperoxidase activity in skim milk: kinetic and thermodynamic analysis, Journal of Food Science 68(1) (2003) 89-93.

[9] D. Driss, Z. Driss, F. Chaari, S.E. Chaabouni, Immobilization of His-tagged recombinant xylanase from Penicillium occitanis on nickel-chelate Eupergit C for increasing digestibility of poultry feed, Bioengineered 5(4) (2014) 274-279.

[10] E.A. Karam, W.A.A. Wahab, S.A. Saleh, M.E. Hassan, A.L. Kansoh, M.A. Esawy, Production, immobilization and thermodynamic studies of free and immobilized Aspergillus awamori amylase, International Journal of Biological Macromolecules 102 (2017) 694-703.

[11] A. Pal, F. Khanum, Characterizing and improving the thermostability of purified xylanase from Aspergillus niger DFR-5 grown on solid-state-medium, Journal of Biochemical Technology 2(4) (2011) 203-209.

[12] A. Pal, F. Khanum, Covalent immobilization of xylanase on glutaraldehyde activated alginate beads using response surface methodology: characterization of immobilized enzyme, Process Biochemistry 46(6) (2011) 1315-1322.

[13] H. Gouzi, C. Depagne, T. Coradin, Kinetics and thermodynamics of the thermal inactivation of polyphenol oxidase in an aqueous extract from Agaricus bisporus, Journal of Agricultural and Food Chemistry 60(1) (2011) 500-506.

[14] M.D. Gouda, S.A. Singh, A.A. Rao, M.S. Thakur, N.G. Karanth, Thermal inactivation of glucose oxidase mechanism and stabilization using additives, Journal of Biological Chemistry 278(27) (2003) 24324-24333.

[15] G. Mainer, L. Sanchez, J. Ena, M. Calvo, Kinetic and thermodynamic parameters for heat denaturation of bovine milk IgG, IgA and IgM, Journal of Food Science 62(5) (1997) 1034-1038.

[16] C. Mateo, J.M. Palomo, G. Fernandez-Lorente, J.M. Guisan, R. Fernandez-Lafuente, Improvement of enzyme activity, stability and selectivity via immobilization techniques, Enzyme and Microbial Technology 40(6) (2007) 1451-1463.

[17] H. Yagar, F. Ertan, B. Balkan, Comparison of some properties of free and immobilized α-Amylase by Aspergillus sclerotiorum in calcium alginate gel beads, Preparative Biochemistry and Biotechnology 38(1) (2007) 13-23.

[18] M. Sharma, V. Sharma, D.K. Majumdar, Entrapment of-amylase in agar beads for biocatalysis of macromolecular substrate, International Scholarly Research Notices 2014 (2014) 1-8.

[19] S.G. Anema, A.B. McKenna, Reaction kinetics of thermal denaturation of whey proteins in heated reconstituted whole milk, Journal of Agricultural and Food Chemistry 44(2) (1996) 422-428.

[20] A. Tanaka, E. Hoshino, Calcium-binding parameter of Bacillus amyloliquefaciens α-amylase determined by inactivation kinetics, Biochemical Journal 364(3) (2002) 635-639.

Chapter 7

Industrial applications of α-amylase immobilized magnetic chitosan

Contents

7.1 Introduction

α-amylase is one of the important starch hydrolyzing enzymes that promote the hydrolysis of α-1,4-glycosidic linkages in starch to yield low molecular weight products like glucose and maltose [1, 2]. Owing to this starch hydrolyzing activity these enzymes are widely implemented in starch processing industries especially in food, detergent, paper, textile desizing and pharmaceutical industries [3, 4].

Detergent industries stand for principal consumers of enzymes and as the enzymes are eco friendly, they are well suited with detergent formulations in order to enhance the stain removing capacity [5, 6]. Amylase constitutes as the second major type of enzymes that widely used with enzymatic detergent formulations that degrade the starchy food residues such as potatoes, gravies, chocolate, sauce etc to smaller oligosaccharides [7, 8]. Amylase exhibited high activity at alkaline pH medium and at lower temperature conditions, although oxidative stability of the enzyme in detergent formulations should be maintained as the washing environs are too oxidizing [9]. The starch hydrolyzing property of enzyme

has been exploited for the starch stain removal from the surface as it is the main polysaccharide presented in the food ingredients and starch removal has become so crucial since it was well attracted to particulate soils [10]. Washing with detergents alone caused much energy loss as the washing performance conducted at higher temperatures in order to improve the washing efficiency. However the use of enzymes in detergents offers lower wash temperature and also shorter periods of agitation. The free form of α-amylase in detergents is generally unstable since it was undergone protease attack and was inhibited its activity by other detergent components. The immobilized form of α-amylase provides better solution to it which protects it from protease attack and also from inhibition of various detergent components such as surfactants. It was recommended the use of laundry detergents at 30 °C and 40 °C wash cycles and preferably in cold filled washing machines as the enzyme tends to be denatured at higher temperatures. But the use of immobilized enzyme instead of free enzyme acquired much stability at higher temperatures as it undergone slow rate of thermal inactivation. Many literatures were reported on which immobilized enzymes as cleaning additive in detergents for the removal of starch stain. Jaiswal et al. reported that immobilized soybean α-amylase on gelatin has found potential application in the cleaning performance of laundry detergents [11]. Soleimani et al. observed the cleaning efficiency of immobilized amylase on silica nanoparticles and found much more than that of free enzyme [12]. They argued that immobilization process has decreased the enzyme sensitivity towards some components of detergents.

In textile industry, the warp yarns are coated with sizing agents in order to get additional strength to prevent the yarn breakage in loom and to improve weaving efficiency by increasing the weft insertion speed [13-15].

Starch is the widely used sizing agent which provides high weaving performance to yarns. The starch on warp yarn tends to resist towards the dye and chemicals that used in wet processing stage and so before attaining this stage the sizing agents must be removed, which termed as desizing. α-amylase is the widely used desizer in textile industry since it do not cause any harm to yarns and it catalyzes the degradation of starch molecules which leads to the enhanced and stable wet processing. The desizing by enzyme required not so much time and can be easily occurred by effective enzyme action. Chimata et al. reported the desizing of cotton cloth by α-amylase from *Aspergillus* species and desizing activities were evaluated by varying the enzyme concentration [16]. Nima Chand et al. observed the high desizing efficiency of Ca^{2+}-independent α-amylase on cotton fabric under acidic conditions [17]. When free enzymes used as desizer, after the reaction some amount remained in the reaction system which cannot be recovered for reuse and this caused contamination of the product. However, the use of immobilized enzyme has become more effective than free enzyme since it can be used repetitively, also due to its longer half life and specific rate of deactivation. Sahinbaskan et al. reported the desizing of cotton fabric by free and immobilized α-amylase using ultra sonic and conventional bath procedures and observed that the multiple use of immobilized enzyme permitted better desizing processes for textile industry [18].

This chapter deals with the two important industrial applications of immobilized α-amylase on magnetic chitosan. The first section describes the washing performance of immobilized α-amylase in laundry detergents and the second section explains the enzymatic desizing of cotton cloth using immobilized α-amylase.

7.2 Experimental

7.2.1 Materials

The materials required for the preparation of immobilized α-amylase on magnetic chitosan were detailed in the chapter 2. Cotton cloth pieces and detergents were purchased from local market. Dinitrosalicylic acid and starch (potato) were acquired from S.d. Fine Chemicals Ltd, Mumbai.

7.2.2 Preparation of immobilized α-amyalse on magnetic chitosan

The preparation of immobilized enzyme and its estimation were discussed in chapter 2.

7.2.3 Measurement of washing performance of immobilized enzyme (CSME) in laundry detergents

The washing performance of immobilized enzyme on starch stain was investigated by using six types of commercially available detergents such as Tide, Ujala, Surf excel, Sunlight, Ariel and Henko. In this study the stock solutions of detergents in 2 g L^{-1} were prepared in distilled water. About 1 % of starch solution was prepared and clean cotton cloth pieces of 3x3 cm were stained with 0.2 mL starch solution. These stained cotton cloth pieces were subjected to wash treatment in separate reaction flasks. In the first case the stained cloth piece was incubated in detergent solution in the presence of immobilized enzyme at 40 °C for 20 min. under continuous agitation. Likewise, in the second reaction flask the stained cloth was washed in distilled water alone and the third cloth piece was washed in another flask by using only detergent solution. The pH of the reaction medium maintained between 9 and 10. After the time period, cloth pieces were taken out from respective reaction flasks and rinsed with definite

amount of distilled water. Then the cloth pieces were squeezed and the volume of wash out made up to 10 mL. About 1 mL of the washout form reaction flasks mixed with 1mL DNS reagent taken in separate reaction tubes and placed in boiling water bath for 5 min. The reaction tubes were cooled to room temperature and maltose produced was determined spectrophotometrically at 540 nm.

7.2.4 Desizing method

For desizing study equal sizes of 3x3 cm clean cotton cloth pieces with starch over that were used and they were weighed on an electronic balance. The weighed cloth strip was then placed in a reaction flask containing immobilized enzyme in buffer at optimum pH. Another weighed cotton strip that dipped in the same buffer without immobilized enzyme stands for control. These reaction systems were incubated at optimum temperature of 35 °C for 1 h. After the time period, the cloth pieces were taken out from the reaction system and rinsed thoroughly. They were washed with tap water, dried in oven and after drying the pieces were again weighed.

7.2.4.1 Desizing efficiency tests Weight loss (%) assay

Desizing efficiency of the immobilized enzyme was evaluated by weight loss (%) assay in which weight of the cotton cloth pieces were measured before and after the desizing process.

The weight loss (%) was calculated by the equation 7.1,

$$Weight\ loss\ \%\ (Wt\ \%) = \frac{(W1 - W2)}{W1} X100 \qquad (7.1)$$

Where W1 is the weight of cotton piece before desizing and W2 is the weight of cotton piece after desizing process.

Reducing sugar assay

The desizing efficiency of immobilized enzyme was also evaluated by reducing sugar assay in which the reducing sugar formed as a result of enzyme action on starch over the cotton cloth was analyzed by dinitrosalicylic acid (DNSA) method. Here 1mL of the supernatant from the reaction system mixed with 1 mL DNS reagent taken in a test tube and then placed in a boiling water bath for 5 min. The reaction tubes were cooled to room temperature and the reducing sugar liberated was spectrophotometrically analyzed at 540 nm.

7.3 Results and Discussion

7.3.1 Washing performance of immobilized α-amylase in laundry detergents

The washing performance of immobilized enzyme supplemented detergents were evaluated by measuring the maltose content released from the starch stained cotton cloth taken for the study. The higher amount of maltose released from the cotton cloth piece indicates better washing. Since the washing capacity of detergents has been based on the degradation of starch stain on the cotton cloth, it also depended on the activity of enzyme towards starch substrate. Hence the washing performance of enzyme in detergents controlled by the temperature of the medium as the enzyme activity varied in accordance with the changes in temperature and also the rise of temperature to higher region leads to the enzyme denaturation.

7.3.1.1 Determination of maltose content in the washout

The maltose content removed from the starch stained cotton cloth pieces in the wash out were determined after they washed in detergents together with immobilized enzyme and in detergents alone. The wash out from the washing of cloth piece in distilled water stands for control. The maltose content removed from both cases of washing are presented in the table 7.1 and here we observed that the washing of cotton cloth piece in detergents supplemented with immobilized α-amylase provided more maltose content than that of washing in detergents alone. This implied the better washing performance of detergents supplemented with immobilized enzyme rather than that of the other.

Table 7.1 Colorimetric determination of maltose content in the washout for the washing of cotton cloth piece in detergents supplemented with immobilized α-amylase and detergents alone

	Maltose content (mg mL^{-1})	
Commercial detergents used	Detergent alone	Detergent + immobilized enzyme
Ariel	0.07	0.2
Henko	0.15	0.825
Surf excel	0.03	0.1
Sunlight	0.09	0.22
Tide	0.02	0.07
Ujala	0.05	0.125

As the reaction medium kept in alkaline, the interaction between the enzyme and the support has become very weak which caused the enzyme desorption from the support surface and promoted to adsorb on to the soil surface [19]. The starch hydrolyzing property of enzyme removes the starch stain from the cotton cloth easily [20]. Here the immobilized α-amylase catalyzed the breakdown of starch molecules in which hydrolysis of

amylose fractions of starch has taken place and yielded maltose and dextrin units. The higher the maltose content in the washout of detergents supplemented with immobilized enzyme indicate enhanced degradation of starch molecules and hence their better washing performance.

The washing performance of immobilized enzyme in terms of its specific activity is presented in the figure 7.1. The enzyme with high specific activity meant for its increased degrading power towards starch stain and hence high washing performance.

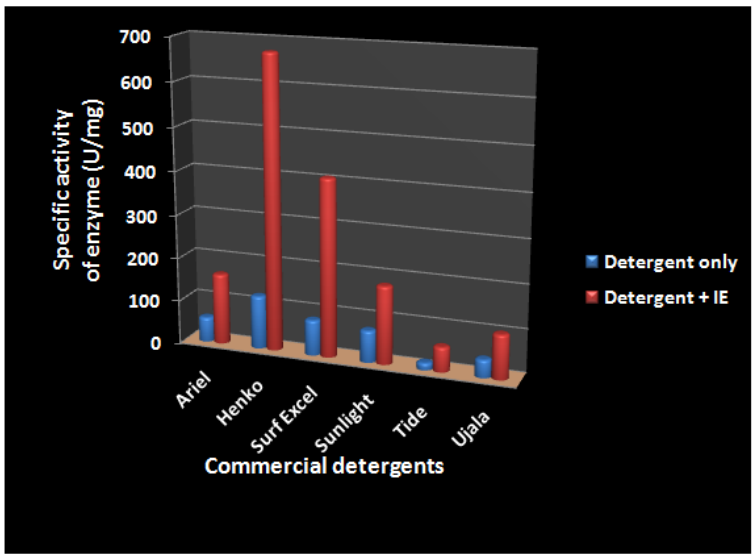

Figure 7.1 Washing performance of detergents supplemented with immobilized enzyme in terms of specific activity

Since the commercial detergents already incorporated with some amount of enzymes, they have been exhibited certain enzyme activity when they were used in the washing of stained cotton cloth pieces. However these detergents supplemented with immobilized enzyme have shown much more specific activity when compared to the detergents alone. Therefore this immobilized enzyme can be successively used in laundry detergents for the degradation of starchy food residues. Here we observed that the detergent

Henko supplemented with immobilized enzyme has shown higher specific activity of about more than 650 U/mg towards the starch stain removal. The immobilized enzyme increased the washing efficiency of detergent without being affected or may be facilitated the action of detergent components. Jaiswal et al. argued that immobilized α-amylase on gelatin could be considered as a potential cleaning additive in detergents as it showed increased washing efficiency in starch stain removal without affected by the components of detergents [11].

7.3.1.2 Effect of temperature on washing performance of free and immobilized enzymes

The effect of temperature on washing performance of immobilized enzymes in various detergents were studied at 40 °C and 50 °C for different time periods and compared with that of free enzyme. The results are depicted in the figure 7.2 to 7.7.

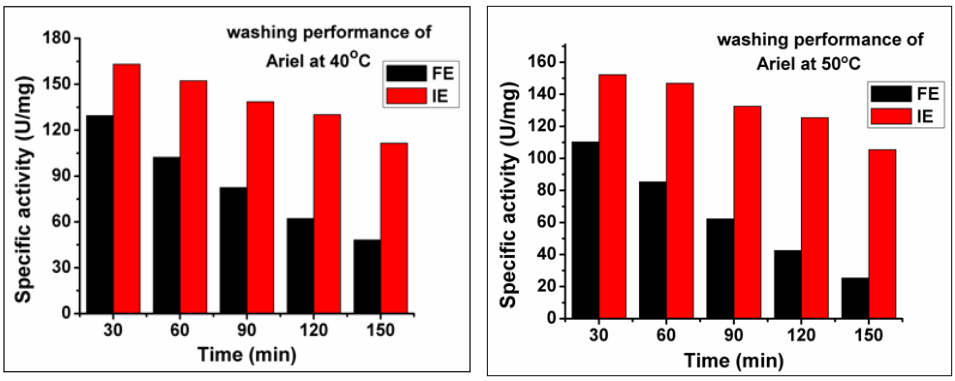

(i) (ii)

Figure 7.2 Effect of temperature on washing performance of free and immobilized enzyme in Ariel at (i) 40 °C (ii) 50 °C

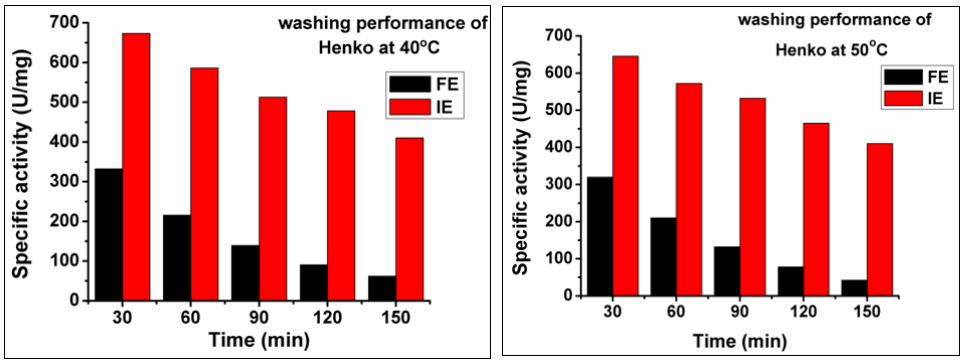

(i) (ii)

Figure 7.3 Effect of temperature on washing performance of free and immobilized enzyme in Henko at (i) 40 °C (ii) 50 °C

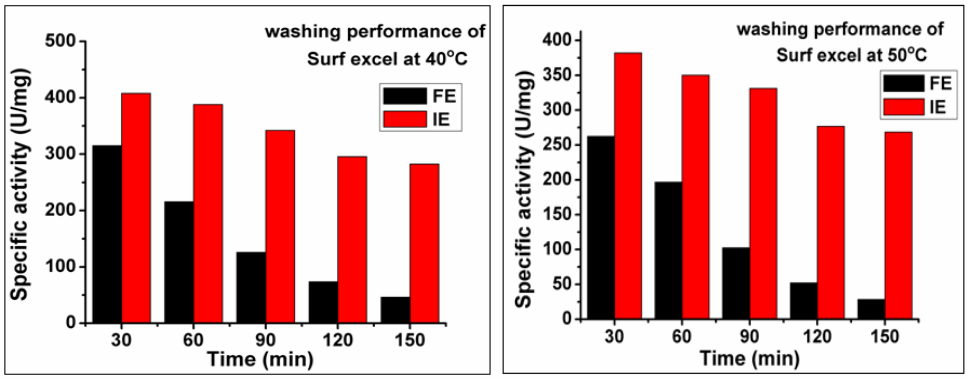

(i) (ii)

Figure 7.4 Effect of temperature on washing performance of free and immobilized enzyme in Surf excel at (i) 40 °C (ii) 50 °C

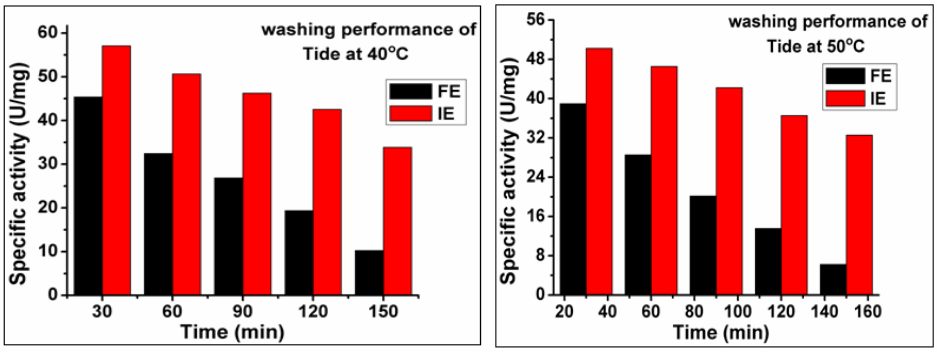

(i) (ii)

Figure 7.5 Effect of temperature on washing performance of free and immobilized enzyme in Tide at (i) 40 °C (ii) 50 °C

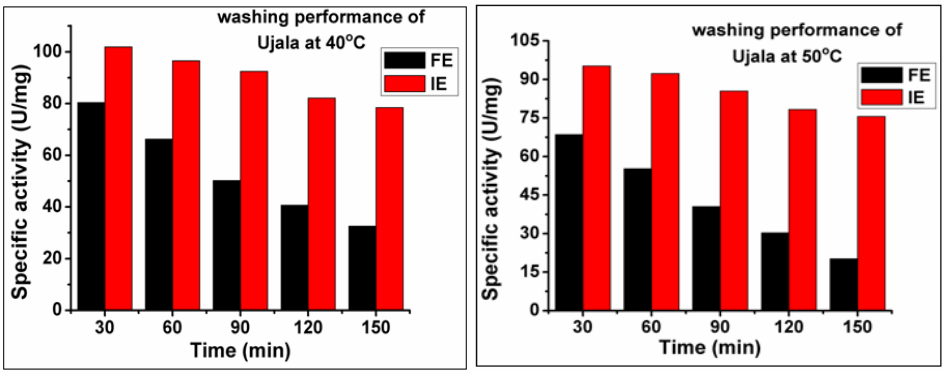

(i) (ii)

Figure 7.6 Effect of temperature on washing performance of free and immobilized enzyme in Ujala at (i) 40 °C (ii) 50 °C

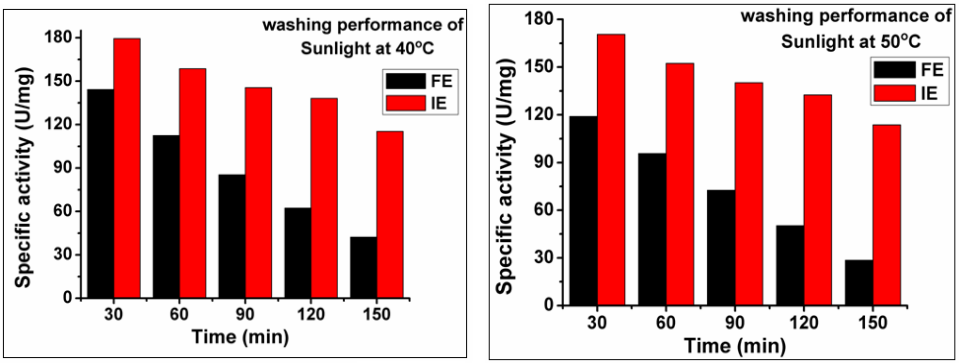

(i) (ii)

Figure 7.7 Effect of temperature on washing performance of free and immobilized enzyme in Sunlight at (i) 40 °C (ii) 50 °C

Here we observed that the washing performance of immobilized enzyme in all detergents was higher than that of free enzyme at both temperatures that we have studied. The free enzyme lost its activity much more than that of immobilized enzyme as the time period for washing process prolonged. When the washing was performed at higher temperature, the activity of both free and immobilized enzymes were found to be decreased. However the decrease in activity for immobilized enzyme was at slower rate when compared to the free enzyme.

As enzymes are denatured at high temperatures and long periods of agitation, the biological laundry detergents were recommended to use at 30 °C and 40 °C wash cycles and preferably in cold fill washing machines. But in this study when detergents supplemented with immobilized enzyme were used for starch stain removal, the immobilized enzyme exhibited slow rate of thermal inactivation as compared to free enzyme and this could be as a result of high thermal stability of the immobilized enzyme. Hence it showed better activity towards starch degradation and can be used for higher temperature washing process without loss of much activity due to thermal denaturation. The similar trend was observed in the cleaning efficiency of immobilized α-amylase on silica nanoparticles on starch soils of cotton fabric at higher temperatures [21].

7.3.2 Enzymatic desizing of cotton cloth using immobilized α-amylase

7.3.2.1 Optimization of parameters for desizing process

The parameters such as amount of immobilized enzyme and incubation time for the desizing process were optimized in order to get maximum desizing efficiency. Weight loss (%) assay and estimation of reducing sugar were carried out for the determination of desizing efficiency of immobilized enzyme.

The enzyme dosage applied for the desizing of cotton cloth was optimized by carrying out the process in the buffer of pH 7 at 50 °C for 1 h. The results are presented in the table 7.2. When the amount of immobilized enzyme increased the desizing efficiency was also found to be increased and this fact was expressed in terms of weigh loss (%) and reducing sugar released. The higher weight loss % confirmed better desizing of the cotton cloth and the reducing sugar estimated was also determines the desizing

efficiency as it gives the amount of starch hydrolyzed. The higher desizing efficiency was observed when the desizing process carried out at 9.75 EU of immobilized enzyme and the desizing efficiency was found to be slightly decreased for further increase of enzyme dosage in the reaction system. At optimum enzyme dosage the desized cotton cloth has shown 12.35 % of weight loss and the reducing sugar released was 1750 μg mL^{-1}. When the amount of immobilized enzyme used in the desizing process again increased both of the weight loss % and the liberated reducing sugar were found to be decreased. This leads to the decrease of desizing efficiency after the optimum value and this decrease was observed at slower rate.

Table 7.2 Optimization of enzyme dosage for desizing process

Enzyme activity (EU)						
Parameter	5.8	7.2	8.85	9.75	10.25	11.86
Weight loss (%)	9.78	10.55	11.24	12.35	12.22	12.14
Reducing sugar (μg mL^{-1})	1055	1250	1525	1750	1735	1725

The incubation time was optimized by carrying out the desizing process in the presence of 9.75 EU of the immobilized enzyme in the buffer of pH 7 at 50 °C by varying the time intervals for incubation. The experimental results are shown in the table 7.3 and the maximum desizing was obtained at 60 min. of incubation. .

Table 7.3 Optimization of incubation time for desizing process

Incubation time (min)						
Weight loss (%)	11.78	12.26	12.78	13.54	13.26	13.15
Reducing sugar (μg mL^{-1})	1250	1525	2575	2815	2810	2798

At optimum incubation time the weight loss % was calculated as 13.54 % and the amount of reducing sugar released from the cloth was 2815 μg mL^{-1}. Further increase of incubation period did not show significant changes in the values of weight loss % and liberated reducing sugar and

hence reflected in the desizing efficiency of immobilized enzyme. Accordingly, 9.75 EU of immobilized enzyme and 60 min. of incubation time were regarded as the optimum desizing conditions for further desizing processes. The sufficient desizing efficiency was observed by Amit Madhu et al. when chitosan and eudragit S-100 immobilized α-amylase used for cotton fabric desizing [22].

7.3.2.2 Effect of pH on desizing efficiency

The effect of pH on enzymatic desizing was investigated in the ranges of pH 3-8 and the optimum was obtained at pH 6. The results are illustrated in the figure 7.8 and showed that the maximum desizing has taken place at acidic pH. This could be due to the increased hydrolysis of glycosidic bonds of starch substrate at lower pH values [23]. At optimum pH 6, the immobilized enzyme exhibited high desizing efficiency of 14.35 % weight loss with specific activity of 7.3 EU/mg. Many reports are there in which enzymatic desizing has taken place in acidic conditions [24, 25].

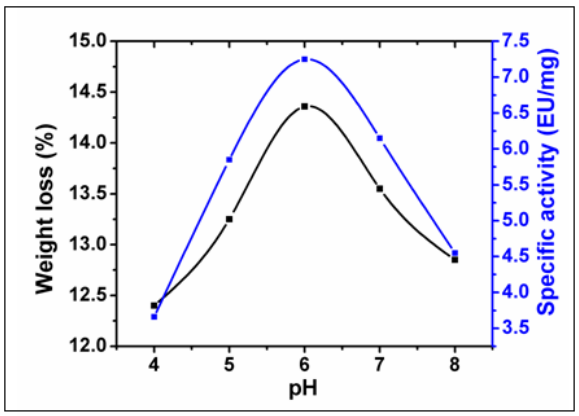

Figure 7.8 Effect of pH on desizing efficiency in terms of weight loss% and specific activity

7.3.2.3 Effect of temperature on desizing efficiency

A study on enzymatic desizing was carried out at optimum pH by varying the temperatures range between 30 °C and 70 °C and the results are

presented in the figure 7.9. The weight loss % of desized cotton cloth and specific activity of enzyme were showed maximum value at 60 °C and this temperature can be considered as the optimum temperature for desizing process. At 60 °C, the desized cloth exhibited 13.3 % of weight loss % and this high weight loss % indicated better desizing as this assay gives high amount of size mix removed from the cotton cloth.

During the desizing process the hydrolysis of starch over the cotton cloth has taken place due to the enzyme action which resulted in the release of reducing sugar. Higher the amount of reducing sugar liberated indicated the higher activity of enzyme and hence better desizing efficiency. Here the immobilized enzyme showed maximum specific activity of 9.2 EU/mg at which maximum desizing can be occurred due to the release of high amount of reducing sugar. The similar optimum desizing temperature was reported by Nima Chand et al. for enzymatic desizing of cotton fabric by Ca^{2+} ion independent α-amylase and they argued that desizing at this low temperature could reduce the energy consumption in the textile industry [17].

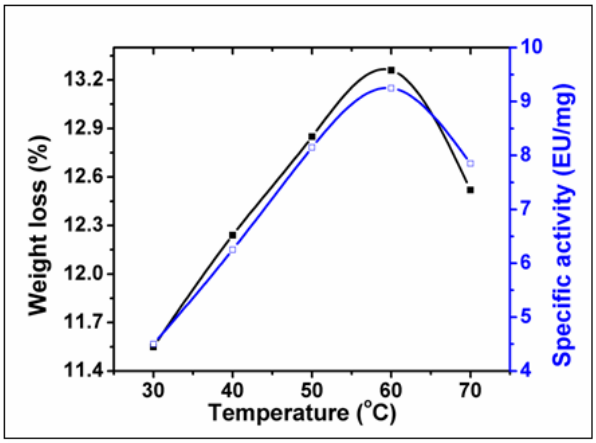

Figure 7.9 Effect of temperature on desizing efficiency in terms of weight loss % and specific activity

7.4 Conclusion

The maltose content released from the cotton cloth by different detergents supplemented with α-amylase immobilized magnetic chitosan was studied. The detergents supplemented with the immobilized enzyme resulted in a better stain removal as compared to that by detergent alone. The cleaning efficiency of immobilized enzyme on starch soils of cotton cloth was found to be more than that of free enzyme at 40 ^{0}C and 50 ^{0}C. The desizing efficiency of immobilized α-amylase on cotton cloth was examined and the higher desizing efficiency was noticed at which the amount of enzyme was increased up to 9.75 EU in the reaction mixture. The desizing was carried out at lower temperatures and with a shorter process time. The optimum temperature for desizing process was obtained at 60 ^{0}C and the weight loss % was about 13.3 %. The maximum desizing was obtained at pH 6 and can be considered as acidic desizing which improved the desizing efficiency at lower pH values.

References

[1] R. Gupta, P. Gigras, H. Mohapatra, V.K. Goswami, B. Chauhan, Microbial α-amylases: a biotechnological perspective, Process Biochemistry 38(11) (2003) 1599-1616.

[2] L. Kandra, α-Amylases of medical and industrial importance, Journal of Molecular Structure: Theochem 666 (2003) 487-498.

[3] P. Ashok, N. Poonam, C. Soccol, V. Soccol, S. Dalel, M. Radjiskumar, Review advances in microbial amylases, Biotechnology and Applied Biochemistry 31(2) (2000) 135-152.

[4] A.R. Ikram-ul-Haq, H. Ashraf, A.H. Shah, Isolation and screening of fungi for the biosynthesis of alpha amylase, Biotechnology 2 (2002) 61-66.

[5] N. Hmidet, N. El-Hadj Ali, A. Haddar, S. Kanoun, S. K. Alya, M. Nasri, Alkaline proteases and thermostable α-amylase co-produced by Bacillus licheniformis NH1: Characterization and potential application as detergent additive, Biochemical Engineering Journal 47(1) (2009) 71-79.

[6] S. Mitidieri, A.H. Souza Martinelli, A. Schrank, M.H. Vainstein, Enzymatic detergent formulation containing amylase from Aspergillus niger: A comparative study with commercial detergent formulations, Bioresource Technology 97(10) (2006) 1217-1224.

[7] A.K. Mukherjee, M. Borah, S.K. Rai, To study the influence of different components of fermentable substrates on induction of extracellular α-amylase synthesis by Bacillus subtilis DM-03 in solid-state fermentation and exploration of feasibility for

inclusion of α-amylase in laundry detergent formulations, Biochemical Engineering Journal 43(2) (2009) 149-156.

[8] H.S. Olsen, P. Falholt, The role of enzymes in modern detergency, Journal of Surfactants and Detergents 1(4) (1998) 555-567.

[9] O. Kirk, T.V. Borchert, C.C. Fuglsang, Industrial enzyme applications, Current Opinion in Biotechnology 13(4) (2002) 345-351.

[10] N. Hmidet, N.E.H. Ali, A. Haddar, S. Kanoun, S.-K. Alya, M. Nasri, Alkaline proteases and thermostable α-amylase co-produced by Bacillus licheniformis NH1: Characterization and potential application as detergent additive, Biochemical Engineering Journal 47(1-3) (2009) 71-79.

[11] N. Jaiswal, O. Prakash, Immobilization of soybean α-amylase on gelatin and its application as a detergent additive, Asian Journal of Biochemistry 6(4) (2011) 337-346.

[12] M. Soleimani, A. Khani, N. Dalali, G.R. Behbehani, Improvement in the cleaning performance towards protein soils in laundry detergents by protease immobilization on the silica nanoparticles, Journal of Surfactants and Detergents 16(3) (2013) 421-426.

[13] R.D. Anandjiwala, D.M. Hall, Textile Sizing, Taylor & Francis First Edition (2004).

[14] A. Cavaco-Paulo, G. Gubitz, Textile processing with enzymes, Elsevier First Edition (2003).

[15] H. Schonberger, T. Schafer, Best available techniques in textile industry, Federal Environmental Agency (2003).

[16] M.K. Chimata, C.S. Chetty, C. Suresh, Fermentative production and thermostability characterization of α-amylase from aspergillus species and its application potential evaluation in desizing of cotton cloth, Biotechnology research international 2011 (2011) 1-8.

[17] N. Chand, A.S. Nateri, R.H. Sajedi, A. Mahdavi, M. Rassa, Enzymatic desizing of cotton fabric using a Ca^{2+} independent α-amylase with acidic pH profile, Journal of Molecular Catalysis B: Enzymatic 83 (2012) 46-50.

[18] B.Y. Sahinbaskan, M.V. Kahraman, Desizing of untreated cotton fabric with the conventional and ultrasonic bath procedures by immobilized and native α-amylase, Starch-Starke 63(3) (2011) 154-159.

[19] M. Soleimani, A. Khani, K. Najafzadeh, α-Amylase immobilization on the silica nanoparticles for cleaning performance towards starch soils in laundry detergents, Journal of Molecular Catalysis B: Enzymatic 74(1) (2012) 1-5.

[20] O. Prakash, N. Jaiswal, Immobilization of a thermostable-amylase on agarose and agar matrices and its application in starch stain removal, World Applied Sciences Journal 13(3) (2011) 572-577.

[21] M. Soleimani, A. Khani, K. Najafzadeh, α-Amylase immobilization on the silica nanoparticles for cleaning

performance towards starch soils in laundry detergents, Journal of Molecular Catalysis B: Enzymatic 74(1-2) (2012) 1-5.

[22] A. Madhu, J.N. Chakraborty, Recovery and reuse of immobilized α-amylase during desizing of cotton fabric, Research Journal of Textile and Apparel 22(3) (2018) 271-290.

[23] M.J. Van Der Maarel, B. Van der Veen, J.C. Uitdehaag, H. Leemhuis, L. Dijkhuizen, Properties and applications of starch-converting enzymes of the α-amylase family, Journal of Biotechnology 94(2) (2002) 137-155.

[24] C. Tomasino, Chemistry & technology of fabric preparation & finishing, North Carolina State University (1992).

[25] P. Dalvi, P. Anthappan, Amylase and pectinase from single source for simultaneous desizing and scouring, Indian Journal of Fibre & Textile Research 32 (2007) 459-465.

Chapter 8

Summary and Conclusion

The enzyme immobilization technique has anchored an inevitable role in the biotechnological industries as it provides new perspectives and facilitates large scale industrial growth. The enzyme immobilization has been widely accepted as it imparts increased availability of the enzyme to the substrate molecules over a substantial period of time. The biocatalysts can be large extent commercialized as they acquired increased shelf life and enhanced reusability. Various immobilization methods and different types of carriers have been applied on both laboratory and industrial level. Several synthetic and natural carriers have been estimated for their effectiveness in enzyme immobilization field and biopolymers gained increased attention due to their easiness to fabricate into different forms and decreased non-specific adsorption.

In this study we have investigated the efficiency of magnetic chitosan as α-amylase carrier. Different modified forms of magnetic chitosan were synthesized and their effectiveness was compared with the base form. The immobilized enzyme was also subjected to industrial applications such as laundry detergents and enzymatic desizing.

The thesis is divided into eight chapters and the brief description on chapter wise summary is given below:

Chapter 1

This chapter contains a general introduction to industrial biocatalysis and literature review on enzymes in industries. A description on enzymes, its chemical nature, structure and types are also given. The activity and

specificity of enzyme and its action was described in shortly. A note on enzyme kinetics explaining kinetic parameters, turn over number and catalytic efficiency is given. A brief discussion on immobilization of enzyme, properties of immobilized enzyme and immobilization methods is carried out. Selection of carrier, importance of chitosan as enzyme carrier and α-amylase for immobilization are mentioned. The scope and objectives of the present work are also outlined in this chapter.

Chapter 2

This chapter deals with the significance of chitosan as carrier for enzyme immobilization and details of physico-chemical techniques implemented for the characterization of composites. The experimental methods for the preparation of immobilized enzyme, total protein assay, optimization of immobilization condition, α-amylase activity assay and biochemical characterization of free and immobilized enzymes are described. Chitosan-metal oxide composites CSM, CSZ and CST are synthesized and characterized by physico-chemical techniques. The efficiency and easy handling of magnetic chitosan as enzyme carrier was recognized. Chemical modification of magnetic chitosan with cross-linking agents was performed. The immobilization of α-amylase on synthesized composites and optimization of immobilization conditions were carried out. The properties of immobilized enzymes, thermal stability, activation energy, reusability and storage stability of immobilized enzymes were analyzed. Kinetic parameters were determined and compared with that of free enzyme.

Chapter 3

This chapter describes the composite formation of magnetic chitosan with polyaniline and polypyrrole and graft copolymerization by methyl

methacrylate and acrlonitrile. The composites were characterized by various physic-chemical techniques. CSM-PANI and CSM-PPY were found to be effectively used as a promising material for α-amylase immobilization. The enzyme immobilized grafted copolymers of magnetic chitosan, CSM-g-PMMA and CSM-g-PAN have shown appreciable immobilization yield and efficiency. The effect of pH and temperature on activity of immobilized enzymes was compared with that of free enzyme. The reusability, thermal and storage stability of immobilized enzymes were studied. The kinetic parameters, turnover number and catalytic efficiency of all immobilized enzymes were compared to that of free enzyme.

Chapter 4

In this chapter the magnetic chitosan was modified with inorganic layered solids such as graphite oxide and montmorillonite. The modified forms were characterized by using different physico-chemical techniques. The α-amylase was immobilized on graphite oxide modified magnetic chitosan by adsorption and covalent binding methods. The activity and stability studies for both methods were compared. The catalytic efficiency and reusability of the immobilized enzymes were evaluated. The effect of incorporation of montmorillonite on magnetic chitosan on α-amylase immobilization was also studied in this chapter. Optimization of immobilization conditions such as immobilization pH, incubation time and enzyme concentration were carried out. The pH and temperature stability, activation energy, thermal and storage stability and reusability of all the immobilized enzymes were described on the basis of MMT concentration in the carrier. The kinetic constants and hence catalytic efficiency were determined for all immobilized enzymes and compared with that of free enzyme.

Chapter 5

This chapter illustrates the modification of magnetic chitosan by PAMAM dendrimers using ethylene diamine and diethylene triamine and exhibits these as new type of carriers for immobilization of α-amylase. The immobilization conditions were optimized and the effect of immobilization efficiency on the increase of PAMAM generation was also studied. The activity of all immobilized enzymes on starch hydrolysis was compared with their free counterpart. The effect of pH and temperature on enzyme activity was studied and activation energies were determined. The stability studies and reusability study were conducted. The enzyme immobilization on second generation of PAMAM modified magnetic chtiosan was performed by adsorption and covalent methods. The activity, stability and reusability of the adsorbed and covalently immobilized enzymes were compared to each other. The kinetic constants were determined for free and immobilized enzymes and their catalytic efficiencies were compared.

Chapter 6

Thermal deactivation study conducted for free and all immobilized enzymes were presented in this chapter. The kinetic parameters such as E_d, $t_{1/2}$, D- and z- values for the thermal deactivation of free and immobilized enzymes were calculated. The variations in these parameters for immobilized enzymes were described with respect to free enzyme and their resistance towards thermal denaturation was explained. The thermodynamic parameters $\Delta H°$, $\Delta S°$ and $\Delta G°$ were derived for thermal deactivation of free and immobilized enzymes. These values for immobilized enzymes were compared with that of free enzyme. The tendency of immobilized enzymes for thermal denaturation was explained on the basis of the interaction between enzyme and carriers.

Chapter 7

This chapter presents the two types of industrial applications for α-amylase immobilized magnetic chitosan. The washing performance of immobilized enzymes in laundry detergents was estimated. The study was conducted using six commercial detergents and the performances of immobilized enzyme on these detergents were compared by determining the maltose content during the starch hydrolysis reaction. The cleaning efficiency of immobilized enzyme was explained on the basis of specific enzyme activity. The effect of temperature on cleaning performances of free and immobilized enzymes was explained for all detergents. This chapter also deals with the performance of α-amylase immobilized magnetic chitosan as desizer. The desizing efficiency was tested by weight loss (%) assay and reducing sugar assay. The parameters such as enzyme concentration and incubation time were optimized for desizing process. The effect of pH and temperature on desizing efficiency was also described in this chapter.

Future outlook

- Development of enzymatic biosensors
- Molecular Modeling and Docking of immobilized enzymes towards perceptive enzyme–substrate interactions
- Synthesis of new modified forms of magnetic chitosan for α-amylase immobilization
- Development of new immobilized systems of these carriers using other industrial enzymes

Publications

Research Publications

- Parameters affecting the improvement of properties and stabilities of immobilized α-amylase on chitosan-metal oxide composites, V.U. Bindu, A. A. Shanty, P. V. Mohanan, International Journal of Biochemistry and Biophysics 6 (2018) 44-57.
- Enhanced stability of α-amylase via immobilization onto chitosan-TiO_2 nanocomposite, V. U. Bindu, P. V. Mohanan, Nanoscience and Technology 4 (2017) 1-9.
- Optimization and immobilization studies of alpha amylase on chitosan-magnetite nanocomposite, V.U. Bindu and P.V. Mohanan, International Conference, ISBN: 978-93-80095-738 (2016) 598-601.
- Chitosan-magnetite nanocomposites as support for enzyme immobilization, V.U. Bindu and P.V. Mohanan, National Seminar, ISBN: 978-81-930558-1-6 (2015) 23-26.
- Preparation, characterisation and thermal studies of composites of polyaniline (doped / undoped forms) with nano magnetite, Maria Augustine, Bindu V. U., P. V. Mohanan, Pauline Journal of Research and Studies 1 (2014) 416-429.

Conference Presentations

- Effect of generations of PAMAM dendrimer on magnetic chitosan for an efficient enzyme carrier, V.U. Bindu and P.V. Mohanan, Presented at international conference on sustainable innovations in green chemistry and new technological developments (ICSIG-2018), Maharaja's college, Ernakulam (2018).
- Studies on activity, stability and kinetics of immobilized α- amylase on Chitosan-TiO_2 nanocomposite, V.U. Bindu and P.V. Mohanan, Presented at National conference CTriC 2018, Cochin University of Science and Technology, Kerala, India (2018).
- Chitosan-TiO_2 nanocomposite as the potential carrier for efficient enzyme immobilization, V.U. Bindu and P.V. Mohanan, Presented at international symposium on new trends in applied chemistry (NTAC-2017).
- Immobilization of α-amylase onto chitosan-ZnO nanocomposite, V.U. Bindu and P.V. Mohanan, Presented at National conference CTriC 2017, Cochin University of Science and Technology, Kerala, India (2017).
- Immobilization of α-amylase onto chitosan-TiO_2 nanocomposite: Optimization of immobilization parameters, V.U. Bindu and P.V. Mohanan, Presented at 26th Swadeshi Science Congress (2017).
- Activity of diastase α-amylase immobilized on chitosan metal oxide nanocomposites, V.U. Bindu and P.V. Mohanan, Presented at World Congress on Drug Discovery & Development, IISc Bengaluru (2016).

- Alpha amylase immobilization on chitosan-magnetite nanocomposite and its chemically modified forms, V.U. Bindu and P.V. Mohanan, National Conference on resent trends in Bio-inorganic and Organometallic Chemistry-NCBOC -2015 (Sri Shakthi Institute of Engineering and Technology, Coimbatore (2015).
- Effect of cross-linking agents on chitosan-magnetite nanocomposite on enzyme immobilization, V.U. Bindu and P.V. Mohanan, Chemistry in Cancer Research-CCR 2015, St. Albert's College, Ernakulam, Kerala, India (2015).
- Immobilization of α-amylase onto cross-linked chitosan-magnetite nano composite, V.U. Bindu and P.V. Mohanan, Presented at National conference CTriC 2014, Cochin University of Science and Technology, Kerala, India (2014).